



Kent Academic Repository

**Bateman, David Christopher (1974) *Models of low energy scattering*.
Doctor of Philosophy (PhD) thesis, University of Kent.**

Downloaded from

<https://kar.kent.ac.uk/94199/> The University of Kent's Academic Repository KAR

The version of record is available from

This document version

UNSPECIFIED

DOI for this version

Licence for this version

CC BY-NC-ND (Attribution-NonCommercial-NoDerivatives)

Additional information

This thesis has been digitised by EThOS, the British Library digitisation service, for purposes of preservation and dissemination. It was uploaded to KAR on 25 April 2022 in order to hold its content and record within University of Kent systems. It is available Open Access using a Creative Commons Attribution, Non-commercial, No Derivatives (<https://creativecommons.org/licenses/by-nc-nd/4.0/>) licence so that the thesis and its author, can benefit from opportunities for increased readership and citation. This was done in line with University of Kent policies (<https://www.kent.ac.uk/is/strategy/docs/Kent%20Open%20Access%20policy.pdf>). If you ...

Versions of research works

Versions of Record

If this version is the version of record, it is the same as the published version available on the publisher's web site. Cite as the published version.

Author Accepted Manuscripts

If this document is identified as the Author Accepted Manuscript it is the version after peer review but before type setting, copy editing or publisher branding. Cite as Surname, Initial. (Year) 'Title of article'. To be published in *Title of Journal*, Volume and issue numbers [peer-reviewed accepted version]. Available at: DOI or URL (Accessed: date).

Enquiries

If you have questions about this document contact ResearchSupport@kent.ac.uk. Please include the URL of the record in KAR. If you believe that your, or a third party's rights have been compromised through this document please see our [Take Down policy](https://www.kent.ac.uk/guides/kar-the-kent-academic-repository#policies) (available from <https://www.kent.ac.uk/guides/kar-the-kent-academic-repository#policies>).

MODELS OF LOW ENERGY

$\pi\pi$ SCATTERING

by

D. C. BATEMAN

Submitted for the degree of Ph.D. in the
Department of Applied Mathematics at the
University of Kent at Canterbury

February, 1974

TO MY WIFE, SANDRA

INDEX

	Page No.
Index	i
Acknowledgments	iv
Summary	v
Foreword	x
 <u>CHAPTER I</u>	
1. Introduction	1
2. Origin and properties of the pion	2
3. S-matrix theory	4
4. The kinematics of elastic pion-pion scattering	8
5. The unitarity condition for partial wave amplitudes	10
6. Isotopic spin and the physical $\pi\pi$ scattering amplitudes	14
7. Crossing symmetry	20
8. Analytic properties of the $\pi\pi$ scattering amplitude	25
 <u>CHAPTER 2</u>	
1. Introduction	29
2. Theoretical determination of real $\pi\pi$ scattering from the reactions $\pi N \rightarrow \pi\pi N$	31
3. Experimental results	
(a) Determination of δ_1^1	38
(b) Determination of δ_0^2	40
(c) Determination of δ_0^0	42
(d) Determination of the $\pi\pi$ s-wave scattering lengths	45
(e) $\pi\pi$ scattering above 1 GeV	46
4. Representation of experimental data	47
5. Current algebra predictions	50
6. A phenomenological analysis - the model of Morgan and Shaw	56
7. The sigma model of $\pi\pi$ scattering	60
8. The Veneziano model	62

	Page No.
<u>CHAPTER 3</u>	
1. Introduction	69
2. Constraints on $\pi\pi$ partial wave amplitudes	71
3. Approximations and parametrisations	75
4. A model for $\pi\pi$ partial wave amplitudes (DCB-I)	98
5. The numerical results	104
6. Conclusion and comments	113
<u>CHAPTER 4</u>	
1. Introduction	116
2. A model for $\pi\pi$ s- p- and d-waves (DCB-II)	117
3. Results of model DCB-II	123
4. Comments, comparisons and conclusions	132
<u>CHAPTER 5</u>	
1. Introduction	137
2. The N/D formalism for $\pi\pi$ scattering	138
3. The pole approximation to $N_0^I(\nu)$	140
4. The pole + cut approximation to $N_0^I(\nu)$	150
Addendum	167a

APPENDICES

Page No.

A1.	Clebsch-Gordan coefficients	168
A3.	Derivation of Balachandran-Nuyts-Roskies crossing relations	169
B3.	Results from model PGM-II	172
C3.	Results from model DCB-I	183
A4.	The behaviour of $\text{Im } A_{\ell}^{\text{I}}(s)$ in the vicinity of $s=0$	192
B4.	Results from model DCB-II	195
C4.	Martin inequalities from DCB-II	196
A5.	Determination of $D_0^{\text{I}}(\nu)$ from the pole approximation to $N_0^{\text{I}}(\nu)$	206
B5.	Determination of $D_0^{\text{I}}(\nu)$ from the pole + cut approximation to $N_0^{\text{I}}(\nu)$	208

ACKNOWLEDGMENTS

I wish to thank the following people without whose help this thesis would never have materialised.

I am most grateful to my supervisor Dr. P.R. Graves-Morris who has provided invaluable guidance and support to the work presented. I should also like to thank Dr. D. Morgan for reading a preliminary version of the thesis, and for his useful comments and suggestions.

My thanks are also due to the Science Research Council for financial support from October 1968 to September 1971.

I am greatly indebted to my wife, Sandra, firstly for her patience and encouragement during the various stages of this work, and secondly for her accurate typing of a difficult text.

SUMMARY

In Chapter 1 the general principles of the theory of $\pi\pi$ elastic scattering are reviewed. Chapter 2 is divided into two parts; firstly, the nature of the indirect experiments and the information they yield are studied, together with some of the techniques that are used to relate the experimental data points to well-defined physical constants; secondly, several theoretical studies are described which are intended to reflect current opinion as to the true state of the $\pi\pi$ system below 1 GeV.

In Chapter 3 various approximation schemes for $\pi\pi$ scattering amplitudes that have been proposed by others are considered, and one such calculation is modified in the light of our present knowledge. The model, referred to as PGM-II, imposes exact crossing symmetry and approximate unitarity on a low energy representation of the $\pi\pi$ scattering amplitudes with the correct threshold behaviour at $s=4$; the coefficients of the parametrisation are determined in terms of a single fixed parameter, chosen to be a_2 , the $I=2$ s-wave scattering length.

The results obtained indicate that there are at least two independent solutions of the $\pi\pi$ amplitudes consistent with the requirements of analyticity, crossing symmetry and unitarity. (We do not rule out the possibility of there being other solutions.) To distinguish between the two solutions it is necessary to impose the additional physical assumption that a

zero exists in each of the s-wave amplitudes in the unphysical region. Although the physical s- and p-wave amplitudes are approximately linear in $[0,4]$ the $\pi^0\pi^0$ s-wave amplitude does not satisfy all the stringent bounds of Martin et al. in this region, and the corresponding values for a_0 , the $I=0$ s-wave scattering length, are found to be smaller than Weinberg's current algebra estimate; in particular PGM-II yields $a_0=0.058$ for $a_2=-0.064$. It is concluded that any representation of the $\pi\pi$ scattering amplitude, designed to be valid in the unphysical region, should take into account the correct behaviour of the partial waves at $s=0$ as well as at $s=4$.

Accordingly, an s- and p- partial wave representation possessing these properties is proposed (the model is called DCB-I). The general approach used to determine the s- and p-waves in $[0,4]$ for fixed values of a_2 is to impose elastic unitarity at $s=4$ and in the crossed-channel at $s=0$, and to impose approximate crossing symmetry in $[0,4]$ via the Balachandran-Nuyts-Roskies relations. DCB-I also yields two independent solutions, both of which exhibit approximately linear s- and p-wave amplitudes in $[0,4]$ and satisfy all the tested Martin-type constraints. The physical solution is again characterised by the presence of a zero in each of the s-wave amplitudes in $[0,4]$, and has scattering lengths, typically $a_0=0.13$, $a_1=0.026$ for $a_2=-0.052$ in satisfactory agreement with most current estimates. The model establishes the Balachandran-Nuyts-Roskies equations as a powerful means

of imposing approximate crossing symmetry in the unphysical region.

It is claimed that the parametrisation of DCB-I is a considerable improvement on PGM-II in the unphysical region, but it is inevitable that this type of model must break down at some order because of the impossibility of satisfying elastic unitarity and crossing symmetry at all energies. For example, in Chapter 4 additional terms are included in the parametrisation of DCB-I and the model is extended to include the $\pi\pi$ d-waves (it is renamed DCB-II); it is found that a solution which simultaneously satisfies p-wave unitarity and the results of DCB-I does not exist, and thus the model is seen to depend upon its approximations. However, if p-wave unitarity is relaxed (it is claimed that this is not an unreasonable approximation to make if one assumes that unitarity is not a strong constraint in the very low energy region) a solution is obtained for fixed values of a second physical parameter, chosen to be a_1 , the p-wave scattering length. Again the possibility of there being solutions other than the one found cannot be eliminated. Although the d-wave scattering lengths $a_{20} = 0.007 \pm 0.002$ $a_{22} = 0.0006 \pm 0.0002$ are larger than most previous estimates, the essential features of DCB-I are preserved in the higher order calculation, and in addition the model does yield a qualitative picture of the d-wave amplitudes in the unphysical region; for example, it is found that $dA_2^0(s)/ds < 0$ $dA_2^2(s)/ds < 0$ in $[0,4]$. The solution is

also shown to satisfy, almost without exception, a large number of Martin-type constraints involving the s- p- and d-wave amplitudes in [0,4].

In retrospect it is felt that although the d-wave calculation does encounter some difficulties, since few model-dependent calculations of the d-wave scattering lengths have so far been performed, the exercise is worthwhile and the results not too unreasonable.

The major drawback of the models proposed in Chapters 3 and 4 is their inability to provide any reliable information on the $\pi\pi$ s-wave amplitudes very far into the physical region because of the range of validity of the series expansions proposed. In Chapter 5 the $\pi\pi$ s-waves are studied from threshold up to 1 GeV using the N/D method. Firstly, a study is made of the pole approximation to the left-hand cut, using the known behaviour of the I=2 s-wave phase shift δ_0^2 and the s-wave Balachandran-Nuyts-Roskies equations to predict the I=0 s-wave phase shift δ_0^0 from threshold up to 1 GeV. It is assumed that (i) the near part of the left-hand cut does not play an essential role in determining low energy $\pi\pi$ scattering, and (ii) the behaviour of δ_0^2 is a strong enough constraint to predict δ_0^0 from threshold up to 1 GeV.

A single-pole approximation to the left-hand cut is rejected because of the absence of zeros in the s-wave amplitudes in the unphysical region for any choice of pole positions on the left-hand cut; a two-pole approximation scheme

is found to possess a zero in each of the s-wave amplitudes in $[0,4]$ for a wide range of positive values of a_0 , but no σ -resonance. It is concluded that (ii) is not a strong enough constraint to furnish reliable information on δ_0^0 in the region of the ρ -resonance, at least for the pole approximation scheme described.

To test the validity of (i) an improved form for the N-function is proposed which exhibits the correct behaviour of the s-wave amplitudes at the edge of the left-hand cut (cut + pole model). It is shown that a cut + one-pole model has a resonance in δ_0^0 for small values of a_0 ; the cut + two-pole model is also shown to provide a good fit to the experimental data of δ_0^2 and to the Up-Down branch of δ_0^0 . The best fit to the δ_0^0 data corresponds to $a_0=0.12$, $M_\sigma=900$ MeV, $\Gamma_\sigma=500$ MeV, indicating our preference for a fairly broad σ -meson resonance at about 900 MeV in the $I=0$ s-wave amplitude.

FOREWORD

The importance of the pion-pion interaction lies in its basic simplicity, which is a consequence of having Bose statistics, no spin, and a reaction which is exactly crossing symmetric. Also, because it is the lightest of the hadrons it is fundamental as far as the study of strong interactions is concerned, but its instability prohibits real $\pi\pi$ scattering experiments.

In recent years there have been many theoretical calculations of the $\pi\pi$ amplitudes based upon quite different methods and it is interesting to see what physical ideas emerge from these calculations. In particular, some progress in understanding the low energy $\pi\pi$ system has come from constructing $\pi\pi$ amplitudes, and constraining them to fulfil the theoretical requirements of analyticity, crossing symmetry and unitarity, and the known experimental data. The aim of this thesis is to use these techniques to further resolve the main uncertainties which surround the $\pi\pi$ partial wave behaviour, namely, scattering lengths and the Up-Down ambiguity in the $I=0$ s-wave.

CHAPTER 1

I. INTRODUCTION

In the world of strong interaction physics, pion-pion scattering is the most fundamental of all the scattering processes and, therefore, the most obvious system upon which to test theories and models. From the many calculations of the low energy $\pi\pi$ scattering amplitudes, often based upon quite different methods, there has emerged a qualitative picture of $\pi\pi$ scattering from threshold up to 1 GeV.

Although different theories exploit different properties of the scattering amplitudes, certain general principles, for example, unitarity, crossing symmetry and analyticity, must be valid in any theory. The purpose of this chapter is to describe the general principles upon which theories and models of the $\pi\pi$ system are necessarily founded. In Section 2, the origin and properties of the pion particle are described, and in Section 3, the idea of the S-Matrix is introduced. The kinematics of $\pi\pi$ elastic scattering are defined in Section 4, and the elastic unitarity condition for partial wave amplitudes is derived in Section 5. In Section 6, the concept of isotopic spin is introduced, and some of the properties of physical $\pi\pi$ scattering amplitudes are established. The symmetry properties of the amplitudes and the crossing symmetry condition for $\pi\pi$ scattering are derived in Section 7; finally in Section 8, the analytic properties of the $\pi\pi$ scattering amplitudes are discussed.

2. ORIGIN AND PROPERTIES OF THE PION

The term 'elementary particle' is used to describe the smallest elements which appear to make up matter as we know it on our planet. Such particles are detected by the effects and tracks they leave in matter which they traverse.

The concept of a 'strong interaction' was introduced by Yukawa⁽¹⁾ in 1935. Before this time only a small number of elementary particles were known to exist, including the electron⁽²⁾, the photon⁽³⁾, the proton⁽²⁾ and the neutron⁽⁴⁾. Of these, the neutron and the proton were known to be manifestations of the same particle carrying different electric charges. It had also been established by this time that an electric field surrounds all electric charges and that the photon acts as the vehicle of the electric field to bring about electromagnetic interactions. Electromagnetic forces could not, however, explain either of the following phenomena: in an atomic nucleus, protons and neutrons are packed so closely together that electric repulsion between two protons can cause an explosion, whereas, if one proton passes sufficiently close to another proton, instead of it first being repelled by the electric field, it is attracted.

Yukawa suggested that nucleons are connected in the atomic nucleus by a field, analogous to the electric field which connects the electron to the atom, but with a force of much shorter range, $\sim 10^{-13}$ cm., and much greater strength. He

further assumed that this field is carried by a particle in the same way as the electric field is carried by the photon, and that nucleons interact with each other by the exchange of this particle, whose mass he predicted to be ~ 100 MeV. This type of interaction he called a strong interaction. The particle predicted by Yukawa was later discovered by studying the effects of cosmic radiation on photographic emulsions⁽⁵⁾. It was called a pion.

In the real world pions are spinless bosons^{*}, existing in three charge states π^+ , π^0 , π^- . They are the lightest of all the strongly interacting particles, and as a result an understanding of the pion-pion interaction is fundamental to any systematic development of strong interaction physics.

The reaction between two nucleons in the atomic nucleus is further explained as follows: the incident proton in its passage through the atomic nucleus removes a virtual pion surrounding the target nucleon according to either $p+p \rightarrow p+p+\pi^0$ or $p+p \rightarrow p+n+\pi^+$. The pion formed, however, has only a very short lifetime, decaying according to either $\pi^+ \rightarrow \mu^+ + \nu$ in $\sim 10^{-8}$ sec.,⁽⁶⁾ or $\pi^0 \rightarrow \gamma + \gamma$ in $\sim 10^{-16}$ sec.⁽⁷⁾. This instability of the pion particle has so far ruled out the possibility of

*Bosons are particles with integral spin which obey Bose Statistics. Bose Statistics is defined as the property of the wave function to be completely symmetric under exchange of all quantum numbers.

the pion-pion scattering experiment being performed. The principal characteristics of the charged states of the pion are shown in Table 1.1⁽⁸⁾.

Particle	Mass (MeV)	Electric Charge	Spin	Mean Lifetime (Secs.)	Mode of Decay
π^+	139.00 ± 0.05	+1	0	$(2.55 \pm 0.03) \times 10^{-8}$	$\mu^+ + \nu$
π^0	135.00 ± 0.05	0	0	$(2.2 \pm 0.8) \times 10^{-16}$	$\gamma + \gamma$
π^-	139.00 ± 0.05	-1	0	$(2.55 \pm 0.03) \times 10^{-8}$	$\mu^- + \bar{\nu}$

Table 1.1

Properties of the Pion

The basic requirement of a mathematical framework upon which studies of all strong interactions could be based began in 1943 when Heisenberg hypothesised the existence of the S-Matrix⁽⁹⁾.

3. S-MATRIX THEORY

An experiment in strong interaction physics may involve observing the initial state $|i\rangle$, representing two or more particles before the interaction, allowing the particles to interact, and then observing the final state $|f\rangle$ of the arbitrary number of particles resulting from the interaction. The state $|i\rangle$ and the state $|f\rangle$ are assumed to contain all the physically relevant information about the system before and after the interaction respectively. They are normalised

according to the relation

$$\langle i|i \rangle = \langle f|f \rangle = 1 . \quad (1.3.1)$$

The S-Matrix is defined to be the operator S, such that the transition amplitude for scattering from a state $|i\rangle$ to a state $|f\rangle$ is given by the matrix element

$$S_{fi} = \langle f|S|i \rangle . \quad (1.3.2)$$

The probability that the given $|f\rangle$ is 'the' final state observed after the interaction is given by

$$P_{fi} = |S_{fi}|^2 = |\langle f|S|i \rangle|^2 , \quad (1.3.3)$$

and since the system must have 'some' final state,

$$\sum_n P_{ni} = 1 = \sum_n \langle i|S^\dagger|n \rangle \langle n|S|i \rangle , \quad (1.3.4)$$

where the summation in Equation (1.3.4) is over all possible final states allowed by energy-momentum conservation laws.

If all permissible final states are assumed to form a complete set of states in the Hilbert Space,

$$\sum_n |n \rangle \langle n| = 1 \quad (1.3.5)$$

and Equation (1.3.4) can be re-written as

$$\langle i|S^\dagger S|i \rangle = 1 . \quad (1.3.6)$$

Since Equation (1.3.6) is true for any initial state $|i\rangle$, it follows that the S-Matrix is a unitary operator

$$S^\dagger S = S S^\dagger = 1 . \quad (1.3.7)$$

In order to calculate the transition probability between an initial state $|i\rangle$ and a final state $|f\rangle$ it is often convenient to introduce reduced matrix operators R and T which may be applied under suitable circumstances. The R -matrix operator is defined by the equation

$$S = 1 + iR \quad (1.3.8)$$

so that

$$S_{fi} = \langle f|1|i\rangle + i\langle f|R|i\rangle = \delta_{fi} + iR_{fi} \quad (1.3.9)$$

where the term δ_{fi} in Equation (1.3.9) implies that no interaction occurs. The unitarity condition for S then yields the relation

$$\langle f|R|i\rangle - \langle f|R^\dagger|i\rangle = i \sum_n \langle f|R^\dagger|n\rangle \langle n|R|i\rangle \quad (1.3.10)$$

between the matrix elements of R .

Invariance of the S -Matrix under Lorentz transformations implies that energy and momentum are conserved in interactions,

$$p_i - p_f = 0 \quad (1.3.11)$$

where p_i and p_f are the energy-momentum 4-vectors of the initial and final states respectively. It is sometimes convenient to take this conservation law out of the matrix element $\langle f|R|i\rangle$ by defining a new matrix element $\langle f|T|i\rangle$ such that

$$R_{fi} = (2\pi)^4 \delta^4(p_f - p_i) T_{fi} \quad (1.3.12)$$

The probability for the transition $|i\rangle \rightarrow |f\rangle$ for the whole of space-time is then given by

$$|R_{fi}|^2 = (2\pi)^8 [\delta^4(p_f - p_i)]^2 |T_{fi}|^2. \quad (1.3.13)$$

A more meaningful quantity is the transition probability per unit volume per unit time, which can be written as

$$\frac{1}{VT} |R_{fi}|^2 = (2\pi)^4 \delta^4(p_f - p_i) |T_{fi}|^2, \quad (1.3.14)^*$$

since in a scattering experiment the quantity of interest is the cross-section σ_{fi} , defined by

$$\sigma_{fi} = \frac{1}{VT} \frac{|R_{fi}|^2}{J_i}, \quad (1.3.15)$$

where J_i is the flux density of the incoming particles. In terms of the transition matrix elements,

$$\sigma_{fi} = \frac{(2\pi)^4 \delta^4(p_f - p_i) |\langle f | T | i \rangle|^2}{2E_1 E_2 |v_1 - v_2|}, \quad (1.3.16)$$

where E_1 and E_2 are the energies of the two incident particles, and $|v_1 - v_2|$ their relative speed.

*Equation (1.3.14) has been derived by writing the double δ -function in Equation (1.3.13) as

$$\delta^4(p_f - p_i) \lim_{\substack{V \rightarrow \infty \\ T \rightarrow \infty}} \int_{VT} d^4x e^{i(p_f - p_i)x} = \delta^4(p_f - p_i) \frac{VT}{(2\pi)^4}.$$

A more complete derivation has been given by Gasiorowicz⁽¹⁰⁾.

4. THE KINEMATICS OF ELASTIC PION-PION SCATTERING

The simplest scattering process between pions, where two pions enter the scattering region and two, not necessarily the same pions, emerge from this region is illustrated in Figure 1.1.

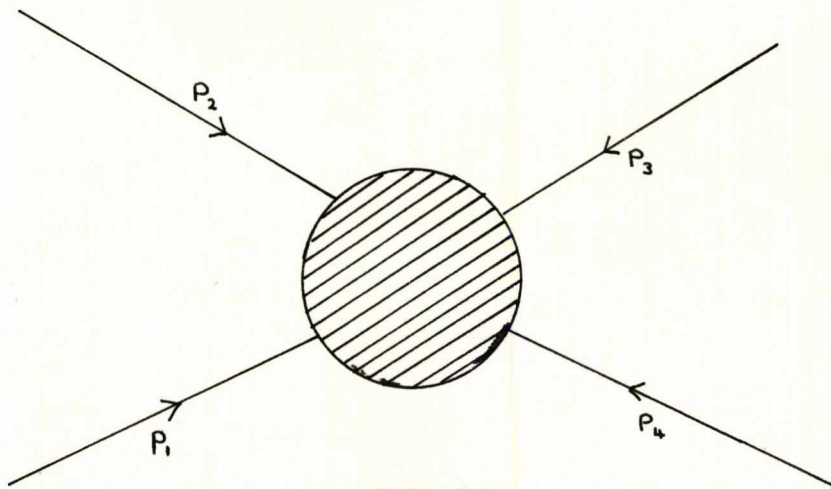


Figure 1.1
The reaction $\pi+\pi\rightarrow\pi+\pi$

p_1, p_2, p_3 and p_4 , the four-momenta of the pions involved in the scattering process, are formally represented as incoming particles. Therefore, at any particular point in time, two of the four-momenta will always be positive-timelike corresponding to the actual incoming particles, and two will always be negative-timelike corresponding to the scattered particles. The scattering amplitude for the process, which is represented by the shaded area in Figure 1.1, is usually written in terms of three Lorentz invariant quantities s, t

and u , defined in terms of the four-momenta of the particles by

$$\left. \begin{aligned} s &= (p_1+p_2)^2 = (p_3+p_4)^2 \\ t &= (p_1+p_3)^2 = (p_2+p_4)^2 \\ u &= (p_1+p_4)^2 = (p_2+p_3)^2 \end{aligned} \right\} \quad (1.4.1)$$

Conservation of energy and momentum in the interaction can be stated as

$$p_1 + p_2 + p_3 + p_4 = 0 \quad , \quad (1.4.2)$$

and since the four-momentum of each pion satisfies the relativistic equation

$$p_i^2 = p_{i0}^2 - \underline{p}_i^2 = m_\pi^2 \quad , \quad (1.4.3)$$

where m_π is the mass of a pion, it is straightforward to show that

$$s + t + u = 4m_\pi^2 \quad , \quad (1.4.4)$$

and so only two of the Mandelstam variables* are independent.

For the corresponding elastic scattering process in the centre of mass frame of reference, which is illustrated in Figure 1.2, the primed particles represent the scattered particles,

$$p_3 = -p_1' \quad , \quad p_4 = -p_2' \quad , \quad (1.4.5)$$

and s , t and u are defined in terms of q , the magnitude of the

*The introduction by Mandelstam⁽¹¹⁾ of an invariant scattering amplitude as a function of s , t and u , has led to the three variables being popularly known as the Mandelstam variables.

three-momentum of a pion in the centre of mass system, and θ , the scattering angle, according to

$$\left. \begin{aligned} s &= 4(m_{\pi}^2 + q^2) \\ t &= -2q^2(1 - \cos \theta) \\ u &= -2q^2(1 + \cos \theta) \end{aligned} \right\} \quad (1.4.6)$$

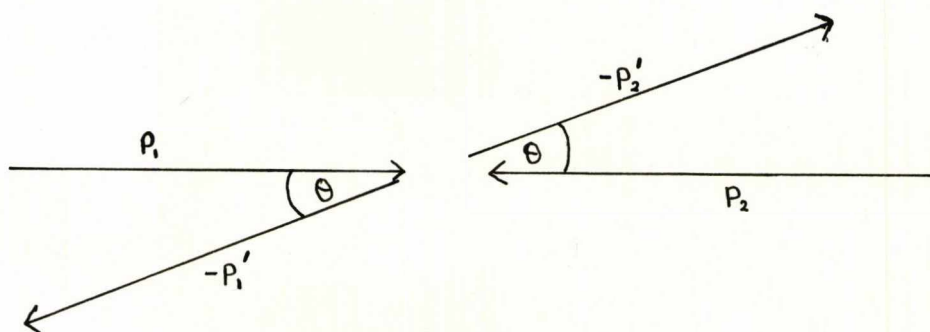


Figure 1.2

The reaction $\pi + \pi \rightarrow \pi + \pi$
in the centre of mass frame

Thus, when p_1 and p_2 are the incident particles, s represents the square of the total energy in the centre of mass system, and t minus the square of the four-momentum transfer. The significance of s , t and u for other pairs of incoming particles is discussed in Section 7.

5. THE UNITARITY CONDITION FOR PARTIAL WAVE AMPLITUDES

The unitarity relation between matrix elements of the transition operator T , for the scattering process represented by Figure 1.2, is defined through Equations (1.3.7), (1.3.8)

and (1.3.12) to be

$$i \langle p_1' p_2' | T^+ - T | p_1 p_2 \rangle = \langle p_1' p_2' | T^+ T | p_1 p_2 \rangle . \quad (1.5.1)$$

In terms of the imaginary part of the scattering amplitude, $\text{Im } A(s, t, u)$, the left-hand-side of Equation (1.5.1) is defined by the expression

$$2\delta^4(p_1 + p_2 - p_1' - p_2') \frac{1}{\sqrt{p_{1_0} p_{2_0} p_{1_0}' p_{2_0}'}} \text{Im } A(s, t, u) , \quad (1.5.2)$$

where $p_{1_0}, p_{2_0}, p_{1_0}', p_{2_0}'$ are the energy components of the corresponding four-momenta. The right-hand-side of Equation (1.5.1) relates $\text{Im } A(s, t, u)$ to a sum over products of matrix elements connecting the initial and final states to all physical states allowed by energy-momentum conservation

$$\delta^4(p_1 + p_2 - p_1' - p_2') \frac{1}{\sqrt{p_{1_0} p_{2_0} p_{1_0}' p_{2_0}'}} \sum_n \frac{1}{n!} \int \frac{d^3 k_1}{p_{k_1}} \dots \frac{d^3 k_n}{p_{k_n}} \delta^4\left(p_1 + p_2 - \sum_i k_i\right) \cdot A^*(p_1' p_2' \rightarrow k_1 \dots k_n) A(p_1 p_2 \rightarrow k_1 \dots k_n) . \quad (1.5.3)$$

To determine the elastic unitarity condition the summation in Equation (1.5.3) is restricted to a sum over two-particle contributions only. Then,

$$\text{Im } A(s, t, u) = \frac{1}{4} \int \frac{d^3 k_1}{p_{k_1}} \frac{d^3 k_2}{p_{k_2}} \delta^4(p_1 + p_2 - k_1 - k_2) A^*(s, t_{p'}, u_{p'}) A(s, t_p, u_p) \quad (1.5.4)$$

where

$$\begin{aligned} t_{p'} &= -2q^2(1 - \cos \theta_{p_1' k_1}) \\ t_p &= -2q^2(1 - \cos \theta_{p_1 k_1}) . \end{aligned}$$

The scattering amplitude can be expanded in terms of its partial wave amplitudes by the equation

$$A(s, t, u) = \sum_{\ell=0}^{\infty} (2\ell+1) A_{\ell}(s) P_{\ell}(\cos \theta) , \quad (1.5.5)$$

where $P_{\ell}(\cos \theta)$ is the usual Legendre polynomial. Since the variable $\cos \theta$ is antisymmetric under interchange of t and u^* , and Bose symmetry requires the amplitude to be completely symmetric, the summation in Equation (1.5.5) is restricted to a sum over even powers of ℓ only. If the d^3k_2 integration in Equation (1.5.4) is performed explicitly and the amplitude replaced by its Legendre expansion,

$$\begin{aligned} \text{Im } A(s, t, u) &= \frac{1}{4} \sum_{\ell, \ell'} (2\ell+1)(2\ell'+1) \int \frac{d^3k}{k_0} \delta(\sqrt{s}-2k_0) \cdot \\ &\cdot A_{\ell}^*(s) A_{\ell'}(s) P_{\ell}(\cos \theta_{kp'}) P_{\ell'}(\cos \theta_{kp}) . \end{aligned} \quad (1.5.6)$$

Using the property of the Legendre polynomials that

$$\int d\Omega_k P_{\ell}(\cos \theta_{kp'}) P_{\ell'}(\cos \theta_{kp}) = \frac{4\pi}{(2\ell+1)} \delta_{\ell\ell'} P_{\ell}(\cos \theta) \quad (1.5.7)$$

Equation (1.5.6) reduces to

$$\text{Im } A(s, t, u) = \sqrt{\frac{s-4m_{\pi}^2}{s}} \sum_{\ell} (2\ell+1) |A_{\ell}(s)|^2 P_{\ell}(\cos \theta) . \quad (1.5.8)$$

*From Equation (1.4.6)

$$\cos \theta = 1 + \frac{2t}{s-4m_{\pi}^2} = - \left(1 + \frac{2u}{s-4m_{\pi}^2} \right) = \frac{t-u}{s-4m_{\pi}^2} = \frac{u-t}{u+t} .$$

If $\text{Im } A(s,t,u)$ is then expanded according to Equation (1.5.5) one obtains the elastic unitarity condition for partial wave amplitudes,

$$\text{Im } A_\ell(s) = \sqrt{\frac{s-4m_\pi^2}{s}} |A_\ell(s)|^2 \quad \text{for all } \ell . \quad (1.5.9)$$

Equation (1.5.9) is an exact relation when the energy variable s is below the threshold of all inelastic processes, but although inelastic processes start at $s=16m_\pi^2 \sim 560 \text{ MeV}$ with the production of two additional pions, Equation (1.5.9) is generally considered to be a good approximation up to an energy of 1 GeV.

A partial wave amplitude which satisfies the elastic unitarity condition can always be written as

$$\begin{aligned} A_\ell(s) &= \sqrt{\frac{s}{s-4m_\pi^2}} e^{i\delta_\ell(s)} \sin \delta_\ell(s) \\ &= \sqrt{\frac{s}{s-4m_\pi^2}} \frac{1}{2i} \left(e^{i\delta_\ell(s)} - 1 \right) , \end{aligned} \quad (1.5.10)$$

where for physical values of ℓ and s the phase shift $\delta_\ell(s)$ is real. Close to the physical threshold* $\delta_\ell(s)$ is small, and its behaviour is conveniently defined in terms of a constant, a_ℓ , the ℓ -wave scattering length, by the equation

$$\delta_\ell(s) \underset{q^2 \rightarrow 0}{\sim} a_\ell q^{(2\ell+1)} . \quad (1.5.11)$$

*The physical threshold is the point $s=4m_\pi^2$, and $\delta_\ell(s)$ is defined in the region $s \geq 4m_\pi^2$, $t < 0$, $u < 0$, c.f. Section 7 of Chapter 1.

At energies greater than 1 GeV, where the contributions from inelastic processes become significant, the phase shifts are complex, and the unitarity relation is then expressed as

$$\text{Im } A_\ell(s) = \sqrt{\frac{s-4m_\pi^2}{s}} R_\ell(s) |A_\ell(s)|^2 \quad \ell=0,1,\dots \quad (1.5.12)$$

where $R_\ell(s)$, the inelasticity parameter for the ℓ th partial wave, satisfies the inequality

$$R_\ell(s) \geq 1 \quad \ell=0,1,\dots \quad (1.5.13)$$

6. ISOTOPIC SPIN AND THE PHYSICAL $\pi\pi$ SCATTERING AMPLITUDES

Although pions exist in three independent charge states π^+ , π^0 , π^- , as far as their strong interactions are concerned these states are simply different manifestations of the same field. The concept of isotopic spin in strong interactions was introduced⁽¹²⁾ to distinguish between those particles which have all their properties, except those associated with electric charge, practically identical.

The isospin of a system is formally similar to angular momentum but is linked to the charge states of the system. Therefore, since a pion exists in three independent charge states, its total isospin is determined from the equation

$$2I + 1 = 3, \quad (1.6.1)$$

and since its charge states are related to the third component of the isospin operator I_3 , it is convenient to define

$$\begin{aligned} I_3(\pi^+) &= +1 \\ I_3(\pi^0) &= 0 \\ I_3(\pi^-) &= -1 \end{aligned} \quad (1.6.2)$$

Total isospin is conserved in strong interactions, and for the interaction between two pions discussed in Section 4 the rules of angular momentum require I to have the three possible values 2, 1 or 0. If $|I, I_3\rangle$ represents a possible state of this two-pion system, the $2I+1$ multiplets that exist for each value of I are given by

$$\begin{aligned} &|2,+2\rangle, |2,+1\rangle, |2,0\rangle, |2,-1\rangle, |2,-2\rangle \\ &|1,+1\rangle, |1,0\rangle, |1,-1\rangle \\ &|0,0\rangle. \end{aligned} \tag{1.6.3}$$

These two-pion states can be written in terms of isotopic spin wave functions of single-pion states; for the state $|2,+2\rangle$ and the state $|2,-2\rangle$ there is only one possible combination of single-pion states, $|1,+1\rangle|1,+1\rangle$ and $|1,-1\rangle|1,-1\rangle$ respectively. The other seven two-pion states are expressed as a combination of possible single-pion states, weighted with the appropriate probabilities of the relevant Clebsch-Gordan coefficients. From Appendix A.1 one can write

$$\left. \begin{aligned} |2,+1\rangle &= \sqrt{\frac{1}{2}}|1,0\rangle|1,1\rangle + \sqrt{\frac{1}{2}}|1,1\rangle|1,0\rangle \\ |2,0\rangle &= \sqrt{\frac{1}{6}}|1,1\rangle|1,-1\rangle + \sqrt{\frac{2}{3}}|1,0\rangle|1,0\rangle + \sqrt{\frac{1}{6}}|1,-1\rangle|1,1\rangle \\ |2,-1\rangle &= \sqrt{\frac{1}{2}}|1,-1\rangle|1,0\rangle + \sqrt{\frac{1}{2}}|1,0\rangle|1,-1\rangle \\ |1,+1\rangle &= \sqrt{\frac{1}{2}}|1,+1\rangle|1,0\rangle - \sqrt{\frac{1}{2}}|1,0\rangle|1,+1\rangle \\ |1,0\rangle &= \sqrt{\frac{1}{2}}|1,+1\rangle|1,-1\rangle - \sqrt{\frac{1}{2}}|1,-1\rangle|1,+1\rangle \\ |1,-1\rangle &= \sqrt{\frac{1}{2}}|1,0\rangle|1,-1\rangle - \sqrt{\frac{1}{2}}|1,-1\rangle|1,0\rangle \\ |0,0\rangle &= \sqrt{\frac{1}{3}}|1,+1\rangle|1,-1\rangle - \sqrt{\frac{1}{3}}|1,0\rangle|1,0\rangle + \sqrt{\frac{1}{3}}|1,-1\rangle|1,+1\rangle \end{aligned} \right\}.$$

The physical nature of the wave functions is exhibited more clearly in Table 1.2, where the isospin states on the left-hand-side of Equation (1.6.3) have been redefined in terms of charge states of the two-pion system.

	I=2	I=1	I=0
$I_3=+2$	$ \pi^+\pi^+\rangle$		
$I_3=+1$	$\frac{ \pi^+\pi^0\rangle + \pi^0\pi^+\rangle}{\sqrt{2}}$	$\frac{ \pi^+\pi^0\rangle - \pi^0\pi^+\rangle}{\sqrt{2}}$	
$I_3=0$	$\frac{ \pi^+\pi^-\rangle + \pi^-\pi^+\rangle + 2 \pi^0\pi^0\rangle}{\sqrt{6}}$	$\frac{ \pi^+\pi^-\rangle - \pi^-\pi^+\rangle}{\sqrt{2}}$	$\frac{ \pi^+\pi^-\rangle + \pi^-\pi^+\rangle - \pi^0\pi^0\rangle}{\sqrt{3}}$
$I_3=-1$	$\frac{ \pi^0\pi^-\rangle + \pi^-\pi^0\rangle}{\sqrt{2}}$	$\frac{ \pi^0\pi^-\rangle - \pi^-\pi^0\rangle}{\sqrt{2}}$	
$I_3=-2$	$ \pi^-\pi^-\rangle$		

Table 1.2

Isotopic Spin States of the Two-Pion System

The I=1 states are antisymmetric under interchange of the two pions and therefore correspond to states with odd angular momenta, while the I=0 states and the I=2 states are symmetric and correspond to states with even angular momenta. If Table 1.2 is inverted the charge states can be expressed in terms of their isotopic content by

$$\begin{aligned}
 |\pi^+ \pi^+ \rangle &= |I=2 \rangle && \text{(even waves only)} \\
 |\pi^+ \pi^0 \rangle &= \begin{cases} \sqrt{\frac{1}{2}} |I=2 \rangle & \text{(even waves)} \\ \sqrt{\frac{1}{2}} |I=1 \rangle & \text{(odd waves)} \end{cases} \\
 |\pi^+ \pi^- \rangle &= \begin{cases} \sqrt{\frac{1}{3}} |I=0 \rangle + \sqrt{\frac{1}{6}} |I=2 \rangle & \text{(even waves)} \\ \sqrt{\frac{1}{2}} |I=1 \rangle & \text{(odd waves)} \end{cases} \\
 |\pi^0 \pi^0 \rangle &= -\sqrt{\frac{1}{3}} |I=0 \rangle + \sqrt{\frac{2}{3}} |I=2 \rangle && \text{(even waves only)} \\
 |\pi^0 \pi^- \rangle &= \begin{cases} \sqrt{\frac{1}{2}} |I=2 \rangle & \text{(even waves)} \\ \sqrt{\frac{1}{2}} |I=1 \rangle & \text{(odd waves)} \end{cases} \\
 |\pi^- \pi^- \rangle &= |I=2 \rangle && \text{(even waves only)}
 \end{aligned}
 \tag{1.6.5}^*$$

Since charge is conserved in all strong interactions, I_3 remains constant during the scattering process. Therefore, in $\pi\pi$ scattering there are only three independent scattering amplitudes, each of which corresponds to a well-defined value of the total isospin. If these amplitudes are denoted by A^0 , A^1 and A^2 , corresponding to $I=0,1,2$ respectively, the $\pi\pi$ transition matrix operator can be written as

$$A^{\pi\pi \rightarrow \pi\pi} = A^0 P_0 + A^1 P_1 + A^2 P_2, \tag{1.6.6}$$

where P_0 , P_1 and P_2 are the projection operators on total isospin states, and total isospin is conserved during the interaction.

*In Equation (1.6.5), the I_3 part of each wave function, which is given by the total charge of the two-pion state, has been omitted.

The physical $\pi\pi$ scattering amplitudes, which correspond to the matrix elements of Equation (1.6.6) between definite charge states, can be readily obtained in terms of the A^I ($I=0,1,2$), through Equation (1.6.5) as

$$\left. \begin{aligned}
 A^{\pi^+ \pi^+ \rightarrow \pi^+ \pi^+} &= A^{\pi^- \pi^- \rightarrow \pi^- \pi^-} = 2A^2 \\
 A^{\pi^+ \pi^0 \rightarrow \pi^+ \pi^0} &= A^{\pi^- \pi^0 \rightarrow \pi^- \pi^0} = A^2 + A^1 \\
 A^{\pi^+ \pi^- \rightarrow \pi^+ \pi^-} &= (2A^0 + A^2)/3 + A^1 \\
 A^{\pi^0 \pi^0 \rightarrow \pi^0 \pi^0} &= (2A^2 + A^0)/3 \\
 A^{\pi^+ \pi^- \rightarrow \pi^0 \pi^0} &= (A^2 - A^0)/3
 \end{aligned} \right\} \quad (1.6.7)$$

It is often useful, by transforming the basis of charge states defined in Equation (1.6.1), to work in a spherical basis of states in isotopic space. The necessary change of basis is obtained by defining the wave functions in terms of their components on the three basis vectors in isotopic space $|\pi^1\rangle$, $|\pi^2\rangle$ and $|\pi^3\rangle$, which are respectively eigenstates of I_1 , I_2 and I_3 with eigenvalues 0, according to

$$\left. \begin{aligned}
 |\pi^+\rangle &= \frac{|\pi^1\rangle + i|\pi^2\rangle}{\sqrt{2}} \\
 |\pi^-\rangle &= \frac{|\pi^1\rangle - i|\pi^2\rangle}{\sqrt{2}} \\
 |\pi^0\rangle &= |\pi^3\rangle
 \end{aligned} \right\} \quad (1.6.8)$$

To define the projection operators P_0 , P_1 and P_2 in this new basis, the reaction is written with the initial pions labelled by indices α and β , and the final pions by indices γ and δ .

Then P_0 , P_1 and P_2 , for the reaction $\pi^\alpha + \pi^\beta \rightarrow \pi^\gamma + \pi^\delta$, are given by

$$\left. \begin{aligned} P_0 &= \frac{1}{3} \delta_{\alpha\beta} \delta_{\gamma\delta} \\ P_1 &= \frac{1}{2} [\delta_{\alpha\gamma} \delta_{\beta\delta} - \delta_{\alpha\delta} \delta_{\beta\gamma}] \\ P_2 &= \frac{1}{2} [\delta_{\alpha\gamma} \delta_{\beta\delta} + \delta_{\alpha\delta} \delta_{\beta\gamma}] - \frac{1}{3} \delta_{\alpha\beta} \delta_{\gamma\delta} \end{aligned} \right\} \quad (1.6.9)$$

If Equation (1.6.9) is compared with Equation (1.6.6) the $\pi\pi$ transition matrix operator can be rewritten as

$$A^{\pi\pi \rightarrow \pi\pi} = A(s,t,u) \delta_{\alpha\beta} \delta_{\gamma\delta} + B(s,t,u) \delta_{\alpha\gamma} \delta_{\beta\delta} + C(s,t,u) \delta_{\alpha\delta} \delta_{\beta\gamma} \quad (1.6.10)$$

where A , B and C depend only on the dynamical variables. If P_0 , P_1 , P_2 , as defined by Equation (1.6.9), then act on Equation (1.6.10), the isospin amplitudes are related to A , B and C through the expressions

$$\left. \begin{aligned} A^0 &= 3A + B + C \\ A^1 &= B - C \\ A^2 &= B + C \end{aligned} \right\} \quad (1.6.11)$$

or in matrix notation

$$\begin{pmatrix} A^0 \\ A^1 \\ A^2 \end{pmatrix} = \begin{pmatrix} 3 & 1 & 1 \\ 0 & 1 & -1 \\ 0 & 1 & 1 \end{pmatrix} \begin{pmatrix} A \\ B \\ C \end{pmatrix} \quad (1.6.12)$$

If Equation (1.6.12) is then inverted, A, B and C are expressed in terms of the isospin amplitudes by the matrix equation

$$\begin{pmatrix} A \\ B \\ C \end{pmatrix} = \begin{pmatrix} \frac{1}{3} & 0 & -\frac{1}{3} \\ 0 & \frac{1}{2} & \frac{1}{2} \\ 0 & -\frac{1}{2} & \frac{1}{2} \end{pmatrix} \begin{pmatrix} A^0 \\ A^1 \\ A^2 \end{pmatrix} . \quad (1.6.13)$$

7. CROSSING SYMMETRY

To determine the symmetry properties of the $\pi\pi$ amplitude consider again the scattering process involving four pions. The six possible processes represented in Figure 1.1 are conveniently classified by pairing the particles into two incoming and two outgoing to define three 'channels'. If the s-channel is the channel for which s is the square of the total energy in the centre-of-mass system, the two reactions which occur in the s-channel, as defined in Section 4, are represented by

$$\left. \begin{array}{l} p_1 + p_2 \rightarrow \bar{p}_3 + \bar{p}_4 \\ \text{and the equivalent anti-particle reaction} \\ p_3 + p_4 \rightarrow \bar{p}_1 + \bar{p}_2 \end{array} \right\} . \quad (1.7.1)^*$$

Reactions with the four-momentum p_1 incoming have the energy component p_{10} positive whilst those with \bar{p}_1 outgoing have p_{10} negative. The signs of the energy components of the other

*In this section, p_1, p_2, p_3, p_4 represent the incoming particles and $\bar{p}_1, \bar{p}_2, \bar{p}_3, \bar{p}_4$ the corresponding outgoing anti-particles.

three four-momenta obey a similar rule, and the physical region of the s-channel is defined to be the region with s positive and greater than a threshold value of $4m_\pi^2$. It follows from Equation (1.4.6) that t and u are then negative in the physical region of the s-channel.

Likewise, scattering in the t-channel describes either of the reactions

$$\left. \begin{aligned} p_1 + p_3 &\rightarrow \bar{p}_2 + \bar{p}_4 \\ p_2 + p_4 &\rightarrow \bar{p}_1 + \bar{p}_3 \end{aligned} \right\} \quad (1.7.2)$$

and occurs when $t \geq 4m_\pi^2$, $s, u \leq 0$, and scattering in the u-channel describes either of the reactions

$$\left. \begin{aligned} p_1 + p_4 &\rightarrow \bar{p}_2 + \bar{p}_3 \\ p_2 + p_3 &\rightarrow \bar{p}_1 + \bar{p}_4 \end{aligned} \right\} \quad (1.7.3)$$

when $u \geq 4m_\pi^2$, $s, t \leq 0$. The physical regions of the three channels are represented by the shaded areas in Figure 1.3

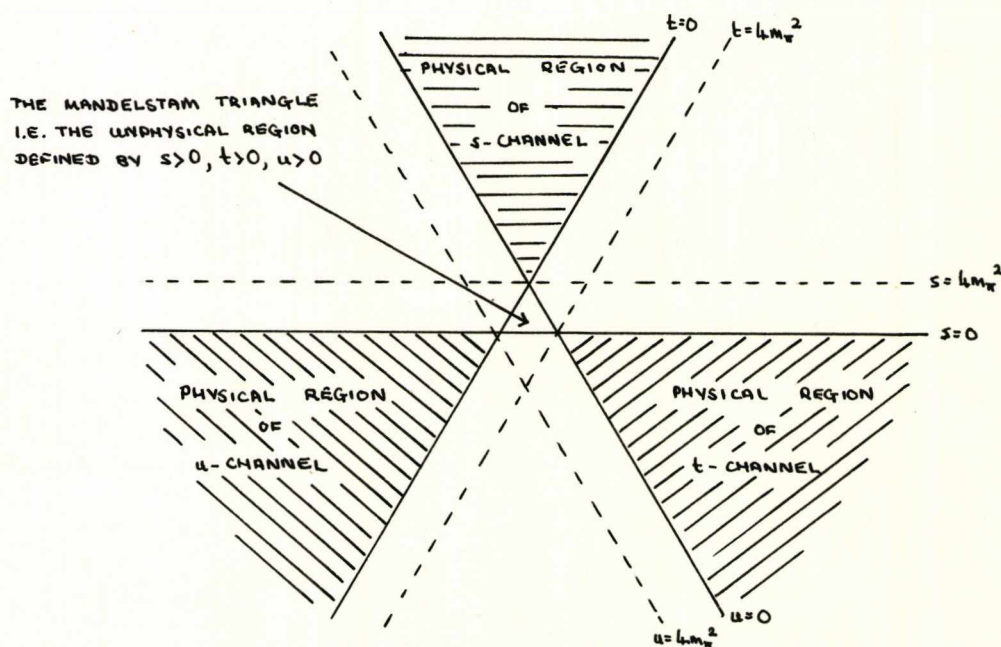


Figure 1.3

The physical regions of $\pi\pi$ scattering

To describe the symmetry of the $\pi\pi$ scattering amplitude it is necessary to postulate that a single analytic function of the variables s , t and u describes the scattering process in all three channels, the channel being selected by assigning values to the variables. It can be seen in Figure 1.3 that the physical regions of the three channels do not overlap, and, therefore, to give the postulate any physical meaning one must have a procedure of analytically continuing from one region to another. Details of the prescription for performing the analytic continuation are described in the next section; for the present it is assumed that such a process is possible. For a scattering process which involves two or more identical particles this postulate leads to the crossing symmetry property, that is, exchanging two identical particles (which requires switching two of the Mandelstam variables and leaving the third unchanged) at most changes the sign of the scattering amplitude*.

To relate $\pi\pi$ scattering in one channel to $\pi\pi$ scattering in another channel, recall the scattering amplitude previously defined in Equation (1.6.10)

$$A_{\alpha\beta,\gamma\delta}^{\pi\pi\rightarrow\pi\pi}(s,t,u) = A(s,t,u)\delta_{\alpha\beta}\delta_{\gamma\delta} + B(s,t,u)\delta_{\alpha\gamma}\delta_{\beta\delta} + C(s,t,u)\delta_{\alpha\delta}\delta_{\beta\gamma}. \quad (1.7.4)$$

*Since pions are bosons the sign of the amplitude is unchanged.

If the indices $\alpha, \beta, \gamma, \delta$ are associated with the four-momenta p_1, p_2, p_3, p_4 , respectively, $A_{\alpha\beta, \gamma\delta}^{\pi\pi \rightarrow \pi\pi}(s, t, u)$ describes the s-channel reaction. In this channel the amplitude is invariant under simultaneous interchange of γ and δ , which corresponds to switching t and u . Therefore,

$$A_{\alpha\beta, \gamma\delta}^{\pi\pi \rightarrow \pi\pi}(s, t, u) = A_{\alpha\beta, \delta\gamma}^{\pi\pi \rightarrow \pi\pi}(s, u, t) \quad (1.7.5)$$

from which the relations

$$\left. \begin{aligned} A(s, t, u) &= A(s, u, t) \\ B(s, t, u) &= C(s, u, t) \end{aligned} \right\} \quad (1.7.6)$$

follow. Crossing symmetry also requires $A_{\alpha\beta, \gamma\delta}^{\pi\pi \rightarrow \pi\pi}(s, t, u)$ to describe the t-channel reactions of Equation (1.7.2).

Interchange of β and δ , and correspondingly of s and u , leads to the relations

$$\left. \begin{aligned} B(s, t, u) &= B(u, t, s) \\ C(s, t, u) &= A(u, t, s) \end{aligned} \right\} . \quad (1.7.7)$$

Finally, in the u-channel, interchange of β and γ , and therefore of s and t , yields

$$\left. \begin{aligned} C(s, t, u) &= C(t, s, u) \\ B(s, t, u) &= A(t, s, u) \end{aligned} \right\} . \quad (1.7.8)$$

If the requirements of crossing symmetry are combined together

in the single equation

$$\left. \begin{aligned} A(s,t,u) &= A(s,u,t) \\ B(s,t,u) &= A(t,s,u) \\ C(s,t,u) &= A(u,t,s) \end{aligned} \right\} , \quad (1.7.9)$$

it is seen that the $\pi\pi$ amplitude depends only on a single function $A(s,t,u)$, which is symmetric under interchange of t and u . To simplify the notation, define

$$\left. \begin{aligned} A &\equiv A(s,t,u) \\ B &\equiv A(t,s,u) \\ C &\equiv A(u,t,s) \end{aligned} \right\} , \quad (1.7.10)$$

and recall the s -channel isospin amplitudes, which were defined in Equation (1.6.12) by the matrix equation

$$\begin{pmatrix} A^0(s,t,u) \\ A^1(s,t,u) \\ A^2(s,t,u) \end{pmatrix} = \begin{pmatrix} 3 & 1 & 1 \\ 0 & 1 & -1 \\ 0 & 1 & 1 \end{pmatrix} \begin{pmatrix} A \\ B \\ C \end{pmatrix} . \quad (1.7.11)$$

If s and t are interchanged in the preceding expression, Equation (1.7.9) implies that

$$s \leftrightarrow t , \quad A \leftrightarrow B , \quad C \leftrightarrow C$$

and, therefore,

$$\begin{pmatrix} A^0(t,s,u) \\ A^1(t,s,u) \\ A^2(t,s,u) \end{pmatrix} = \begin{pmatrix} 1 & 3 & 1 \\ 1 & 0 & -1 \\ 1 & 0 & 1 \end{pmatrix} \begin{pmatrix} A \\ B \\ C \end{pmatrix} . \quad (1.7.12)$$

From Equation (1.7.11) and Equation (1.7.12) it is clear that there exists a linear relationship between $A^I(s,t,u)$ and $A^I(t,s,u)$,

$$A^I(s,t,u) = \alpha_{st}^{II'} A^{I'}(t,s,u) \quad (1.7.13)$$

where $\alpha_{st}^{II'}$ is called the $s \leftrightarrow t$ isospin crossing matrix and is readily obtained, by using Equation (1.6.13), as

$$\alpha_{st}^{II'} = \begin{pmatrix} \frac{1}{3} & 1 & \frac{5}{3} \\ \frac{1}{3} & \frac{1}{2} & -\frac{5}{6} \\ \frac{1}{3} & -\frac{1}{2} & \frac{1}{6} \end{pmatrix} . \quad (1.7.14)$$

Similarly, under interchange of s and u , it can be shown that

$$A^I(s,t,u) = \alpha_{su}^{II'} A^{I'}(u,t,s) \quad (1.7.15)$$

with the $s \leftrightarrow u$ crossing matrix given by

$$\alpha_{su}^{II'} = \begin{pmatrix} \frac{1}{3} & -1 & \frac{5}{3} \\ -\frac{1}{3} & \frac{1}{2} & \frac{5}{6} \\ \frac{1}{3} & \frac{1}{2} & \frac{1}{6} \end{pmatrix} . \quad (1.7.16)$$

8. ANALYTIC PROPERTIES OF THE $\pi\pi$ SCATTERING AMPLITUDE

It was pointed out in the previous section that in order to make the principle of crossing symmetry precise, it is necessary to regard $A(s,t,u)$ as a function of the complex variables s , t and u . $A(s,t,u)$ corresponds to a physical amplitude only when s , t and u take appropriate real values.

To determine the analytic properties of the $\pi\pi$ scattering amplitude it is convenient to consider the special case of forward scattering* for the s-channel process defined in Equation (1.7.1). The forward amplitude for this process, $A(s,0)$, is then an analytic function of the complex variable s throughout the complex s-plane, except for branch cuts along the real axis, as shown in Figure 1.4.

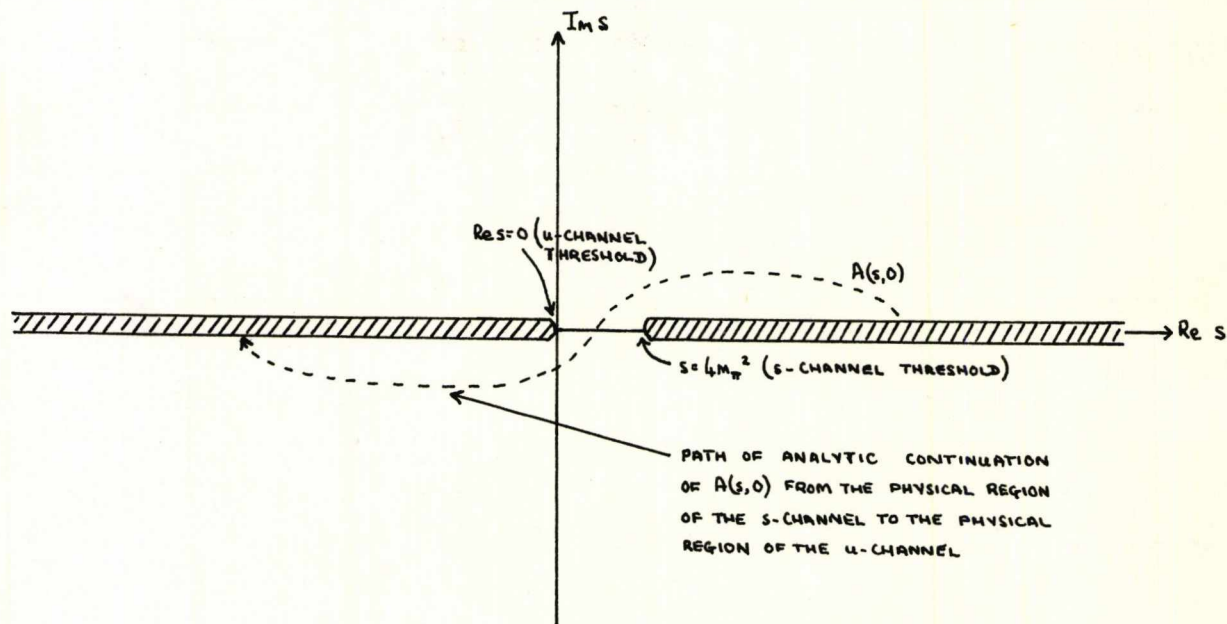


Figure 1.4

The Complex s-plane for $t=0$

$A(s,0)$ has a branch point at $s=4m_\pi^2$, which is the threshold for which the s-channel process becomes a physical process as

*For forward scattering in the s-channel, $t=0$.

allowed by the kinematic conditions (c.f. Figure 1.3 along the line $t=0$). There are other branch points in the s -plane, at $s=(4m_\pi)^2$, $s=(6m_\pi)^2$, ... , which are the thresholds for the production of additional pions. These branch points all lie along the positive real axis. In addition there are also branch points at the corresponding values of u for the u -channel process, for which the leading branch point is at $u=4m_\pi^2$. In this case (with $t=0$), the threshold $u=4m_\pi^2$ corresponds to the point $s=0$, and the resulting branch cut is drawn along the negative real s -axis.

Between the branch points at $s=0$ and $s=4m_\pi^2$, $A(s,0)$ is real and therefore hermitian, so that

$$A(s^*,0) = A^*(s,0) , \quad (1.8.1)$$

where the asterisk in Equation (1.8.1) denotes complex conjugation. The physical amplitude for the s -channel process, is obtained, as indicated in Figure 1.4, by taking the limit from above the right-hand branch cut. Thus, when s is real and greater than $4m_\pi^2$,

$$\text{Physical } A(s,0) = \lim_{\epsilon \rightarrow +0} A(s+i\epsilon,0) . \quad (1.8.2)$$

The physical amplitude for the u -channel process is obtained in the s -plane by taking the limit onto the real axis from below the left-hand branch cut. Analytic continuation by the path indicated in Figure 1.4 establishes the analytic statement of crossing symmetry, which relates the s -channel and u -channel processes, for the forward amplitude.

REFERENCES

1. H. YUKAWA, Proc. Phys. Math. Soc. Japan 17, 48 (1935).
2. J. J. THOMSON, Phil. Mag. 44, 293, 311 (1897).
3. A. EINSTEIN, Ann. der Phys. 17, 132 (1905).
4. J. CHADWICK, Proc. Roy. Soc. A136, 692 (1932).
5. C. M. G. LATTES, G. P. S. OCCHIALINI and C. F. POWELL, Nature 160, 453, 486 (1947).
6. U. CAMERINI, H. MUIRHEAD, C. F. POWELL and D. M. RITSON, Nature 162, 433 (1948).
J. R. RICHARDSON, Phys. Rev. 74, 1720 (1948).
7. A. G. CARLSON, J. E. HOOPER and D. T. KING, Phil. Mag. 41, 701 (1950).
8. A. H. ROSENFELD ET AL., Data on Particles and Resonant States UCRL-8030 (1967).
9. W. HEISENBERG, Z. für Phys. 120, 513, 673 (1943).
10. S. GASIOROWICZ, Fortschr. der Phys. 8, 665 (1960).
11. S. MANDELSTAM, Phys. Rev. 112, 1344 (1958); Phys. Rev. 115, 1741, 1752 (1959).
12. B. CASSEN and E. H. CONDON, Phys. Rev. 50, 846 (1936).

CHAPTER 2

I. INTRODUCTION

The instability of the pion prevents one forming pion targets, and although it may one day be possible, by using colliding beam accelerators, to perform the pion-pion elastic scattering experiment described in Chapter 1, for the present one has to rely upon indirect information obtained from processes in which pions appear. Reactions yielding information on the $\pi\pi$ system come mainly from two sources; firstly from experiments which produce a single pion in pion-nucleon collisions, and secondly from experiments, such as K-decays, in which pions appear as the only strongly interacting particle. Because of the indirect nature of the experiments, the process of extracting information about the $\pi\pi$ system relies upon some kind of analytic extrapolation being performed on the experimental data.

In Chapter 1 it was stressed that the structure of $\pi\pi$ elastic scattering is particularly simple. This simplicity is a consequence of having Bose Statistics, no spin, and a reaction which is exactly crossing symmetric. It appears also that because of the very short range of the forces involved, and the almost negligible contribution from other production processes below 1 GeV, $\pi\pi$ scattering is, in this region, accurately described by contributions from the lowest order (s and p) partial waves only.

In this chapter both the experimental results and some of the more successful theoretical treatments of $\pi\pi$ elastic scattering are reviewed. In Section 2, the functional forms for the s- and p-wave phase shifts which follow from a theoretical analysis of physical $\pi N \rightarrow \pi\pi N$ scattering are derived; the experimental results obtained from both pion-production processes and K-decay processes are discussed in Section 3. The results outlined in this section suggest that, with the exception of the I=0 s-wave phase shift, a fairly comprehensive picture of the $\pi\pi$ interaction between 500 MeV and 1 GeV has been established experimentally, but that below 500 MeV the amplitude has not been accurately determined, and above 1 GeV information is limited to the identification of some $\pi\pi$ resonances. Some of the techniques used to interpret sets of experimental data points in terms of well-defined physical constants (scattering lengths, effective ranges, resonance parameters and asymptotic behaviour) are described in Section 4.

The uncertainties that exist in the $\pi\pi$ system make it an ideal testing ground for theories and theoretical models*. The most successful calculation of the very low energy $\pi\pi$ interaction, say from threshold up to 400 MeV, has been the current algebra model of $\pi\pi$ scattering, originally proposed by Weinberg.⁽¹⁾

*A comprehensive review of $\pi\pi$ theories and models has been given elsewhere in the literature⁽⁵⁾. The topics discussed in Sections 5-8 are selective, but the predictions made are intended to reflect, as far as is possible, current feeling as to the true state of the $\pi\pi$ system below 1 GeV.

The model and the results obtained are discussed in Section 5. In recent years phenomenological analyses have become very popular. These analyses usually rely upon some kind of physical assumption being used as input to the model; for example, in the analysis made by Morgan and Shaw⁽²⁾, which is described in Section 6, estimates for the $\pi\pi$ scattering lengths are obtained which follow from assumptions made about the partial wave phase shifts in the range 500 MeV to 1 GeV. Other model dependent analyses have been used to determine the partial wave phase shifts between 500 MeV and 1 GeV; both the σ -model of Basdevant and Lee⁽³⁾, which is discussed in Section 7, and the Veneziano model⁽⁴⁾, discussed in Section 8, favour a fairly broad resonance in the $I=0$ s-wave amplitude at ~ 765 MeV.

2. THEORETICAL DETERMINATION OF REAL $\pi\pi$ SCATTERING FROM THE REACTIONS $\pi N \rightarrow \pi\pi N$

Most of the information on the $\pi\pi$ interaction comes from a study of the final states $\pi^+\pi^-$ and $\pi^\pm\pi^0$ in the reactions $\pi N \rightarrow \pi\pi N$, which are thought to be dominated by the one pion exchange (OPE) process corresponding to diagram (a) of Figure 2.1, on the next page. In this figure, π' represents the exchanged pion which is virtual, and if the OPE process does dominate the reaction, then the upper vertex of (a) describes the scattering of a real and a virtual pion to two real pions.

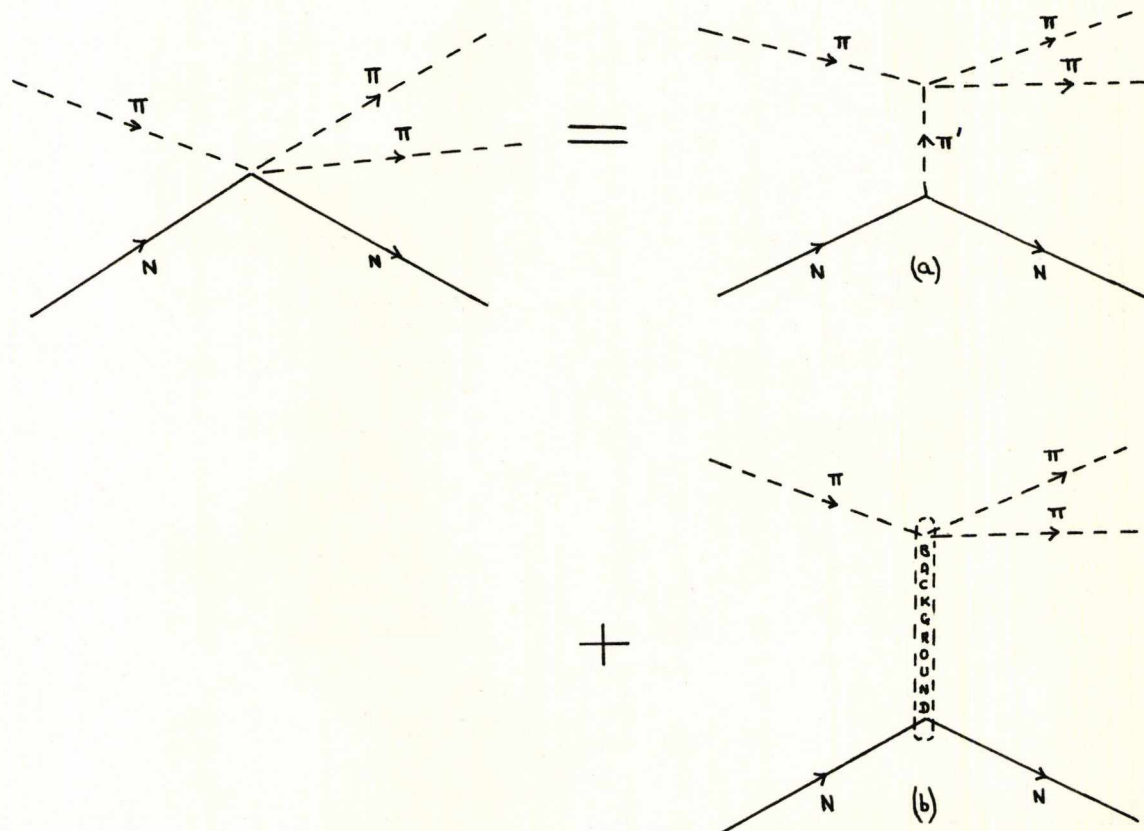


Figure 2.1

OPE process in the reaction $\pi N \rightarrow \pi\pi N$

Contributions other than OPE, which are represented by the 'background' term in diagram (b) of Figure 2.1 are important and great care is needed in order to isolate the OPE contribution. Another difficulty arises because of the virtual nature of the exchanged pion; if the $\pi\pi$ phase shifts could be obtained they would be functions of the square of the mass of the virtual

pion, Δ^2 , and in the physical region $\Delta^2 < 0$. Therefore, to determine the phase shifts for real $\pi\pi$ scattering it would be necessary to extrapolate the values to $\Delta^2 = m_\pi^2 \equiv 1$.*

In spite of the technical difficulties to be overcome, the need for reliable experimental results is emphasised if one looks at a qualitative picture of the $\pi\pi$ interaction based on the theoretical OPE model and our knowledge of real $\pi\pi$ scattering.

From Equation (1.5.5) and Equation (1.5.10) the $\pi\pi$ isospin amplitudes can be written as

$$A^I(q^2, \theta) = \frac{(1+q^2)^{\frac{1}{2}}}{q} \sum_{\ell=0}^{\infty} (1+(-1)^{I+\ell}) (2\ell+1) P_\ell(\cos \theta) e^{i\delta_\ell^I} \sin \delta_\ell^I, \quad (2.2.1)$$

where δ_ℓ^I is the phase shift corresponding to partial wave ℓ and total isospin I , and the term $(1+(-1)^{I+\ell})$ the symmetry factor which combines odd partial waves with odd isospin states and even partial waves with even isospin states. For the reactions

$$(a) \quad \pi^+ + \pi^- \rightarrow \pi^+ + \pi^-$$

and

$$(b) \quad \pi^- + \pi^0 \rightarrow \pi^- + \pi^0, \quad ,$$

the relevant charge states of the two-pion system were defined in Equation (1.6.5) by

$$\left. \begin{aligned} |\pi^+\pi^- \rangle &= \sqrt{\frac{1}{6}} |2,0\rangle + \sqrt{\frac{1}{2}} |1,0\rangle + \sqrt{\frac{1}{3}} |0,0\rangle \\ |\pi^-\pi^0 \rangle &= \sqrt{\frac{1}{2}} (|2,1\rangle + |1,-1\rangle) \end{aligned} \right\}, \quad (2.2.2)$$

*The more usual convention of normalising the pion mass to unity will be adopted from now on.

and from Equation (2.2.1) and Equation (2.2.2) the scattering amplitudes for these two reactions can be written as

$$\left. \begin{aligned}
 A_a(q^2, \theta) &= \frac{(1+q^2)^{\frac{1}{2}}}{q} \sum_{\ell=0}^{\infty} (2\ell+1) \left\{ [1+(-1)^\ell] \left(\frac{1}{6} e^{i\delta_\ell^2} \sin \delta_\ell^2 + \frac{1}{3} e^{i\delta_\ell^0} \sin \delta_\ell^0 \right) \right. \\
 &\quad \left. + [1-(-1)^\ell] \frac{1}{2} e^{i\delta_\ell^1} \sin \delta_\ell^1 \right\} P_\ell(\cos \theta) \\
 A_b(q^2, \theta) &= \frac{(1+q^2)^{\frac{1}{2}}}{q} \sum_{\ell=0}^{\infty} (2\ell+1) \left\{ [1+(-1)^\ell] \frac{1}{2} e^{i\delta_\ell^2} \sin \delta_\ell^2 \right. \\
 &\quad \left. + [1-(-1)^\ell] \frac{1}{2} e^{i\delta_\ell^1} \sin \delta_\ell^1 \right\} P_\ell(\cos \theta)
 \end{aligned} \right\} .$$

(2.2.3)

The differential cross-sections are obtained by taking the absolute squares of the scattering amplitudes, and if $\pi\pi$ scattering below 1 GeV is assumed to be dominated by contributions from the s- and p-waves only, the contributions from partial waves $\ell \geq 2$ can be neglected. The differential cross-sections can then be written as

$$\begin{aligned}
 \left(\frac{d\sigma}{d\Omega} \right)_a &= \frac{(1+q^2)}{q^2} \left\{ \left(\frac{4}{9} \sin^2 \delta_0^0 + \frac{1}{9} \sin^2 \delta_0^2 + \frac{4}{9} \cos(\delta_0^0 - \delta_0^2) \sin \delta_0^0 \sin \delta_0^2 \right) \right. \\
 &\quad \left. + (4 \cos(\delta_0^0 - \delta_1^1) \sin \delta_0^0 \sin \delta_1^1 + 2 \cos(\delta_0^2 - \delta_1^1) \sin \delta_0^2 \sin \delta_1^1) \cos \theta \right. \\
 &\quad \left. + 9 \sin^2 \delta_1^1 \cos^2 \theta \right\} ,
 \end{aligned} \tag{2.2.4}$$

and

$$\begin{aligned}
 \left(\frac{d\sigma}{d\Omega} \right)_b &= \frac{(1+q^2)}{q^2} \left\{ \sin^2 \delta_0^2 + 6 [\cos(\delta_0^2 - \delta_1^1) \sin \delta_0^2 \sin \delta_1^1] \cos \theta \right. \\
 &\quad \left. + 9 \sin^2 \delta_1^1 \cos^2 \theta \right\} ,
 \end{aligned} \tag{2.2.5}$$

where δ_0^0, δ_0^2 are the s-wave phase shifts corresponding to isospin

0,2 respectively, and δ_1^1 the p-wave phase shift. The right-hand sides of both Equation (2.2.4) and Equation (2.2.5) are of the form $A + B \cos \theta + C \cos^2 \theta$, and in principle the phase shifts δ_0^0, δ_0^2 and δ_1^1 can be determined by measuring the angular distributions of the two reactions (a) and (b). The coefficients associated with the $\cos^2 \theta$ terms theoretically determine the p-wave behaviour, those associated with the $\cos \theta$ terms measure the s-p interference, and the constant terms measure the s-waves only.

In practice, contributions from processes other than the OPE process introduce a degree of uncertainty into Equation (2.2.4) and Equation (2.2.5) which mainly affect the isotropic term, and when determining the $\pi\pi$ phase shifts this term is usually ignored. The s-wave phase shifts are therefore determined from the s-p interference term, once the p-wave is known, using reaction (b) to determine δ_0^2 and reaction (a) to determine δ_0^0 . Experimentally, δ_0^2 is found to be small and negative from threshold up to at least 1 GeV*, and in order to discuss the qualitative behaviour of δ_0^0 it is convenient as a first approximation to put δ_0^2 equal to zero in this region. δ_0^0 can then be obtained from the term

$$4 \cos(\delta_0^0 - \delta_1^1) \sin \delta_0^0 \sin \delta_1^1 . \quad (2.2.6)$$

*Experimental data points for δ_0^2 below 1 GeV are given in Figure 2.4 on page 41.

Equation (2.2.6) gives rise to two ambiguities since it remains unchanged under both the transformations

$$\delta_0^0 \rightarrow \delta_0^{0'} = \delta_0^0 + \pi \quad (2.2.7)$$

and

$$\delta_0^0 \rightarrow \delta_0^{0'} = \frac{\pi}{2} - (\delta_0^0 - \delta_1^1) . \quad (2.2.8)$$

Equation (2.2.7) represents a trivial change of phase by π , but this ambiguity has been resolved in studies of the reaction $\pi^+\pi^-\rightarrow\pi^0\pi^0$ which indicate that $\delta_0^0 > 0$ in the region below 1 GeV⁽⁶⁾. The ambiguity represented by Equation (2.2.8) has proved more difficult to resolve, since if at some energy

$$\delta_0^0 = \frac{\pi}{4} + \frac{\delta_1^1}{2} , \quad (2.2.9)$$

then

$$\delta_0^{0'} = \delta_0^0 . \quad (2.2.10)$$

This is approximately what is thought to happen at about 765 MeV, where the p-wave is characterised by the ρ -resonance

$$\left. \delta_1^1 \right|_{765 \text{ MeV}} \approx \frac{\pi}{2} . \quad (2.2.11)$$

For Equations (2.2.9) and (2.2.10) to meet the requirements of (2.2.11), δ_0^0 must satisfy the condition

$$\left. \delta_0^{0'} \right|_{765 \text{ MeV}} \approx \left. \delta_0^0 \right|_{765 \text{ MeV}} \approx \left. \delta_1^1 \right|_{765 \text{ MeV}} \approx \frac{\pi}{2} . \quad (2.2.12)$$

Ample evidence is to be found in the literature in support of a δ_0^0 which rises to approximately 90° in the vicinity of the ρ -resonance⁽⁷⁾. Then, according to Equation (2.2.8), four

possible solutions for δ_0^0 exist, as shown in Figure 2.2.

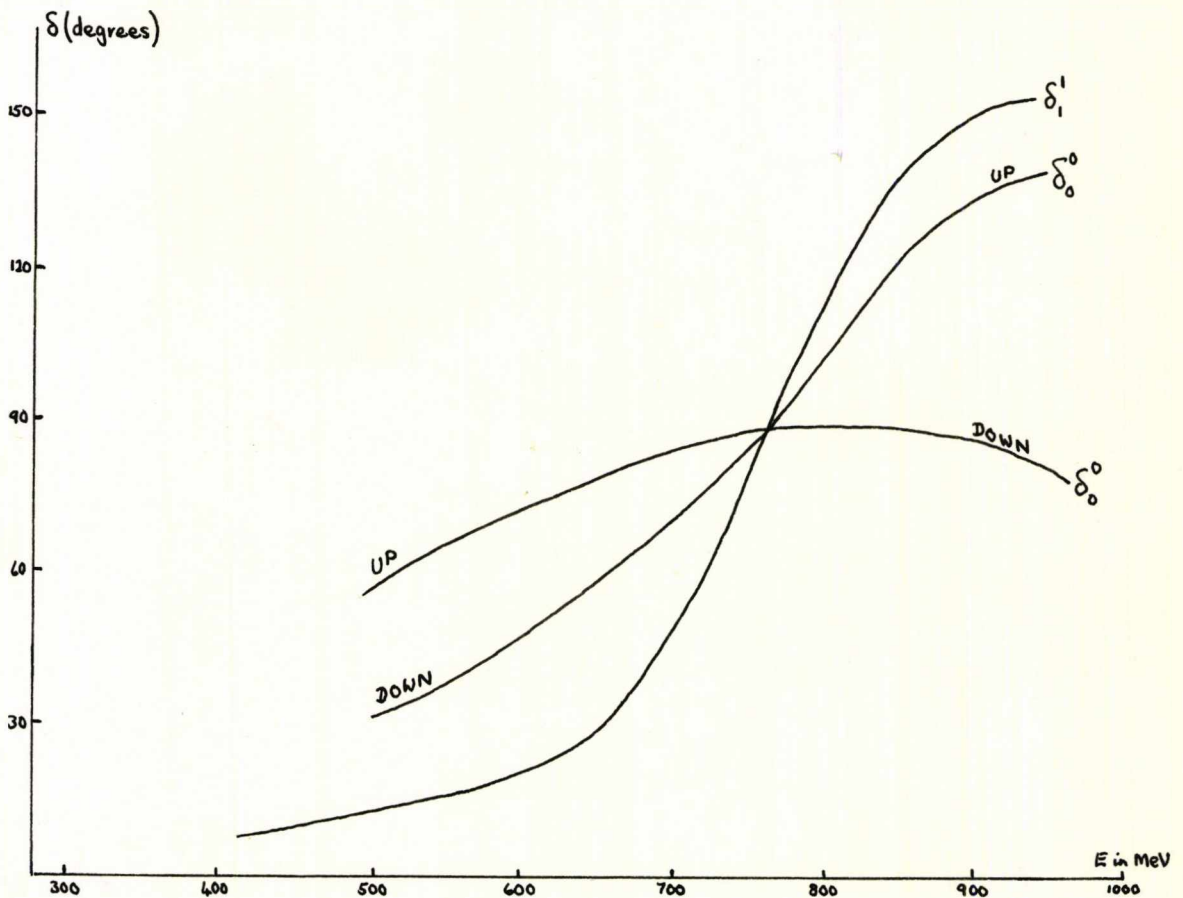


Figure 2.2

Possible solutions for δ_0^0 compared with δ_1^{1*}

These solutions, which are characterised by 'Up' and 'Down' branches above and below the ρ -resonance, are commonly labelled 'Up-Up', 'Up-Down', 'Down-Up' and 'Down-Down'.

*The qualitative nature of the phases in Figure 2.2 are intended to reflect the situation resulting from Equations (2.2.8) to (2.2.12).

3. EXPERIMENTAL RESULTS

(a) Determination of δ_1^1

It has been known for a long time that the low energy $\pi\pi$ p-wave is dominated by the ρ -meson resonance⁽⁸⁾. Although agreement on the position of the resonance peak has been reached, the most widely published estimate being

$$M_\rho = (765 \pm 10)\text{MeV} , \quad (2.3.1)^{(9)}$$

the width of the resonance, Γ_ρ , has not been so accurately determined. The experimental data points indicate a width of between 150 MeV and 170 MeV, but estimates of the extrapolated data suggest values as low as 110 MeV. Results are quoted from two independent analyses, one by Malamud and Schlein⁽¹⁰⁾, the other by Baton, Laurens and Reignier⁽¹¹⁾, which illustrate the uncertainty in our knowledge of Γ_ρ . Both of the analyses assume OPE dominance for small values of Δ^2 , and the raw experimental data points obtained for δ_1^1 are shown in Figure 2.3, on the next page.

The analysis by Malamud and Schlein was on data obtained from 20,555 events of the reaction $\pi^-p \rightarrow \pi^+\pi^-n$, collected from five experiments performed at incident beam momenta within the range $2.1 < p_{\text{Lab}} < 3.2$ GeV. From a sub-sample of 7319 small momentum transfer events, the value

$$\Gamma_\rho = (148.1 \pm 4.7)\text{MeV} \quad (2.3.2)^*$$

was obtained for the width of the ρ -resonance peak.

*In Reference 10 a revised estimate for Γ_ρ , obtained from the extrapolated data, is given as $\Gamma_\rho = (132 \pm 13)\text{MeV}$.

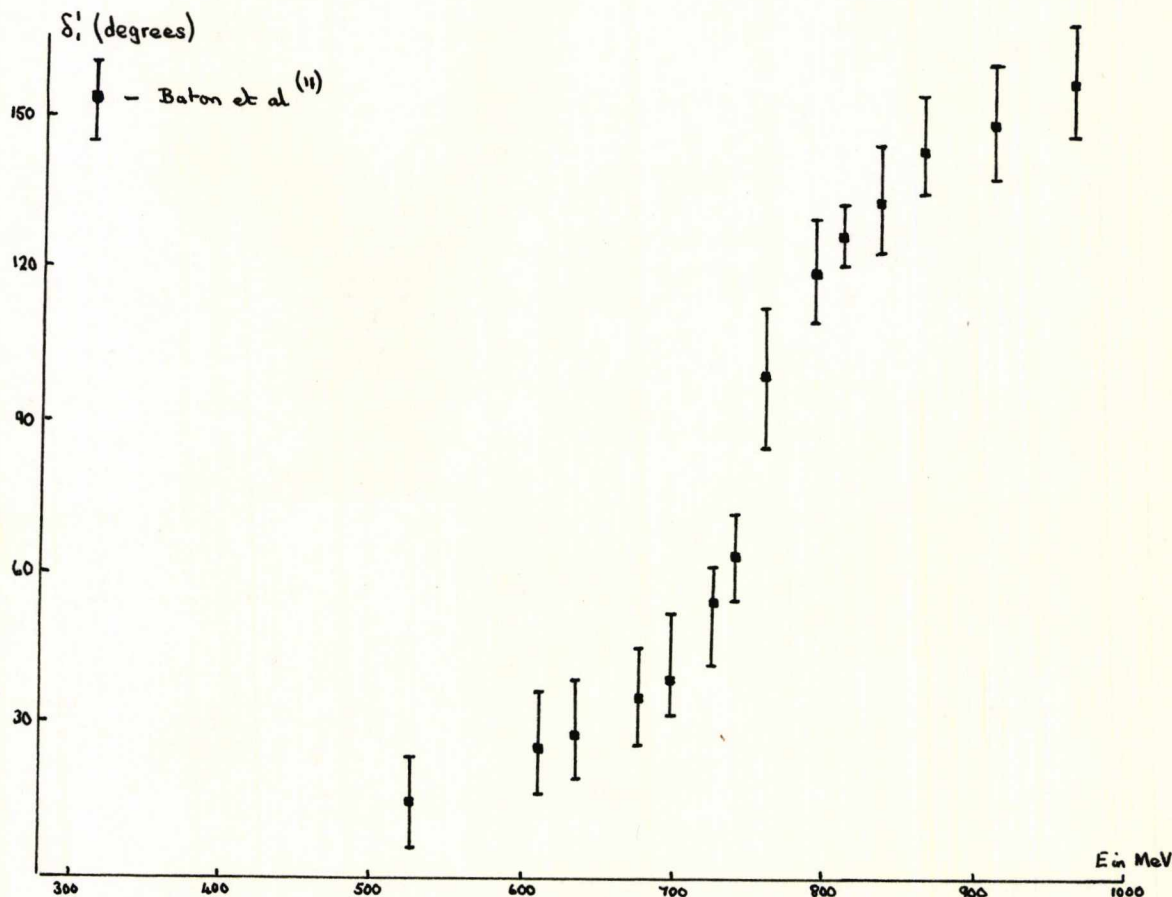


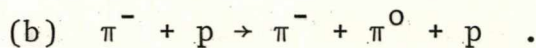
Figure 2.3

Experimental data on δ_1^1 below 1 GeV

The analysis by Baton, Laurens and Reignier was on data compiled from the reactions



and



Both the reactions were studied at an incident beam momentum of $p_{\text{Lab}} = 2.77$ GeV. Reaction (b) was studied first because the events with small momentum transfer were easier to identify and

measure; 7,666 events with $|\Delta^2| < 13$ were measured, and although the OPE contribution could not be isolated, it was assumed to dominate for small values of $|\Delta^2|$. The ρ -resonance parameters were determined as

$$(M_\rho, \Gamma_\rho) = (755 \pm 5, 110 \pm 9) \text{ MeV} . \quad (2.3.3)$$

Reaction (a) was then studied in the same way using 10,634 events with $|\Delta^2| < 13$ and the ρ -parameters of Equation (2.3.3) were again reproduced.

(b) Determination of δ_0^2

The wealth of experimental evidence on the $I=2$ s-wave phase shift is strongly in favour of a δ_0^2 which is small and negative from threshold up to 1 GeV. Small discrepancies do exist in the experimental data; for example, in the analysis by Malamud and Schlein, they found

$$\left. \begin{aligned} \delta_0^2 &\approx -17^\circ & \text{at } v &= m_K^{2*} \\ \delta_0^2 &\approx -30^\circ & \text{at } v &= m_\rho^2 \end{aligned} \right\} \quad (2.3.4)$$

whereas Baton et al. obtained

$$\left. \begin{aligned} \delta_0^2 &\approx -6^\circ & \text{at } v &= m_K^2 \\ \delta_0^2 &\approx -18^\circ & \text{at } v &= m_\rho^2 \end{aligned} \right\} . \quad (2.3.5)$$

* m_K , the mass of the K-meson, ≈ 494 MeV.

The experimental data points shown in Figure 2.4 point to a numerical majority in favour of the smaller phase shifts obtained by Baton et al..

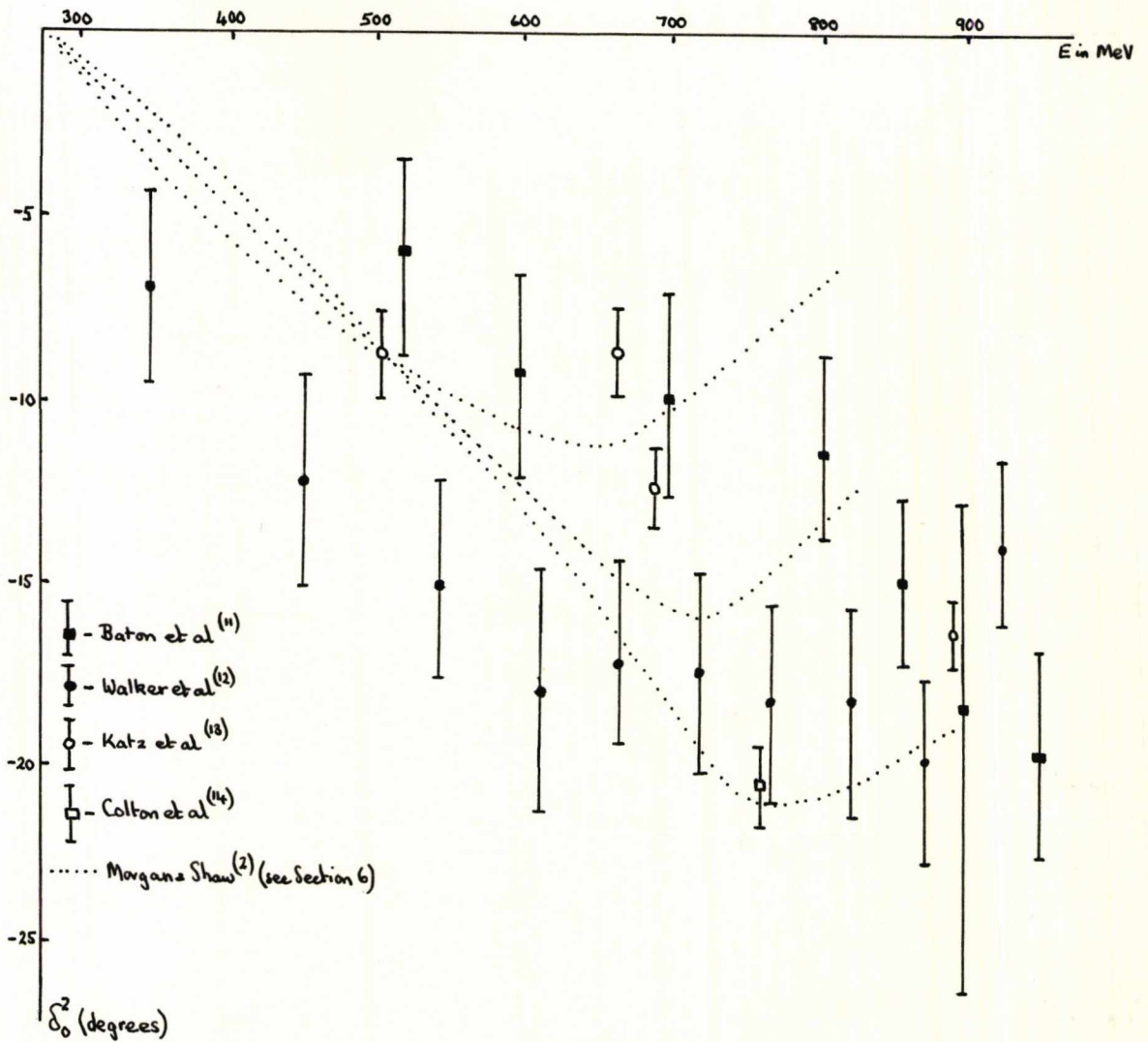


Figure 2.4

Experimental data on δ_0^2 below 1 GeV

(c) Determination of δ_0^0

In Section 2 of this chapter, it was shown that studies of the s-p interference term in pion-production experiments lead via a two-way ambiguity to the possibilities Up-Up, Up-Down, Down-Up and Down-Down for the functional form of δ_0^0 below 1 GeV. The ambiguity has been illustrated by Scharenguivel et al.⁽¹⁵⁾ who obtained alternative forms for δ_0^0 from $\pi^+\pi^-$ production data by a method of extrapolation of the forward-backward asymmetry to the pion pole. The ratio $\frac{\text{FORWARD} - \text{BACKWARD}}{\text{FORWARD} + \text{BACKWARD}}$ produced phase shifts which established the existence of distinct up and down branches both above and below the region of the ρ -resonance. Numerous experimental determinations have so far failed to resolve this ambiguity; for example, in their compilation of data on the reaction $\pi^-p \rightarrow \pi^+\pi^-n$, Malamud and Schlein⁽¹⁰⁾ favoured the Up-Up solution, whereas the Up-Down solution was preferred by Walker et al.⁽¹²⁾. Baton et al.⁽¹¹⁾ favoured the Down-branch below the ρ -resonance, and a δ_0^0 consistent with the Down-Up solution was obtained by Marateck et al.⁽¹⁶⁾. The experimental situation for δ_0^0 is summarised in Figure 2.5, on the next page. The values obtained for δ_0^0 in the above experimental analyses rest upon attempts to isolate the s-wave contribution in the $\cos \theta$ term of Equations (2.2.4) and (2.2.5), and since the s-wave contribution is obscured by the large contribution in the p-wave resulting from the ρ -meson, it is not surprising that different attempts have led to contradictory results. In theory,

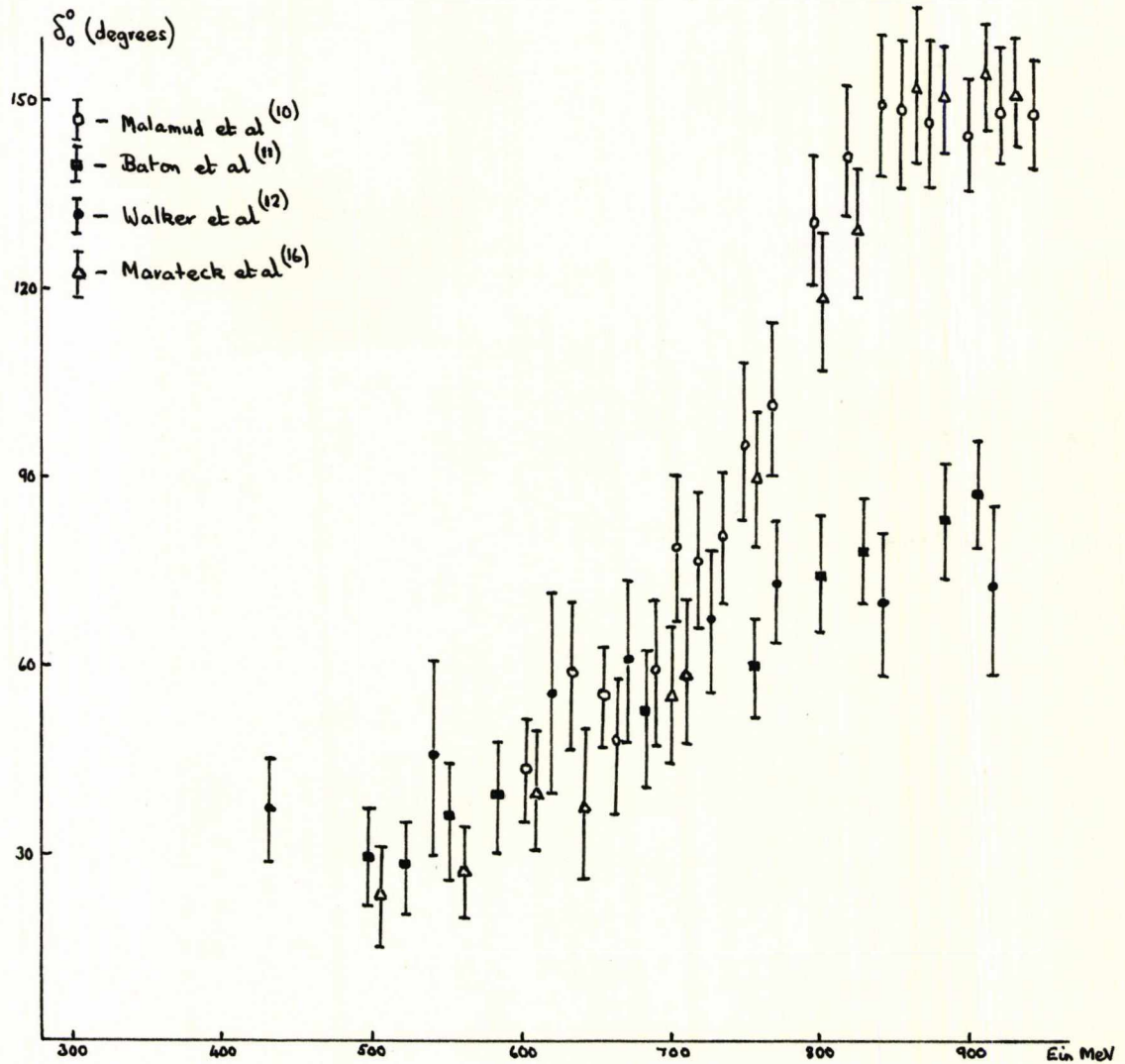


Figure 2.5

Experimental data on δ_0^0 below 1 GeV

the best way to study the s-wave $\pi\pi$ interaction is through the reaction $\pi^- p \rightarrow \pi^0 \pi^0 n$, since the s-wave is not masked by the dominating ρ -contribution. An analysis of this reaction by Deinet et al. (17) indicates that δ_0^0 stays near 90° from about 400 MeV to 800 MeV. Only the Up-Down solution for δ_0^0 is

consistent with this data.

There are sources other than pion-production experiments from which information about the $\pi\pi$ phase shifts can be extracted; for example, K-decays, although the poor statistics of the experiments performed so far (only a few hundred events) render the results rather unreliable.

The branching ratio

$$\frac{K_S^0 \rightarrow \pi^+ \pi^-}{K_S^0 \rightarrow \pi^0 \pi^0}$$

obtained from $K_S^0 \rightarrow 2\pi$ decays yields information about the phase difference $\delta_0^0 - \delta_0^2$ at the K-meson mass. The results obtained by Morfin and Sinclair⁽¹⁸⁾

$$(\delta_0^0 - \delta_0^2) \Big|_{m_K} = (68 \pm 11)^\circ \quad (2.3.6)$$

favour the Up-branch below the ρ -resonance, for which

$$(\delta_0^0 - \delta_0^2) \Big|_{m_K} = (55 \pm 10)^\circ \quad (2.3.7)$$

rather than the Down-branch, for which

$$(\delta_0^0 - \delta_0^2) \Big|_{m_K} = (32 \pm 10)^\circ \quad (2.3.8)$$

K_{e4} decay experiments, $K \rightarrow 2\pi e\nu$, provide information on $\pi\pi$ scattering from threshold up to 400 MeV. The theory has been discussed in detail by Pais and Treiman⁽¹⁹⁾. The results indicate the average for the phase difference $\delta_0^0 - \delta_1^1$ over this

region to be given by

$$\langle \delta_0^0 - \delta_1^1 \rangle = \pm(25 \pm 8)^{\circ} \quad . \quad (2.3.9)$$

This result was obtained from a poor statistics experiment of only 300 events, and its validity is therefore questionable, although Equation (2.3.9) does agree with estimates obtained from pion-production data. In the future, K-decay experiments may well provide essential pieces of information on $\pi\pi$ scattering, but higher statistics data have to be obtained before drawing any serious conclusions.

(d) Determination of the $\pi\pi$ s-wave scattering lengths

Information on the $\pi\pi$ s-wave scattering lengths has been acquired by studying the reaction $\pi N \rightarrow \pi\pi N$ near threshold. Batusov et al.⁽²⁰⁾ concentrated on the reaction $\pi^- p \rightarrow \pi^+ \pi^- n$ and obtained a $\pi^+ \pi^-$ cross-section at threshold which corresponds to

$$|2a_0 + a_2| = 1.0 \pm 0.3 \quad , \quad (2.3.10)$$

where $a_{0,2}$ are the $I=0,2$ s-wave scattering lengths. The same group also analysed the energy and angular distributions of the final three particles, from which they deduced

$$a_0 - a_2 = 0.25 \pm 0.05 \quad . \quad (2.3.11)$$

There have recently been two independent experimental determinations of the ratio a_0/a_2 . Firstly, Gutay, Meiere and Scharenguivel⁽²¹⁾ studied the relation between Δ^2 and s at the point where the forward-backward asymmetry vanishes in peripheral

$\pi^+\pi^-$ production. Assuming an exact linear form in s , t and u for the real part of the $\pi\pi$ amplitude, they obtained

$$\frac{a_0}{a_2} = -3.2 \pm 0.1 \quad (2.3.12)$$

which indicates that a_0 and a_2 are of opposite signs. The same ratio has been deduced by Cline, Braun and Scherer⁽²²⁾ from a study of the charge branching ratios $R_1 = \sigma(\pi^0\pi^0)/\sigma(\pi^+\pi^+)$ and $R_2 = \sigma(\pi^0\pi^0)/\sigma(\pi^+\pi^-)$ near threshold. R_1 and R_2 both depend essentially on the value a_0/a_2 , with corrections applied for p- and d-waves. A consistent fit to both branching ratios was obtained for

$$\frac{a_0}{a_2} = -3.2 \pm 1.1 \quad (2.3.13)$$

in agreement with the independent result of Gutay et al. referred to above.

(e) $\pi\pi$ scattering above 1 GeV

Above 1 GeV, the $I=0$ d-wave resonance f_0 , with its parameters

$$(M_{f_0}, \Gamma_{f_0}) = (1260 \pm 10, 150 \pm 25)\text{MeV} \quad (2.3.14)$$

and the $I=1$ f-wave resonance g , with its parameters

$$(M_g, \Gamma_g) = (1680 \pm 20, 110 \pm 10)\text{MeV} \quad (2.3.15)$$

are both well-established resonances. It has been suggested that

there is an $I=0$ s-wave resonance accompanying the $f_0^{(23)}$, and at higher energies, one would expect to see evidence of an $I=0$ d-wave resonance f' , at about 1550 MeV, but none has been seen yet; and at still higher energies the situation is equally uncertain.

To summarise the experimental situation of low energy pion-pion scattering at the present time, the general picture is of an $I=1$ p-wave dominated by the rho meson, a large positive $I=0$ s-wave and a small negative $I=2$ s-wave. Higher statistics experiments offer the best method of resolving many of the ambiguities still further; indeed, the most recent experimental analyses claim to have partly resolved the δ_0^0 -ambiguity by definitely selecting the Down-branch above the ρ -resonance⁽²⁴⁾.

4. REPRESENTATION OF EXPERIMENTAL DATA

The experimental data discussed in the previous section, for example, phase shifts and cross-sections, are determined as sets of experimental values with error bars, but are usually presented in the more readable form of smooth analytic functions containing a small number of parameters. These parameters often correspond to physical constants, such as scattering lengths, positions and widths of resonances etc., and in such cases it is essential that the representation should have a firm theoretical basis.

Using Equation (1.5.10)* the partial wave amplitudes in the physical region can be expanded in terms of the phase shifts $\delta_\ell(v)$ by

$$A_\ell(v) = \sqrt{\frac{v+1}{v}} (\cot \delta_\ell(v) - i)^{-1} \quad \text{for } v > 0. \quad (2.4.1)$$

A particularly simple parametrisation for $\sqrt{v/v+1} \cot \delta_\ell(v)$ close to the physical threshold is given by the effective-range formula⁽²⁵⁾,

$$\sqrt{\frac{v}{v+1}} \cot \delta_\ell(v) = \frac{1}{v^\ell} \left\{ \frac{1}{a_\ell} + \frac{r_\ell}{2} v + \dots \right\} \quad (2.4.2)$$

where a_ℓ is the ℓ -wave scattering length, and r_ℓ the effective-range. $A_\ell(v)$, as defined by Equations (2.4.1) and (2.4.2), satisfies both the elastic unitarity condition

$$\text{Im}[A_\ell(v)]^{-1} = -\sqrt{\frac{v}{v+1}} \quad \text{for } v \in [0, 3], \quad (2.4.3)$$

and the threshold condition

$$A_\ell(v) \approx a_\ell v^\ell \quad \text{as } v \rightarrow 0, \quad (2.4.4)$$

but because of the presence of a left-hand cut in the v -plane beginning at $v=-1$, Equation (2.4.2) is a valid parametrisation close to the physical threshold only.

Olsson⁽²⁶⁾ has extended the domain of application of the p -wave effective-range formula to above the region of the ρ -resonance as follows: a resonance is theoretically associated with a pole of the partial wave amplitude located close to the

*With the change of variable $v = q^2 = \frac{s}{4} - 1$.

physical region and on the second sheet of the v -plane. To the experimentalist, it is also related to the behaviour of the phase shift which passes through $\pi/2$ with a positive gradient. In the vicinity of a resonance, the behaviour of the phase shift, $\delta_\ell(v)$, is given by the Breit-Wigner⁽²⁷⁾ formula

$$\cot \delta_\ell(v) = - \frac{2(v-v_R)}{\omega_R \Gamma_R}, \quad (2.4.5)$$

where ω_R is the mass and Γ_R the width of the resonance, and the corresponding form for the partial wave amplitude close to the resonance is then given by

$$A_\ell(v) = \frac{\frac{1}{2}\Gamma_R}{\sqrt{v/v+1}(v_R-v-\frac{1}{2}i\Gamma_R)}. \quad (2.4.6)$$

Olsson's idea was to develop an expression for the p-wave amplitude, $A_1^1(v)$, which has the correct threshold behaviour and which blends smoothly into a Breit-Wigner form in the region of the ρ -resonance. To achieve this, he chose an effective-range formula

$$\frac{q^3}{\omega} \cot \delta_1^1(v) = \frac{1}{a_1} \left(1 - \frac{v}{v_\rho} \right) \quad (2.4.7)$$

with a_1 , the p-wave scattering length, defined in terms of the ρ -resonance parameters by

$$a_1 \equiv \frac{\omega_\rho^2 \Gamma_\rho}{2q_\rho^5}. \quad (2.4.8)^*$$

* For $\omega_\rho=774$ MeV, $\Gamma_\rho=150$ MeV, Equation (2.4.8) implies that $a_1=0.036 \text{ m}^{-3}$, in agreement with the value obtained by Morgan and Shaw⁽²⁾ (see Section 6 of this chapter).

Although the asymptotic behaviour of cross-sections appears to approach constant values, our detailed knowledge of the high energy region is rather uncertain, and as a result, whatever representation is used to describe the amplitude in this region its influence on the results below 1 GeV should be minimised. It is usually assumed that the asymptotic behaviour of the amplitudes are Regge-behaved⁽²⁸⁾, that is, for fixed values of t ,

$$\text{Im } A(s,t) \propto \sum_i s^{\alpha_i(t)} \quad \text{as } s \rightarrow \infty \quad (2.4.9)$$

where each α_i represents a linear trajectory

$$\alpha_i(t) = \alpha_i(0) + t\alpha_i' \quad (2.4.10)$$

To satisfy the asymptotic condition for forward scattering

$$\text{Im } A(s,0) \approx s \quad \text{as } s \rightarrow \infty \quad (2.4.11)$$

the leading trajectory must be characterised by $\alpha_p(0)=1$, the Pomeranchuk trajectory; other terms in the right-hand side of (2.4.9) are usually restricted to contributions from the ρ and f_0 resonances. For the ρ -resonance,

$$\alpha_\rho(0) \approx 0.5 \quad , \quad \alpha_\rho' \approx 0.018 m_\pi^{-2} \quad (2.4.12)$$

provide a good fit to the experimental data⁽²⁹⁾

5. CURRENT ALGEBRA PREDICTIONS

Current algebra, which was introduced by Gell-Mann⁽³⁰⁾, provided the essential break-through in the quantitative understanding of strong interaction physics, and in particular, enabled the first quantitative predictions of the low energy

$\pi\pi$ parameters to be made. The general aspects of the theory have been discussed in the literature⁽³¹⁾. The assumptions are based upon the fact that weak interaction processes can provide precise information on some features of strong interactions. In $\pi\pi$ scattering, the partially conserved axial current (PCAC) hypothesis is used to define the pion amplitudes off the mass-shell*, and the commutation relations of current algebra, which are non-linear, are used to obtain absolute quantitative predictions.

The PCAC hypothesis⁽³²⁾, which states that the divergence of the axial-vector current is proportional to the pion field, can be written as

$$\partial_{\mu} A_{\mu}^{\alpha}(x) = f_{\pi} m_{\pi}^2 \pi^{\alpha}(x) \quad (2.5.1)$$

where α is an isospin index, and f_{π} the pion decay constant ($f_{\pi} \approx 95$ MeV). Equation (2.5.1) is used to define pion amplitudes off the mass-shell, which in turn leads to Adler's self-consistency condition for $\pi\pi$ scattering⁽³³⁾: if, in the reaction $\pi^{\alpha}(p_1) + \pi^{\beta}(p_2) \rightarrow \pi^{\gamma}(p_3) + \pi^{\delta}(p_4)$, one of the four-momenta, say p_1 , goes off the mass-shell, then as $p_{1\mu} \rightarrow 0$, the $\pi\pi$ scattering amplitude also vanishes

$$\lim_{p_{1\mu} \rightarrow 0} A_{\alpha\beta,\gamma\delta}^{\pi\pi}(p_1, p_2; p_3, p_4) = 0. \quad (2.5.2)$$

If the other pions involved in the reaction remain on the mass-shell, the invariant quantities s , t and u satisfy the condition

$$s = t = u = m_{\pi}^2 \quad (2.5.3)$$

*i.e. when one or more of the pions involved in the scattering process fails to satisfy the relativistic equation $p_i^2 = m_{\pi}^2$.

and, therefore,

$$A_{\alpha\beta,\gamma\delta}^{\pi\pi}(s=t=u=m_\pi^2) = 0 \quad . \quad (2.5.4)$$

$A_{\alpha\beta,\gamma\delta}^{\pi\pi}$ of Equation (2.5.4) is a continuation of the physical $\pi\pi$ scattering amplitude discussed in Chapter 1, but the point $s=t=u=m_\pi^2$ is close enough to the physical region for the Adler condition to imply the presence of zeros in the physical amplitude.

To investigate the consequences of the current algebra, it is necessary to consider $A_{\alpha\beta,\gamma\delta}^{\pi\pi}$ with two pions off the mass-shell. If $p_{1\mu}$ and $p_{3\mu}$ both vanish it can be proved that $A_{\alpha\beta,\gamma\delta}^{\pi\pi}$ exhibits the behaviour

$$A_{\alpha\beta,\gamma\delta}^{\pi\pi}(p_1,p_2;p_3,p_4) \underset{\substack{p_{1\mu} \rightarrow 0 \\ p_{3\mu} \rightarrow 0}}{\approx} M_{\alpha\beta,\gamma\delta}^0 + \frac{2p_1 \cdot p_2}{f_\pi^2} (\delta_{\alpha\beta} \delta_{\gamma\delta} - \delta_{\alpha\delta} \delta_{\beta\gamma})$$

(with $p_2^2 = p_4^2 = m_\pi^2$) (2.5.5)

where $M_{\alpha\beta,\gamma\delta}^0$ is a constant, symmetric under the interchange $\alpha \leftrightarrow \gamma, \beta \leftrightarrow \delta$.

Weinberg⁽¹⁾ was the first person to use the assumption of PCAC and current algebra to calculate the low energy $\pi\pi$ amplitude. Combining Equations (1.7.4) and (1.7.9) he wrote the total $\pi\pi$ amplitude as

$$A_{\alpha\beta,\gamma\delta}^{\pi\pi}(s,t,u) = A(s,t,u) \delta_{\alpha\beta} \delta_{\gamma\delta} + A(t,s,u) \delta_{\alpha\gamma} \delta_{\beta\delta} + A(u,t,s) \delta_{\alpha\delta} \delta_{\beta\gamma}$$

(2.5.6)

and expanded $A(s,t,u)$ to first order in the Mandelstam variables

$$A(s,t,u) = \frac{1}{f_\pi^2} (a + bs + c(t+u)) \quad . \quad (2.5.7)$$

Equation (2.5.7) exhibits the $t \leftrightarrow u$ symmetry of the $\pi\pi$ amplitude and the factor $\frac{1}{f_\pi^2}$ is included in the expansion for convenience. The constraints π imposed by PCAC and current algebra were used to determine the constants a , b and c as follows: if $A(s,t,u)$ vanishes at $s=t=u=m_\pi^2$,

$$a + (b+2c)m_\pi^2 = 0 \quad (2.5.8)$$

and in the limit $p_{1\mu} \rightarrow 0$, $p_{3\mu} \rightarrow 0$,

$$A_{\alpha\beta,\gamma\delta}^{\pi\pi}(p_1,p_2;p_3,p_4) = M_{\alpha\beta,\gamma\delta}^0 + \frac{2p_1 \cdot p_3}{f_\pi^2} (b-c) [\delta_{\alpha\beta} \delta_{\gamma\delta} - \delta_{\alpha\delta} \delta_{\beta\gamma}] , \quad (2.5.9)$$

with

$$M_{\alpha\beta,\gamma\delta}^0 = \frac{1}{f_\pi^2} \left\{ [a+(b+c)m_\pi^2] (\delta_{\alpha\beta} \delta_{\gamma\delta} + \delta_{\alpha\delta} \delta_{\beta\gamma}) + [a+2cm_\pi^2] \delta_{\alpha\gamma} \delta_{\beta\delta} \right\} . \quad (2.5.10)$$

Comparing Equation (2.5.9) with (2.5.5) imposes the constraint

$$b - c = 1 \quad (2.5.11)$$

on the coefficients of $A(s,t,u)$, which together with (2.5.8) determines $A(s,t,u)$ up to a constant value; taking the coefficient c as parameter,

$$A(s,t,u) = \frac{1}{f_\pi^2} \left[-m_\pi^2 + (1+c)s + c(t+u-3m_\pi^2) \right] . \quad (2.5.12)$$

If the off-shell amplitude $A(s,t,u)$ is assumed to be valid also on the mass-shell, $s+t+u=4m_\pi^2$, and Equation (2.5.12) simplifies to

$$A(s,t,u) = \frac{1}{f_\pi^2} \left[s - m_\pi^2(1-c) \right] . \quad (2.5.13)$$

Using Equations (1.7.10) and (1.7.11) the corresponding isospin amplitudes are given by

$$\left. \begin{aligned} A^0(s,t,u) &= \frac{1}{f_\pi^2} (2s - m_\pi^2 + 5cm_\pi^2) \\ A^1(s,t,u) &= \frac{1}{f_\pi^2} (t-u) = \frac{(s-4m_\pi^2)}{f_\pi^2} \cos \theta \\ A^2(s,t,u) &= \frac{1}{f_\pi^2} (2m_\pi^2 - s + 2cm_\pi^2) \end{aligned} \right\} \quad (2.5.14)$$

and the corresponding scattering lengths, which are defined in terms of the s-wave amplitudes by

$$a_O^I = A^I(s=4m_\pi^2, t=0, u=0) \quad (I=0,2) \quad (2.5.15)$$

become

$$\left. \begin{aligned} a_O^0 &= (7+5c) \frac{m_\pi^2}{f_\pi^2} \\ a_O^2 &= (-2+2c) \frac{m_\pi^2}{f_\pi^2} \end{aligned} \right\} \quad (2.5.16)$$

In order to obtain a value for the parameter c , Weinberg observed that $M_{\alpha\beta,\gamma\delta}^0$, as defined by Equation (2.5.10), has only even partial wave contributions in the t-channel. He then assumed that the $I=2$ part of $M_{\alpha\beta,\gamma\delta}^0$ vanishes, and obtained the supplementary condition

$$a + (b+c)m_\pi^2 = 0 \quad (2.5.17)$$

which, together with Equation (2.5.8), requires $c=0$. For

$f_{\pi} = \frac{2}{3}m_{\pi}$ and $c=0$, Equation (2.5.16) yields

$$\left. \begin{aligned} a_0^0 &= 0.16 m_{\pi}^{-1} \\ a_0^2 &= -0.045 m_{\pi}^{-1} \\ \frac{a_0^0}{a_0^2} &= -\frac{7}{2} \end{aligned} \right\} \quad (2.5.18)$$

One interesting consequence of the Weinberg amplitude, Equation (2.5.14), is that A^0 and A^2 vanish at the points

$$\left. \begin{aligned} s_0 &= m_{\pi}^2(1-5c) \\ s_2 &= 2m_{\pi}^2(1+c) \end{aligned} \right\} \quad (2.5.19)$$

respectively. In Weinberg's case with $c=0$

$$\left. \begin{aligned} s_0 &= m_{\pi}^2 \\ s_2 &= 2m_{\pi}^2 \end{aligned} \right\} \quad (2.5.20)$$

which implies the existence of zeros in an exact amplitude, although their exact position may be shifted by unitarity effects.

Many attempts have since been made to obtain additional information on low energy $\pi\pi$ scattering from the Weinberg amplitude⁽³⁴⁾, but above the physical threshold unitarity plays an essential role and one problem has been precisely how to take unitarity into account*. Brown and Goble⁽³⁵⁾, for example,

*The Weinberg amplitude, being a real function, does not satisfy the elastic unitarity condition of Equation (1.5.9).

started with Equation (2.5.14) with $c=0$, $A_{\ell}^{I,CA}$, and introduced a function

$$h(s) = \frac{1}{\pi} \sqrt{\frac{s-4}{s}} \log \left(\frac{\sqrt{s-4} + \sqrt{s}}{2} \right) . \quad (2.5.21)$$

They then defined partial wave amplitudes which are exactly unitary

$$A_{\ell}^I(s) = \frac{A_{\ell}^{I,CA}(s)}{P^I(s) + h(s) A_{\ell}^{I,CA}(s)} \quad (2.5.22)$$

where $P^I(s)$ is an arbitrary polynomial. To introduce a resonance pole into the partial wave amplitude and maintain $A_{\ell}^I(s) \approx A_{\ell}^{I,CA}(s)$ at low energies, Brown and Goble used the parametrisation

$$P^I(s) = 1 + \alpha_I A_{\ell}^{I,CA}(s) , \quad (2.5.23)$$

and by adjusting the constant α_I were able to obtain a suitable value for the ρ -meson width after fixing the ρ -meson mass. The method also predicted a broad σ -resonance in the $I=0$ s-wave, but it was pointed out by Roskies⁽³⁶⁾ that Brown and Goble's calculation ignored crossing symmetry completely. Attempts, which have since been made to restore crossing symmetry to the formalism⁽³⁷⁾, have reaffirmed the conclusions of Brown and Goble.

6. A PHENOMENOLOGICAL ANALYSIS - THE MODEL OF MORGAN & SHAW

Forward dispersion relations have been extensively used over the last few years to correlate experimental data on $\pi\pi$ scattering⁽³⁸⁾, although the techniques used encounter

difficulties in the $\pi\pi$ system because of the absence of reliable experimental information in the high and very low energy regions, and because of the very obscure situation concerning the $I=0$ s-wave.

In order to study the influence of the $I=0$ s-wave, Morgan and Shaw tabulated values for the scattering lengths and low energy $\pi\pi$ phase shifts which correspond to various assumptions about the mass and width of the σ -resonance. The method used forward and first derivative dispersion relations for amplitudes with definite isospin in the crossed t-channel,

$$T^I(\nu) = \alpha_{st}^{II'} A^{I'}(\nu) \quad (2.6.1)$$

$$\text{and } D^I(\nu) = \alpha_{st}^{II'} B^{I'}(\nu) \quad (2.6.2)$$

where

$$B^I(\nu) \equiv \left[\frac{d}{dt} A^I(\nu, t) \right] \Big|_{t=0}$$

$$= \frac{1}{4} \sum_{\substack{(I+\ell) \\ \text{even}}} (2\ell+1) [\ell(\ell+1)\nu A_\ell^I(\nu) - \frac{1}{2} \frac{d}{d\nu} A_\ell^I(\nu)]. \quad (2.6.3)$$

Using the crossing symmetric variable

$$z = \frac{s-u}{4} = 2\nu+1 \quad (2.6.4)$$

they wrote forward dispersion relations for $T^I(z)$,

$$\left. \begin{aligned} \text{Re } T^{0,2}(z) &= \frac{2}{\pi} \mathcal{P} \int_1^\infty \frac{dz' z' \text{Im } T^{0,2}(z')}{z'^2 - z^2} \\ \text{Re } T^1(z) &= \frac{2z}{\pi} \mathcal{P} \int_1^\infty \frac{dz' \text{Im } T^1(z')}{z'^2 - z^2} \end{aligned} \right\} \quad (2.6.5)$$

and completely similar equations for the derivatives $D^I(z)$. The integrations on the right-hand-side of Equation (2.6.5) were divided into three regions:

- I) A very low energy region, from threshold up to ~ 500 MeV, in which the phase shifts were to be determined.
- II) An intermediate energy region, from 500 MeV to ~ 1.5 GeV, where the phase shifts were assumed to be known. Results were tabulated for various assumptions about the mass and width of the σ -meson.
- III) The high energy region above 1.5 GeV. Its influence on the left-hand-side of Equation (2.6.5) was represented at least up to the ρ -mass by a polynomial expansion in z (even or odd powers of z contributing to even or odd isospin states).

The coefficients of these polynomials were determined by imposing definite values for the A^I amplitudes and their first derivatives at the ρ -mass.

Accordingly, Equation (2.6.5) was re-written

$$\left. \begin{aligned} \text{Re } T^{0,2}(z) &= \frac{2}{\pi} \mathcal{P} \left\{ \int_1^{z_1} + \int_{z_1}^{z_2} \right\} \frac{dz' z' \text{Im } T^{0,2}(z')}{z'^2 - z^2} + e_0^{0,2} + e_2^{0,2} z^2 \\ \text{Re } T^1(z) &= \frac{2z}{\pi} \mathcal{P} \left\{ \int_1^{z_1} + \int_{z_1}^{z_2} \right\} \frac{dz' \text{Im } T^1(z')}{z'^2 - z^2} + e_1^1 z \end{aligned} \right\}$$

for $0 \leq z \leq z_0 < z_2$. The dispersion relations of Equation (2.6.6) were solved firstly for the s- and p-waves, assuming the d-waves to be known. They were solved iteratively, using (2.6.6) to pass from $\text{Im } T^I$ to $\text{Re } T^I$ and unitarity to pass from $\text{Re } T^I$ to $\text{Im } T^I$, and the constants e_j^I were adjusted at each stage of the calculation. A stable solution was quickly obtained, and it was found that the final results were not too sensitive to the assumed form for the d-waves. The derivative dispersion relations were then treated similarly to provide a check on the d-waves.

A discussion of the parameters e_j^I suggested that both the Down-Down and the Up-Up solutions for δ_0^0 had to be rejected. An analysis of the remaining forms for δ_0^0 favoured a rather broad σ -resonance in the $I=0$ s-wave, an $I=0$ d-wave which was positive and non-negligible in this region, and an $I=2$ d-wave which was always less than 0.2° below 1 GeV. Estimates for the s-p- and d-wave scattering lengths obtained by Morgan and Shaw are given in Table 2.1.

S-wave Scattering Lengths	$\left\{ \begin{array}{l} a_0^0 \\ a_0^2 \end{array} \right.$	$\begin{array}{l} 0.16 \pm 0.04 \\ -0.05 \pm 0.01 \end{array}$
P-wave Scattering Length	a_1^1	0.035 ± 0.002
D-wave Scattering Lengths	$\left\{ \begin{array}{l} a_2^0 \\ a_2^2 \end{array} \right.$	$\begin{array}{l} 0.0016 \pm 0.0002 \\ 0.0003 \pm 0.0001 \end{array}$

Table 2.1

$\pi\pi$ Scattering Lengths of Morgan and Shaw⁽²⁾

7. THE SIGMA MODEL OF $\pi\pi$ SCATTERING

The stability of the ϕ^4 model of $\pi\pi$ scattering⁽³⁹⁾, and its failure to produce s-wave phase shifts in agreement with the experimental data, appears to indicate that the physical content of the ϕ^4 Lagrangian does not correspond to the physical situation. It was suggested by Lee⁽⁴⁰⁾ that the extra physical information apparently lacking in the ϕ^4 model could be taken from current algebra considerations. This was the motivation behind the study of the σ -model of Gell-Mann and Lévy⁽⁴¹⁾ along the same lines. In the $\pi\pi$ calculation, Basdevant and Lee⁽³⁾ considered a Lagrangian

$$\mathcal{L} = \frac{1}{2} \left[(\partial_\mu \sigma)^2 + (\partial_\mu \vec{\pi})^2 \right] - \frac{\mu^2}{2} (\vec{\pi}^2 + \sigma^2) - \frac{g}{4} (\sigma^2 + \vec{\pi}^2) + c\sigma \quad (2.7.1)$$

where σ and $\vec{\pi}$ are the isoscalar, scalar and isovector, pseudoscalar meson fields, and where, except for the last term $c\sigma$, the Lagrangian of Equation (2.7.1) is invariant under $SU(2) \times SU(2)$ transformations. The axial-vector current

$$\vec{A}_\mu(x) = \vec{\pi} \partial_\mu \sigma - \sigma \partial_\mu \vec{\pi} \quad (2.7.2)$$

satisfies

$$\partial_\mu \vec{A}_\mu(x) = c \vec{\pi}(x) \quad , \quad (2.7.3)$$

so that if PCAC is to be satisfied to first order,

$$c = f_\pi m_\pi^2 \quad . \quad (2.7.4)$$

Furthermore, it is possible to renormalise the theory in such a way as to preserve the current algebra and PCAC constraints at each order of the perturbation expansion. Under the translation

$$\sigma = \tilde{\sigma} + f_\pi \quad (2.7.5)$$

the resulting Lagrangian is given by

$$\begin{aligned} \mathcal{L} = & \frac{1}{2} \left[(\partial_\mu \overset{\sim}{\sigma})^2 - m_\sigma^2 \overset{\sim}{\sigma}^2 \right] + \frac{1}{2} \left[(\partial_\mu \overset{\sim}{\pi})^2 - m_\pi^2 \overset{\sim}{\pi}^2 \right] - \frac{g}{4} (\overset{\sim}{\sigma}^2 + \overset{\sim}{\pi}^2)^2 \\ & - (gf_\pi) \overset{\sim}{\sigma} (\overset{\sim}{\sigma}^2 + \overset{\sim}{\pi}^2) \end{aligned} \quad (2.7.6)$$

where the π and σ masses are related by

$$m_\sigma^2 = m_\pi^2 + 2gf_\pi^2 \quad . \quad (2.7.7)$$

The theory, therefore, involves the three parameters m_π^2 , f_π and a dimensionless constant g . Basdevant and Lee obtained the s-wave phase shifts shown in Figure 2.6 by requiring $g \approx 6$ in order to satisfy $\delta_0^0(m_\rho) \approx 90^\circ$.

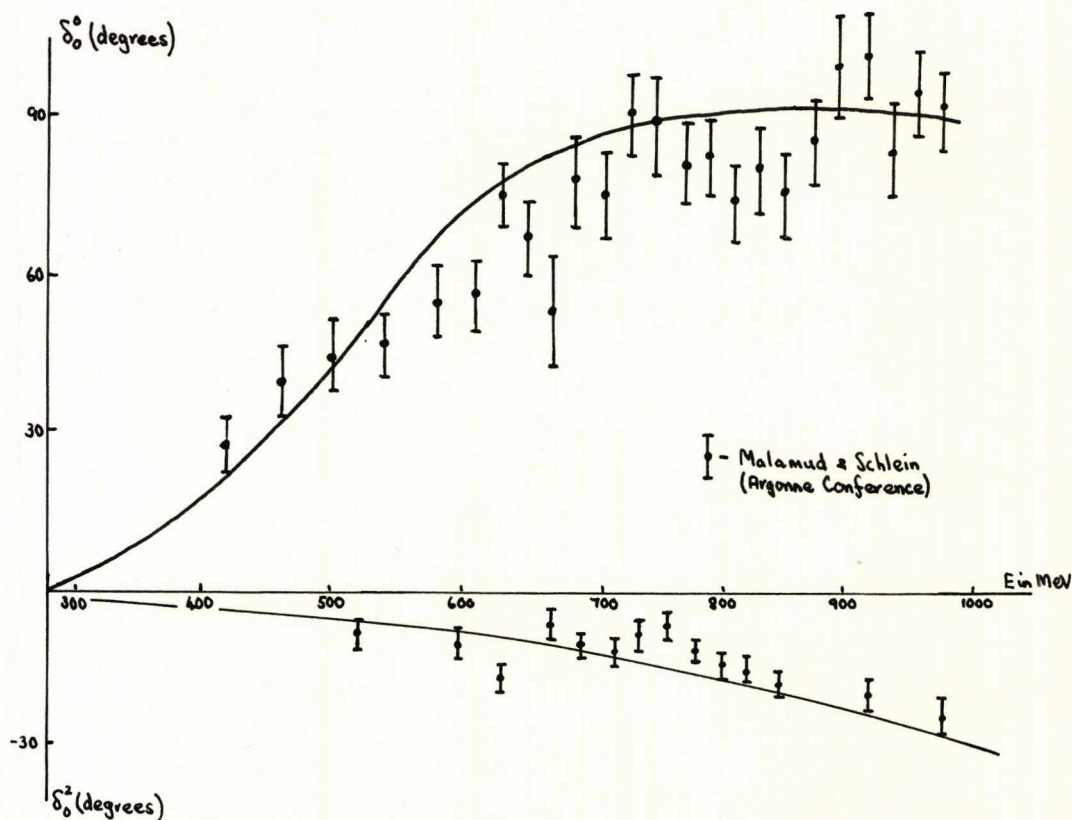


Figure 2.6

$\pi\pi$ s-wave phase shifts from the σ -model

A very broad σ -resonance

$$M_{\sigma} \approx 500 \text{ MeV} , \quad \Gamma_{\sigma} \approx 300 \text{ MeV}$$

was obtained, and the ρ and f_0 resonances, not present in the original Lagrangian, were generated dynamically with

$$M_{\rho} \approx 780 \text{ MeV} , \quad \Gamma_{\rho} \approx 35 \text{ MeV}$$

$$M_{f_0} \approx 1115 \text{ MeV} , \quad \Gamma_{f_0} \approx 180 \text{ MeV}$$

in fair agreement with experiment, at least as a first approximation.

Close to the physical threshold the amplitudes were approximated to the Weinberg amplitudes. Crossing symmetry constraints were found to be well-satisfied, and for this reason the model would appear to be more satisfactory than the arbitrary unitarisation of the current algebra amplitude proposed by Brown and Goble.

8. THE VENEZIANO MODEL

In discussions on finite energy sum rules and duality models, scattering amplitudes were written either as a sum of direct-channel resonances or as a sum of crossed-channel Regge poles.

The Veneziano formula for $\pi\pi$ scattering was introduced by Lovelace⁽⁴²⁾

$$V(s,t) = -\lambda \frac{\Gamma[1 - \alpha_{\rho}(s)] \Gamma[1 - \alpha_{\rho}(t)]}{\Gamma[1 - \alpha_{\rho}(s) - \alpha_{\rho}(t)]} \quad (2.8.1)$$

where α_{ρ} is the linear ρ -trajectory

$$\alpha_{\rho}(s) = \alpha_{\rho}(0) + s\alpha'_{\rho} \quad (2.8.2)$$

and λ is an unknown constant. The $\pi\pi$ isospin amplitudes, defined by

$$\left. \begin{aligned} A^0(s,t,u) &= \frac{3}{2}[V(s,t) + V(s,u)] - \frac{1}{2}V(t,u) \\ A^1(s,t,u) &= V(s,t) - V(s,u) \\ A^2(s,t,u) &= V(t,u) \end{aligned} \right\} \quad (2.8.3)$$

are crossing symmetric. The Adler condition of Equation (2.5.4) was satisfied by imposing a pole in the denominator of (2.8.1) at $s=t=u=m_\pi^2$. This yielded the constraint

$$\alpha_\rho(m_\pi^2) = \frac{1}{2} \quad (2.8.4)$$

in agreement with the experimental data*. The constant λ was determined by imposing Weinberg's condition when two pions go off the mass-shell. In the limit $s \approx u \approx m_\pi^2$, $t \rightarrow 0$

$$\lambda = \frac{1}{\pi f_\pi^2 \alpha'_\rho} \quad (2.8.5)$$

The Veneziano representation is both crossing symmetric and Regge-behaved, and because of the current algebra constraints imposed, it reproduces the scattering lengths of (2.5.18). However, the model is non-unitary, and in order to compute resonance widths it was proposed by Lovelace⁽⁴³⁾ that the partial wave projections of (2.8.3) be used as K-matrices.

*For $\alpha'_\rho \approx 0.018 \text{ m}^{-2}$, as suggested by Equation (2.4.12), $\alpha_\rho(m_\pi^2) = \frac{1}{2}$ requires $\alpha_\rho(0) \approx 0.48$.

Using this prescription he was able to obtain a ρ -width

$$\Gamma_{\rho} \approx 100 \text{ MeV} ,$$

a very broad σ -resonance

$$\Gamma_{\sigma} \approx \frac{9}{2} \Gamma_{\rho} \approx 450 \text{ MeV}$$

and an f_0 -resonance with parameters

$$M_{f_0} \approx 1289 \text{ MeV} , \quad \Gamma_{f_0} \approx 110 \text{ MeV} ,$$

but, as with the Brown-Goble model, Lovelace's unitarisation procedure destroys the crossing symmetry originally present in the Veneziano representation. Later attempts⁽⁴⁴⁾ have at least partially restored crossing to the model without changing the phenomenological predictions of Lovelace.

REFERENCES

1. S. WEINBERG, Phys. Rev. Letts. 17, 616 (1966).
2. D. MORGAN and G. SHAW, Phys. Rev. D2, 520 (1970).
3. J. L. BASDEVANT and B. W. LEE, Phys. Rev. D2, 1680 (1970).
Phys. Letts. 29B, 437 (1969).
4. G. VENEZIANO, Nuovo Cimento 57A, 190 (1968).
5. J. L. BASDEVANT and J. REIGNIER, "Pion-Pion Interactions II" - Herceg, Novi Lectures (1970).
J. L. BASDEVANT, " $\pi\pi$ Theories" - Contribution to G. Höhler Festival, published in Springer Tracts in Modern Physics 61, 1 (1970).
D. MORGAN and J. PISUT, Springer Tracts in Modern Physics 55, 1 (1970).
D. MORGAN, Rutherford Laboratory preprint RPP/T/27
6. W. D. WALKER, "Proceedings of the Conference on $\pi\pi$ and $K\pi$ interactions" Argonne National Laboratory (1969), edited by F. Loeffler and E. Malamud.
7. M. FELDMAN et al., Phys. Rev. Letts. 22, 316 (1969).
J. BARTSCH et al., Nuclear Physics B22, 1 (1970).
R. BIZZARRI et al., Nuclear Physics B14, 169 (1969).
J. DIAZ et al., Nuclear Physics B16, 239 (1970),
and also References 10,11,12,13,14,16 and 17.
8. V. P. KENNEY et al., Phys. Rev. 126, 736 (1962).
W. R. FRAZER and J. R. FULCO, Phys. Rev. 117, 1609 (1960),
and other references contained in Reference 9, p.129.
9. PARTICLE DATA GROUP, Review of Modern Physics 42, 87 (1970).
10. E. MALAMUD and P. E. SCHLEIN, Phys. Rev. Letts. 19, 1056 (1967).

REFERENCES

11. J. P. BATON, G. LAURENS and J. REIGNIER, Nuclear Physics B3, 349 (1967). Phys. Letts. 25B, 419 (1967); 26B, 471 (1968).
12. W. D. WALKER, J. CARROLL, A. GARFINKEL and B. OH, Phys. Rev. Letts. 18, 630 (1967).
13. W. M. KATZ et al., University of Rochester preprint UR-875-282 (1969).
14. E. COLTON, E. MALAMUD and P. E. SCHLEIN, Argonne (1969) p.93.
15. J. H. SCHARENGUIVEL et al., Phys. Rev. 186, 1387 (1969).
16. S. MARATECK, et al., Phys. Rev. Letts. 21, 1613 (1968).
17. W. DEINET et al., Phys. Letts. 30B, 359 (1969).
18. J. MORFIN and D. SINCLAIR, Argonne (1969) p.337.
19. A. PAIS and S. B. TREIMAN, Phys. Rev. 168 1858 (1968).
20. Y. A. BATUSOV et al., Soviet Journal of Nuclear Phys. 1, 492 (1965).
21. L. J. GUTAY, F. T. MEIERE and J. H. SCHARENGUIVEL, Phys. Rev. Letts. 23, 431 (1969).
22. D. CLINE, K. J. BRAUN and V. R. SCHERER, Nuclear Phys. B18, 77 (1970).
23. J. T. CARROLL et al., Phys. Rev. Letts. 28, 318 (1972).
J. BARTSCH et al., Nuclear Phys. B22, 109 (1970).
C. WHITEHEAD et al., Rutherford Laboratory preprint RPP/H/85 (1972).
24. S. D. PROTOPODESCU et al., Berkeley preprint LBL-787.
25. N. F. MOTT and H. F. MASSEY, "The theory of atomic collisions" 3rd edition, Oxford (1965).
T. Y. WU and T. OHMURA, "Quantum theory of scattering", Prentice Hall Inc., New Jersey (1962).

REFERENCES

26. M. OLSSON, Phys. Rev. 162, 1338 (1967).
27. G. BREIT and E. WIGNER, Phys. Rev. 49, 519 (1936).
G. BREIT, Phys. Rev. 58, 506 (1940).
28. T. REGGE, Nuovo Cimento 14, 951 (1959); 18, 947 (1960).
29. C. LOVELACE, Phys. Letts. 28B, 264 (1968).
30. M. GELL-MANN, Phys. Rev. 125, 1067 (1962); Physics 1,
63 (1964).
31. S. L. ADLER and R. DASHEN, "Current Algebras" -
W. A. Benjamin, New York (1968).
32. M. GELL-MANN and M. LÉVY, Nuovo Cimento 16, 705 (1960).
Y. NAMBU, Phys. Rev. Letts. 4, 380 (1960).
J. BERNSTEIN, S. FUBINI, M. GELL-MANN and W. THIRRING,
Nuovo Cimento 17, 757 (1960).
J. BERNSTEIN, M. GELL-MANN and W. THIRRING, Nuovo Cimento
16, 560 (1960).
33. S. L. ADLER, Phys. Rev. 137B, 1022 (1965); 140B, 736 (1965).
Phys. Rev. Letts. 14, 1051 (1965).
34. J. ILIOPOULOS, Nuovo Cimento 52A, 192 (1967); 53A, 552 (1968).
R. ARNOWITT, M. H. FRIEDMAN, P. NATH and R. SUITOR,
Phys. Rev. Letts. 20, 475 (1968).
A. M. S. AMATYA, A. PAGNAMENTA and B. RENNER, Phys. Rev.
172, 1755 (1968).
D. F. GREENBERG, Phys. Rev. 184, 1934 (1969).
35. L. S. BROWN and R. L. GOBLE, Phys. Rev. Letts. 20, 346
(1968).
36. R. ROSKIES, Nuovo Cimento 65A, 467 (1970).
37. S. KRINSKY, Phys. Rev. D2, 1168 (1970).

REFERENCES

38. P. CASTOLDI, Nuclear Phys. B12, 567 (1969).
J. R. FULCO and D. Y. WONG, Phys. Rev. Letts. 19,
1399 (1967).
N. G. ANTONIOU and C. PALEV, Phys. Letts. 26B, 301 (1968).
N. PAVER and C. VERZEGNASSI, Phys. Letts. 26B, 388 (1968).
39. D. BESSIS and M. PUSTERLA, Nuovo Cimento 54A, 243 (1968).
J. L. BASDEVANT, D. BESSIS and J. ZINN-JUSTIN, Nuovo
Cimento 60A, 185 (1969).
40. B. W. LEE, Nuclear Phys. B9, 649 (1969).
41. M. GELL-MANN and M. LÉVY, Nuovo Cimento 16, 705 (1960).
42. C. LOVELACE, Phys. Letts. 28B, 265 (1968).
43. C. LOVELACE, Argonne (1969) p.562.
44. K. KANG, M. LACOMBE, R. VINH MAU, IPNO-TH 71-22 July 1971.

CHAPTER 3

I. INTRODUCTION

One of the unanswered questions of $\pi\pi$ scattering, whether one should consider the total $\pi\pi$ amplitude or restrict oneself to partial waves, has been discussed at length in the literature⁽¹⁾. The problems involved were encountered in some of the models described in Chapter 2; if one deals with partial waves unitarity can be imposed exactly, but crossing symmetry, which relates all partial wave amplitudes to each other, is at best only approximate; and if one uses the total amplitude, which is exactly crossing symmetric, it is the unitarity condition that is difficult to impose.

For the most part $\pi\pi$ theorists have dealt with partial waves. There are two reasons for this. Firstly, it is expected that the unitarity condition plays an essential role in $\pi\pi$ dynamics, even at quite low energies, and secondly, there now exist a large number of restrictions on partial wave amplitudes which follow from the theoretical requirements of analyticity, crossing symmetry and unitarity (ACU), which were described in Chapter 1. One way to use these restrictions has been suggested by Wanders⁽²⁾. His method is discussed in detail in Section 3, but the general idea is to start with a model that is unitary but which contains some free parameters, and then adjust the parameters until the various requirements are satisfied. The results obtained from this type of approach^(2,3) suggest that the requirements of ACU on partial

wave amplitudes are quite restrictive, at least in the very low energy region.

On the other hand, by working with the total amplitude, Atkinson⁽⁴⁾ has shown that there exists an infinite set of functions which satisfy ACU. The two apparently contradictory results would be reconciled if all of Atkinson's solutions become identical in the very low energy region, but there is no a priori reason to believe that this should happen, and it has been suggested⁽⁵⁾ that the methods of Wanders et al. may have overlooked solutions.

The purpose of this chapter is to confirm that there exists at least one other family of solutions which is perfectly acceptable on the basis of ACU requirements. In Section 2 some of the crossing symmetry constraints, and the restrictions they impose on the $\pi\pi$ partial wave amplitudes in the unphysical region, are discussed. Section 3 contains details of approximation schemes and low energy partial wave parametrisations that have been used by others. One of the calculations is modified in the light of our present knowledge. In Section 4, a parametrisation for partial wave amplitudes, designed to be valid in the unphysical region, is proposed. The general approach used to determine the $\pi\pi$ scattering lengths is to impose elastic unitarity at the physical threshold and approximate crossing symmetry over the region $0 \leq s \leq 4$. The numerical results are presented in Section 5 and some tentative conclusions are drawn in Section 6.

2. CONSTRAINTS ON $\pi\pi$ PARTIAL WAVE AMPLITUDES

The requirements of unitarity and analyticity were first applied to the $\pi\pi$ problem by Chew and Mandelstam⁽⁶⁾. The model, which was exactly crossing symmetric had only s- and p-waves possessing non-zero absorptive parts. Since partial waves with $\ell \geq 2$ are expected to be small in the low energy region this was considered a reasonable approximation, but the numerical calculation yielded strong s-wave solutions and a small p-wave with no ρ -resonance.

The first attempts at putting crossing constraints on partial wave amplitudes was initiated by Martin⁽⁷⁾, and since then considerable effort has been devoted to the derivation of rigorous properties of the lower $\pi\pi$ partial waves, particularly in the unphysical region. The constraints derived so far fall into two main categories:

- (i) linear inequalities between the values of partial wave amplitudes at two points of the interval $0 \leq s \leq 4$, or between their value at one point and given integrals over this region;
- (ii) linear equalities between integrals in the region $0 \leq s \leq 4$.

Most of the restrictions of type (i), which are a consequence of analyticity and crossing symmetry plus positivity properties of the absorptive parts which follow from unitarity, have been

obtained on the s-waves of the total $\pi^0\pi^0 \rightarrow \pi^0\pi^0$ scattering amplitude $A^{00}(s,t,u)$,

$$A^{00}(s,t,u) = \frac{1}{3}[A^0(s,t,u) + 2A^2(s,t,u)]. \quad (3.2.1)$$

Being a sum over even partial waves, $A^{00}(s,t,u)$ is completely symmetric under interchange of s, t and u. The following constraints on $A_0^{00}(s)$, the s-wave projection of the total $\pi^0\pi^0$ amplitude, severely restricts its possible shape in the unphysical region. For example, the inequalities

$$\frac{dA_0^{00}}{ds}(s) < 0 \quad 0 \leq s \leq 1.127 \quad (3.2.2) \quad (7,8)$$

$$\frac{dA_0^{00}}{ds}(s) > 0 \quad 1.7 \leq s \leq 4 \quad (3.2.3) \quad (7,9,10)$$

$$\frac{d^2A_0^{00}}{ds^2}(s) > 0 \quad 0 \leq s \leq 1.7 \quad (3.2.4) \quad (9)$$

indicate that the $\pi^0\pi^0$ s-wave has a minimum in the interval $1.127 \leq s \leq 1.7$, and that this minimum is the only one in the unphysical region. The additional inequalities

$$A_0^{00}(0) < A_0^{00}(4) \quad (3.2.5) \quad (10)$$

$$A_0^{00}(0) > A_0^{00}(3.189) \quad (3.2.6) \quad (10)$$

$$A_0^{00}(4) > -3 \quad (3.2.7) \quad (11,12)$$

$$A_0^{00}(0) \geq \frac{1}{2} \int_2^4 ds A_0^{00}(s) \quad (3.2.8) \quad (10)$$

$$\int_0^4 ds A_0^{00}(s) \leq \int_0^4 ds A_0^2(s) + 6A_0^2(0) \quad (3.2.9) \quad (13)$$

$$A_0^{00}(3.205) > A_0^{00}(0.2134) > A_0^{00}(2.9863) \quad (3.2.10)^{(14)}$$

establish $A_0^{00}(s)$ in the unphysical region to be qualitatively depicted by Figure 3.1.

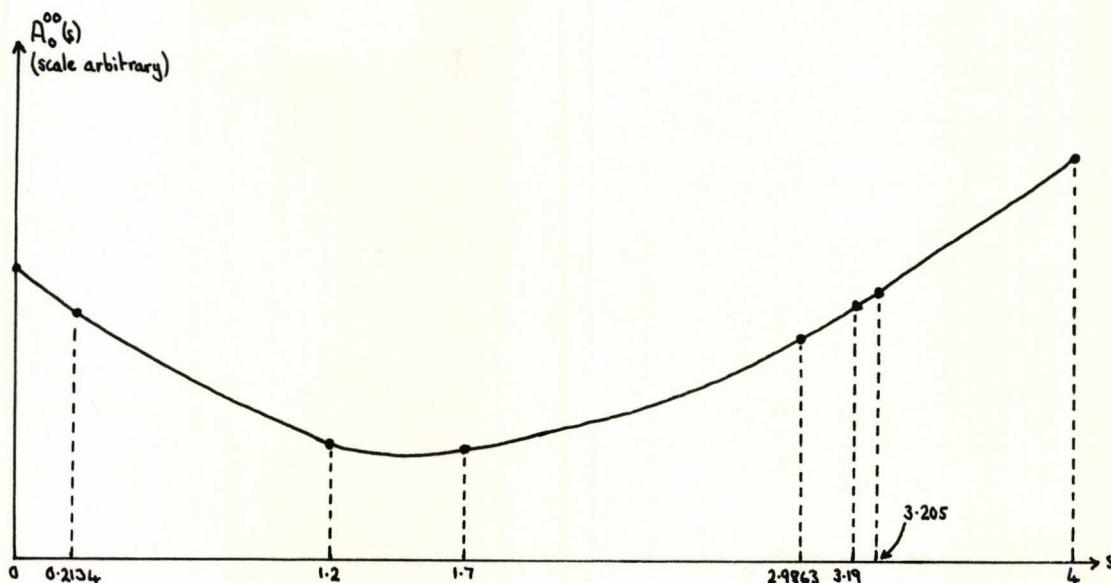


Figure 3.1

$A_0^{00}(s)$ as defined by Equations (3.2.2) to (3.2.10)

The physical implications of these constraints are not self-evident and their relevance is difficult to estimate because of two obvious failings. Firstly, apart from Equation (3.2.7), which is in any case only a very poor lower bound on the $\pi^0\pi^0$ s-wave scattering length, the inequalities provide no information about an absolute scale for $A_0^{00}(s)$. Secondly, the conditions affect the unphysical region only, hence their range of application would appear to be limited. In spite of these shortcomings the constraints do appear to be very useful, either when constructing low energy models^(2,3) or

when testing existing ones⁽¹⁵⁾. At the very least one can say that these constraints do furnish some reliable information, and all models connecting the physical and unphysical regions have to take these inequalities into account.

The second method of finding crossing constraints on partial wave amplitudes stems from the work of Balachandran and Nuyts⁽¹⁶⁾, and later of Roskies⁽¹⁷⁾. They showed that there exists an infinite set of constraint equations which are linear equalities between partial wave integrals evaluated over the region $0 \leq s \leq 4$. To derive these equations, consider an amplitude $A(s,t,u)$ which is totally symmetric (or antisymmetric) under interchange of its three variables. If one multiplies this function by an antisymmetric (or symmetric) polynomial $P(s,t,u)$ and then integrates the product of the two functions over the symmetric domain $\Delta \equiv (s>0, t>0, u>0)$ of the Mandelstam plane, the integral must be identically zero,

$$\iint_{\Delta} A(s,t,u) P(s,t,u) ds dt \equiv 0 . \quad (3.2.11)$$

For example, the total $\pi^0\pi^0$ amplitude is symmetric under interchange of s , t and u , and $(s-u)$ is a function antisymmetric under interchange of s and u . Then, according to (3.2.11)

$$\int_0^4 (4-s) \int_{-1}^1 A^{00}(s,t,u) (s-u) d(\cos \theta) = 0 , \quad (3.2.12)$$

and if $A^{00}(s,t,u)$ is expanded in terms of its partial waves,

$$\int_0^4 (4-s) \int_{-1}^1 \sum_{\substack{\ell=0 \\ \text{even } \ell}}^{\infty} (2\ell+1) A_{\ell}^{00}(s) \left[\frac{(3s-4)}{2} - \frac{(4-s)}{2} \cos \theta \right] P_{\ell}(\cos \theta) d(\cos \theta) = 0 . \quad (3.2.13)$$

For $\ell > 0$ the $\cos \theta$ integration is zero, and Equation (3.2.13) simplifies to

$$\int_0^4 (4-s)(3s-4) A_0^{00}(s) ds = 0, \quad (3.2.14)$$

which is an integral equation involving s-waves only. (3.2.14) is of special significance because it is the only integral equation of its kind involving the $\pi^0 \pi^0$ s-wave amplitude. By choosing different polynomial forms for $P(s,t,u)$ one could derive an infinite set of such relations, and although each relation involves only a finite number of partial waves, the set is complete in the sense that if all the equations are satisfied exactly, the amplitude is crossing symmetric. Roskies⁽¹⁸⁾ has also proved that for $\ell > 0$ there exist $2\ell+1$ integral equations relating the ℓ th partial wave to all the lower partial waves. The three equations relating the p-waves to the s-waves and the five equations relating the d-waves to the s- and p-waves are given explicitly with their means of derivation in Appendix A3.

3. APPROXIMATIONS AND PARAMETRISATIONS

In the region of the Mandelstam plane $s > 0$, $t > 0$, $u > 0$ the $\pi\pi$ isospin amplitudes $A^I(s,t,u)$ are analytic. Therefore, one can expand these amplitudes in powers of s , t and u about a point in this region. All things being equal, the most natural choice for such a point would be the symmetry point $s=t=u=\frac{4}{3}$.

In Section 7 of Chapter 1 it was established that all $\pi\pi$ amplitudes are determined by a single function $A(s,t,u)$ symmetric under interchange of t and u . Therefore, if $A(s,t,u)$ is expanded about the point $s=t=u=\frac{4}{3}$,

$$A(s,t,u) = \alpha + \beta(s - \frac{4}{3}) + \gamma_1(s - \frac{4}{3})^2 + \gamma_2 \left[(t - \frac{4}{3})^2 + (u - \frac{4}{3})^2 \right] + \dots$$

(3.3.1)

where, because of its symmetry properties the on mass-shell amplitude $A(s,t,u)$ has no terms linear in t and u ; similarly the tu term is related to s^2 and $(t+u)^2$ by $(s+t+u)^2=16$, etc.. It is not clear what kind of physical information can be obtained from such an expansion, since (3.3.1) diverges at $s=4$ and is real for all values of s , whereas the $\pi\pi$ amplitude is constant at the physical threshold and becomes complex above this point. If (3.3.1) is to be a realistic approximation of the $\pi\pi$ scattering amplitude $A(s,t,u)$ must be small and smooth over the region in which (3.3.1) is defined and unitarity must be assumed not to be a strong constraint. This smoothness assumption is not a new idea; it was used by Weinberg in his current algebra calculation of the $\pi\pi$ scattering lengths, and although he used only a linear form for the amplitude the small values he obtained for the scattering lengths were consistent with his initial assumption.

The simplest approximation to (3.3.1), which was also the starting point of the Chew-Mandelstam dynamical scheme for $\pi\pi$ scattering⁽⁶⁾, is a constant approximation

$$A(s,t,u) = \lambda \quad . \quad (3.3.2)$$

The isospin amplitudes then become

$$\left. \begin{aligned} A^0(s,t,u) &= 5\lambda \\ A^1(s,t,u) &= 0 \\ A^2(s,t,u) &= 2\lambda \end{aligned} \right\} \quad (3.3.3)$$

and at the symmetry point

$$\frac{A^0\left(\frac{4}{3}, \frac{4}{3}, \frac{4}{3}\right)}{A^2\left(\frac{4}{3}, \frac{4}{3}, \frac{4}{3}\right)} = \frac{5}{2} \quad (3.3.4)$$

In this approximation only the s-wave amplitudes exist. The scattering lengths have the same sign and are also in the ratio

$$\frac{a_0}{a_2} = \frac{5}{2} \quad (3.3.5)$$

Evidence is to be found in this chapter which suggests that there does exist a solution of the $\pi\pi$ scattering amplitude consistent with both crossing symmetry and unitarity and which has s-wave scattering lengths very close to this ratio.

If one keeps both the first two terms in (3.3.1), one can define a linear approximation to the $\pi\pi$ amplitude in terms of two parameters λ and μ by writing

$$A(s,t,u) = \lambda + \mu s \quad (3.3.6)$$

The corresponding isospin amplitudes are then given by

$$\left. \begin{aligned} A^0(s,t,u) &= 5\lambda + 4\mu + 2\mu s \equiv A_0^0(s) \\ A^1(s,t,u) &= \mu(t-u) \equiv \mu(s-4)\cos\theta \\ A^2(s,t,u) &= 2\lambda + 4\mu - \mu s \equiv A_0^2(s) \end{aligned} \right\} \quad (3.3.7)$$

In this approximation both s- and p-waves exist, with the p-wave amplitude given by

$$A_1^1(s) = \frac{\mu}{3}(s - 4) \quad . \quad (3.3.8)$$

Therefore, the gradients of the s- and p-wave amplitudes are in the ratio $2:\frac{1}{3}:-1$ for isospin 0, 1 and 2 respectively. If, in addition, one assumes the p-wave scattering length

$$a_1 = \frac{4}{3}\mu \quad (3.3.9)$$

to be positive, μ must be positive, in which case as s increases, $A_0^0(s)$ increases - like $6A_1^1(s)$, and $A_0^2(s)$ decreases, but more slowly - like $-\frac{1}{2}A_0^0(s)$. From (3.3.7) and (3.3.9) the scattering lengths satisfy

$$2a_0 - 5a_2 = 18a_1 \quad , \quad (3.3.10)$$

with a_0 and a_2 in the ratio

$$\frac{a_0}{a_2} = \frac{5\lambda + 12\mu}{2\lambda} \quad . \quad (3.3.11)$$

To obtain a numerical estimate for a_0/a_2 an additional assumption is necessary which will specify the relationship between λ and μ . For example, if the Adler condition is imposed on (3.3.6), $\lambda = -\mu$, and

$$\frac{a_0}{a_2} = -3.5 \quad . \quad (3.3.12)$$

Furthermore, if zeros exist in each of the s-wave amplitudes they would occur at

$$\left. \begin{aligned} s_0 &= - \frac{(5\lambda + 4\mu)}{2\mu} \\ s_2 &= \frac{(2\lambda + 4\mu)}{\mu} \end{aligned} \right\} \quad (3.3.13)$$

which leads to a further constraint equation⁽¹⁹⁾

$$4s_0 + 5s_2 = 12 \quad (3.3.14)$$

between the position of the two s-wave zeros if they exist.

Equation (3.3.12) implies that the s-wave scattering lengths obtained from a linear form for the $\pi\pi$ amplitude are of opposite signs, and, therefore, belong to a solution other than that suggested by the constant form for the amplitude. The existence of a second solution, which is also consistent with crossing symmetry and unitarity, and which exhibits the properties illustrated above will be confirmed later in this chapter.

However, $A_0^{00}(s)$, as defined either by the constant or the linear form for the $\pi\pi$ amplitude, is a constant for all values of s and therefore violates all of the so-called Martin inequalities of (3.2.2) to (3.2.10). Although on their own these inequalities do not determine $A_0^{00}(s)$ absolutely, when used with additional physical assumptions they can prove extremely useful, as has been illustrated by Wanders⁽²⁾. His method was to construct unitary amplitudes and then constrain

them to fulfil the Martin inequalities. He defined s-wave amplitudes

$$A_0^I(s) = \frac{\sqrt{s}}{2\phi^I(s) - i\sqrt{s-4}} \quad (3.3.15)$$

with the functions $\phi^I(s)$ consistent with the known analytic properties of $A_0^I(s)$. Under the transformation

$$s = 4\cos^2 v \quad (3.3.16)$$

the s-plane is mapped onto the interval $\text{Re } v \in [0, \pi/2]$, as illustrated in Figure 3.2.

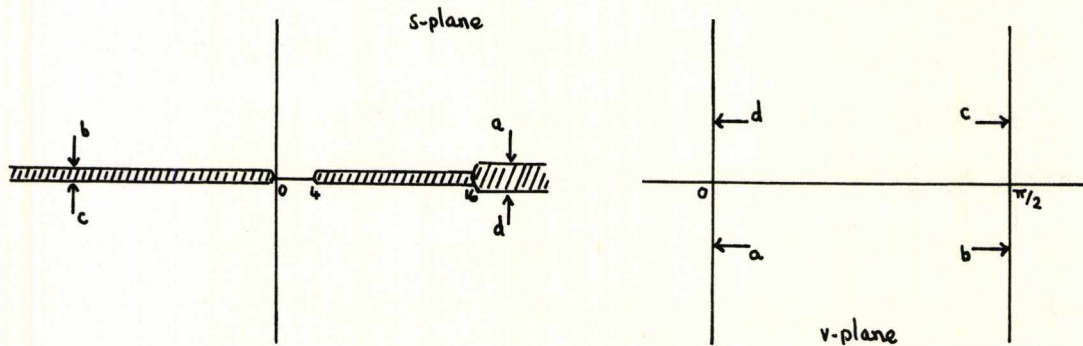


Figure 3.2

Mapping of the S-plane under the transformation $s=4\cos^2 v$

Using the v-variable, the s-wave amplitudes are then given by

$$A_0^I(v) = \frac{\cos v}{\phi^I(v) + \sin v} \quad (3.3.17)$$

with the $\phi^I(v)$ defined to be real even meromorphic functions of v with their poles corresponding to zeros of the s-wave

amplitudes. As parametrisations for $\phi^I(v)$, Wanders chose

$$\left. \begin{aligned} \phi^0(v) &= \frac{A + Bv^2 + Cv^4 + Dv^6}{\alpha^2 - \sin^2 v} \\ \phi^2(v) &= \left[a_2 \left(1 - \left[\frac{2v}{\pi} \right]^2 \right) \right]^{-1} \end{aligned} \right\} \quad (3.3.18)$$

with a_2 , the $I=2$ s-wave scattering length, assumed to be known. Equation (3.3.18) imposes real zeros in both s-wave amplitudes - in $A_0^0(s)$ at $s_0=4(1-\alpha^2)$ and in $A_0^2(s)$ at $s_2=0$. For suitable values of a_2 the degree of the polynomial in the numerator of $\phi^0(v)$ was found to be minimal in order to satisfy all the Martin inequalities, and then a solution could only be obtained for s_0 lying in the range $3 < s_0 < 7$. This method of saturating the Martin inequalities yields a solution which it is claimed is approximately crossing symmetric, and therefore should satisfy the two Balachandran-Nuyts-Roskies integral equations involving s-wave amplitudes only.

Wanders' Solution			$\left \int_0^4 (4-s) (2A_0^0(s) - 5A_0^2(s)) ds \right $	$\left \int_0^4 (4-s) (3s-4) (A_0^0(s) + 2A_0^2(s)) ds \right $
a_2	a_0	s_0		
-0.05	0.022	3.2	0.01	0.00
	-0.089	7.2	0.46	0.00
-0.07	0.033	3.2	0.02	0.00
	-0.123	7.2	0.63	0.00
-0.09	0.045	3.2	0.02	0.01
	-0.160	7.2	0.82	0.01

Table 3.1

Table 3.1 illustrates that the integral equations are only well-satisfied if s_0 lies in the unphysical region and Equation (3.3.14) is approximately satisfied. Furthermore, the value of a_0 is related to the position of s_0 , and if, as is implied by (3.3.14), s_0 depends upon s_2 , a_0 will also depend upon any initial assumption made about s_2 .

To illustrate further the usefulness of the Balachandran-Nuyts-Roskies equations when constraining partial wave amplitudes to be approximately crossing symmetric in the unphysical region, consider a parametrisation

$$A_0^{00}(s) \propto (s - \eta)^2 \quad 0 \leq s \leq 4 \quad (3.3.19)$$

which is suggested by Figure 3.1. Substituting for (3.3.19) in (3.2.14), one obtains a minimum in the $\pi^0\pi^0$ s-wave amplitude at $s=\eta=1.6$ and a form for $A_0^{00}(s)$ which satisfies all the Martin inequalities, including the very restrictive ones of (3.2.6) and (3.2.10)*.

To obtain a realistic parametrisation of the $\pi\pi$ scattering amplitude there must be two important deviations from (3.3.1); the first, near $s=0$, comes from the existence of a $(-s)^{3/2}$ term in the amplitude due to the presence of a left-hand cut beginning at $s=0$; the second is expected at $s=4$ due to the presence of the right-hand cut.

*A general quadratic form for $A_0^{00}(s)$ also satisfies (3.2.2) to (3.2.10) if the position of the minimum lies between $s=1.5$ and $s=1.7$.

The simplest way of introducing the correct behaviour into the amplitude above $s=4$ has been suggested by Iliopoulos⁽²⁰⁾, who proposed that a suitable representation of the $\pi\pi$ scattering amplitude in its three isotopic spin states is given by a series expansion in the variables $\sqrt{4-s}$, $\sqrt{4-t}$, $\sqrt{4-u}$.

$$\left. \begin{aligned} A^0(s,t,u) &= a_0 + b_0\sqrt{4-s} + c_0(\sqrt{4-t} + \sqrt{4-u}) + \dots \\ A^1(s,t,u) &= c_1(\sqrt{4-t} - \sqrt{4-u}) + \dots \\ A^2(s,t,u) &= a_2 + b_2\sqrt{4-s} + c_2(\sqrt{4-t} + \sqrt{4-u}) + \dots \end{aligned} \right\} (3.3.20)$$

As well as being exactly crossing symmetric under interchange of s , t and u the isospin amplitudes have a square-root branch cut at $s=4$, corresponding to the elastic unitarity cut, and also crossed-channel normal thresholds. The corresponding s -wave amplitudes can be written as a power series in $\sqrt{4-s}$ such that

$$A_0^{00}(s) = \alpha + \beta\sqrt{4-s} + \gamma(4-s) + \dots \quad (3.3.21)$$

where α, β, γ are linear combinations of the coefficients a_I, b_I, c_I ($I=0,2$). To enable $A_0^{00}(s)$ of (3.3.21) to satisfy

$$\int_0^4 (4-s)(3s-4) A_0^{00}(s) ds = 0$$

and

$$A_0^{00}(3.205) > A_0^{00}(0.2134) > A_0^{00}(2.9863)$$

one requires $\beta < 0$, which in turn is found to violate two of the remaining Martin inequalities, namely (3.2.3) and (3.2.8). We conclude that in order to simultaneously satisfy all known

constraints in the region $0 \leq s \leq 4$ it may be necessary to impose the correct behaviour on the amplitude at $s=0$ as well as at $s=4$.

However, the Iliopoulos expansion has formed the basis of several theoretical calculations of the low energy $\pi\pi$ parameters. For example, Dilley⁽⁵⁾ started with the exactly crossing symmetric amplitude of (3.3.20), and then imposed elastic unitarity on the corresponding partial wave amplitudes over a fixed region just above the physical threshold. To be more precise, he defined, for the s-wave amplitudes, a function

$$R(\nu) \equiv \frac{\text{Im } A_0^I(\nu)}{\sqrt{\nu/\nu+1} |A_0^I(\nu)|^2} \quad (I=0,2) \quad (3.3.22)$$

where $R(\nu)=1$ for elastic unitarity. He then measured the root-mean-square deviation of $R(\nu)$ from 1 over an interval $0 \leq \nu \leq \bar{\nu}=1$,

$$\delta R(\bar{\nu}) = \frac{1}{\sqrt{n}} \left\{ \sum_{i=1}^n [R(\nu_i) - 1]^2 \right\}^{\frac{1}{2}}, \quad (3.3.23)$$

where ν_i are equally spaced points in the interval $[0, \bar{\nu}]$. The coefficients in the Iliopoulos expansion were then determined by minimising $\delta R(\bar{\nu})$ over this interval. Dilley found, contradictory to previous investigations, two distinct types of scattering amplitudes which are both consistent with results which follow from analyticity, crossing symmetry and unitarity. The values he obtained for the s-wave scattering lengths are compared with our own results in Figure 3.3 on page 91.

A previous formulation of the low energy $\pi\pi$ interaction⁽²¹⁾, hereafter referred to as PGM-I, has shown that an approximately crossing symmetric amplitude, obtained by expanding the amplitude as a Taylor series about the point $s=4, t=u=0$ using variables $\sqrt{4-s}, t, u$, and the exactly crossing symmetric amplitude of (3.3.20), lead to almost identical results for the low energy $\pi\pi$ parameters. The values obtained in PGM-I for the s-wave scattering lengths, however, are shown in Table 3.2 to differ considerably from either of Dilley's solution.

	a_2	a_0
Graves-Morris (PGM-I)	0.029	0.77
Dilley $\left\{ \begin{array}{l} \text{Solution A} \\ \text{Solution B} \end{array} \right.$	0.029	0.078
	0.029	-0.045

Table 3.2

$\pi\pi$ S-wave Scattering Length Predictions

We shall now show that the method used by Graves-Morris does yield at least one other solution consistent with known properties of analyticity, crossing symmetry and unitarity, and that it is the "overlooked" solution that corresponds to the physical solution. The model will be referred to as PGM-II.

If the physical amplitudes are expanded to second order in the variables $\sqrt{4-s}, t, u,$

$$\left. \begin{aligned} A^0(s,t,u) &= a_0 + b_0 \sqrt{4-s} + c_0(t+u) + d_0(4-s) + f_0(t^2+u^2) + h_0 \sqrt{4-s}(t+u) + k_0 tu \\ A^1(s,t,u) &= c_1(t-u) + h_1 \sqrt{4-s}(t-u) + f_1(t^2-u^2) \\ A^2(s,t,u) &= a_2 + b_2 \sqrt{4-s} + c_2(t+u) + d_2(4-s) + f_2(t^2+u^2) + h_2 \sqrt{4-s}(t+u) + k_2 tu \end{aligned} \right\} \quad (3.3.24)$$

To impose crossing symmetry on the mass-shell, it is convenient to re-expand the amplitudes about the symmetry point $s=t=u=\frac{4}{3}$ to the same order*. Then, equating the isospin combinations

$$\left. \begin{aligned} A^0(s,t,u) + 2A^2(s,t,u) \\ A^0(s,t,u) + 2A^1(s,t,u) \end{aligned} \right\} \quad (3.3.25)$$

which are symmetric under interchange of s and t , and

$$2A^0(s,t,u) - 3A^1(s,t,u) - 5A^2(s,t,u) \quad (3.3.26)$$

which is antisymmetric under interchange of s and t , one obtains nine linearly independent equations between the coefficients of the Taylor expansion. In terms of v , the centre of mass momentum $v=(s-4)/4$, the s - and p -wave projections of

*In PGM-I the amplitudes were re-expanded about the point $s=t=u=0$ which is off the mass-shell. This amendment changes the numerical estimates of the parameters by a negligible amount.

(3.3.24) are given by

$$\left. \begin{aligned} A_0^0(v) &= a_0 - 2ib_0\sqrt{v} - 4(c_0+d_0)v + 8ih_0v^{3/2} + \frac{8}{3}(4f_0+k_0)v^2 \\ A_1^1(v) &= \frac{4}{3}v(c_1-2ih_1\sqrt{v} - 4f_1v) \\ A_0^2(v) &= a_2 - 2ib_2\sqrt{v} - 4(c_2+d_2)v + 8ih_2v^{3/2} + \frac{8}{3}(4f_2+k_2)v^2 \end{aligned} \right\} \quad (3.3.27)$$

and if the elastic unitarity condition

$$\text{Im } A_\ell^I(v) = \sqrt{\frac{v}{v+1}} |A_\ell^I(v)|^2 \quad 0 \leq v \leq 3 \quad (3.3.28)$$

is imposed to second order on each of these partial wave amplitudes, the following five additional constraint equations

$$\left. \begin{aligned} b_0 &= -a_0^2/2 \\ -b_0 + 8h_0 &= 4b_0^2 - 8a_0(c_0 + d_0) \\ b_2 &= -a_2^2/2 \\ -b_2 + 8h_2 &= 4b_2^2 - 8a_2(c_2 + d_2) \\ h_1 &= 0 \end{aligned} \right\} \quad (3.3.29)$$

are obtained between the coefficients of the Taylor expansion. Since $h_1=0$, the p-wave is real and therefore non-unitary in the second order model. If the coefficients c_0, d_0 and c_2, d_2 are redefined by

$$\left. \begin{aligned} c_0 + d_0 &\equiv nc_0 \\ c_2 + d_2 &\equiv nc_2 \end{aligned} \right\} , \quad (3.3.30)$$

the theory involves fifteen parameters, five unitarity equations and nine linearly independent crossing symmetry equations, and the scattering amplitudes can, therefore, be determined in terms of a single fixed parameter. This parameter is chosen to be a_2 , the $I=2$ s-wave scattering length, which it is assumed lies within the range $-0.07 \leq a_2 \leq 0.07$.

The linear constraint equations, which follow from crossing symmetry, satisfy the matrix equation

$$\underline{Ax} = \underline{By} \quad (3.3.31)$$

where A is the 9×9 square matrix

$$A \equiv \begin{bmatrix} 0 & -2 & 0 & 0 & 0 & -3 & -6 & 0 & 0 \\ 0 & 0 & -1 & 0 & -2 & -\frac{1}{8} & -\frac{1}{4} & 0 & 0 \\ 0 & 0 & 0 & 0 & 0 & -\frac{1}{2} & -1 & -1 & -2 \\ -2 & 0 & 0 & 0 & 0 & -3 & 0 & 0 & 0 \\ 0 & 0 & -1 & -2 & 0 & -\frac{1}{8} & 0 & 0 & 0 \\ 0 & 0 & 0 & 0 & 0 & -\frac{1}{2} & 0 & -1 & 0 \\ 0 & 0 & 2 & -3 & -5 & -\frac{1}{4} & \frac{5}{8} & 0 & 0 \\ 0 & 0 & 0 & 0 & 0 & -1 & \frac{5}{2} & 2 & -5 \\ -6 & -10 & 0 & 0 & 0 & \frac{128}{9} & -\frac{320}{9} & 0 & 0 \end{bmatrix} \quad (3.3.32)$$

B is the 9×5 matrix

$$B \equiv \begin{bmatrix} 0 & 0 & \frac{3}{8} & \frac{3}{4} & 1 \\ 0 & 0 & \frac{3}{64} & \frac{3}{32} & 0 \\ 0 & 0 & 0 & 0 & 0 \\ 0 & 0 & \frac{3}{8} & 0 & 1 \\ 0 & 0 & \frac{3}{64} & 0 & 0 \\ 0 & 0 & 0 & 0 & 0 \\ 0 & 0 & \frac{3}{32} & -\frac{15}{64} & 0 \\ 0 & 0 & 0 & 0 & 0 \\ -2 & 5 & -5 & \frac{25}{2} & -4 \end{bmatrix} \quad (3.3.33)$$

and \underline{x} and \underline{y} are the column vectors

$$\underline{x} \equiv \begin{bmatrix} c_1 \\ nc_2 \\ f_0 \\ f_1 \\ f_2 \\ H_0 \\ H_2 \\ k_0 \\ k_2 \end{bmatrix} \quad \underline{y} \equiv \begin{bmatrix} a_0 \\ a_2 \\ B_0 \\ B_2 \\ nc_0 \end{bmatrix} \quad (3.3.34)$$

In Equation (3.3.34) the coefficients B_0 , B_2 , H_0 and H_2 are defined as $\sqrt{3/8} b_0$, $\sqrt{3/8} b_2$, $\sqrt{3/8} h_0$ and $\sqrt{3/8} h_2$ respectively. The unitarity equations, which are quadratic, can be solved for using a generalised Newton-Raphson method⁽²²⁾. The precise method of solution is as follows: fix a_2 and guess suitable initial values for a_0 and nc_0 . B_0 and B_2 can be found from (3.3.29), and the remaining coefficients are determined by solving the matrix equation

$$\underline{x} = A^{-1} B \underline{y} . \quad (3.3.35)$$

Then, using the Newton-Raphson method, new estimates are obtained for a_0 and nc_0 , which replace the previous values, and the entire procedure is repeated until stable values are obtained for all the coefficients.

It was found* that a simultaneous solution of (3.3.29) and (3.3.35) is not unique. For suitable values of a_2 there exist at least two independent sets of parameters and therefore at least two representations of $\pi\pi$ scattering which are approximately crossing symmetric and unitary in the very low energy region. The two solutions obtained are labelled PGM-II Solution A and PGM-II Solution B, and in Figure 3.3 we compare the s-wave scattering lengths belonging to each of these solutions with similar estimates obtained by Dilley⁽⁵⁾.

*Details of the computer programs and the results are given in Appendix B3.

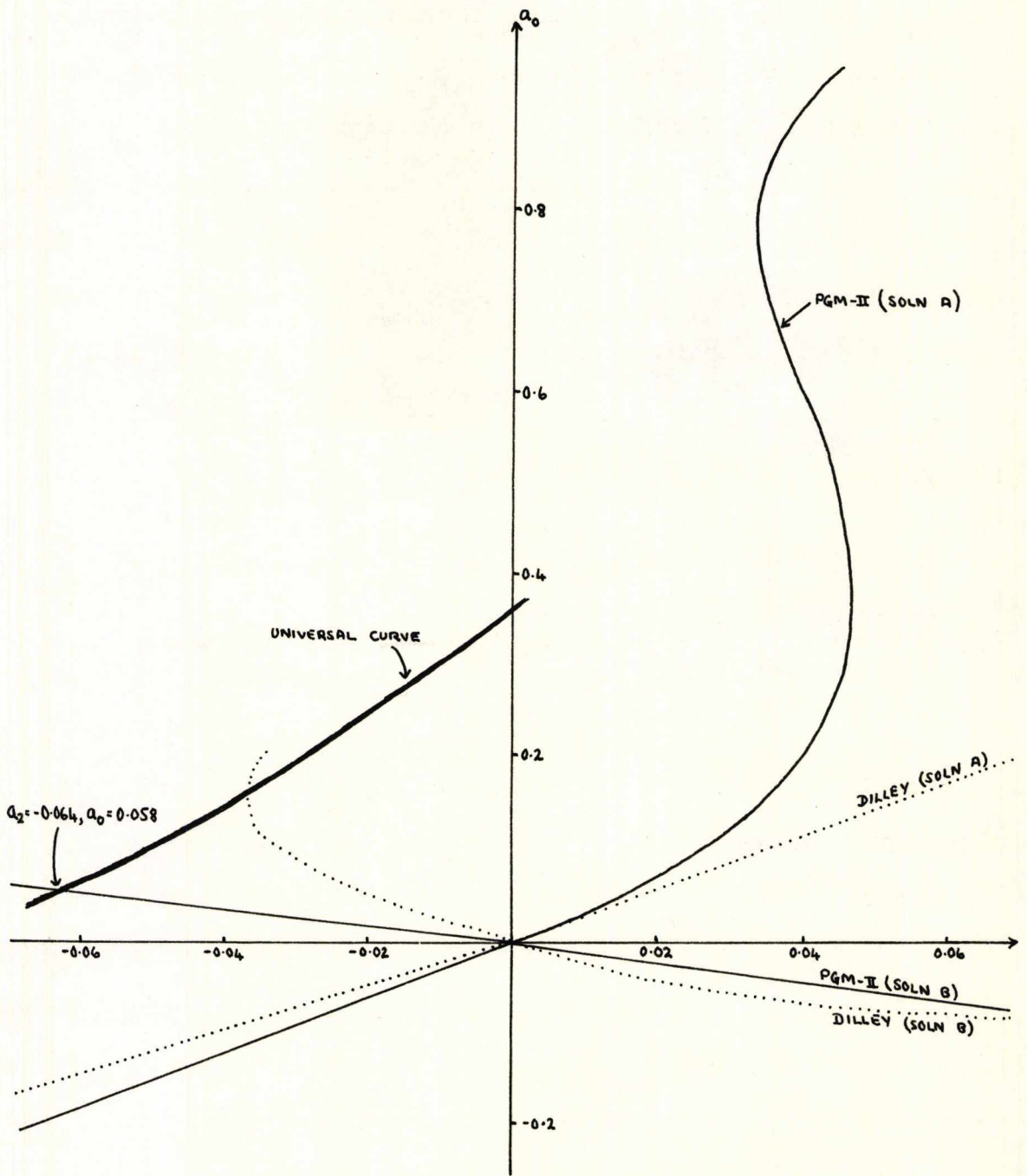


Figure 3.3

$\pi\pi$ s-wave scattering lengths from PGM-II

The obvious questions to ask now are: (i) which of our two solutions, if either, corresponds to physical reality?; and (ii) on what grounds can one reject the unphysical solution? Differences do exist between the two solutions; for example, Figure 3.3 shows that the ratio a_0/a_2 is positive for Solution A and negative for Solution B. However, to compare the properties of each solution more fully it is convenient to define four sub-solutions such that a_0 and a_2 obey the following sign convention:

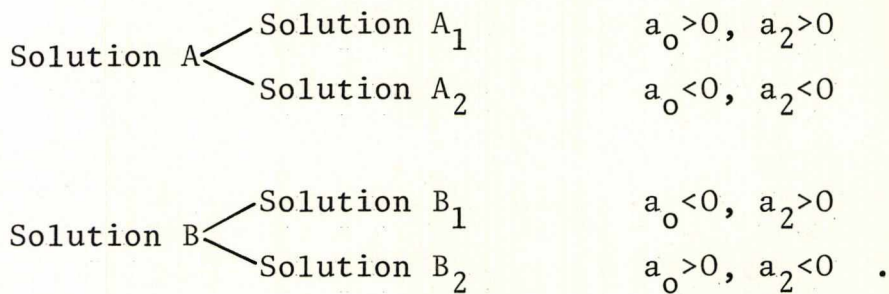


Figure 3.3 also shows that for $0.034 \leq a_2 \leq 0.047$ Solution A₁ has three possible values for a_0 , and therefore three independent sets of parameters which belong to Solution A₁^(a), Solution A₁^(b) and Solution A₁^(c).

The solutions defined above exhibit a wide range of possible values for a_0 and a_1 as is shown in Table 3.3 on the next page. The p-wave scattering length

$$a_1 = \frac{4}{3}c_1 \tag{3.3.36}$$

is obtained from the threshold condition of Equation (2.4.4)

		Solution A ₁	Solution A ₂	Solution B ₁	Solution B ₂
a ₂		0.04	-0.04	0.04	-0.04
a ₀	A ₁ ^(a)	0.18			
	A ₁ ^(b)	0.55	-0.11	-0.05	0.04
	A ₁ ^(c)	0.88			
a ₁	A ₁ ^(a)	0.008			
	A ₁ ^(b)	0.032	-0.001	-0.017	0.015
	A ₁ ^(c)	0.04			
$\frac{a_0}{a_2}$	A ₁ ^(a)	4.50			
	A ₁ ^(b)	13.75	2.75	-1.25	-1.00
	A ₁ ^(c)	22.00			

Table 3.3

$\pi\pi$ S- and P-wave Scattering Lengths from PGM-II

The values given in PGM-I for the s-wave scattering lengths are from Solution A₁^(c). They were obtained by comparing the resulting s-wave phase shifts with known experimental values in the low energy region. This method would appear to be rather unreliable because Equation (3.3.24) cannot be claimed to be a valid representation of the $\pi\pi$ scattering amplitude very far into the physical region. Also, with the exception of δ_0^2 of Solution A₁, all of our s-wave phase shifts either rise or fall

smoothly below 500 MeV, and none of the solutions possess a δ_0^0 which goes through or near 90° anywhere below 1 GeV*.

In the unphysical region, all of our solutions have s- and p-wave amplitudes which are approximately linear, and which saturate the Martin inequalities*. The essential features of the s- and p-wave behaviour in this region are summarised in Table 3.4*.

	Solution A ₁	Solution A ₂	Solution B ₁	Solution B ₂
s ₀	A ₁ ^(a) -			
	A ₁ ^(b) -	-	1.82	2.40
	A ₁ ^(c) -			
s ₂	A ₁ ^(a) 5.4			
	A ₁ ^(b) 6.0	-	0.95	0.48
	A ₁ ^(c) 10.7			
4s ₀ +5s ₂	-	-	12.03	12.00
$\frac{dA_0^0(s)}{ds}$	>0	~0	<0	>0
$\frac{dA_0^2(s)}{ds}$	<0	>0	>0	<0
$\frac{dA_1^1(s)}{ds}$	>0	<0	<0	>0

Table 3.4

Properties of $\pi\pi$ S- and P-wave Amplitudes in $0 \leq s \leq 4$ from PGM-II[†]

*Further details are given in Appendix B3.

[†]The values of s₀ and s₂ in Table 3.4 correspond to the s-wave scattering lengths of Table 3.3.

The most obvious difference between the two solutions in the unphysical region is that whereas a zero exists in each s-wave amplitude of Solution B, no such zeros exist for Solution A. Several arguments have been put forward in favour of the existence of zeros in the s-wave amplitudes in the unphysical region, and it was emphasised earlier that Wanders parametrised the amplitudes so as to force a zero in $A_0^2(s)$ at $s=0$, which eliminates the possibility of him finding a solution which corresponds to Solution A.

Solution B also satisfies several conditions which follow from a linear approximation of the $\pi\pi$ scattering amplitude, and which were derived in the previous section. For example, the s-wave scattering lengths are of opposite signs, and they approximately satisfy the condition $2a_0 - 5a_2 = 18a_1$; the positions of the zeros in the s-wave amplitudes also satisfy the constraint equation $4s_0 + 5s_2 = 12$.

It has been suggested by Olsson⁽²³⁾, and independently by Morgan and Shaw⁽²⁴⁾, that there exists an approximately linear relationship between the $\pi\pi$ s-wave scattering lengths. In Figure 3.3 it is shown that their "universal curve" intersects only Solution B₂.

The evidence produced suggests that Solution B corresponds to the physical solution, and a negative value for the I=2 s-wave scattering length is strongly favoured. The s-wave

phase shifts, for the preferred scattering lengths

$$a_0 = 0.058, \quad a_2 = -0.064$$

which lie on Olsson's universal curve, are shown in Figure 3.4.*

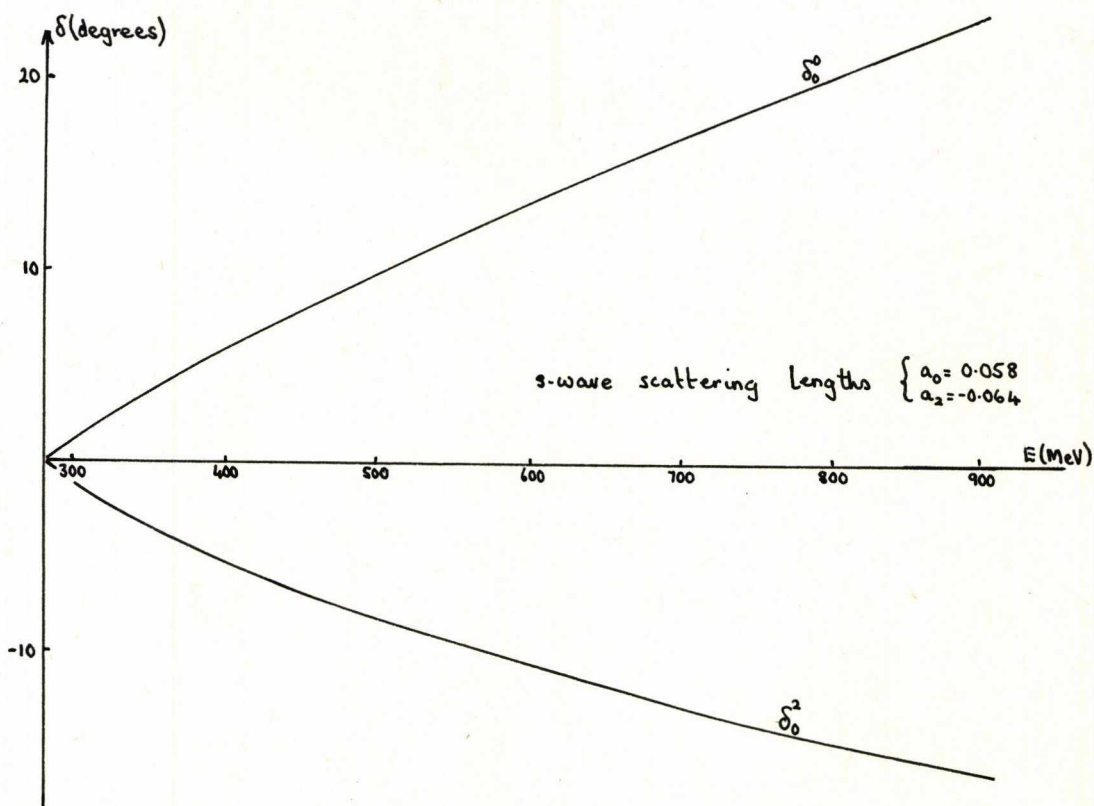


Figure 3.4

$\pi\pi$ s-wave phase shifts from PGM-II Solution B₂

*It seems impossible to establish a precise domain of convergence for the series expansion of PGM-II. However, it is claimed that (3.3.20) is at least valid in the range 0→400 MeV. One would expect the constraints imposed on the model to produce at least a positive δ_0^0 and a negative δ_0^2 which are smoothly varying close to the physical threshold. For the sake of completeness, all phase shifts in this thesis are shown up to about 900 MeV, but it should be emphasised that the models proposed in Chapters 3 and 4 cannot be justified very far into the physical region.

and the behaviour of the s- and p-wave amplitudes in the unphysical region is illustrated in Figure 3.5.

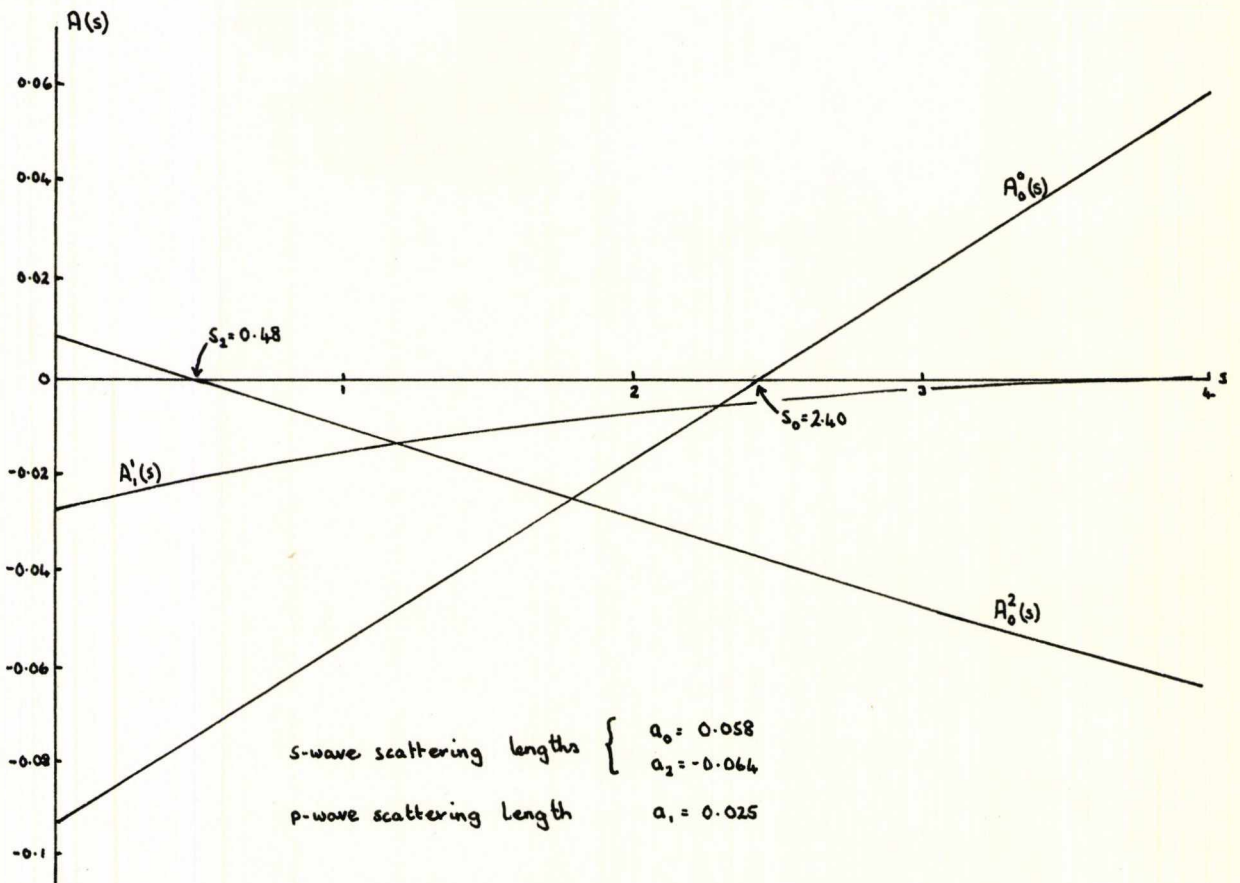


Figure 3.5

$\pi\pi$ S- and P-wave Amplitudes in the Unphysical Region
from PGM-II Solution B_2

The values obtained for the s-wave scattering lengths compare favourably with the results of Wanders. The existence of a small positive value for a_0 , which is common to both models, is governed by s_2 being at, or close to, $s=0$, the constraint equation $4s_0 + 5s_2 = 12$, and the sign of $dA_0^0(s)/ds$ in

the unphysical region*.

4. A MODEL FOR $\pi\pi$ PARTIAL WAVE AMPLITUDES

In the previous section, $\pi\pi$ scattering lengths have been determined by imposing exact crossing symmetry and approximate unitarity on a suitable low energy representation of the total $\pi\pi$ scattering amplitude. It was suggested in Section 2 of this chapter that the Balachandran-Nuyts-Roskies equations, which are integral equalities between partial wave amplitudes in the region $0 \leq s \leq 4$, could be used to constrain amplitudes to be approximately crossing symmetric over this region⁽²⁵⁾. It was also suggested that any $\pi\pi$ partial wave representation, designed to be valid in the unphysical region, should take into account the behaviour of the partial waves at $s=0$ as well as at $s=4$.

A consequence of elastic unitarity and normal threshold behaviour is the particular expansion of $\text{Im } A_{\ell}^I(s)$ in the vicinity of $s=0$, for at this point $A_{\ell}^I(s)$ has a square-root singularity, and can be expanded by⁽²⁶⁾

$$A_{\ell}^I(s) = a_{\ell}^I + b_{\ell}^I s + c_{\ell}^I s^{3/2} + \dots \quad (3.4.1)$$

where the coefficients associated with the $s^{3/2}$ terms are related via crossed-channel unitarity constraints to non-linear

*If s_2 is fixed at $s=1.5$, we obtain $a_0=0.19$, $a_2=-0.064$ for the s-wave scattering lengths, and $s_0=1.03$ for the position of the $I=0$ s-wave zero. Equation (3.3.14) is again approximately satisfied.

combinations of the s-wave scattering lengths. Elastic unitarity requires

$$\left. \begin{aligned} \operatorname{Re} A^{\text{I}}(s) &\approx (s-4)^{\ell} \\ \operatorname{Im} A^{\text{I}}(s) &\approx (s-4)^{(4\ell+1)/2} \end{aligned} \right\} \quad (3.4.2)$$

in the neighbourhood of $s=4$. Combining (3.4.1) and (3.4.2) a suitable representation for the $\pi\pi$ s- and p-wave amplitudes in the unphysical region is given by

$$\left. \begin{aligned} A_0^{\text{O}}(s) &= a_0^{\text{S}} + b_0^{\text{S}}s + c_0^{\text{S}}s^{3/2} + \sqrt{4-s}(z_0^{\text{S}} + y_0^{\text{S}}(4-s)) \\ A_1^{\text{1}}(s) &= b_1^{\text{P}}(s-4) + c_1^{\text{P}}(s^{3/2} - 8) \\ A_2^{\text{O}}(s) &= a_2^{\text{S}} + b_2^{\text{S}}s + c_2^{\text{S}}s^{3/2} + \sqrt{4-s}(z_2^{\text{S}} + y_2^{\text{S}}(4-s)) \end{aligned} \right\} \quad (3.4.3)$$

with the corresponding scattering lengths

$$\left. \begin{aligned} a_0 &= a_0^{\text{S}} + 4b_0^{\text{S}} + 8c_0^{\text{S}} \\ a_1 &= 4(b_1^{\text{P}} + 3c_1^{\text{P}}) \\ a_2 &= a_2^{\text{S}} + 4b_2^{\text{S}} + 8c_2^{\text{S}} \end{aligned} \right\} \quad (3.4.4)$$

defined such that each partial wave amplitude satisfies the normal threshold condition of (2.4.4). The p-wave amplitude is real for $s \geq 4$ and is, therefore, non-unitary in the direct channel. If, however, unitarity is imposed on $A_1^{\text{1}}(s)$ in the crossed-channel, one obtains

$$c_1^{\text{P}} = -\frac{1}{18}a_0^2 + \frac{5}{36}a_2^2 \quad (3.4.5)^*$$

*This equation is derived in Appendix A4.

where a_0 and a_2 are defined by (3.4.4). c_0^S and c_2^S are likewise determined by imposing crossed-channel unitarity on the s-wave amplitudes,

$$c_0^S = \frac{1}{18}a_0^2 + \frac{5}{18}a_2^2 \quad (3.4.6)^*$$

$$c_2^S = \frac{1}{18}a_0^2 + \frac{1}{36}a_2^2 \quad (3.4.7)^*$$

which leads to the linear relation

$$2c_0^S - 3c_1^P - 5c_2^S = 0 \quad (3.4.8)$$

between the coefficients of (3.4.3).

Our aim is to find solutions of (3.4.3) which are approximately crossing symmetric and unitary over the threshold region, and from which one can obtain reliable information about the low energy $\pi\pi$ parameters, in particular, scattering lengths and positions of s-wave zeros, if they exist.

It is impossible for the s-wave amplitudes of (3.4.3) to satisfy exactly the elastic unitarity condition

$$\text{Im } A_\ell^I(s) = \sqrt{\frac{s-4}{s}} |A_\ell^I(s)|^2 \quad (3.4.9)$$

for all values of s in the region $4 \leq s \leq 16$. The best one can hope to do is satisfy (3.4.9) as accurately as possible over the region where the parametrisation is designed to be valid.

*These equations are derived in Appendix A4.

For example, in the model PGM-II described in the previous section, elastic unitarity is imposed on the s-wave amplitudes and their first derivatives at $s=4$. Each s-wave amplitude is then exactly unitary at the physical threshold, and if the parametrisation is well-behaved in the neighbourhood of $s=4$, it is hoped that (3.4.9) is approximately satisfied elsewhere in the low energy region*.

A more flexible method is to impose elastic unitarity on each s-wave amplitude at a series of points $s=s', s'', s''', \dots$ in the region where the parametrisation is designed to be valid. In principle, there is no restriction on the number of constraint equations that could be imposed in this way; in practice, though, (3.4.3) involves twelve coefficients, three of which, as we have seen, can be determined from crossed-channel unitarity constraints, and another five, we shall see, can be determined from the Balachandran-Nuyts-Roskies relations involving only s- and p-waves. This leaves four coefficients which are conveniently determined by imposing elastic unitarity on the s-wave amplitudes of (3.4.3) at two independent values of s , say $s=s'$ and $s=s''$, in the region where the parametrisation is valid. In this way, the constraint equations at $s=s'$

$$\left. \begin{aligned} -\sqrt{s'} \left(z_0^S - (s'-4)y_0^S \right) &= \left[\left(a_0^S + b_0^S s' + c_0^S s'^{3/2} \right)^2 + (s'-4) \left(z_0^S - (s'-4)y_0^S \right)^2 \right] \\ -\sqrt{s'} \left(z_2^S - (s'-4)y_2^S \right) &= \left[\left(a_2^S + b_2^S s' + c_2^S s'^{3/2} \right)^2 + (s'-4) \left(z_2^S - (s'-4)y_2^S \right)^2 \right] \end{aligned} \right\} \quad (3.4.10)$$

*A measure of elastic unitarity violation in PGM-II is given in Appendix B3.



and at $s=s''$

$$\left. \begin{aligned} -\sqrt{s''} \left(z_0^S - (s''-4)y_0^S \right) &= \left[\left[a_0^S + b_0^S s'' + c_0^S s''^{3/2} \right]^2 + (s''-4) \left[z_2^S - (s''-4)y_2^S \right]^2 \right] \\ -\sqrt{s''} \left(z_2^S - (s''-4)y_2^S \right) &= \left[\left[a_2^S + b_2^S s'' + c_2^S s''^{3/2} \right]^2 + (s''-4) \left[z_2^S - (s''-4)y_2^S \right]^2 \right] \end{aligned} \right\}$$

(3.4.11)

determine the coefficients z_0^S , z_2^S , y_0^S and y_2^S , once the other coefficients are known. Suitable values for s' and s'' will be discussed in the next section.

The five remaining coefficients a_0^S , b_0^S , a_2^S , b_2^S and b_1^P , are determined by requiring the coefficients of (3.4.3) to satisfy the Balachandran-Nuyts-Roskies relations

$$\left. \begin{aligned} \int_0^4 (4-s)(3s-4)(A_0^0(s) + 2A_0^2(s)) ds &= 0 \\ \int_0^4 (4-s)(2A_0^0(s) - 5A_0^2(s)) ds &= 0 \\ \int_0^4 s(4-s)(2A_0^0(s) - 5A_0^2(s)) ds + 3 \int_0^4 (4-s)^2 A_1^1(s) ds &= 0 \\ \int_0^4 s(4-s)^2 (2A_0^0(s) - 5A_0^2(s)) ds + 3 \int_0^4 s(4-s)^2 A_1^1(s) ds &= 0 \\ \int_0^4 s(4-s)^3 (2A_0^0(s) - 5A_0^2(s)) ds + 3 \int_0^4 s(4-s)^2 (3s-4) A_1^1(s) ds &= 0 \end{aligned} \right\}$$

(3.4.12)

which lead to a set of five linearly independent equations between the coefficients of (3.4.3).*

*The result of evaluating the integrals is given in Appendix C3.

Attempts to find a simultaneous solution of the twelve constraint equations consistent with the properties of crossing symmetry and unitarity defined above failed. Further investigation revealed that (3.4.8) is approximately a linear combination of the constraint equations which follow from crossing symmetry, and is therefore redundant. A simple solution to this problem is to relax one of the crossed-channel unitarity conditions; since the sign of c_1^p depends upon the absolute values of the s-wave scattering lengths and c_0^s and c_2^s are both positive with $c_0^s > c_2^s$, it would appear that (3.4.7) is the least important of the crossed-channel unitarity equations, and is therefore relaxed*. A method of solving this type of system of linear and non-linear simultaneous equations has been outlined in the previous section. The necessary amendments to the computer program, which are a consequence of solving a different set of equations, are described in Appendix C3.

*Alternatively, we could have chosen to relax one of the crossing symmetry conditions which follow from (3.4.12). However, since crossing symmetry appears to be such a strong constraint we prefer the method described in the text.

5. THE NUMERICAL RESULTS

Since the representation of the $\pi\pi$ partial wave amplitudes is designed to be valid in the region $0 \leq s \leq 4$ and we wish to determine $\pi\pi$ scattering lengths, one obvious place to impose elastic unitarity is at $s=4$. Equation (3.4.10) then simplifies to

$$\left. \begin{aligned} z_0^s &= -\frac{a_0^2}{2} \\ z_2^s &= -\frac{a_2^2}{2} \end{aligned} \right\} \quad (3.5.1)$$

If s'' is then chosen close enough to the physical threshold, the method of imposing elastic unitarity is equivalent to PGM-II, that is, each s-wave amplitude and its first derivative satisfies (3.4.8) at $s=4$.

For $-0.07 \leq a_2 \leq 0.07$ and $s''=4.001$ two independent solutions, DCB-I Solution A and DCB-I Solution B, have been found*. The values obtained for a_0 are compared with the results of PGM-II in Figure 3.6 on the next page. It is seen that, for $-0.0645 \leq a_2 \leq -0.039$, DCB-I Solution B_2 has two possible values for a_0 ; the smaller value belongs to Solution $B_2^{(a)}$, and the larger value to Solution $B_2^{(b)}$. The essential properties of each solution in the threshold region, which correspond to either $a_2=0.05$ or $a_2=-0.05$, are summarised in Table 3.5 on page 106.

*These solutions are defined by $a_0/a_2 > 0$ and $a_0/a_2 < 0$ as in PGM-II.

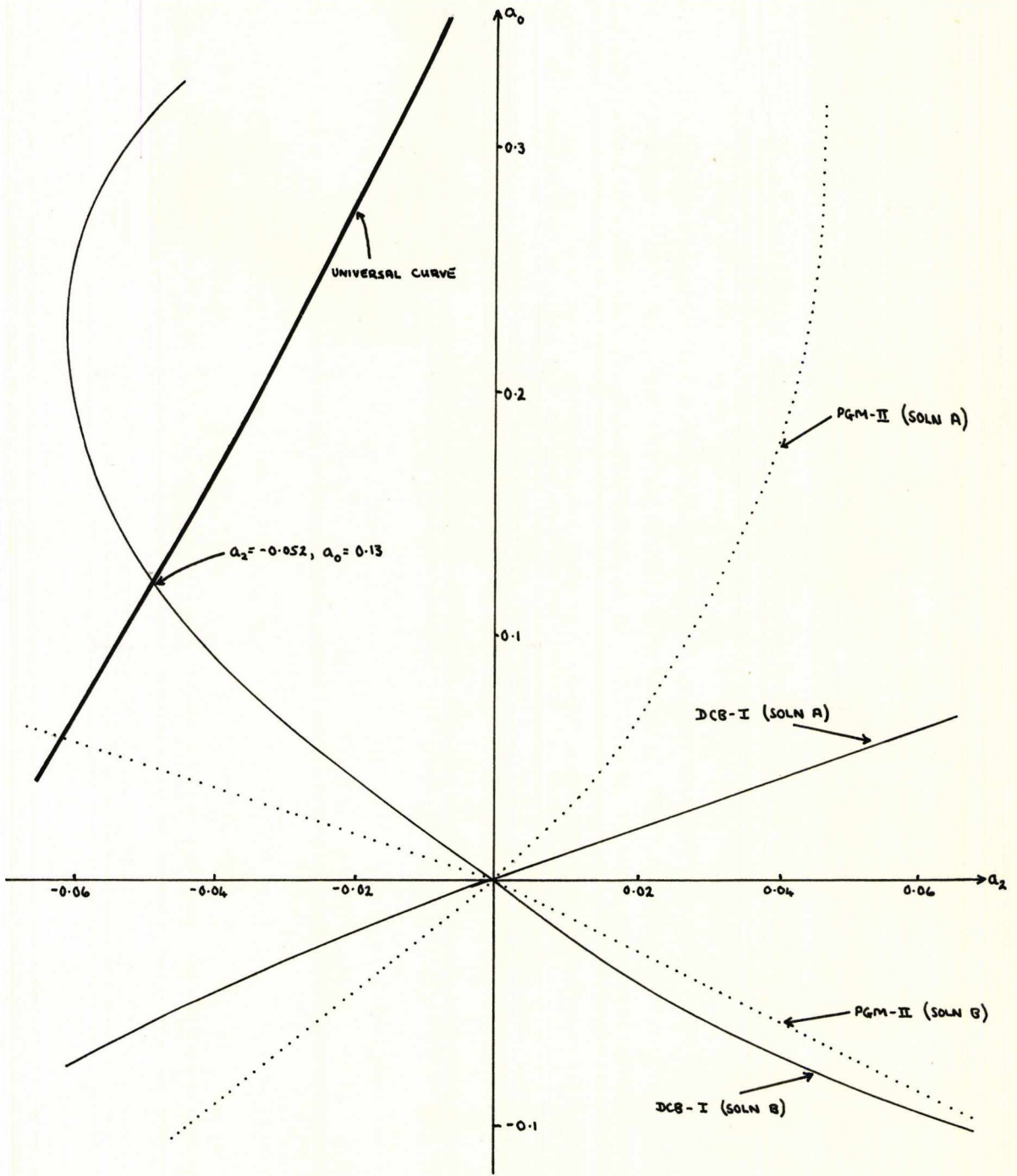


Figure 3.6

$\pi\pi$ s-wave scattering lengths from DCB-I

	Solution A ₁	Solution A ₂	Solution B ₁	Solution B ₂	
a ₂	0.05	-0.05	0.05		-0.05
a ₀	0.057	-0.06	-0.078	B ₂ ^(a)	0.123
				B ₂ ^(b)	0.320
a ₁	-0.007	0.008	-0.023	B ₂ ^(a)	0.026
				B ₂ ^(b)	0.025
$\frac{a_0}{a_2}$	1.14	1.20	-1.56	B ₂ ^(a)	-2.46
				B ₂ ^(b)	-6.40
s ₀	-	-	1.47	B ₂ ^(a)	1.36
				B ₂ ^(b)	0.38
s ₂	-	-	1.22	B ₂ ^(a)	1.32
				B ₂ ^(b)	1.92
4s ₀ +5s ₂	-	-	11.98	B ₂ ^(a)	12.04
				B ₂ ^(b)	11.12
$\frac{dA_0^0(s)}{ds}$	<0	>0	<0	B ₂ ^(a)	>0
				B ₂ ^(b)	>0
$\frac{dA_0^2(s)}{ds}$	>0	<0	>0	B ₂ ^(a)	<0
				B ₂ ^(b)	<0
$\frac{dA_1^1(s)}{ds}$	<0	>0	<0	B ₂ ^(a)	>0
				B ₂ ^(b)	>0

Table 3.5

Properties of $\pi\pi$ S- and P-wave Amplitudes in $0 \leq s \leq 4$ from DCB-I*

*Further details are given in Appendix C3.

Solution B exhibits the same characteristics as Solution B of PGM-II and, for the reasons discussed in Section 3, is again preferred as the physical solution. For negative values of a_2 it is necessary to distinguish between values of a_0 belonging to Solutions $B_2^{(a)}$ and $B_2^{(b)}$. The ratio

$$\frac{a_0}{a_2} = -3.1 \pm 1.1 \quad (3.5.2)$$

of Equation (2.3.13), which has been suggested by recent experimental analyses, is satisfied by Solutions $B_2^{(a)}$ and $B_2^{(b)}$ for s-wave scattering lengths lying within the range

$$-0.039 \geq a_2 \geq -0.0645, \quad 0.08 \leq a_0 \leq 0.26.$$

The preferred solution, which lies on Olsson's universal curve, is from Solution $B_2^{(a)}$; its s-wave scattering lengths

$$a_2 = -0.052, \quad a_0 = 0.13$$

are in the ratio $a_0/a_2 = -2.50$.

The behaviour of the corresponding s- and p-wave amplitudes in the unphysical region is shown in Figure 3.7 on the next page; the s-wave zeros, at $s_0=1.35$ and $s_2=1.33$ satisfy $4s_0+5s_2=12$ to within 1%.

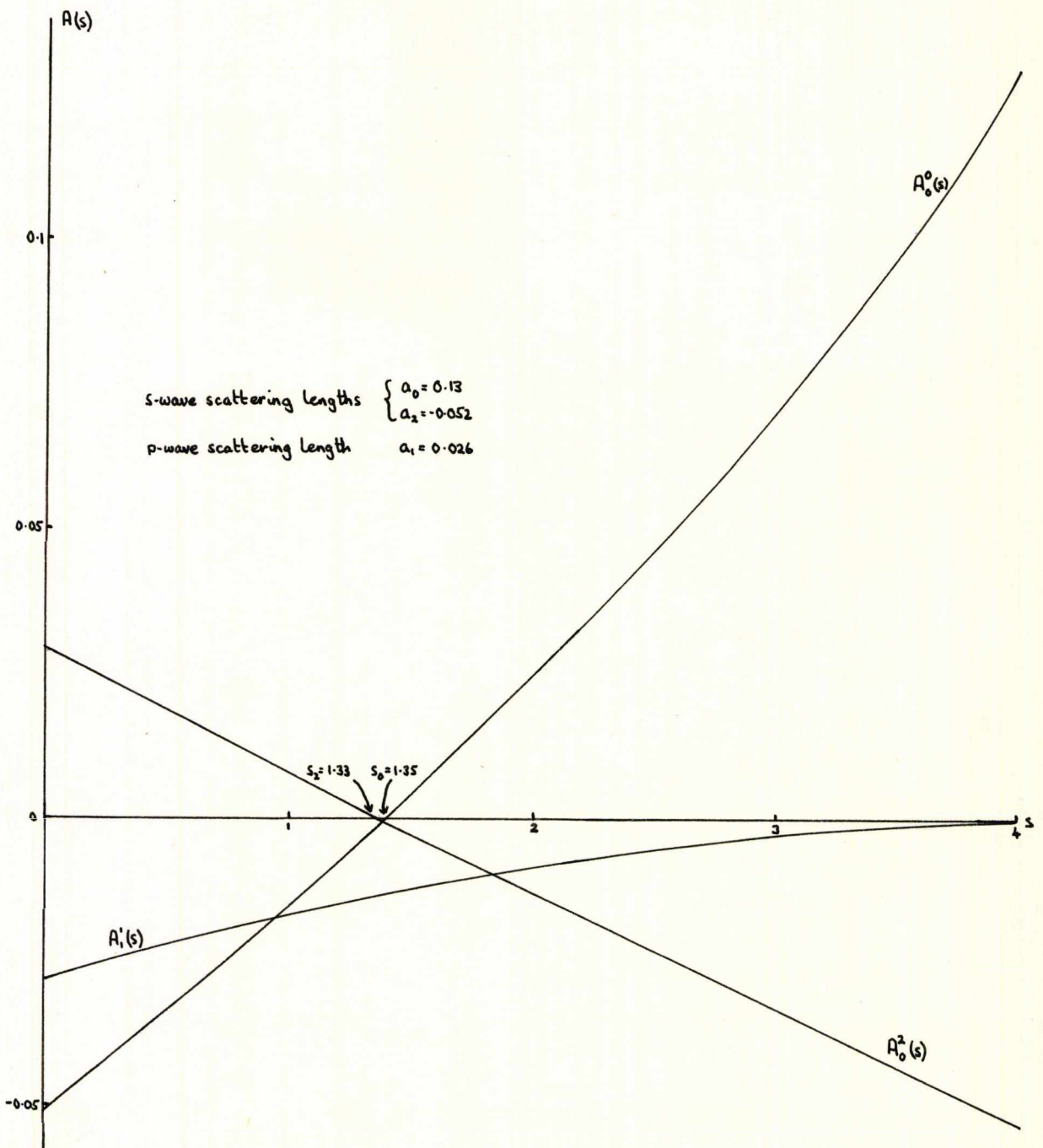


Figure 3.7

Behaviour of the S- and P-wave Amplitudes in $0 \leq s \leq 4$
from DCB-I Solution $B_2^{(a)}$

Although the $I=2$ s-wave phase shift (see Figure 3.8) is small and negative and in satisfactory agreement with the theoretical predictions of Morgan and Shaw⁽²⁴⁾, the range of validity of (3.4.3) is such that we cannot obtain any direct information on the possible existence of an $I=0$ s-wave resonance.

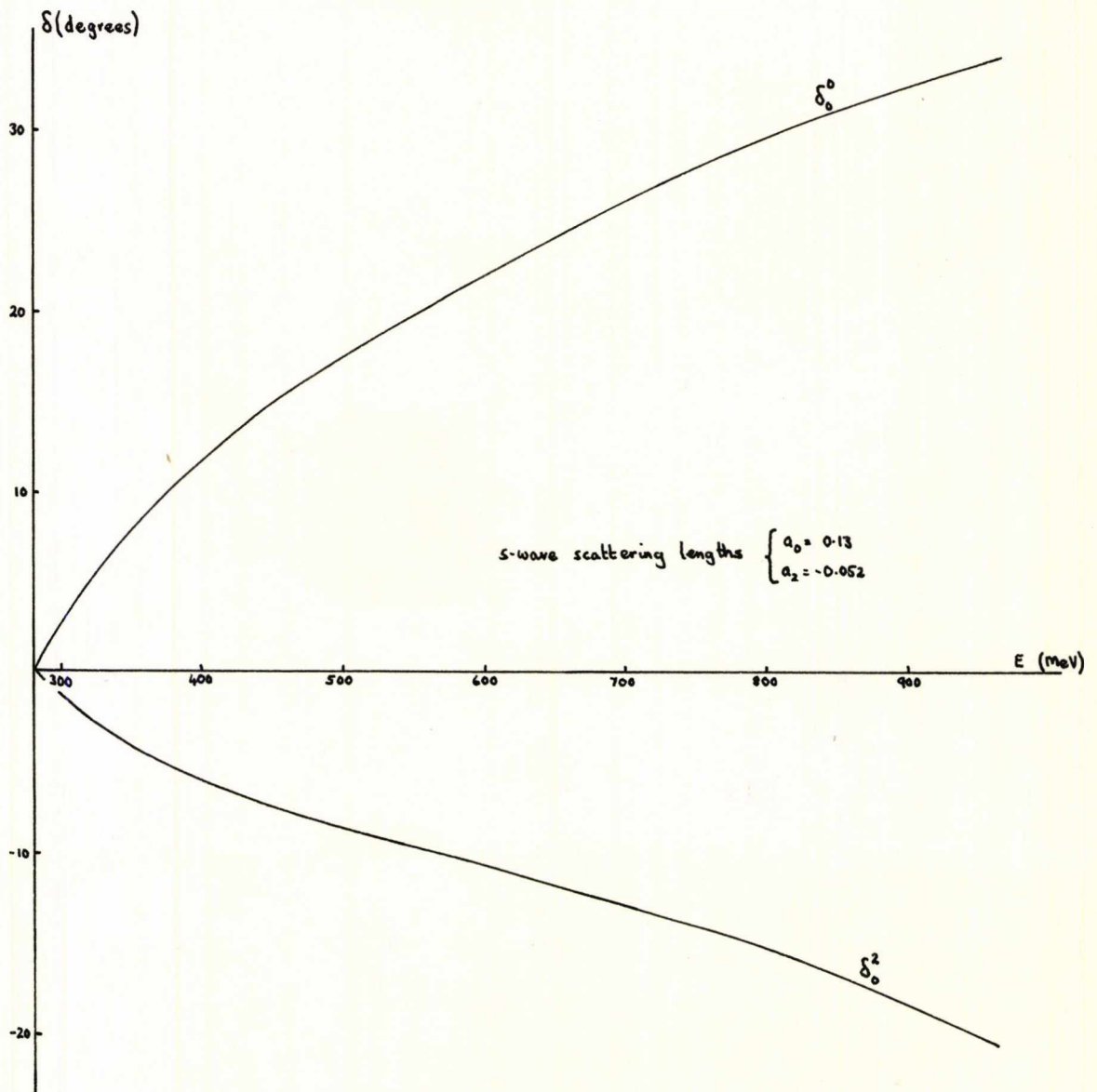


Figure 3.8

$\pi\pi$ S-wave Phase Shifts from DCB-I Solution $B_2^{(a)}$

Finally, we investigate the consequences of choosing s'' other than close to the physical threshold. Although the elastic unitarity condition of Equation (3.4.9) holds for all values of s in the range $4 \leq s \leq 16$, it is found that for $a_2 = -0.052$ and $s'' > 4.85$ a simultaneous solution of the system of equations does not exist. However, since (3.4.3) is only designed to be valid in the unphysical region, it is assumed that (3.4.10) can be imposed for values of s'' in the region $0 < s \leq 4^*$. For $a_2 = -0.052$ the behaviour of a_0 for $1 \leq s'' \leq 4.85$ is illustrated in Figure 3.9.

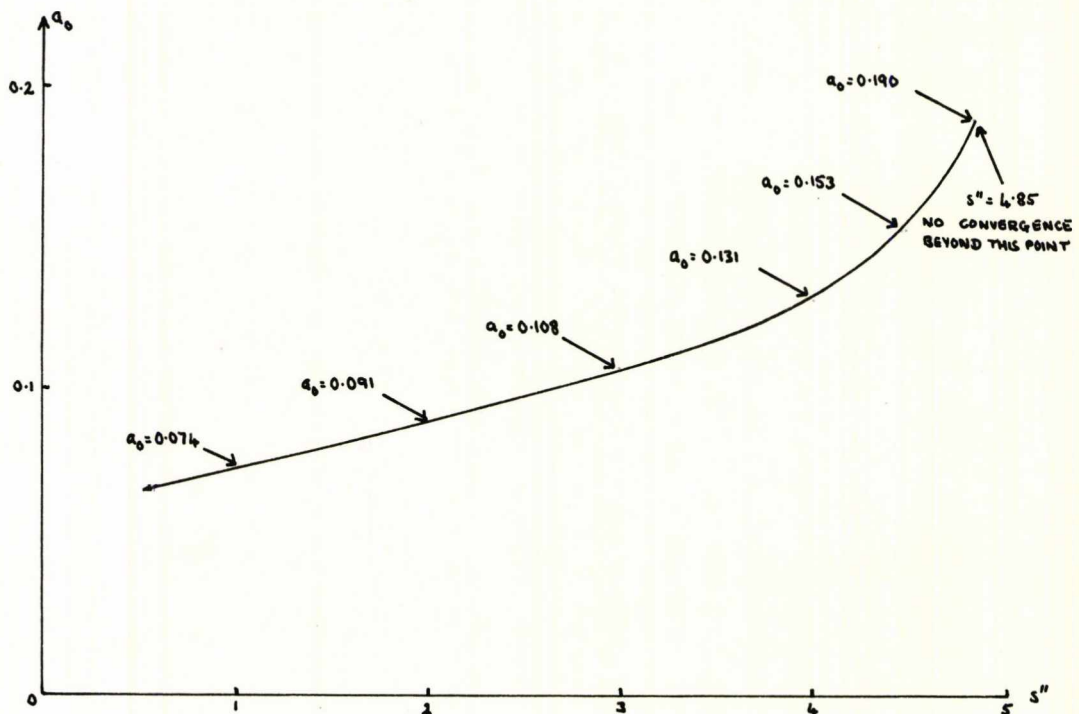


Figure 3.9

Values of a_0 for $a_2 = -0.052$, $s' = 4$, $1 \leq s'' \leq 4.85$
 from DCB-I Solution $B_2^{(a)}$

* Since $\sqrt{s''-4/s''}$ is infinite at $s''=0$, elastic unitarity can never be satisfied at $s''=0$.

The properties of the partial wave amplitudes are unaltered by variations in s'' ; for example, approximate linearity of the s- and p-wave amplitudes in the unphysical region is preserved, as are all the Martin inequalities. Specific changes in the values of the low energy parameters are recorded in Table 3.6.

s''	a_0	s_0	s_2	$4s_0+5s_2$
1.0	0.074	1.97	0.82	11.98
2.0	0.091	1.75	1.01	12.05
3.0	0.108	1.57	1.15	12.03
4.001	0.131	1.36	1.32	12.04
4.5	0.154	1.19	1.46	12.06

Table 3.6

Low Energy $\pi\pi$ Parameters for $a_2 = -0.052$, $1 \leq s'' \leq 4.85$

from DCB-I Solution $B_2^{(a)}$

The percentage violation of s-wave elastic unitarity at various points in the physical region, for values of s'' in

the range $1 \leq s'' \leq 4.85$ are presented in Table 3.7. The results indicate that there is no virtue in choosing s'' in the unphysical region, although values of s'' in the physical region can "improve" upon elastic unitarity violation in the low energy region. The upper limit of $s''_{\max} = 4.85$ imposes an upper bound on the $I=0$ s-wave scattering length of $a_0 < 0.19$ for $a_2 = -0.052^*$.

s'' Energy in MeV	1.0		3.0		4.001		4.5	
	I=0	I=2	I=0	I=2	I=0	I=2	I=0	I=2
284	11.3	3.1	2.5	1.1	0.4	0.2	0.5	0.3
291	20.3	5.9	5.0	2.3	1.3	0.6	0.3	0.2
298	27.6	8.5	7.5	3.5	2.6	1.3	0.4	0.2
305	-	10.9	9.9	4.8	4.0	2.1	1.5	0.8
312	-	13.1	12.3	6.0	5.6	2.9	2.8	1.4
326	-	17.9	17.7	9.0	9.9	5.2	6.6	3.3
340	-	22.0	22.5	11.8	14.1	7.4	10.6	5.3
355	-	25.4	26.7	14.4	18.0	9.6	14.6	7.3
368	-	28.5	-	16.8	21.8	11.8	18.4	9.2
381	-	-	-	19.0	25.1	13.6	21.9	10.9
393	-	-	-	20.9	28.3	15.4	25.2	12.5

Table 3.7

Percentage Violation of S-wave Elastic Unitarity in the
Very Low Energy Region for $a_2 = -0.052$, $1 \leq s'' \leq 4.5$
from DCB-I Solution $B_2^{(a)\dagger}$

*For DCB-I Solution $B_2^{(a)}$, if $a_2 > -0.052$ then $s''_{\max} > 4.85$ whereas if $a_2 < -0.052$ then $s''_{\max} < 4.85$.

†Percentages >30% are not shown in the table.

6. CONCLUSION AND COMMENTS

Using only constraints imposed by the requirements of analyticity, crossing symmetry and elastic unitarity, two distinct types of pion-pion scattering amplitudes have been shown to exist. The unphysical solution corresponds approximately to the 's-wave dominant' solution, originally found by Chew, Mandelstam and Noyes⁽²⁷⁾ more than a decade ago. This solution can only be rejected using assumptions which do not follow from either crossing symmetry or unitarity. The physical solution has scattering lengths in agreement with other theoretical estimates, and although no current algebra is used in the model, the zeros in the s-wave amplitudes closely resemble the Adler zeros which follow from the hypothesis of PCAC.

Although the models studied do not provide any reliable information about the intermediate energy region, we gain from two important aspects. Firstly, physical assumptions, namely the value of the $I=2$ s-wave scattering length, are kept to a minimum, which results in a greater generality than has been obtained in many previous theoretical investigations. This produces the extra solutions and enables us to see why they were excluded before as well as clarifying certain other aspects of previous models. Secondly, in limiting the range of applicability we feel that we improve on the accuracy of the s-wave behaviour in the unphysical region.

REFERENCES

1. J. L. BASDEVANT, " $\pi\pi$ Theories" Springer Tracts in Modern Physics 61, 1 (1972).
2. G. WANDERS and O. PIGUET, Nuovo Cimento 56A, 417 (1968).
G. AUBERSON, O. PIGUET and G. WANDERS, Phys. Letts. 28B, 41 (1968).
3. B. BONNIER, Nuclear Physics B10, 467 (1969); B17, 525 (1970).
4. D. ATKINSON, Nuclear Physics B7, 375 (1968); B8, 377 (1968); B13, 415 (1969); B23, 397 (1970).
see also
J. KUPSCH, Nuclear Physics B11, 573 (1969); B12, 155 (1969);
Nuovo Cimento 66A, 202 (1970).
5. J. DILLEY, Nuclear Physics B25, 227 (1971).
6. G. F. CHEW and S. MANDELSTAM, Phys. Rev. 119, 467 (1960);
Nuovo Cimento 19, 752 (1961).
7. Y. S. JIN and A. MARTIN, Phys. Rev. 135B, 1369 (1964).
8. G. AUBERSON, Nuovo Cimento 68A, 281 (1970).
9. A. K. COMMON, Nuovo Cimento 53A, 946 (1968).
10. A. MARTIN, Nuovo Cimento 47A, 265 (1967).
11. B. BONNIER and R. VINH MAU, Phys. Rev. 165, 1923 (1968).
12. A. K. COMMON, Nuovo Cimento 63A, 451 (1969).
13. G. AUBERSON, O. BRANDER, G. MAHOUX and A. MARTIN, Nuovo Cimento 65A, 743 (1970).
14. A. MARTIN, Nuovo Cimento 58A, 303 (1968).
15. J. L. BASDEVANT, G. COHEN-TANNOUDJI and A. MOREL, Nuovo Cimento 64A, 585 (1969).

REFERENCES

16. A. P. BALACHANDRAN and J. NUYTS, Phys. Rev. 172, 1821 (1968).
17. R. ROSKIES, Phys. Letts. 30B, 42 (1969); Journal of Mathematical Physics 11, 482 (1970).
18. R. ROSKIES, Nuovo Cimento 65A, 467 (1970).
19. M. R. PENNINGTON and P. POND, Nuovo Cimento 3A, 548 (1971).
20. J. ILIOPOULOS, Nuovo Cimento 52A, 192 (1967); 53A, 552 (1968).
21. P. R. GRAVES-MORRIS, Phys. Rev. 177, 285 (1969).
22. J. HAWGOOD, "Numerical Methods in Algol" published by McGraw-Hill (1965) pp.63-65.
23. M. G. OLSSON, University of Wisconsin preprint C00-270 (January, 1970).
24. D. MORGAN and G. SHAW, Phys. Rev. D2, 520 (1970).
25. The Balachandran-Nuyts-Roskies relations have since been used to constrain many models to be approximately crossing symmetric in the unphysical region. See, for example
B. BONNIER and P. GAURON, Nuclear Physics B21, 465 (1970).
J. S. KANG and B. W. LEE, Phys. Rev. D3, 2814 (1971).
K. KANG, M. LACOMBE and R. VINH MAU, Phys. Rev. D4, 3005 (1971).
26. For a proof of the existence of this type of expansion at $s=0$, see the Appendix of
G. WANDERS and O. PIGUET, Nuovo Cimento 56A, 417 (1968).
27. G. F. CHEW, S. MANDELSTAM and H. P. NOYES, Phys. Rev. 119, 478 (1960).

CHAPTER 4

I. INTRODUCTION

Restrictions on the behaviour of the $\pi\pi$ d-wave amplitudes in the unphysical region follow from a few Martin-type constraint equations involving the $\pi^0\pi^0$ s- and d-waves at points in the region $0 \leq s \leq 4$ ⁽¹⁾, and also from the Balachandran-Nuyts-Roskies relations between the s- p- and d-wave amplitudes. Although estimates of the d-wave scattering lengths have been obtained in several recent model-dependent analyses⁽²⁾, it would be highly instructional if, for example, the model DCB-I introduced in the previous chapter could be extended to include the $\pi\pi$ d-waves.

It is a feature of all self-consistent models that one assumes that the self-consistency is not generated by either numerical or theoretical approximations. A d-wave model would necessitate terms in the partial wave parametrisations up to order s^2 and possibly higher, but since one does not know a priori at what order the parametrisation is a good approximation to the amplitude in the unphysical region, one would feel much more at ease with the results if the higher order terms could be calculated and compared with the lower order terms.

In the next section DCB-I is extended to include the $\pi\pi$ d-waves; the model is accordingly renamed DCB-II. Values obtained for the d-wave scattering lengths and the behaviour of the d-wave amplitudes in the unphysical region are described in Section 3.

2. A MODEL FOR $\pi\pi$ S- P- AND D-WAVES (DCB-II)

To introduce d-waves into DCB-I it is convenient to include terms up to the order $s^{5/2}$ in the partial wave expansions.* Following (3.4.2) and (3.4.3) the s- p- and d-wave amplitudes become

$$\left. \begin{aligned} A_0^I(s) &= a_I^S + b_I^S s + c_I^S s^{3/2} + d_I^S s^2 + e_I^S s^{5/2} + \sqrt{4-s} (z_I^S + y_I^S (4-s) + x_I^S (4-s)^2) \\ A_1^I(s) &= b_1^P (s-4) + c_1^P (s^{3/2} - 8) + d_1^P (s^2 - 16) + e_1^P (s^{5/2} - 32) + x_1^P (4-s)^{5/2} \\ A_2^I(s) &= c_I^d (s^{3/2} - 3s + 4) + d_I^d (s-4)^2 + e_I^d (s^{5/2} - 20s + 48) \end{aligned} \right\} \quad \text{(where } I=0,2) \quad (4.2.1)$$

respectively, and their corresponding scattering lengths

$$\left. \begin{aligned} a_{0I} &= a_I^S + 4b_I^S + 8c_I^S + 16d_I^S + 32e_I^S \\ a_{11} &= 4(b_1^P + 3c_1^P + 8d_1^P + 20e_1^P) \\ a_{2I} &= 8\left(\frac{3}{8}c_I^d + 2d_I^d + \frac{15}{2}e_I^d\right) \end{aligned} \right\} \quad \text{(where } I=0,2) \quad (4.2.2)$$

satisfy the threshold condition of Equation (3.4.2). Once again, (4.2.1) is claimed to be a valid representation of the $\pi\pi$ partial wave amplitudes at least in the region $0 \leq s \leq 4$, although the d-waves are real and therefore non-unitary above $s=4$.

*Terms up to order s^2 in the parametrisations are sufficient to introduce d-waves into the model. However, at this order additional constraint equations follow from crossing symmetry alone. The presence of $s^{5/2}$ terms in the expansions allows one to impose additional unitarity constraints on the model as well.

The behaviour of these amplitudes at the beginning of the left-hand cut can be obtained by expanding the unitarity equation as a Taylor series about the point $s=4^*$; the resulting constraint equations for c_0^S , c_2^S and c_1^D have been given in Equations (3.4.5)-(3.4.7) and remain unaltered. The additional constraint equations which verify crossed-channel unitarity to order $(-s)^{5/2}$ can be written as

$$\left. \begin{aligned}
 c_0^d &= c_0^s \equiv c_0^{s,d} \\
 c_2^d &= c_2^s \equiv c_2^{s,d} \\
 e_0^s &= \frac{13}{240} \left(\frac{1}{3} a_{00}^2 + \frac{5}{3} a_{02}^2 \right) - \frac{1}{10} \left(\frac{1}{3} \alpha_0 + \frac{5}{3} \alpha_2 \right) \\
 e_2^s &= \frac{13}{240} \left(\frac{1}{3} a_{00}^2 + \frac{1}{6} a_{02}^2 \right) - \frac{1}{10} \left(\frac{1}{3} \alpha_0 + \frac{1}{6} \alpha_2 \right) \\
 e_1^p &= -\frac{7}{80} \left(\frac{1}{3} a_{00}^2 - \frac{5}{6} a_{02}^2 \right) + \frac{1}{10} \left(\frac{1}{3} \alpha_0 - \frac{5}{6} \alpha_2 \right) \\
 e_0^d &= \frac{37}{240} \left(\frac{1}{3} a_{00}^2 + \frac{5}{3} a_{02}^2 \right) - \frac{1}{10} \left(\frac{1}{3} \alpha_0 + \frac{5}{3} \alpha_2 \right) \\
 e_2^d &= \frac{37}{240} \left(\frac{1}{3} a_{00}^2 + \frac{1}{6} a_{02}^2 \right) - \frac{1}{10} \left(\frac{1}{3} \alpha_0 + \frac{1}{6} \alpha_2 \right)
 \end{aligned} \right\} (4.2.3)^\dagger$$

where

$$\begin{aligned}
 \alpha_I &\equiv \left. \frac{d}{ds} |A_0^I(s)|^2 \right|_{s=4} \\
 &= 2a_{0I}^s (b_I^s + 3c_I^{s,d} + 8d_I^s + 20e_I^s) + z_I^{s^2}
 \end{aligned}$$

*It is assumed also that the effect of the remainder of the left-hand cut is negligible when determining the behaviour of the partial waves in the region $[0,4]$.

†For details of derivation, see Appendix A4.

If the p-wave amplitude satisfies elastic unitarity at $s=4$, x_1^p is defined explicitly in terms of the p-wave scattering length according to

$$x_1^p = -\frac{1}{32} a_{11}^2 . \quad (4.2.4)$$

Imposing elastic unitarity on the s-wave amplitudes to third order yields the constraint equations

$$\left. \begin{aligned} z_I^s &= -\frac{1}{2} a_{0I}^2 \\ -z_I^s + 8y_I^s &= 2a_{0I} (4b_I^s + 12c_I^{s,d} + 32d_I^s + 80e_I^s) + 4z_I^{s^2} \\ \frac{z_I^s}{4} + 4y_I^s - 32x_I^s &= (4b_I^s + 12c_I^{s,d} + 32d_I^s + 80e_I^s)^2 + \\ &\quad 2a_{0I} (3c_I^{s,d} + 16d_I^s + 60e_I^s) - 32z_I^s y_I^s \end{aligned} \right\} (4.2.5)$$

(for $I=0,2$) .

The five integral crossing symmetry equations which relate the d-waves to the s- and p-waves are derived in Appendix A3. They can be written as

$$\left. \begin{aligned} 4 \int_0^4 (4-s)^2 (s-1) (A_0^0(s) + 2A_0^2(s)) ds + \int_0^4 (4-s)^3 (A_2^0(s) + 2A_2^2(s)) ds &= 0 \\ \int_0^4 (4-s)^3 (5s-4) (A_0^0(s) + 2A_0^2(s)) ds + \int_0^4 (4-s)^3 (4+s) (A_2^0(s) + 2A_2^2(s)) ds &= 0 \\ 2 \int_0^4 (4-s)^3 (2A_0^0(s) - 5A_0^2(s)) ds + \int_0^4 (4-s)^3 (2A_2^0(s) - 5A_2^2(s)) ds - \\ &\quad 9 \int_0^4 (4-s)^3 A_1^1(s) ds = 0 \\ 2 \int_0^4 s^2 (4-s)^3 (2A_0^0(s) - 5A_0^2(s)) ds + \int_0^4 s^2 (4-s)^3 (2A_2^0(s) - 5A_2^2(s)) ds + \\ &\quad 9 \int_0^4 s^2 (4-s)^3 A_1^1(s) ds = 0 \\ \int_0^4 s (4-s)^3 (2A_0^0(s) - 5A_0^2(s)) ds - \int_0^4 s (4-s)^3 (2A_2^0(s) - 5A_2^2(s)) ds &= 0 \end{aligned} \right\} (4.2.6)$$

and combine with Equation (3.4.13) to form a set of ten linear constraint equations between the coefficients of the partial wave expressions.

The method of imposing crossing symmetry and unitarity again yields the same number of constraint equations as there are unknown coefficients. Following DCB-I in the first instance, the only physical constraint imposed on the model is a fixed value of a_{02} ; therefore, it is necessary to relax only one of the derived constraint equations. Because of the existence of a comprehensive set of inequality constraints which follow from crossing symmetry and which provide an excellent independent means of testing crossing symmetry violation in the unphysical region, it is convenient to relax the highest order Balachandran-Nuyts-Roskies equation, namely

$$2 \int_0^4 s^2 (4-s)^3 (2A_0^0(s) - 5A_0^2(s)) ds + \int_0^4 s^2 (4-s)^3 (2A_0^0(s) - 5A_2^2(s)) ds + 9 \int_0^4 s^2 (4-s)^3 A_1^1(s) ds = 0 \quad (4.2.7)$$

Substituting for $A_\ell^I(s)$ from (4.2.1) into the nine remaining Balachandran-Nuyts-Roskies equations and doing the integration explicitly yields the following system of linear constraint equations between the coefficients of $A_\ell^I(s)$

$$\begin{pmatrix}
 0 & 2310 & 3696 & 7392 & -2640 & -5280 & 0 & 0 & 0 \\
 -1575 & -2100 & 1680 & -4200 & 2880 & -7200 & 0 & 0 & 0 \\
 -5775 & -11550 & 11088 & -27720 & 7040 & -17600 & -20790 & -99792 & 120960 \\
 -75075 & -120120 & 96096 & -240240 & 116480 & -291200 & -108108 & -576576 & 483840 \\
 -45045 & -60060 & 41184 & -102960 & 80640 & -201600 & 0 & -41184 & -96768 \\
 0 & 18018 & 24024 & 48048 & -21840 & -43680 & 0 & 0 & 0 \\
 0 & 6006 & 6864 & 13728 & -7560 & -15120 & 0 & 0 & 0 \\
 -225225 & -180180 & 96096 & -240240 & 524160 & -1310400 & 648648 & 3027024 & -3991680 \\
 -225225 & -300300 & 205920 & -514800 & 403200 & -1008000 & 0 & 0 & 0
 \end{pmatrix}
 \begin{pmatrix}
 a_2^s \\
 b_2^s \\
 d_0^s \\
 d_2^s \\
 y_0^s \\
 y_2^s \\
 b_1^p \\
 d_1^p \\
 x_1^p
 \end{pmatrix}
 =$$

0	396	-1155	-2112	-4224	-6400	11200	792	-12800	a_0^s
-630	-1008	-840	-1152	2880	-2560	-8960	2520	6400	z_0^s
-2310	-3168	-4620	-7040	17600	-17920	-17920	7920	44800	b_0^s
-30030	-45760	-48048	-66560	166400	-143360	-322560	114400	358400	$c_0^{s,d}$
-18018	-29120	-24024	-30720	76800	-57344	-236544	72800	143360	$c_2^{s,d}$
0	2860	-9009	-42978	-85956	-38400	100800	5720	-76800	e_0^s
0	910	-3003	-20529	-41058	-10240	36960	1820	-20480	x_0^s
-90090	-160160	-72072	-191880	479700	-122880	-1774080	400400	307200	z_2^s
-90090	-145600	-120120	0	0	-286720	-1182720	364000	716800	e_2^s
22400	0	0	0	0	0	0	0	0	x_2^s
22400	0	0	0	0	0	0	0	0	c_1^p
44800	46992	206400	0	0	0	0	0	0	e_1^p
80640	260520	1226400	0	0	0	0	0	0	d_0^d
591360	10632	116256	0	0	0	0	0	0	d_2^d
201600	0	0	-120120	-240240	-375720	-751440			e_0^d
73920	0	0	-68640	-137280	-215468	-430936			e_2^d
4435200	-1441908	-6210000	-480480	1201200	-1502880	3757200			
2956800	0	0	686400	-1716000	2208640	-5521600			

3. RESULTS OF MODEL DCB-II

Although there are now considerably more equations to solve than for DCB-I the method of solution is identical and the details are not repeated. However, computational difficulties do exist in obtaining a convergent solution at this order*; in particular, it becomes increasingly important to choose a good first approximation to the solution. The scattering lengths shown in Table 4.1 are from the preferred physical solution, labelled DCB-II Solution A.

<u>s-wave</u>	<u>p-wave</u>	<u>d-wave</u>
$a_{00} = 0.084$	$a_{11} = 0.114$	$a_{20} = 0.027$
$a_{02} = -0.05$ (fixed)		$a_{22} = 0.001$

Table 4.1
s- p- and d-wave scattering lengths
from DCB-II Solution A[†]

*It is well-known that in order to solve a system of non-linear simultaneous equations, as N the number of equations increases, the problem becomes very cumbersome and the results are sometimes unreliable(3).

†The numerical values of the coefficients for this solution are tabulated in Appendix B4.

In Table 4.2 and Figures 4.1 and 4.2 the behaviour of the s-wave amplitudes in the unphysical region are compared with the corresponding results of DCB-I Solution $B_2^{(a)}$.

	DCB-II A	DCB-I $B_2^{(a)}$
a_{02}	-0.05 (fixed)	-0.05 (fixed)
a_{00}	0.084	0.123
a_{00}/a_{02}	-1.67	-2.46
Posn. of zero in $A_0^0(s)$, s_0	2.12	1.36
Posn. of zero in $A_0^2(s)$, s_2	0.64	1.32
$4s_0 + 5s_2$	11.68	12.04
Posn. at which $A_0^{00}(s)$ is a minimum	1.53	1.60
a_{11}	0.11	0.03

Table 4.2

Comparison of s-wave behaviour in [0,4]
from DCB-I Solution $B_2^{(a)}$ and DCB-II Solution A

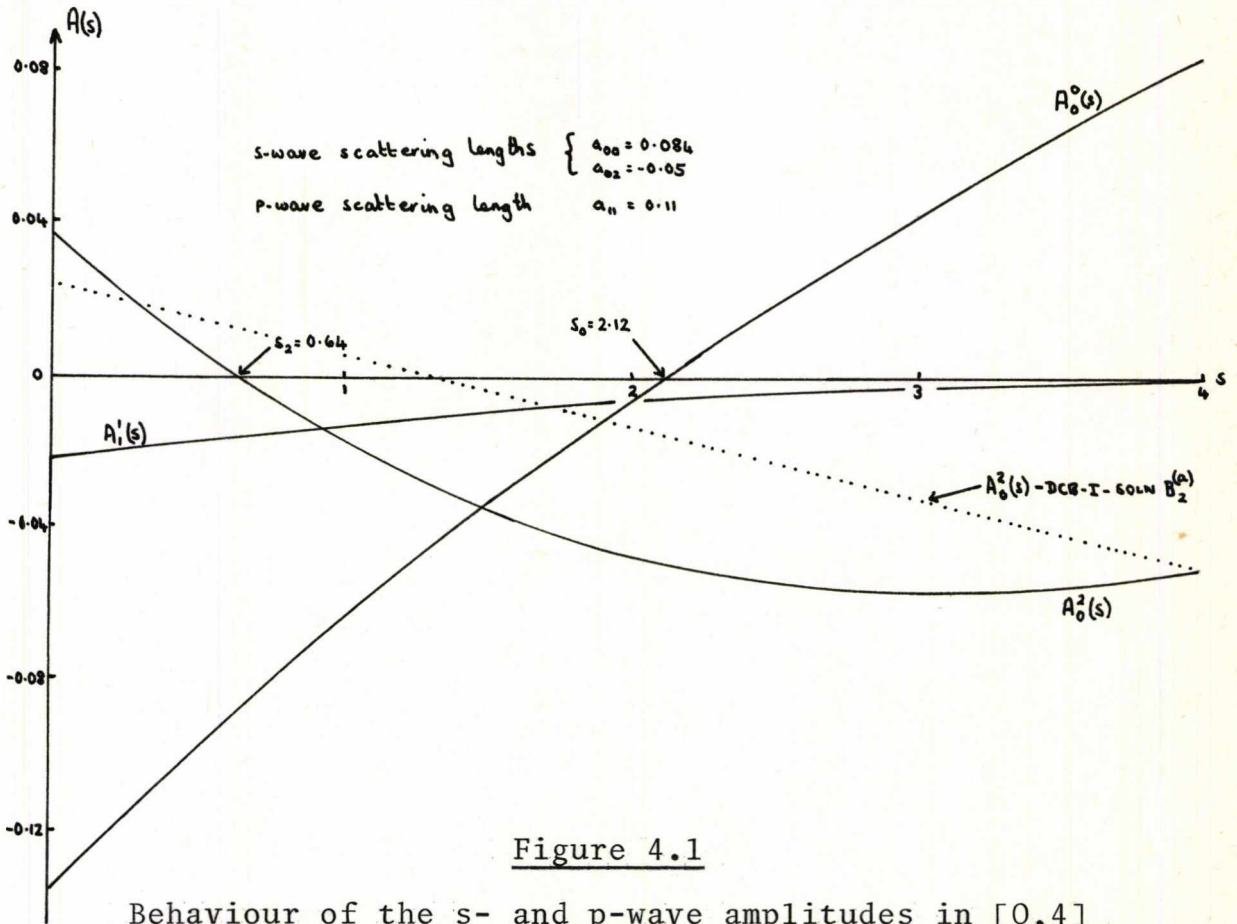


Figure 4.1

Behaviour of the s- and p-wave amplitudes in $[0, 4]$
from DCB-II Solution A

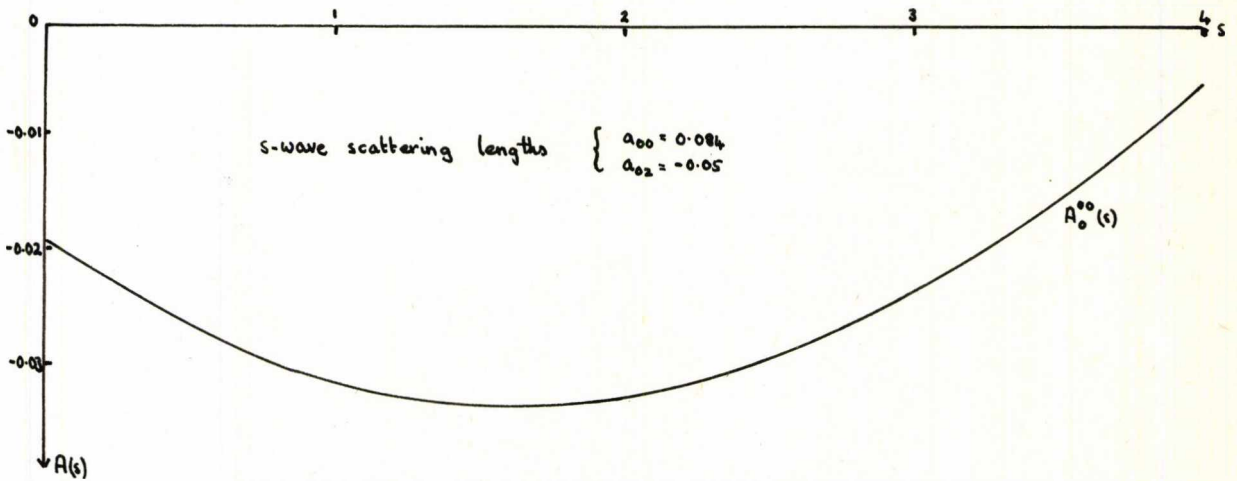


Figure 4.2

Behaviour of $A_0^{00}(s)$ in $[0, 4]$ from DCB-II Solution A

The behaviour of the d-wave amplitudes in the unphysical region is shown in Figure 4.3.

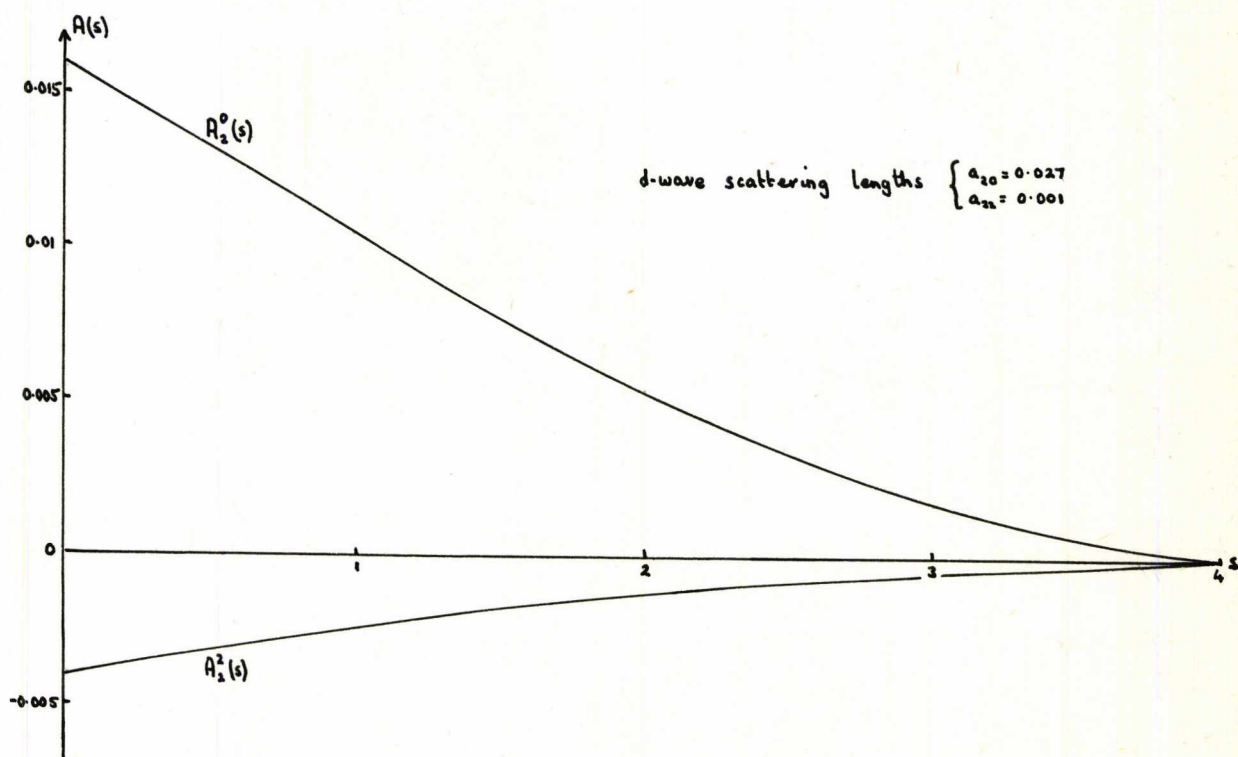


Figure 4.3

Behaviour of the d-wave amplitudes in $[0,4]$ from DCB-II Solution A

It can be seen that $A_2^2(s)$ and $A_2^0(s)$ have positive and negative slopes respectively over this region. A numerical check of some of the Martin-type constraints in $[0,4]$ is given in Appendix C4. With the exception of a few inequalities between the $\pi^0\pi^0$ s- and d-wave amplitudes, all the chosen constraint equations are satisfied by the above solution.

Although many of the essential features of the lower order model are reproduced, for example, small s-wave scattering lengths and a zero in each of the s-wave amplitudes in the unphysical region, other predictions are not nearly so impressive. In particular, the value obtained for the p-wave scattering length is much larger than has been previously suggested, and is in general disagreement with recent theoretical estimates listed in Table 4.3. Furthermore, $A_0^2(s)$ has a second zero just above the physical threshold (at ~ 300 MeV), which contradicts the known experimental data*.

Author	Method	a_{11}
M. G. Olsson ⁴	Effective-range formula	0.040±0.005
D. Morgan and G. Shaw ²	Forward dispersion relations	0.035±0.002
J. Iliopoulos ⁵	Unitarity corrections to a current algebra model	0.03
K. Kang, M. Lacombe ⁶ and R. Vinh Mau	Unitarised Veneziano model	0.035
B. Bonnier and P. Gauron ²	Model satisfying crossing symmetry and elastic unitarity	0.052±0.012

Table 4.3

Recent theoretical estimates of the p-wave scattering length

*c.f. Figure 2.4.

It is interesting to note that the solution of Bonnier and Gauron⁽²⁾, referred to in Table 4.3, also exhibits a second zero in $A_0^2(s)$ in the physical region. Their model aims to be far more predictive than DCB-II; for example, a more elaborate parametrisation of the partial wave amplitudes, designed to be valid from $0 \leq s \leq 30$, is used. Then, using the ρ -meson parameters as input they determine the threshold parameters by imposing the crossing sum-rules of Balachandran, Nuyts and Roskies.

For $-0.07 \leq a_{02} \leq -0.03$, DCB-II Solution A requires

$$x_1^p \sim -(0.5 \pm 0.2) \times 10^{-3} \quad , \quad (4.3.1)$$

a value which can never simultaneously satisfy a p-wave scattering length suggested by Table 4.3 and the elastic unitarity condition

$$x_1^p = -\frac{1}{32} a_{11}^2 \quad . \quad (4.3.2)$$

It would appear that at least as far as our model is concerned, and it may well be that all models of this type suffer from a similar drawback at higher order, more physical information is required as input to the model in order to be able to make predictions that are realistic in the light of our present knowledge. It is convenient then to relax the p-wave elastic unitarity condition of Equation (4.3.2), and impose instead a fixed value for the p-wave scattering length, defined by

$$4(b_1^p + 3c_1^p + 8d_1^p + 20e_1^p) = a_{11}^{\text{fixed}} \quad . \quad (4.3.3)$$

The calculation was then repeated, and solutions 'B', 'C' and 'D' were obtained for the physical parameters defined in Table 4.4.

DCB-II	a_{02}	a_{11} fixed
B	-0.05	0.04
C	-0.05	0.03
D	-0.07	0.03

Table 4.4

Physical input parameters for DCB-II

The corresponding values obtained for a_{00} , a_{20} and a_{22} are given in Table 4.5 and the behaviour of the partial wave amplitudes in the unphysical region is illustrated in Figures 4.4, 4.5 and 4.6.*

DCB-II	a_{00}	a_{20}	a_{22}
B	0.104	0.0096	0.0004
C	0.099	0.0072	0.0008
D	0.118	0.0059	0.0006

Table 4.5

Scattering length predictions from DCB-II

*The coefficients of each solution and numerical verification of some Martin-type constraints are tabulated in Appendices B4 and C4 respectively.

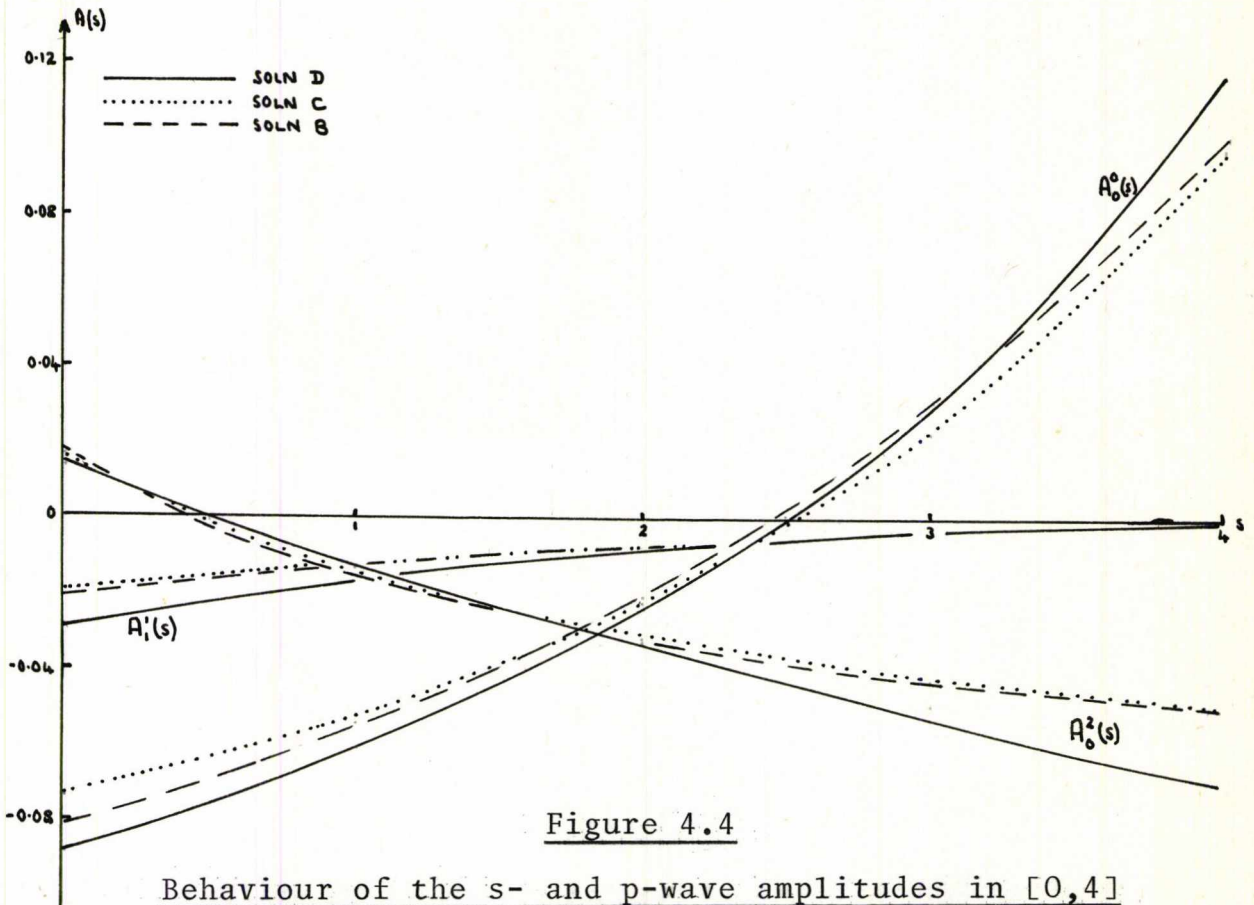


Figure 4.4

Behaviour of the s- and p-wave amplitudes in [0,4]
from DCB-II Solutions B, C and D

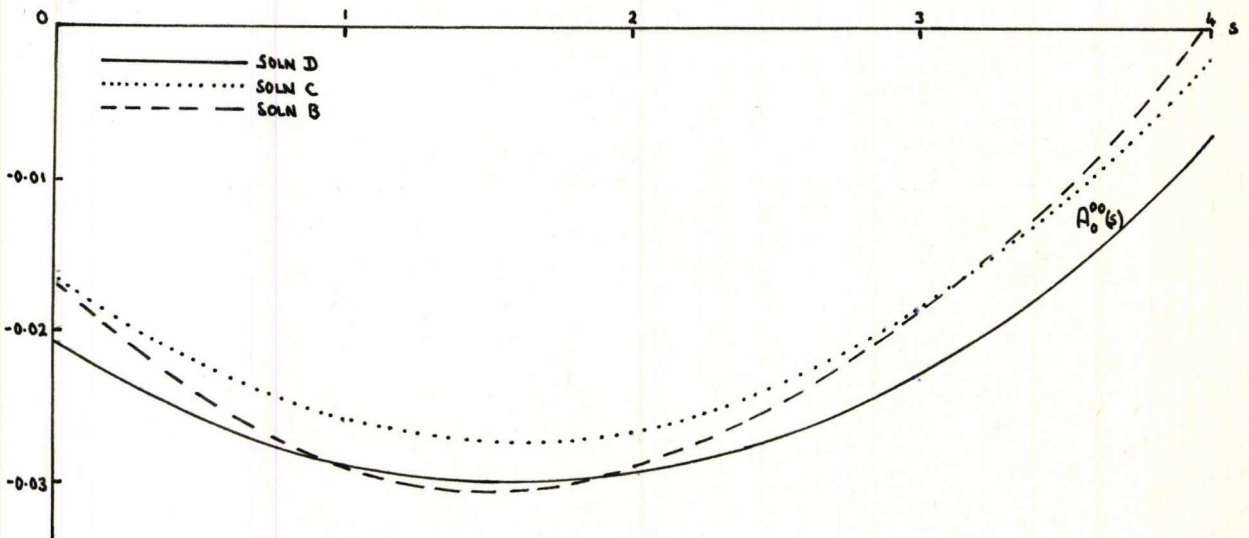


Figure 4.5

Behaviour of $A_0^{00}(s)$ in [0,4]
from DCB-II Solutions B, C and D

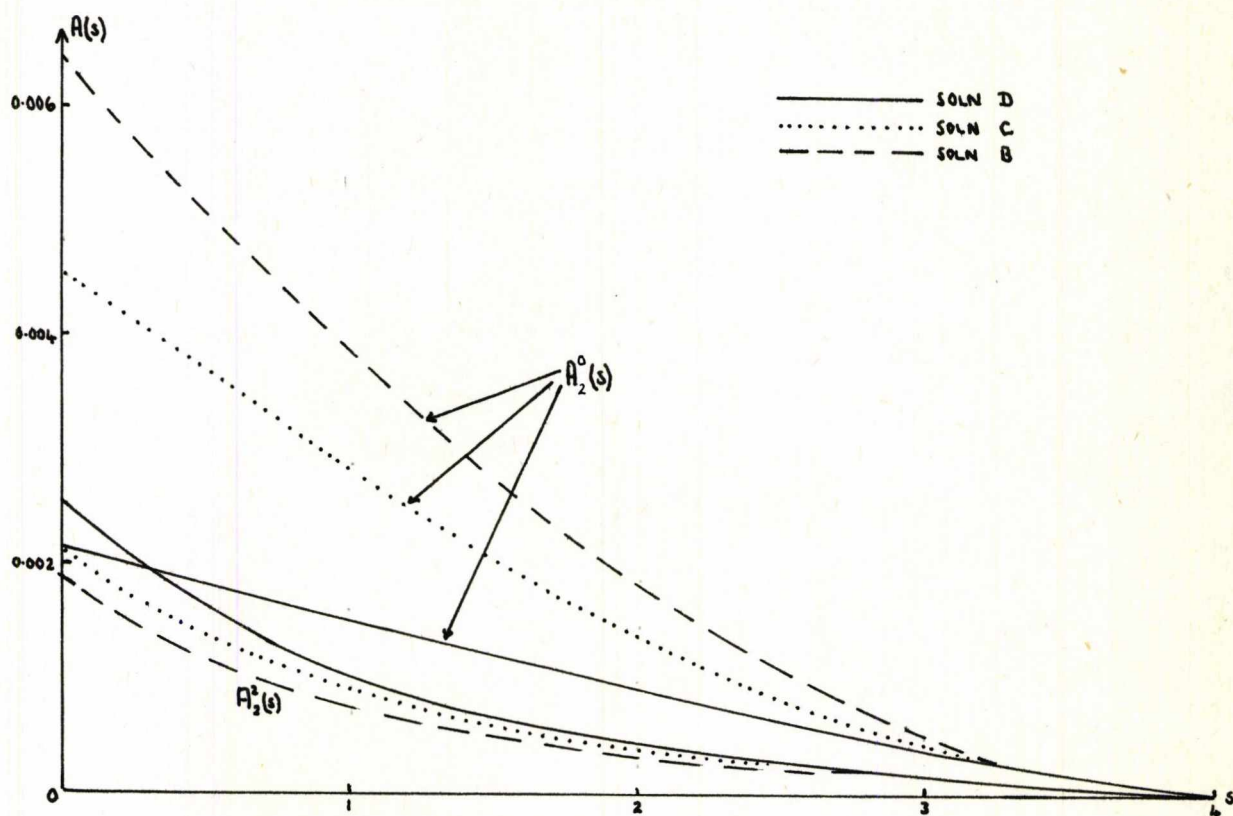


Figure 4.6

Behaviour of the d-wave amplitudes in $[0,4]$ from DCB-II Solutions B, C and D

Although the behaviour of $A_1^1(s)$ in $0 \leq s \leq 4$ is virtually unchanged by the additional physical information present in Solutions B, C and D, the behaviour of both $A_0^2(s)$ and $A_2^2(s)$ in this region is altered. In particular, $A_2^2(s)$ and $dA_2^2(s)/ds$ are of opposite signs to those obtained in Solution A, and $A_0^2(s)$ is restored to the approximately linear form exhibited by DCB-I. However, $A_0^2(s)$ still retains its second zero just above the physical threshold and its unrealistic phase shift below 1 GeV, as is illustrated in Figure 4.7.

Since DCB-II has no physical structure in the region of the ρ -resonance it would perhaps have been surprising if realistic phase shifts had been produced.

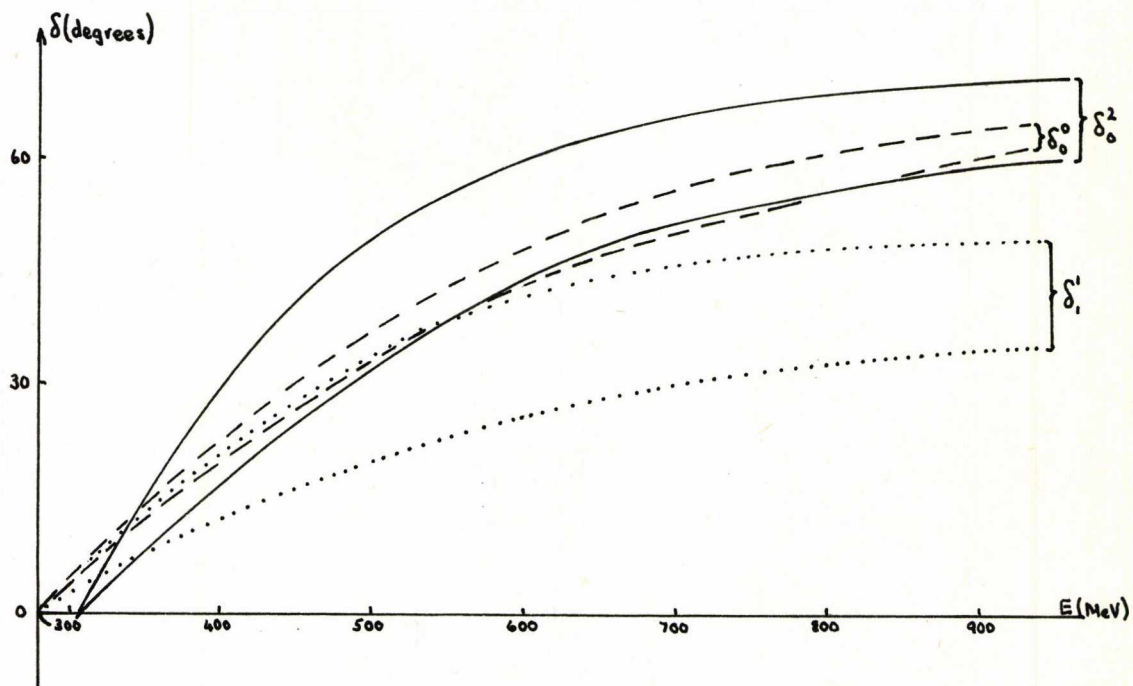


Figure 4.7

$\pi\pi$ s- and p-wave phase shifts from
DCB-II Solution B, C and D

4. COMMENTS, COMPARISONS AND CONCLUSIONS

Few detailed studies have so far been made of the $\pi\pi$ d-wave behaviour in the unphysical region. Previous analyses^(2,7,8,9) have determined the d-wave threshold behaviour by combining the general features of the experimental partial waves with the requirements of crossing, unitarity and analyticity, using the ρ -resonance parameters as known

physical quantities. By restricting the range of applicability of our model to the region $[0,4]$ it was hoped to improve on the reliability of the results in the domain of interest, as well as provide a useful check of the model's self-consistency, c.f. Table 4.6.

	DCB-I	DCB-II
a_{00}	0.123	0.11 ± 0.01
a_{02}	-0.05	-0.06 ± 0.01
a_{11}	0.026	0.035 ± 0.005
a_{20}	-	0.007 ± 0.002
a_{22}	-	0.0006 ± 0.0002
a_{00}/a_{02}	-2.46	-2.0 ± 0.4
s_0	1.36	2.5 ± 0.1
s_2	1.32	0.5 ± 0.1
$4s_0 + 5s_2$	12.04	12.5 ± 1.0
Posn. at which $A_0^{00}(s)$ is a minimum	1.60	1.55 ± 0.05
$dA_0^0(s)/ds$	>0	>0
$dA_0^2(s)/ds$	<0	<0
$dA_1^1(s)/ds$	>0	>0
$dA_2^0(s)/ds$	-	<0
$dA_2^2(s)/ds$	-	<0

Table 4.6

A comparison of s- p- d-wave predictions
in $[0,4]$ from DCB-I and DCB-II

Both d-wave scattering lengths are small and positive and satisfy the lower bounds⁽¹⁰⁾

$$a_{20} > 0, \quad a_{22} > -\frac{1}{2} a_{20},$$

and in Figure 4.8 the behaviour of the d-waves in the un-physical region is shown to compare favourably with the results of Bonnier and Gauron⁽⁷⁾, and Arbab and Donohue⁽²⁾.

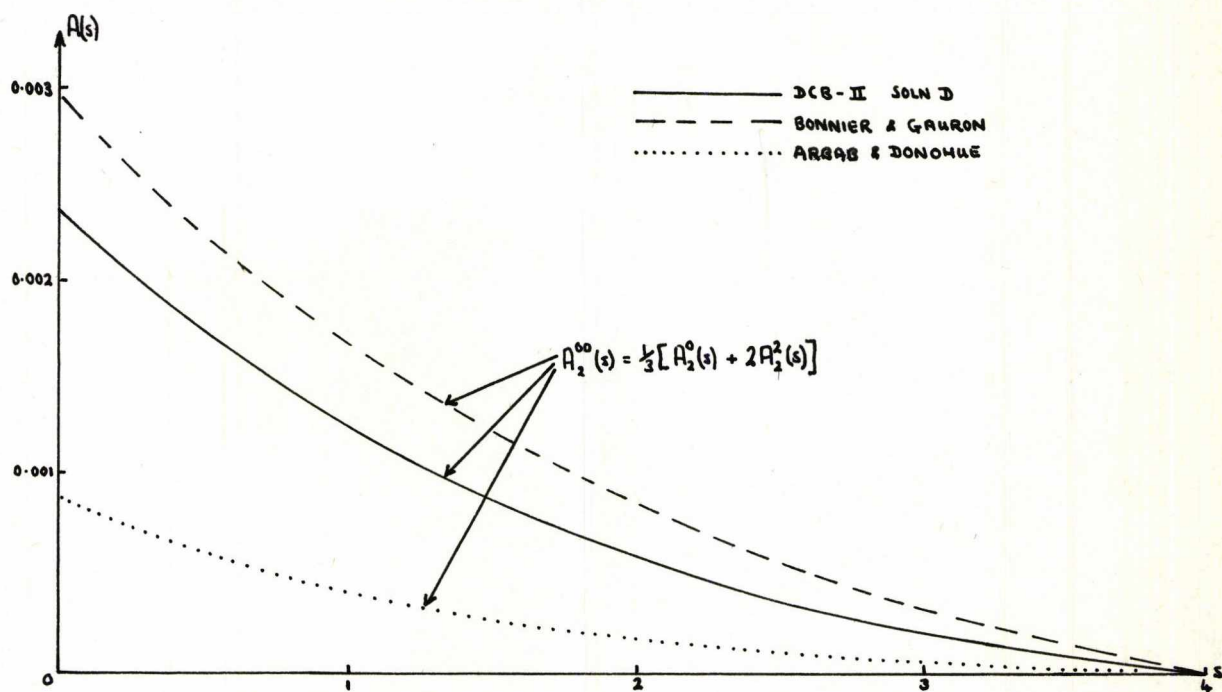


Figure 4.8

$\pi\pi$ d-waves in $[0,4]$ from DCB-II, Bonnier and Gauron⁽⁷⁾,
and Arbab and Donohue⁽²⁾.

However, the d-wave scattering lengths of Bonnier and Gauron⁽⁷⁾

$$a_{20} \sim 0.0056, \quad a_{22} \sim 0.0018$$

are preferred to the somewhat smaller values of Morgan and Shaw⁽²⁾

$$a_{20} = 0.0017 \pm 0.0003, \quad a_{22} = 0.0003 \pm 0.0001$$

and Arbab and Donohue⁽²⁾

$$a_{20} \sim 0.0012, \quad a_{22} \sim -0.0001$$

and it would appear that further calculations of the d-wave threshold behaviour are desirable before any firm conclusions can be drawn.

REFERENCES

1. A. MARTIN, Nuovo Cimento 44A, 1219 (1966); 58A, 303 (1968); 63A, 169 (1969).
G. AUBERSON, Nuovo Cimento 68A, 281 (1970).
2. D. MORGAN and G. SHAW, Phys. Rev D2, 520 (1970).
B. BONNIER, Nuclear Physics B17, 525 (1970).
B. BONNIER and P. GAURON, Nuclear Physics B21, 465 (1970).
F. ARBAB and J. T. DONOHUE, Phys. Rev. D1, 217 (1970).
3. J. HAWGOOD, "Numerical Methods in Algol" McGraw-Hill p.70.
4. M. G. OLSSON, Phys. Rev. 162, 1338 (1967).
5. J. ILIOPOULOS, Nuovo Cimento 53A, 552 (1968).
6. K. KANG, M. LACOMBE and R. VINH MAU, preprint IPNO-TH 71-22 (July, 1971).
7. B. BONNIER and P. GAURON, Nuclear Physics B36, 11 (1972).
8. A. ARNEODO and J. T. DONOHUE, preprint N-TH 72/4 (July, 1972).
9. J. L. BASDEVANT, C. D. FROGGATT and J. L. PETERSON, CERN preprint TH.1519 (June, 1972).
10. L. LUBASZUK and A. MARTIN, Phys. Letters 21, 96 (1966).
G. WANDERS, Phys. Letters 19, 331 (1965).

CHAPTER 5

I. INTRODUCTION

The essential drawback of the models proposed in Chapters 3 and 4 is their inability to provide any insight into the behaviour of the $\pi\pi$ partial waves in the region of the ρ -resonance. It has been indicated in Chapter 2 that the outstanding uncertainty in this region has been narrowed down to the detailed behaviour of the s-waves, especially the $I=0$ s-wave. Further information on these phases is required in many areas of hadron physics, both in the phenomenology of various processes (e.g. πN , NN scattering, $K_{\ell 4}$ decay, $K_{S,L} \rightarrow 2\pi$ etc.) and as a simple testing ground for theoretical ideas.

In this chapter a study is made of the $\pi\pi$ s-waves from threshold up to 1 GeV using a knowledge of δ_0^2 to furnish reliable information on δ_0^0 . The main ingredient of such a model must be a suitable representation of the $\pi\pi$ s-wave amplitudes over this region; accordingly the N/D formalism of Chew and Mandelstam⁽¹⁾ is used.

In Section 2 we recall the basic N/D method; the results will, of course, be dependent upon the choice of approximation for the left-hand cut. In Section 3, both a one-pole and a two-pole approximation scheme are considered, and a calculation of some $I=0$ s-wave parameters is made. By improving the left-hand cut approximation by a square-root

branch cut + poles in Section 4, a suitable form for both s-wave phases from threshold up to 1 GeV is obtained. The assumption that a fairly broad σ -meson resonance exists in the $I=0$ s-wave is found to be consistent with small positive values of a_0 , the $I=0$ s-wave scattering length.

2. THE N/D FORMALISM FOR $\pi\pi$ SCATTERING

The basic N/D technique was proposed by Chew and Low⁽²⁾, working with the static model of the pion-nucleon interaction, and was subsequently modified by Chew and Mandelstam for use in a more general class of problem. The method is used to solve the fundamental dynamical problem in S-matrix theory of determining the partial wave amplitude when one is given the discontinuity across its unphysical (otherwise called left-hand) cuts and has been extensively referred to in the literature.

The s-wave amplitudes are defined by

$$A_0^I(v) = \sqrt{\frac{v+1}{v}} e^{i\delta_0^I(v)} \sin \delta_0^I(v) \quad (I=0,2) \quad (5.2.1)$$

with δ_0^I real in the elastic region. $A_0^I(v)$ has cuts along the intervals $-\infty \leq v \leq -1$ and $0 \leq v \leq \infty$ (the reader is referred back to Figure 1.4), but one can separate these two cuts by performing the N/D decomposition

$$A_0^I(v) = \frac{N_0^I(v)}{D_0^I(v)}, \quad (5.2.2)$$

where $N_0^I(v)$ and $D_0^I(v)$ are both real analytic functions; the numerator contains the branch point at $v=-1$ with the left-hand cut, and the denominator contains the branch point at $v=0$ with the right-hand cut. From these assumptions, one can write

$$\left. \begin{aligned} \text{Im } N_0^I(v) &= D_0^I(v) \text{Im } A_0^I(v) \\ \text{Im } D_0^I(v) &= 0 \end{aligned} \right\} \text{ for } v < -1 \quad (5.2.3)$$

$$\text{Im } N_0^I(v) = \text{Im } D_0^I(v) = 0 \quad \text{for } -1 < v < 0 \quad (5.2.4)$$

$$\left. \begin{aligned} \text{Im } N_0^I(v) &= 0 \\ \text{Im } D_0^I(v) &= N_0^I(v) \text{Im } \frac{1}{A_0^I(v)} \end{aligned} \right\} \text{ for } v > 0, \quad (5.2.5)$$

and if elastic unitarity is imposed along the right-hand cut, the imaginary part of the D-function becomes

$$\text{Im } D_0^I(v) = -\sqrt{\frac{v}{v+1}} N_0^I(v) \quad \text{for } v > 0 \quad (5.2.6)$$

The Cauchy integral formulae for $N_0^I(v)$ and $D_0^I(v)$ are dependent upon the asymptotic behaviour of the numerator and denominator functions. For example, if one assumes that $N_0^I(v)$ has constant asymptotic behaviour, once-subtracted dispersion integrals for $N_0^I(v)$ and $D_0^I(v)$ are required to guarantee convergence of the integrals. Hence

$$N_0^I(v) = a_I + \frac{(v-v_0)}{\pi} \int_{-\infty}^{-1} \frac{dv' \text{Im } A_0^I(v') D_0^I(v')}{(v'-v)(v'-v_0)} \quad (5.2.7)$$

and

$$D_0^I(v) = 1 - \frac{(v-v_0)}{\pi} \int_0^\infty dv' \sqrt{\frac{v'}{v'+1}} \frac{N_0^I(v')}{(v'-v)(v'-v_0)} \quad (5.2.8)$$

where the normalisation $N_0^I(v_0) = a_I$, $D_0^I(v_0) = 1$ has been used. The existence of the parameter v_0 in the equations does not correspond to any arbitrariness in the amplitude $A_0^I(v)$; changing v_0 alters the normalisation of $D_0^I(v)$, but since $N_0^I(v)$ changes by the same amount, $A_0^I(v)$ remains unaltered. Since partial wave amplitudes satisfy the general requirement

$$A_\ell^I(v) \sim a_\ell v^\ell \quad \text{near } v=0,$$

a choice of $v_0=0$ eliminates the subtraction constant in all but the s-wave amplitudes where one free parameter appears to be inescapable in the relativistic problem.

3. THE POLE APPROXIMATION TO $N_0^I(v)$

Using the conventions outlined in Section 8 of Chapter 1

$$\left. \begin{aligned} D_0^I(v) &= \lim_{\epsilon \rightarrow +0} D_0^I(v+i\epsilon) \\ N_0^I(v) &= \lim_{\epsilon \rightarrow +0} N_0^I(v+i\epsilon) \end{aligned} \right\} \quad (5.3.1)$$

and (5.2.8) becomes

$$D_0^I(v) = 1 - \frac{(v-v_0)}{\pi} \int_0^\infty dv' \sqrt{\frac{v'}{v'+1}} \frac{N_0^I(v')}{(v'-v-i\epsilon)(v'-v_0)}. \quad (5.3.2)$$

To give the integral in (5.3.2) a meaning $1/(v'-v-i\epsilon)$ is written in terms of its Principal Value function,

$$\frac{1}{v'-v-i\epsilon} = \mathcal{P} \frac{1}{v'-v} + i\pi\delta(v'-v) \quad (5.3.3)$$

so that, for $v_0=0$,

$$D_0^I(v) = 1 - \frac{v}{\pi} \mathcal{P} \int_0^\infty dv' \sqrt{\frac{v'}{v'+1}} \frac{N_0^I(v')}{v'(v'-v)} - i \sqrt{\frac{v}{v+1}} N_0^I(v) \quad (5.3.4)$$

Using a one-pole approximation for $N_0^I(v)$, defined by

$$N_0^I(v) = \frac{\Gamma^I}{v+v^I} \quad (5.3.5)$$

the D-functions are given by^(*)

$$D_0^I(v) = 1 + \frac{\Gamma^I}{v+v^I} \left\{ h(v) + \frac{v}{\pi\sqrt{v^I(v^I-1)}} \ln \left| \frac{1+\sqrt{(v^I-1)/v^I}}{1-\sqrt{(v^I-1)/v^I}} \right| - i \sqrt{\frac{v}{v+1}} \right\} \quad (5.3.6)$$

where $h(v)$ is the real positive function,

$$h(v) = \frac{1}{\pi} \sqrt{\frac{v}{v+1}} \ln \left| \frac{1 + \sqrt{v/v+1}}{1 - \sqrt{v/v+1}} \right| \quad (5.3.7)$$

and the corresponding phase shifts are given by

$$\sqrt{\frac{v}{v+1}} \cot \delta_0^I(v) = \frac{\text{Re } D_0^I(v)}{N_0^I(v)} = \frac{v+v^I}{\Gamma^I} + h(v) + \frac{v}{\pi\sqrt{v^I(v^I-1)}} \ln \left| \frac{1+\sqrt{(v^I-1)/v^I}}{1-\sqrt{(v^I-1)/v^I}} \right| \quad (5.3.8)$$

(*) More generally the integral in (5.3.4) can be solved for a series of n poles, as is shown in Appendix A5.

In the original N/D calculation⁽³⁾, v^I and Γ^I were determined by making use of crossing symmetry relations that exist between the amplitudes and their derivatives on the left- and right-hand cuts. To test the predictive powers of the one-pole approximation for the left-hand cut it is useful to recall the unambiguous properties of the $\pi\pi$ s-waves; for example, the $I=2$ s-wave scattering length is known to be small and negative

$$a_2 = -0.05 \pm 0.02 \quad (5.3.9)$$

with its phase shift $\delta_0^2(v)$ also small, negative, and increasing in magnitude, such that at the ρ -mass

$$\delta_0^2(v=v_\rho) = -15^\circ \pm 5^\circ \quad (5.3.10)$$

These two constraints on $A_0^2(v)$ will be extensively used in this chapter and are assumed to describe the physical $I=2$ s-wave behaviour from the threshold region to 1 GeV. Our knowledge of the s-wave amplitudes also extends to the unphysical region where the existence of zeros, compatible with the current algebra zeros imposed by the Adler condition, have been confirmed. The single-pole approximation suffers from the drawback that for any choice of pole position on the left-hand cut, (5.3.5) never changes sign in the region $v \geq -1$, thus excluding the possible existence of zeros in the amplitudes in the unphysical region. Furthermore, the small values obtained for $\delta_0^2(v=v_\rho)$, and which are given in Table 5.1,

suggest that a one-pole approximation for the left-hand cut is very limited in its predictions.

$\begin{matrix} v^{I=2} \\ a_2 \end{matrix}$	10	20	30	50	100
-0.03	-1°	-2°	-2°	-2°	-2°
-0.05	-2°	-3°	-3°	-3°	-3°
-0.07	-3°	-4°	-4°	-4°	-4°

Table 5.1

$\delta_0^2(v=v_\rho)$ from a one-pole approximation of the left-hand cut

However, a two-pole approximation, with its numerator function

$$N_0^I(v) = \frac{\Gamma_1^I}{v+v_1^I} + \frac{\Gamma_2^I}{v+v_2^I} \quad (5.3.11)$$

has enough free parameters to allow the existence of a zero in each of the s-wave amplitudes if one pole is attractive and the other repulsive, i.e. one residue is greater than zero, the other less than zero. To calculate the s-wave phase shifts, one has to determine eight unknown parameters, namely the four pole positions and their corresponding residues. For convenience, the four pole positions are reduced to two by choosing

$$\left. \begin{aligned} v_1^0 &= v_1^2 = v_1 \\ v_2^0 &= v_2^2 = v_2 \end{aligned} \right\} \quad (5.3.12)$$

which leaves six unknown parameters. Any results will, of course, depend upon the conditions imposed on the s-wave amplitudes. The locations of the poles are arbitrary, and are chosen intuitively, but if one assumes that the near part of the left-hand cut does not play a significant role in low energy $\pi\pi$ scattering a suitable choice appears to be

$$v_1 = 10 \quad , \quad v_2 = 15 \quad . \quad (5.3.13)^*$$

The known behaviour of $\delta_0^2(v)$ is used to determine the residues Γ_1^2 and Γ_2^2 by imposing the constraints (5.3.9) and (5.3.10) on

$$\frac{\Gamma_1^2}{v_1} + \frac{\Gamma_2^2}{v_2} = a_2 \quad (5.3.14)$$

and

$$\sqrt{\frac{v_\rho}{v_\rho+1}} \cot \delta_0^2(v_\rho) = h(v_\rho) + \sum_{i=1}^2 \left\{ \frac{v_\rho + v_i}{\Gamma_i^2} + \frac{v_\rho}{\pi \sqrt{v_i(v_i-1)}} \ln \left| \frac{1 + \sqrt{(v_i-1)/v_i}}{1 - \sqrt{(v_i-1)/v_i}} \right| \right\} . \quad (5.3.15)$$

The values obtained for Γ_1^2 and Γ_2^2 are given in Table 5.2 and the corresponding $I=2$ s-wave phase shifts are shown in Figure 5.1.

*The qualitative nature of the solution is found to be stable against small variations in v_1 and v_2 .

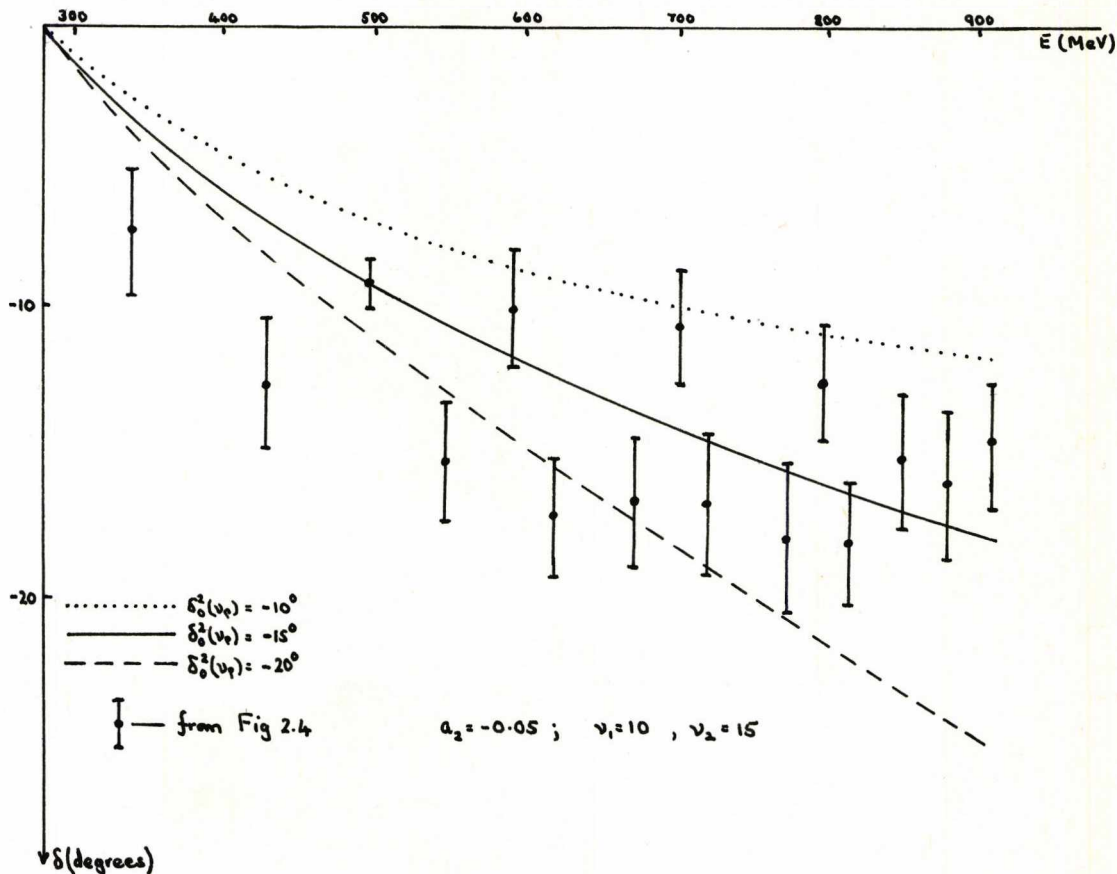


Figure 5.1

$\delta_0^2(v)$ from the two-pole model

The $I=0$ s-wave phase shifts cannot be used to calculate Γ_1^0 and Γ_2^0 in a similar way because of the uncertainty surrounding δ_0^0 in the region of the ρ -resonance. However, using the solution for $A_0^2(v)$ the residues in the $I=0$ amplitude are determined by requiring the s-wave amplitudes to satisfy the two independent Balachandran-Nuyts-Roskies equations

involving s-waves only, namely

$$\left. \begin{aligned} \int_{-1}^0 v [2A_0^0(v) - 5A_0^2(v)] dv &= 0 \\ \int_{-1}^0 v (3v+2) [A_0^0(v) + 2A_0^2(v)] dv &= 0 \end{aligned} \right\} \quad (5.3.16)$$

The $I=0$ s-wave phase shifts obtained are shown in Figure 5.2; Γ_1^0 , Γ_2^0 and related parameters are given in Table 5.2 on the next page.

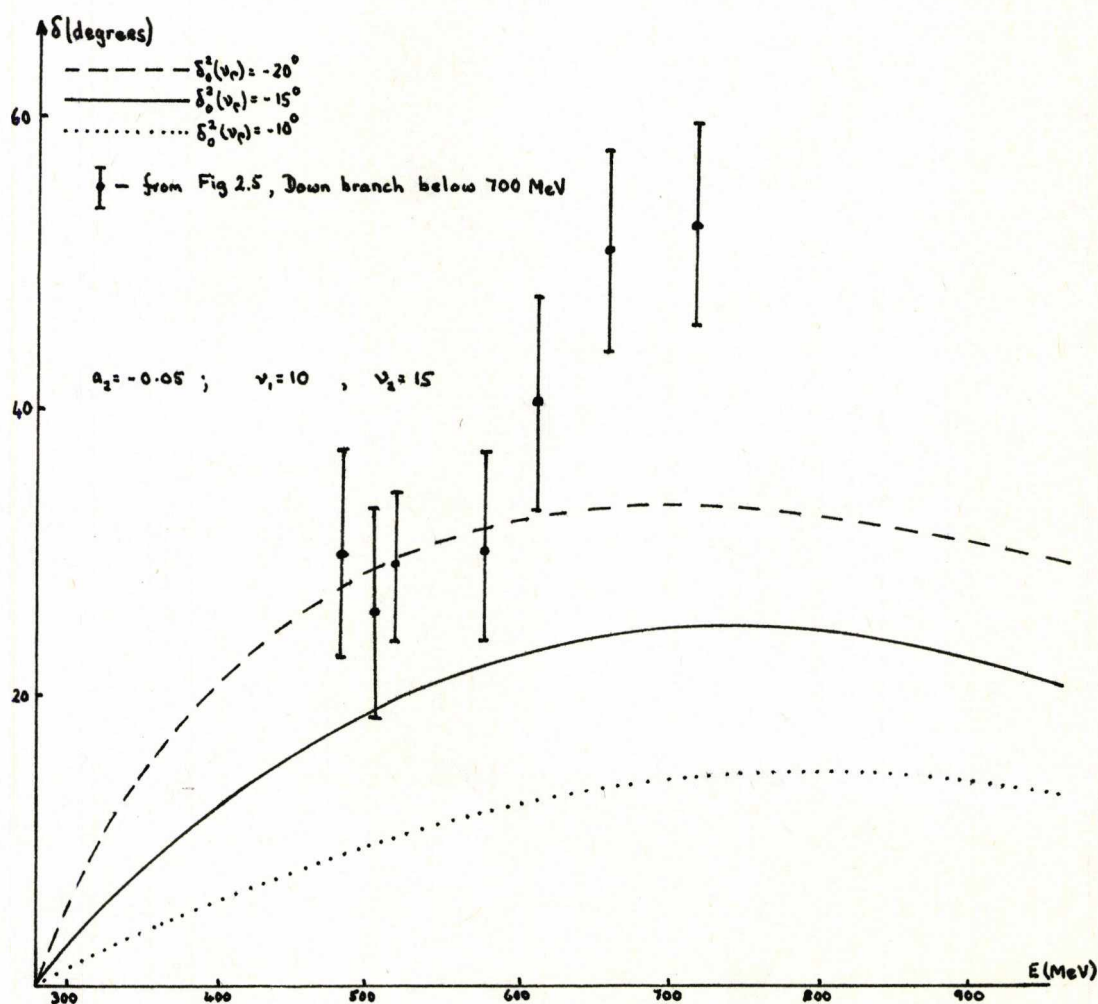


Figure 5.2

$\delta_0^0(v)$ from the two-pole model

$\delta_0^2(v_\rho)$	Γ_1^0	Γ_2^0	Γ_1^2	Γ_2^2	a_0	v_0^{zero}	v_2^{zero}
-10°	-32.52	49.41	15.22	-23.58	0.04	-0.37	-0.90
-15°	-58.03	89.58	24.66	-37.74	0.17	-0.81	-0.56
-20°	-86.02	133.75	34.25	-52.12	0.31	-0.99	0.42

Table 5.2

Parameters from the two-pole model

for $a_2 = -0.05$, $v_1 = 10$, $v_2 = 15$

Although δ_0^0 is somewhat larger than δ_0^2 in the ρ -resonance region no evidence is found to support the existence of an $I=0$ s-wave resonance below 1 GeV. In the unphysical region, however, the s-wave behaviour is more conclusive; zeros are obtained in each of the s-wave amplitudes (see Figure 5.3) and all solutions are found to satisfy the Martin inequalities in this region. Furthermore, Figure 5.4 shows that a_0 is small and positive for a wide range of pole positions on the left-hand cut.

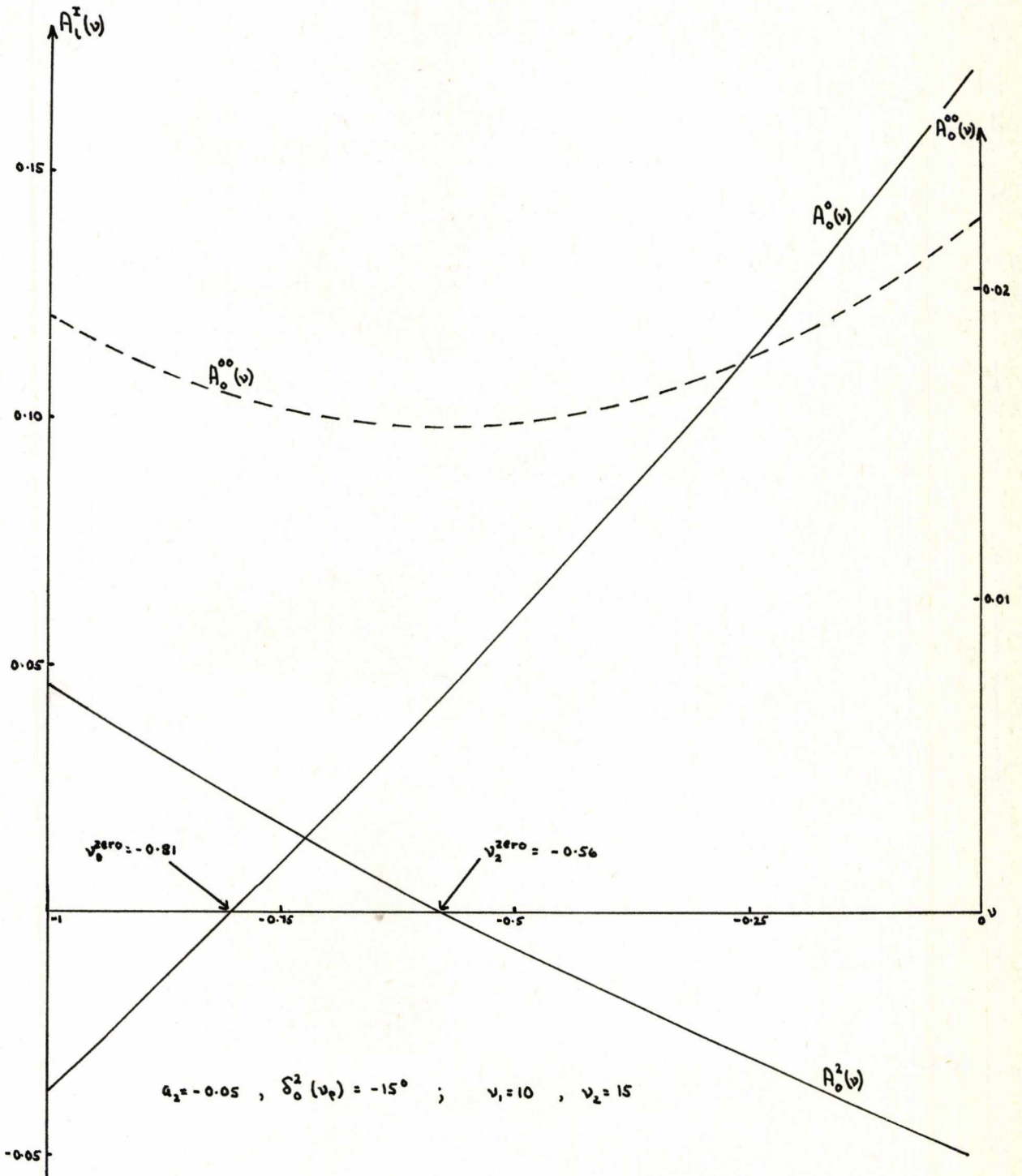


Figure 5.3

$\pi\pi$ s-wave amplitudes in $[-1,0]$ from the two-pole model

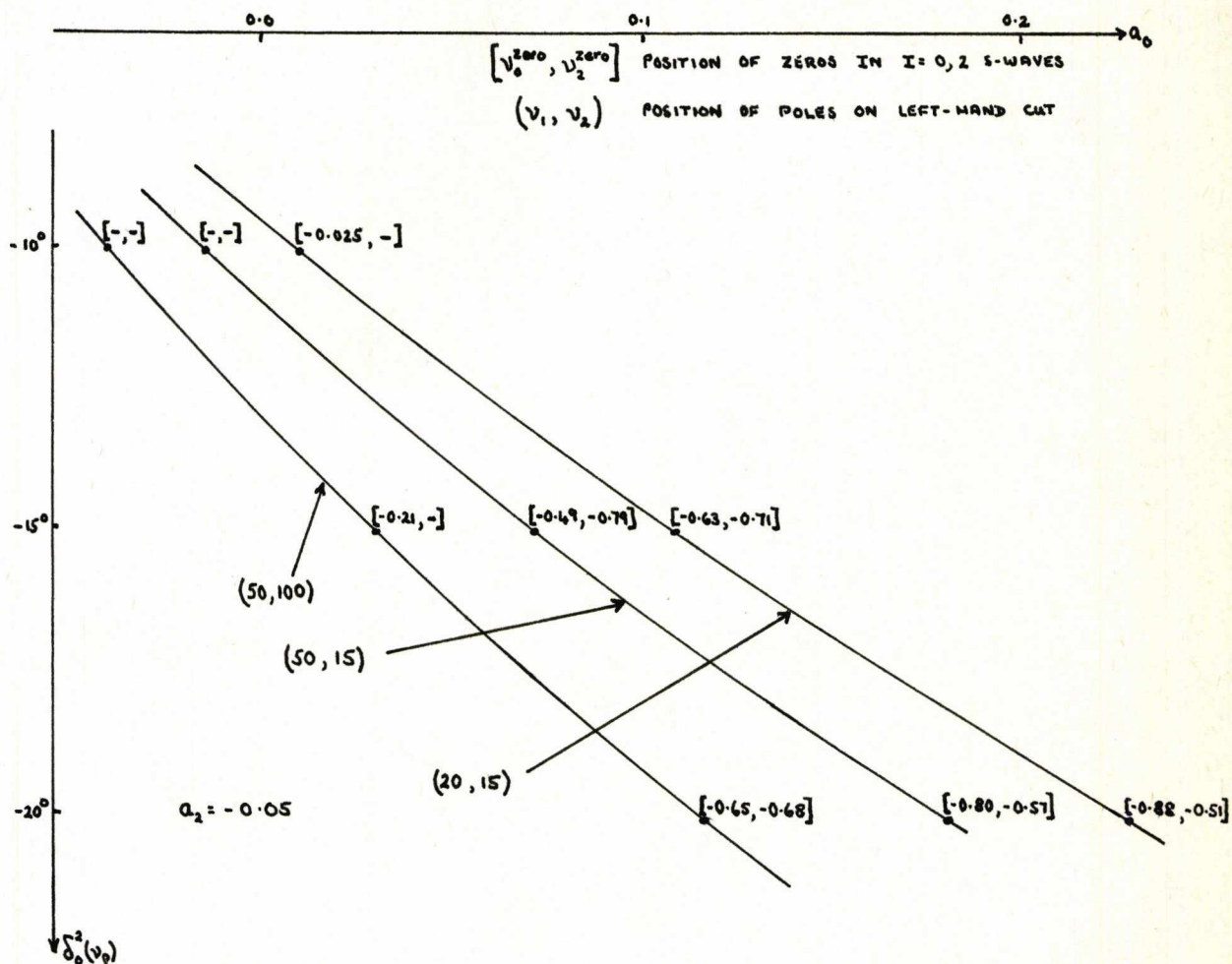


Figure 5.4

a_0 versus $\delta_0^2(v)$ from the two-pole model

The approximately linear form for $A_0^0(v)$ and $A_0^2(v)$ in the unphysical region is reflected in the 1:1 correspondence between a_0 and the positions of the zeros in the unphysical region $[v_0^{\text{zero}}, v_2^{\text{zero}}]$. The current algebra zeros, $[-0.75, -0.5]$, correspond to $a_0 \sim 0.21$, and those of DCB-I, $[-0.66, -0.66]$, to $a_0 \sim 0.11$, so that although the technique of fitting a two-pole approximation of the left-hand cut to the known s-wave

behaviour does not predict a δ_0^0 in agreement with any experimental data it does have the virtue of providing further confirmation of the threshold behaviour established in earlier chapters.

4. THE POLE + CUT APPROXIMATION TO $N_0^I(\nu)$

Further information could possibly be obtained by adding more and more poles to the N-function⁽⁴⁾, but each additional pole introduces two more degrees of freedom into the model. It is proposed instead to make use of the fact that the amplitudes have a square-root type of singularity at $\nu=-1$, and amend the pole approximation by defining

$$N_0^I(\nu) = (\nu+1)^{3/2} \frac{\Gamma^I}{\nu+\nu^I} \quad (5.4.1)$$

which approximates the left-hand cut by a square-root branch cut beginning at $\nu=-1^*$, and a single pole located at $\nu=-\nu^I$, where $\nu^I \gg 1$. Equation (5.4.1) has one obvious advantage over (5.3.1) in that it imposes a zero in each of the s-wave amplitudes in the unphysical region, although both zeros are fixed artificially at $\nu=-1$. Substituting (5.4.1) into (5.3.4) and doing the integration explicitly (the details for the more general problem of a cut + n poles is given in

*The $(\nu+1)^{3/2}$ term provides the correct functional form for $\text{Im } A_0^I(\nu)$ at $\nu=-1$ ⁽⁵⁾ (see also Equation (3.4.1)).

Appendix B5) yields

$$\operatorname{Re} D_0^I(\nu) = 1 - \frac{\Gamma^I}{\nu + \nu^I} \left[\frac{\nu^I - 1}{\sqrt{\nu^I}} \right] \nu, \quad (5.4.2)$$

and phase shifts given by

$$\tan \delta_0^I(\nu) = \frac{\sqrt{\nu}(\nu+1)}{\frac{\nu + \nu^I}{\Gamma^I} - \left[\frac{\nu^I - 1}{\sqrt{\nu^I}} \right] \nu}. \quad (5.4.3)$$

For fixed values of a_2 and $\nu^{I=2}$, the behaviour of $\delta_0^2(\nu)$ below 1 GeV is illustrated in Figure 5.5, and the parameter $\delta_0^2(\nu_\rho)$ is tabulated in Table 5.3.

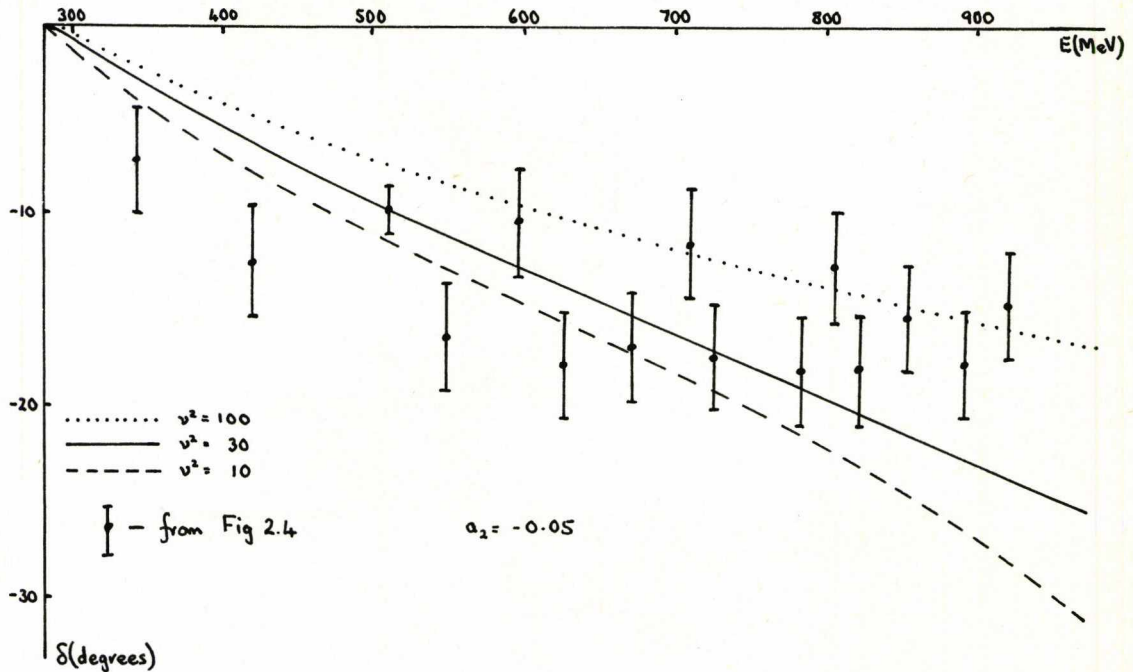


Figure 5.5

δ_0^2 from the cut + one-pole model

$\nu^{I=2}$ \ / \ a_2	10	20	30	50	100
-0.03	-15°	-16°	-15°	-14°	-11°
-0.05	-21°	-20°	-19°	-16°	-13°
-0.07	-25°	-24°	-21°	-18°	-14°

Table 5.3

$\delta_0^2(\nu_0)$ from the cut + one-pole model

The condition for the existence of a resonance in the I=0 s-wave amplitude is

$$\frac{\nu + \nu^0}{\Gamma^0} - \left[\frac{\nu^0 - 1}{\sqrt{\nu^0}} \right] \nu = 0 \quad (5.4.4)$$

For a suitable range of a_0 and ν^0 a resonance is obtained; its location is indicated in Table 5.4 and the corresponding I=0 s-wave phase shifts are shown in Figure 5.6.

$\nu^{I=0}$ \ / \ a_0	12	25	38
0.1	638 MeV	502 MeV	460 MeV
0.15	523 MeV	436 MeV	407 MeV
0.2	466 MeV	401 MeV	378 MeV

Table 5.4

Position of I=0 s-wave resonance from the cut + one-pole model

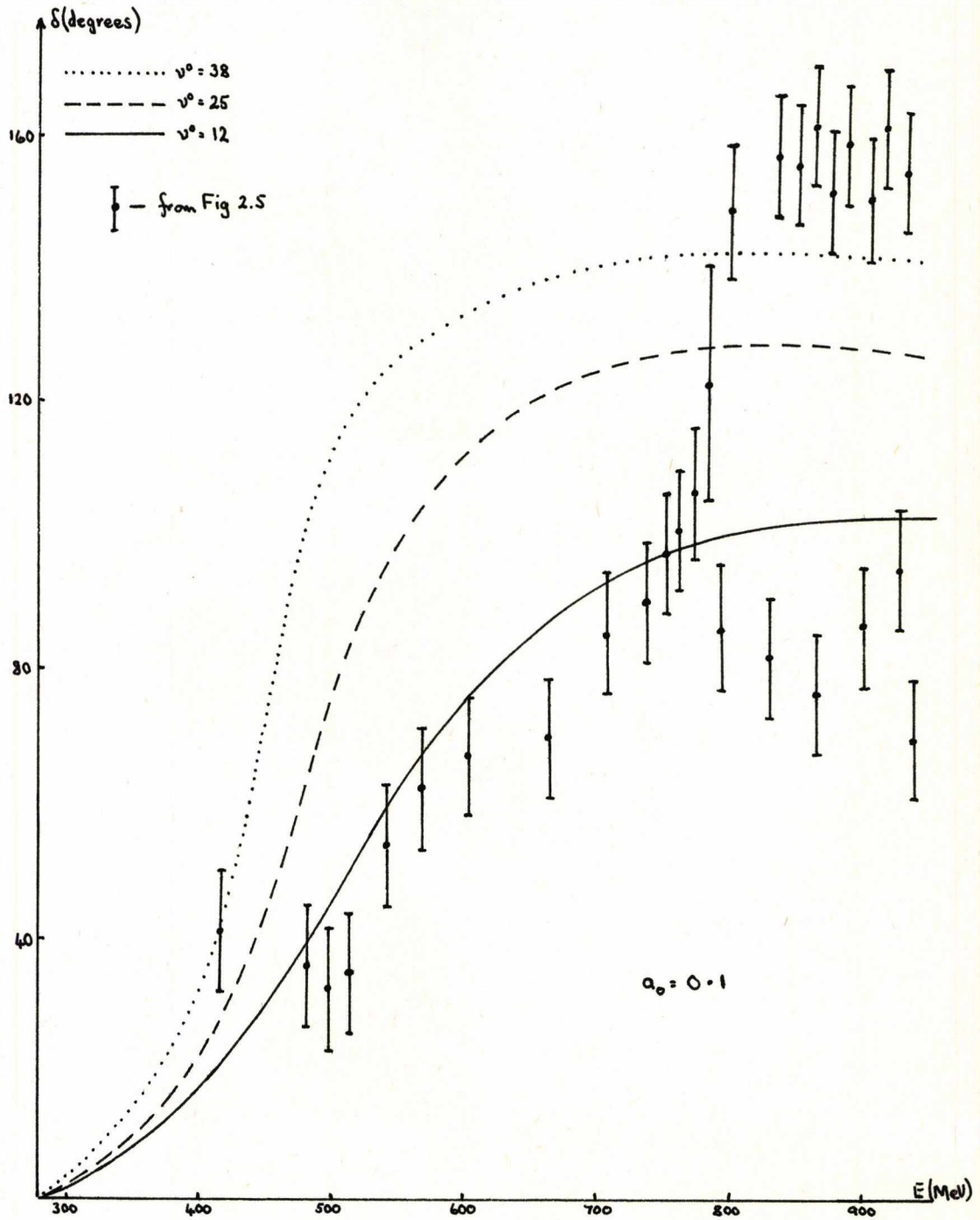


Figure 5.6

δ_0^0 from the cut + one-pole model

The model can be extended as before by adding another pole; the approximation to the left-hand cut is then given by

$$N_0^I(\nu) = (\nu+1)^{3/2} \left\{ \frac{\Gamma_1^I}{\nu+\nu_1^I} + \frac{\Gamma_2^I}{\nu+\nu_2^I} \right\} \quad (5.4.5)$$

and its D-function (from Appendix B5) by

$$D_0^I(\nu) = 1 - \left\{ \frac{\Gamma_1^I}{\nu+\nu_1^I} \left[\frac{\nu_1^I-1}{\sqrt{\nu_1^I}} \right] + \frac{\Gamma_2^I}{\nu+\nu_2^I} \left[\frac{\nu_2^I-1}{\sqrt{\nu_2^I}} \right] \right\} \nu - i \sqrt{\frac{\nu}{\nu+1}} N_0^I(\nu) . \quad (5.4.6)$$

Since each s-wave amplitude has a zero at $\nu=-1$, $A_0^I(\nu)$ derived from (5.4.5) and (5.4.6) is not a suitable representation of the s-wave amplitudes in the unphysical region. However, for pole positions far from the edge of the left-hand cut the parametrisation is claimed to be a valid representation of the s-wave amplitudes from threshold up to 1 GeV. Once again, with

$$\nu_1^0 = \nu_1^2 = \nu_1 \quad \text{and} \quad \nu_2^0 = \nu_2^2 = \nu_2$$

the constraints

$$a_2 = -0.05 \pm 0.02$$

$$\text{and} \quad \delta_0^2(\nu_\rho) = -15^\circ \pm 5^\circ$$

lead to the residues of Table 5.5 and the I=2 s-wave phase shifts of Figure 5.7.

$\delta_0^2(\nu_\rho)$ \ a_2	-0.03	-0.05	-0.07
-10°	(-9.05, 4.53)	(-22.15, 11.79)	(-35.26, 19.05)
-15°	(0.52, -1.21)	(-3.83, 0.80)	(-8.18, 2.81)
-20°	(3.27, -2.86)	(1.44, -2.36)	(-0.39, -1.87)

Table 5.5

(Γ_1^2, Γ_2^2) from the cut + two-pole model for $\nu_1=50, \nu_2=30$

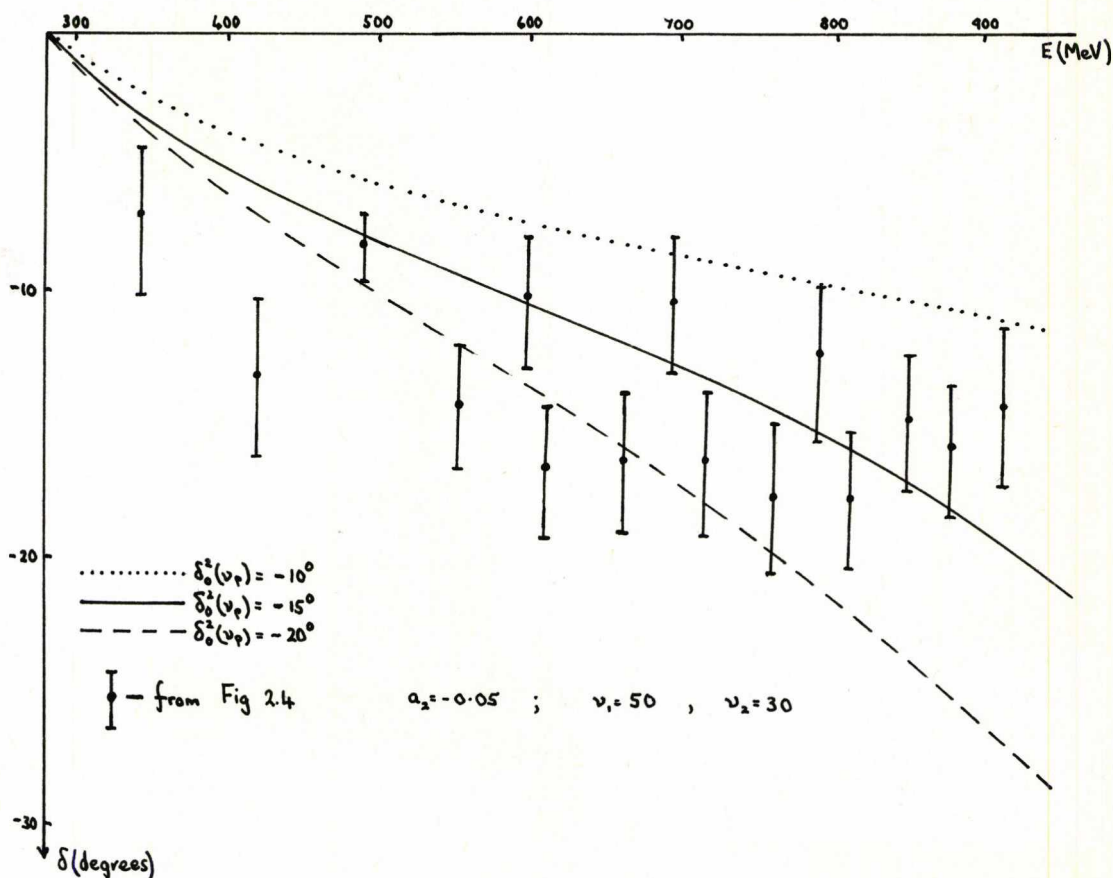


Figure 5.7

δ_0^2 from the cut + two-pole model

Since the amplitudes are not well-defined in the unphysical region the constraints of (5.3.16) cannot be used to determine Γ_1^0 and Γ_2^0 . Instead, a model is proposed which assumes the existence of a σ -meson resonance in the range 600 to 900 MeV. Calculations are reported over a mesh of possibilities for the mass and width of the σ -resonance.

In Section 4 of Chapter 2 it was shown that the Breit-Wigner formula

$$A_\ell(\nu) = \frac{\frac{1}{2}\Gamma_R}{\sqrt{\nu/\nu+1} (\nu - \nu_R - \frac{1}{2}\Gamma_R)} \quad (5.4.7)$$

is a suitable parametrisation for a partial wave amplitude close to a resonance. The residues of the poles in the $I=0$ s-wave amplitude are determined by requiring $A_0^I(\nu)$ to approximate to the Breit-Wigner form near $\nu=\nu_0$. This leads to the two constraint equations

$$\frac{1}{2}\Gamma_\sigma = N_0^0(\nu_\sigma) = (\nu_\sigma+1)^{3/2} \left\{ \frac{\Gamma_1^0}{\nu_\sigma+\nu_1} + \frac{\Gamma_2^0}{\nu_\sigma+\nu_2} \right\} \quad (5.4.8)$$

$$\text{Re } D_0^0(\nu_\sigma) = 0 = 1 - \left\{ \frac{\Gamma_1^0}{\nu_\sigma+\nu_1} \left[\frac{\nu_1-1}{\sqrt{\nu_1}} \right] + \frac{\Gamma_2^0}{\nu_\sigma+\nu_2} \left[\frac{\nu_2-1}{\sqrt{\nu_2}} \right] \right\}. \quad (5.4.9)$$

The values of Γ_1^0 and Γ_2^0 , obtained by solving (5.4.8) and (5.4.9) for fixed values M_σ and Γ_σ are given in Tables 5.6 and 5.7 respectively, the corresponding scattering length a_0 in Table 5.8 and the $I=0$ s-wave phase shifts in Figures 5.8, 5.9 and 5.10 for different values of M_σ and Γ_σ .

$M_\sigma \backslash \Gamma_\sigma$	140 MeV	250 MeV	400 MeV	500 MeV	650 MeV	800 MeV
600 MeV	-1.64	0.89	4.33	6.63	10.08	13.53
765 MeV	-1.40	0.08	2.10	3.46	5.46	7.48
900 MeV	-1.31	-0.25	1.21	2.18	3.64	5.10

Table 5.6

Γ_1^0 from the cut + two-pole model for $\nu_1=10, \nu_2=15$

$M_\sigma \backslash \Gamma_\sigma$	140 MeV	250 MeV	400 MeV	500 MeV	650 MeV	800 MeV
600 MeV	3.17	0.46	-3.25	-5.72	-9.43	-13.14
765 MeV	2.34	0.82	-1.25	-2.62	-4.69	-6.76
900 MeV	2.01	0.96	-0.48	-1.45	-2.89	-4.33

Table 5.7

Γ_2^0 from the cut + two-pole model for $\nu_1=10, \nu_2=15$

$M_\sigma \backslash \Gamma_\sigma$	140 MeV	250 MeV	400 MeV	500 MeV	650 MeV	800 MeV
600 MeV	0.05	0.12	0.22	0.28	0.38	0.48
765 MeV	0.02	0.06	0.13	0.17	0.23	0.30
900 MeV	0.00	0.04	0.09	0.11	0.17	0.22

Table 5.8

a_0 from the cut + two-pole model for $\nu_1=10, \nu_2=15$

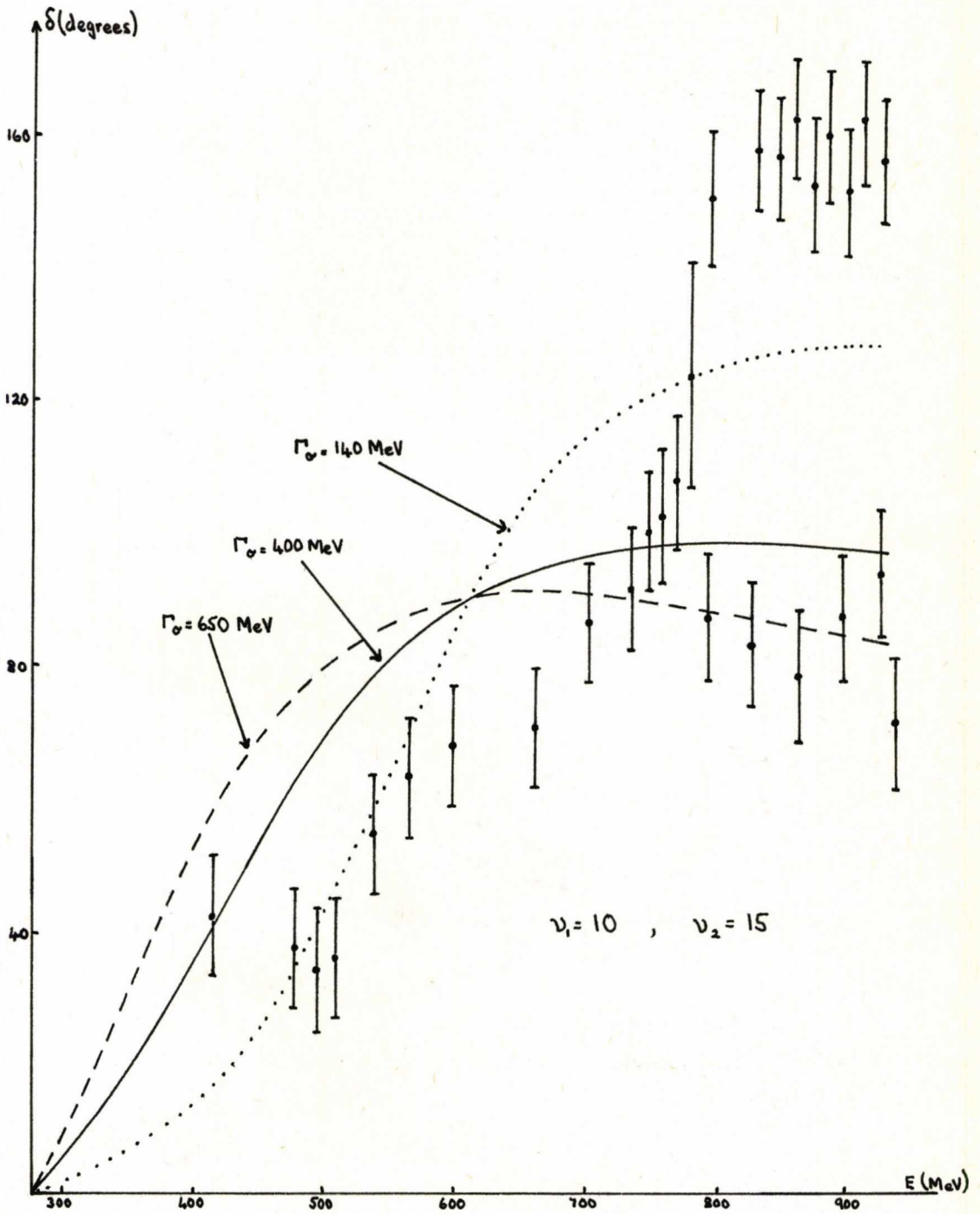


Figure 5.8

δ_0^0 from the cut + two-pole model for $M_0 = 600 \text{ MeV}$

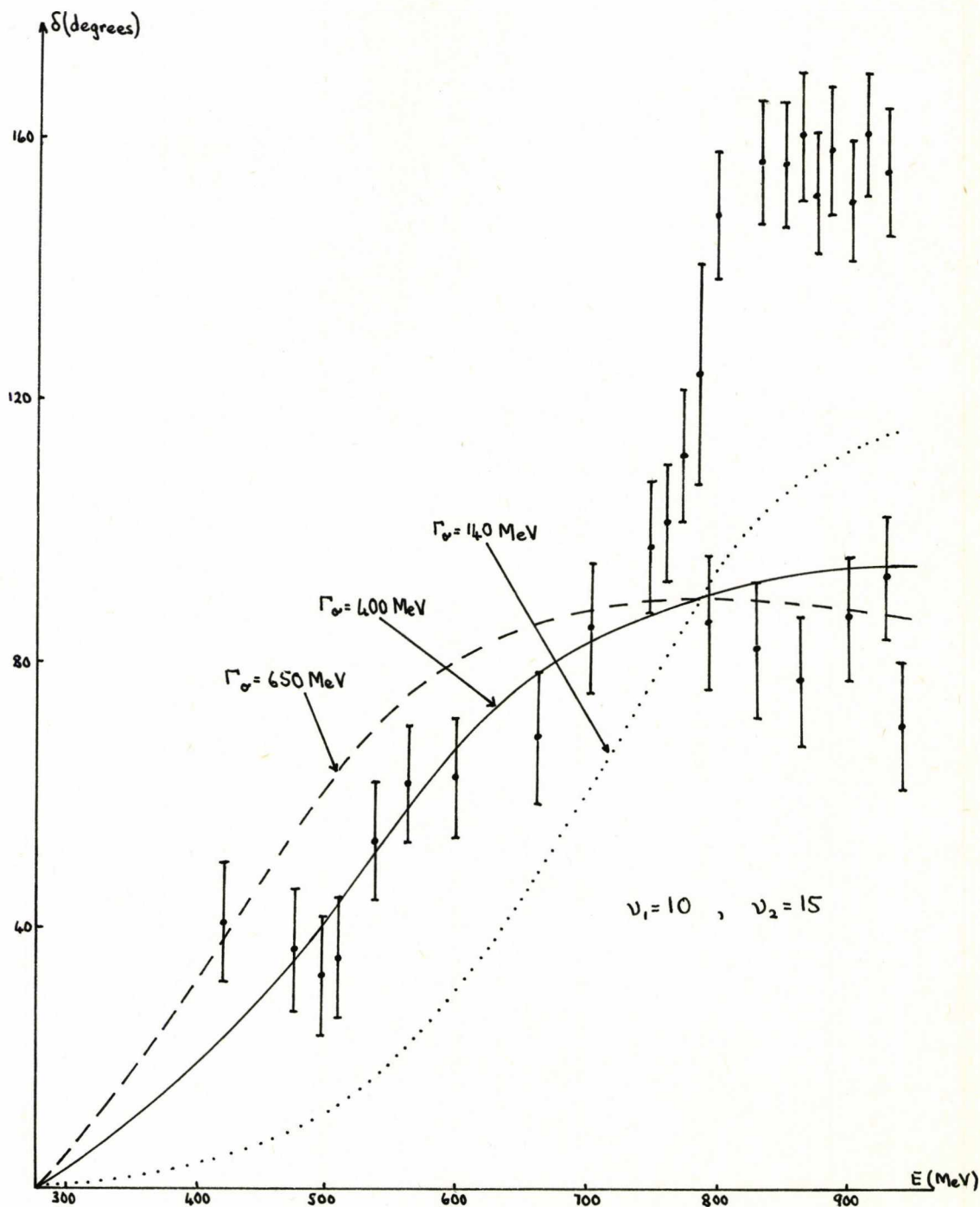


Figure 5.9

δ_0^0 from the cut + two-pole model for $M_\sigma = 765 \text{ MeV}$

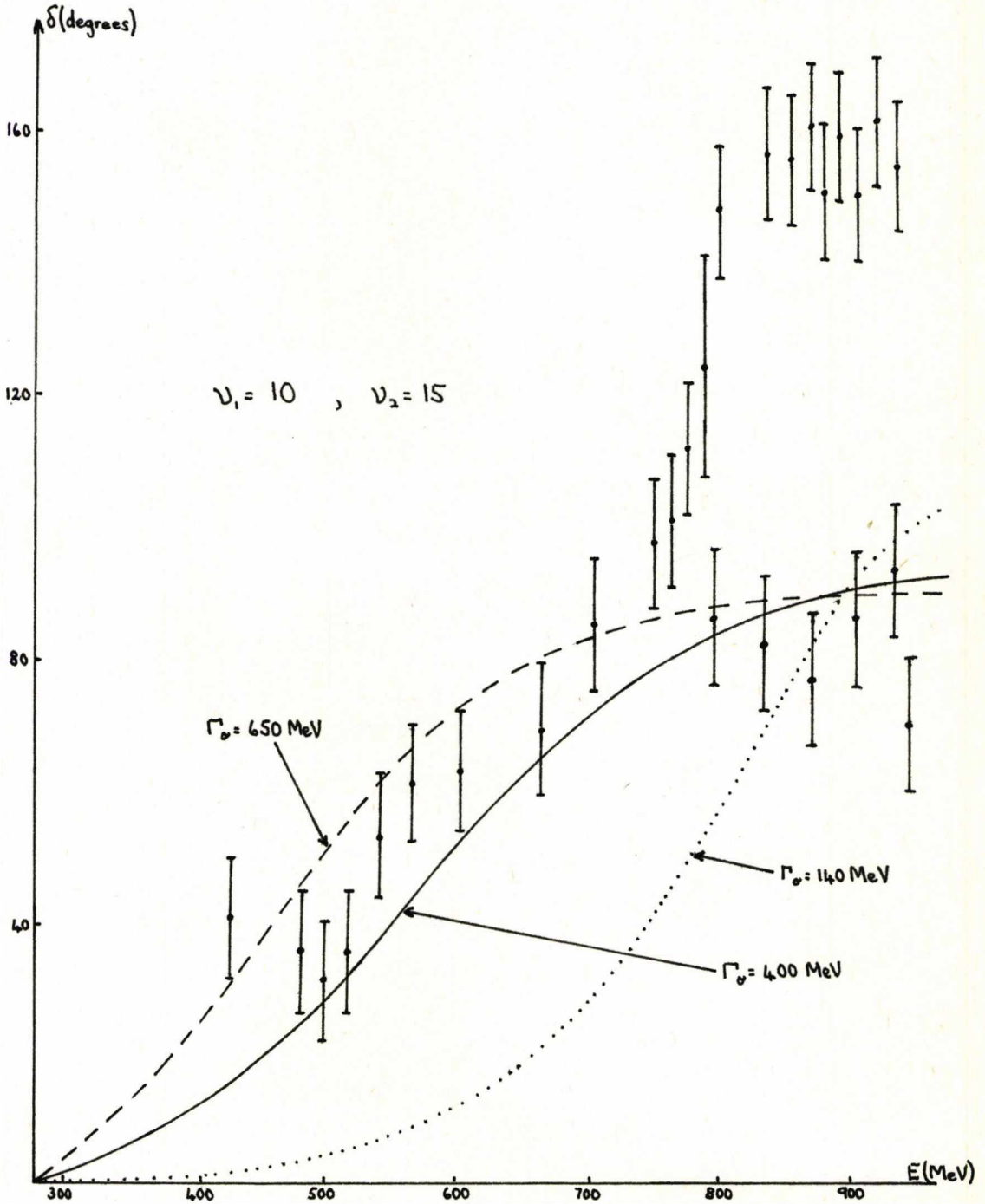


Figure 5.10

δ_0^0 from the cut + two-pole model for $M_0 = 900 \text{ MeV}$

The approximately linear relationship that exists between a_0 and the σ -parameters is illustrated in Figure 5.11.

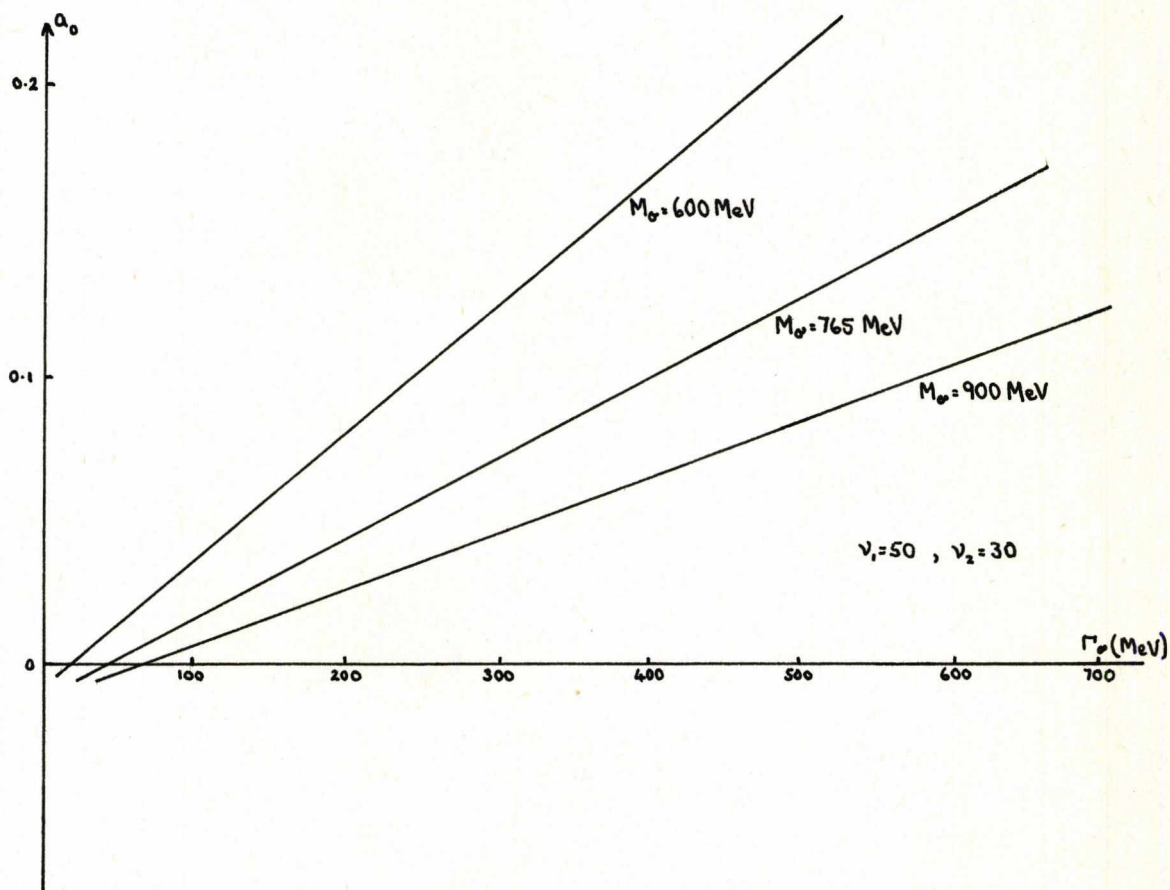


Figure 5.11

A plot of a_0 against Γ_σ from the cut + two-pole model

However, a_0 and δ_0^0 depend upon the position of the poles on the left-hand cut, but for ν_1 and ν_2 lying within the range

$$\nu_1: 10 \rightarrow 50$$

$$\nu_2: 15 \rightarrow 30$$

Figures 5.12 and 5.13 indicate that both of these s-wave

parameters remain fairly insensitive to a wide variation in the pole positions.

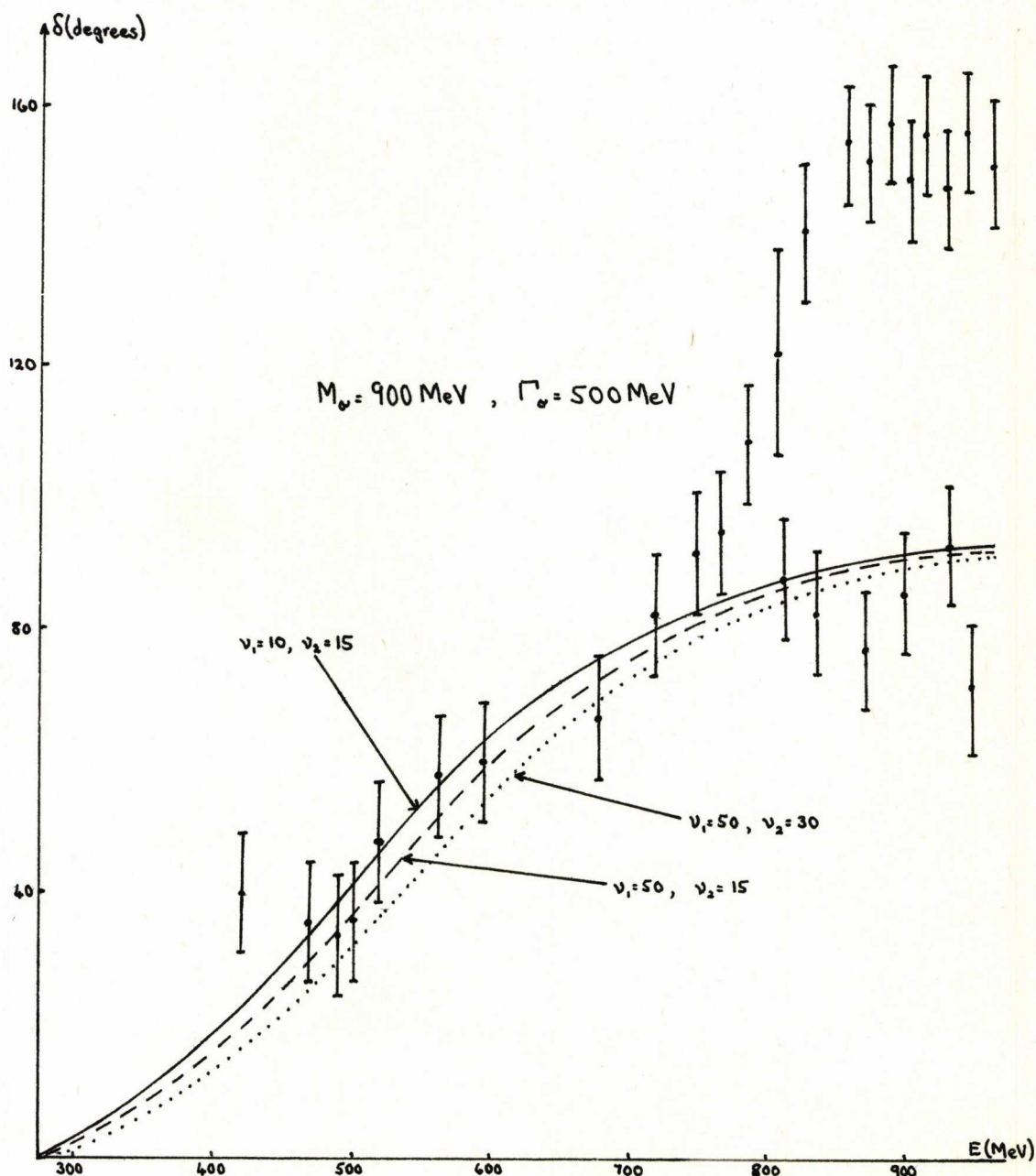


Figure 5.12

Range of δ_0^0 from the cut + two-pole model
for different pole positions

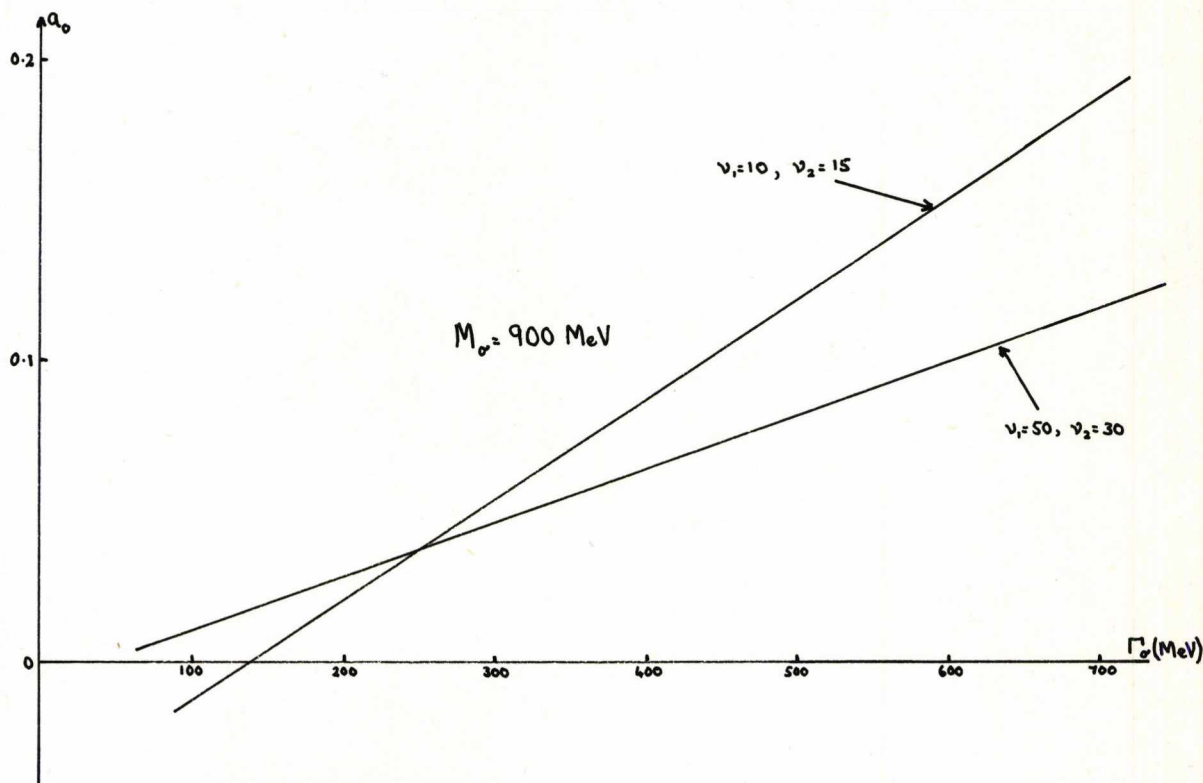


Figure 5.13

a_0 versus Γ_σ from the cut + two-pole model
for different pole positions

The pole + cut model comes out strongly in favour of a δ_0^0 which keeps fairly close to 90° from the region of the ρ -resonance to 1 GeV. Below 600 MeV the results are not so conclusive; the Up-Down solution is favoured by a broad σ -resonance, say >400 MeV and the Down-Down solution by a fairly narrow σ -resonance, say <250 MeV. The preferred solution, shown in Figure 5.14, is the one that gives the best fit to the experimental data. It corresponds to the

parameters

$$\begin{aligned} \nu_1 &= 10 & , & \nu_2 = 15 \\ \Gamma_1^0 &= 2.18 & , & \Gamma_2^0 = -1.44 \\ \Gamma_1^2 &= -1.64 & , & \Gamma_2^2 = 2.01 \\ a_0 &= 0.12 & , & \delta_0^0(\nu_\rho) = 83^\circ \\ a_2 &= -0.03 & , & \delta_0^2(\nu_\rho) = -10^\circ \\ M_\sigma &= 900 \text{ MeV} & , & \Gamma_\sigma = 500 \text{ MeV} \end{aligned}$$

indicating our preference for a very broad σ -resonance at about 900 MeV.*

The major drawback of the pole + cut parametrisation is its inability to describe the pion-pion amplitude in the unphysical region because the zeros in the amplitude are constrained to lie at $\nu=-1$. However, it has been suggested⁽⁶⁾ that this difficulty can be overcome by combining the pole + cut model with the pole model described in Section 3. The left-hand cut was defined by

$$N_0^I(\nu) = (\nu+1)^{3/2} \left[\frac{\Gamma_1^I}{\nu+\nu_1} + \frac{\Gamma_2^I}{\nu+\nu_2} \right] , \quad (5.4.10)$$

and the parameters $\nu_1, \nu_2, \Gamma_1^I, \Gamma_2^I$ ($I=0,2$) were determined by a method similar to that described in Section 3, except that the

*Further reference to the pole model and the pole + cut model has been made by A. Angus⁽⁶⁾.

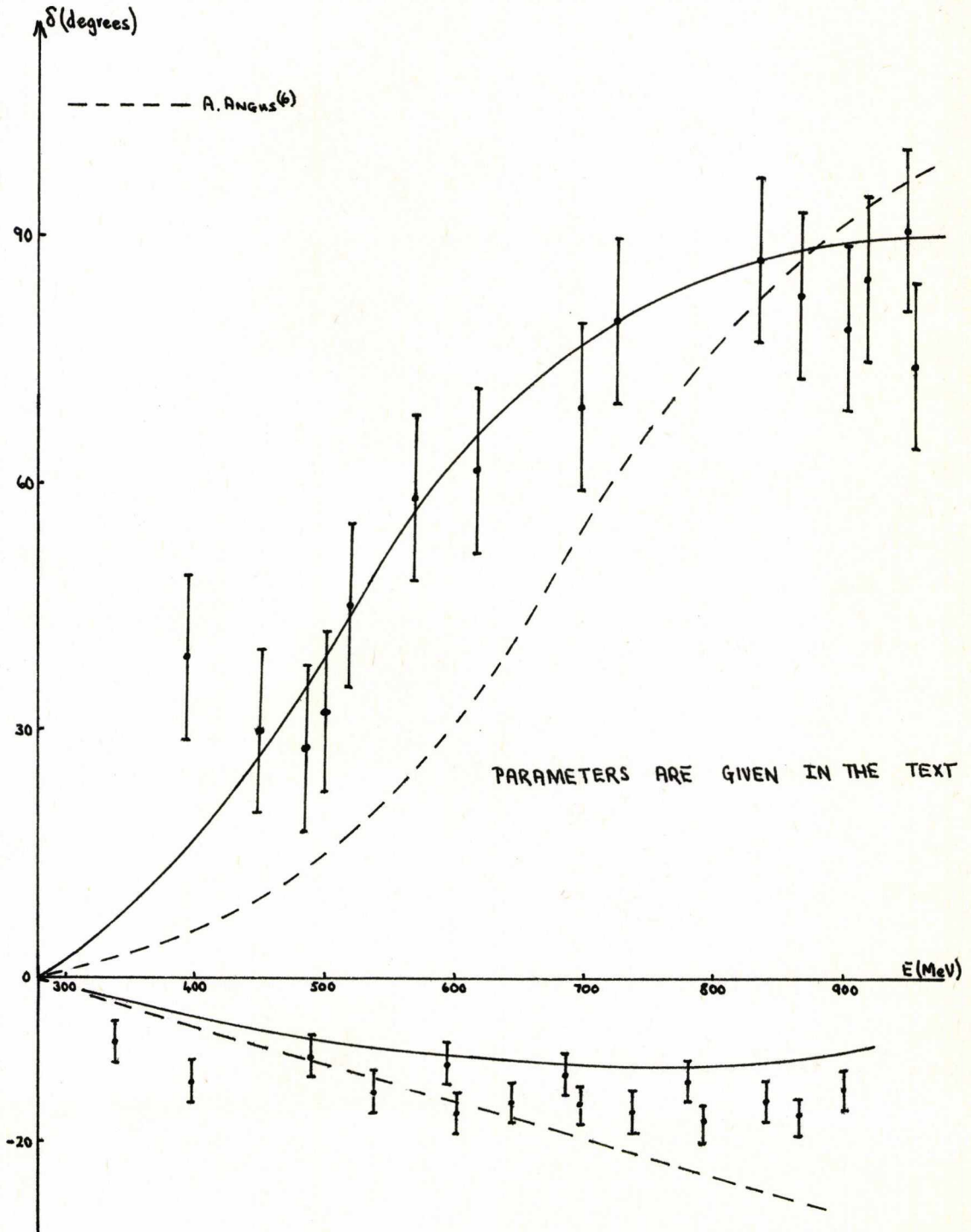


Figure 5.14

$\pi\pi$ s-wave phase shifts from the cut + two-pole model
- 'the preferred solution'

current algebra zeros were imposed on the amplitudes in the unphysical region instead of the Balachandran-Nuyts-Roskies equations of (5.3.16). The resulting phase shifts shown in Figure 5.14 are from a "best fit" of the Balachandran-Nuyts-Roskies constraints and correspond to parameters

$$\begin{aligned}v_1 &= 14 & , & & v_2 &= 40 \\ \Gamma_1^0 &= 0.73 & , & & \Gamma_2^0 &= -0.10 \\ \Gamma_1^2 &= -1.10 & , & & \Gamma_2^2 &= 1.14 \\ a_0 &= 0.05 & , & & \delta_0^0(v_\rho) &= 75^\circ \\ a_2 &= -0.05 & , & & \delta_0^2(v_\rho) &= -20^\circ\end{aligned}$$

but although the $I=0$ s-wave phase shift again indicates a σ -resonance at about 900 MeV the results are not entirely conclusive because of the critical dependence of the $I=0$ s-wave behaviour upon the choice of pole positions.

REFERENCES

1. G. F. CHEW and S. MANDELSTAM, Phys. Rev. 119, 467 (1960).
2. G. F. CHEW and F. LOW, Phys. Rev. 101, 1570 (1956).
3. G. F. CHEW and S. MANDELSTAM, Nuovo Cimento 19, 752 (1961).
4. J. S. KANG and B. W. LEE, Phys. Rev. D3, 2814 (1971).
5. G. WANDERS and O. PIGUET, Nuovo Cimento 56A, 417 (1968).
6. A. ANGUS, Ph.D. Thesis (University of Kent at Canterbury).

ADDENDUM

During the preparation of this thesis, Basdevant, Froggatt and Peterson* have published an important series of papers on $\pi\pi$ phenomenology below 1100 MeV. They use the partial wave equations of Roy[†] which express crossing and analyticity properties at physical energies, and establish that, on the basis of analyticity, crossing and unitarity requirements alone, there exists a two-dimensional domain of possibilities for the $\pi\pi$ partial wave amplitudes. This multiplicity of solutions confirms the somewhat less important result obtained in Chapter 3 of this thesis, and also by Dilley - that there exists a second solution of the low energy $\pi\pi$ partial wave amplitudes consistent with the requirements of analyticity, crossing symmetry and unitarity.

*J. L. Basdevant, C. D. Froggatt and J. L. Peterson

Phys. Letts., 41B, 173, 178 (1972).

International Conference on $\pi\pi$ Scattering and
Associated Topics - Tallahassee (1973).

Contributions to Aix en Provence International
Conference on Elementary Particles (September, 1973).

†S. M. Roy, Phys. Letts., 36B, 353 (1971).

APPENDIX A1

CLEBSCH-GORDAN COEFFICIENTS

If a two-pion state is defined by $\psi(J,M)$, where J is the total angular momentum of the system and M the third component of the angular momentum, and two single-pion states by $\phi_1(j_1,m_1)$, $\phi_2(j_2,m_2)$, then

$$\psi(J,M) = \sum_{m_1, m_2} C(J,M,j_1,m_1,j_2,m_2) \phi_1(j_1,m_1) \phi_2(j_2,m_2). \quad (A1.1)$$

For pions, $j_1=j_2=1$ and the relevant Clebsch-Gordan coefficients $C(J,M,j_1=1,m_1,j_2=1,m_2)$ are given in Table A1.1 (in all cases the squares of the coefficients are given)

		J										
		2	2	1	2	1	0	2	1	2		
$m_1 \quad m_2$		M										
		+2	+2	+1	0	0	0	-1	-1	-2		
+1	+1	1										
+1	0		$\frac{1}{2}$	$\frac{1}{2}$								
0	+1		$\frac{1}{2}$	$-\frac{1}{2}$								
+1	-1				$\frac{1}{6}$	$\frac{1}{2}$	$\frac{1}{3}$					
0	0				$\frac{2}{3}$	0	$-\frac{1}{3}$					
-1	+1				$\frac{1}{6}$	$-\frac{1}{2}$	$\frac{1}{3}$					
0	-1							$\frac{1}{2}$	$\frac{1}{2}$			
-1	0							$\frac{1}{2}$	$-\frac{1}{2}$			
-1	-1									1		

Table A1.1

APPENDIX A3

DERIVATION OF BALACHANDRAN-NUYTS-ROSKIES CROSSING RELATIONS

Using the identities

$$\iint_{\Delta} A(s,t,u) P(s,t,u) ds dt \equiv 0 \quad (A3.1)$$

choose $P(s,t,u)$ as functions which are either symmetric or antisymmetric under $s \leftrightarrow u$ interchange and combine these with isospin combinations possessing the opposite symmetry properties

$$\begin{aligned} (a) \quad A(s,t,u) &= A^0(s,t,u) + 2A^2(s,t,u) \\ (b) \quad A(s,t,u) &= A^0(s,t,u) - 2A^1(s,t,u) \end{aligned} \left. \vphantom{\begin{aligned} (a) \\ (b) \end{aligned}} \right\} \text{Symmetric under } s \leftrightarrow u \text{ interchange}$$

$$(c) \quad A(s,t,u) = 2A^0(s,t,u) + 3A^1(s,t,u) - 5A^2(s,t,u)$$

|
Antisymmetric under $s \leftrightarrow u$ interchange

Expand $A^I(s,t,u)$ in terms of their partial wave amplitudes according to

$$A^I(s,t,u) = \sum_{\ell=0}^{\infty} (2\ell+1) \left[1 + (-1)^{I+\ell} \right] A_{\ell}^I(s) P_{\ell}(\cos \theta) \quad (A3.2)$$

and multiply by $P(s,t,u)$ as outlined in Table A3.1. Each $\cos \theta$ integral is then done explicitly resulting in the set of ten integral equations of Table A3.2 which involve the s- p- and d-wave amplitudes in the unphysical region.

Equation Number	$P(s,t,u)$	$A(s,t,u)$	Non-zero partial waves
I	1	(c)	s
II	(s-u)	(a)	s
III	t	(c)	s & p
IV	su	(c)	s & p
V	$\left\{ \begin{array}{l} (s-u)su \\ stu \end{array} \right\}$	(b)	s & p
		(c)	
VI	(s-u)t	(a)	s & d
VII	(s-u)t ²	(a)	s & d
VIII	t ²	(c)	s, p & d
IX	s ² u ²	(c)	s, p & d
X	$\left\{ \begin{array}{l} (s-u)stu \\ st^2u \end{array} \right\}$	(b)	s & d
		(c)	

Table A3.1

Eq. No.	Balachandran-Nuyts-Roskies integral equation
I	$\int_0^4 (4-s) (2A_0^0(s) - 5A_0^2(s)) ds = 0$
II	$\int_0^4 (4-s) (3s-4) (A_0^0(s) + 2A_0^2(s)) ds = 0$
III	$\int_0^4 s(4-s) (2A_0^0(s) - 5A_0^2(s)) ds + 3 \int_0^4 (4-s)^2 A_1^1(s) ds = 0$
IV	$\int_0^4 s(4-s)^2 (2A_0^0(s) - 5A_0^2(s)) ds + 3 \int_0^4 s(4-s)^2 A_1^1(s) ds = 0$
V	$\int_0^4 s(4-s)^3 (2A_0^0(s) - 5A_0^2(s)) ds + 3 \int_0^4 s(4-s)^2 (3s-4) A_1^1(s) ds = 0$
VI	$4 \int_0^4 (4-s)^2 (s-1) (A_0^0(s) + 2A_0^2(s)) ds$ $+ \int_0^4 (4-s)^3 (A_2^0(s) + 2A_2^2(s)) ds = 0$
VII	$\int_0^4 (4-s)^3 (5s-4) (A_0^0(s) + 2A_0^2(s)) ds$ $+ \int_0^4 (4-s)^3 (4+s) (A_2^0(s) + 2A_2^2(s)) ds = 0$
VIII	$2 \int_0^4 (4-s)^3 (2A_0^0(s) - 5A_0^2(s)) ds + \int_0^4 (4-s)^3 (2A_2^0(s) - 5A_2^2(s)) ds$ $- 9 \int_0^4 (4-s)^3 A_1^1(s) ds = 0$
IX	$2 \int_0^4 s^2 (4-s)^3 (2A_0^0(s) - 5A_0^2(s)) ds + \int_0^4 s^2 (4-s)^3 (2A_2^0(s) - 5A_2^2(s)) ds$ $+ 9 \int_0^4 s^2 (4-s)^3 A_1^1(s) ds = 0$
X	$\int_0^4 s(4-s)^3 (2A_0^0(s) - 5A_0^2(s)) ds - \int_0^4 s(4-s)^3 (2A_2^0(s) - 5A_2^2(s)) ds = 0$

Table A3.2

APPENDIX B3

RESULTS FROM MODEL PGM-II

The results presented in this thesis were obtained from a series of computer programs written in Algol and run on an I.C.L. 4130 computer at the University of Kent at Canterbury.

A library of Algol procedures is used to perform all the standard operations of matrix arithmetic. The procedures, which must be declared within the main program, operate in the following manner when called (unless otherwise stated the parameters of the procedures must be declared as two-dimensional real arrays within the block in which the procedure is called).

READMX(A); ————— reads real numbers from cards and stores them row by row in the array A.

MXPROD(A,B,C); ——— performs the matrix product $B * C$ storing the result in array A; both B and C are preserved.

INVERT(A,N); ————— inverts the $N \times N$ matrix A where N must be declared as an integer variable. A real variable DET must also be declared in the main program.

An assembly listing of the program which determines the coefficients of PGM-II follows; since all lower-case letters must be transformed to upper-case letters in the program it was necessary to redefine H_0 and H_2 in the text as NHO and NH2 in the program. Otherwise, the method and notation is as explained in Section 3 of Chapter 3.

Computer program

The following program, written in Algol, computes the coefficients of PGM-II.

```
PROGRAM CP1;

1  "BEGIN""INTEGER" I, J, M, N, CYC, COUNT;
2  "REAL" A0, A2, B0, B2, NC0, C1, NC2, F0, F1, F2,
3  H0, NH0, H2, NH2, K0, K2, DA0, DNC0, DET;
4  "ARRAY" A[1:9, 1:9], B[1:9, 1:5], ARR[1:2, 0:2], BRR[1:2, 1:2];

5  "COMMENT" LIST PROCEDURES REQUIRED;
6  "LIBRARY" READMX, MXPROD, INVERT;

7  "PROCEDURE" EVCO;
8  "COMMENT" EVCO EVALUATES THE COEFFICIENTS AT EACH STAGE
9  OF THE ITERATION;
10 "BEGIN""ARRAY" C, X[1:9, 1:1], Y[1:5, 1:1];
11 Y[1, 1] := A0;
12 Y[2, 1] := A2;
13 Y[3, 1] := B0 * SQRT(3 / R);
14 Y[4, 1] := B2 * SQRT(3 / R);
15 Y[5, 1] := NC0;
16 MXPROD(C, B, Y);
17 MXPROD(X, A, C);
18 "IF" COUNT = 10 "THEN"
19     "BEGIN""IF" CYC = 0 "THEN"
20         "BEGIN""FOR" I := 1 "STEP" 1 "UNTIL" N "DO""PRINT" X[I, 1];
21         "END";
22     "END";
23 C1 := X[1, 1];
24 NC2 := X[2, 1];
25 F0 := X[3, 1];
26 F1 := X[4, 1];
27 F2 := X[5, 1];
28 NH0 := X[6, 1];
29 NH2 := X[7, 1];
30 K0 := X[8, 1];
31 K2 := X[9, 1];
32 H0 := NH0 * SQRT(R / 3);
33 H2 := NH2 * SQRT(R / 3);
34 ARR[1, CYC] := B0 * (1 + 4 * B0) - 8 * A0 * NC0 - 8 * H0;
35 ARR[2, CYC] := B2 * (1 + 4 * B2) - 8 * A2 * NC2 - 8 * H2;
36 "COMMENT" PRINT ARR[I, 0], I = 1, 2 AT EACH ITERATION,
37 IF CONVERGENCE OBTAINED ARR[I, 0] → 0;
38 "IF" CYC = 0 "THEN""PRINT" ALIGNED(1, 8), ARR[1, CYC],
39 SAMELINE, "S5", ARR[2, CYC];
40 "END";
```

```
41 "COMMENT" PROGRAM STARTS;
42 "COMMENT" READ IN VALUES FOR M AND N, M=2, N=9;
43 "READ" M, N;
44 "COMMENT" READ IN THE N*N MATRIX A, EQTN 3.3.32;
45 READMX(A);
46 "COMMENT" DETERMINE  $A^{-1}$ ;
47 INVERT(A, N);
48 "COMMENT" READ IN THE N*5 MATRIX B, EQTN 3.3.33;
49 READMX(B);
50 "COMMENT" READ IN A2, AND GUESS INITIAL VALUES
51 FOR A0 AND NCO (SEE TABLE B3.1). PUT DAO=DNCO=0.00001;
52 "READ" A2, A0, NCO, DAO, DNCO;
53 B2:=- (1/2)*A2*A2;
54 "COMMENT" COUNT IS A COUNT OF THE NUMBER OF ITERATIONS;
55 COUNT:=0;
56 AGAIN:COUNT:=COUNT+1;
57 B0:=- (1/2)*A0*A0;
58 CYC:=0;
59 EVCO;
60 "COMMENT" CALCULATE NEW VALUES FOR A0 AND NCO
61 USING THE NEWTON-RAPHSON METHOD;
62 "COMMENT" SOLUTION OBTAINED AFTER 10 ITERATIONS;
63 "IF" COUNT=10 "THEN" "GOTO" EXIT;
64 CYC:=1;
65 A0:=A0+DAO;
66 B0:=- (1/2)*A0*A0;
67 EVCO;
68 CYC:=2;
69 NCO:=NCO+DNCO;
70 A0:=A0-DAO;
71 B0:=- (1/2)*A0*A0;
72 EVCO;
73 NCO:=NCO-DNCO;
74 "FOR" I:=1 "STEP" 1 "UNTIL" M "DO" "FOR" J:=1 "STEP" 1 "UNTIL" M "DO"
75     "BEGIN" BRR[I, J]:=(ARR[I, J]-ARR[I, 0])/0.00001;
76     BRR[I, J]:=-BRR[I, J];
77     "END";
78 INVERT(BRR, M);
79 A0:=A0+BRR[1, 1]*ARR[1, 0]+BRR[1, 2]*ARR[2, 0];
80 NCO:=NCO+BRR[2, 1]*ARR[1, 0]+BRR[2, 2]*ARR[2, 0];
81 "IF" COUNT<10 "THEN" "GOTO" AGAIN;
82 EXIT: "COMMENT" PRINT COEFFICIENTS, COMPUTE PHASE SHIFTS ETC;
83 "END";
```

The phase shifts are determined from the K-matrix formula

$$\tan \delta = \frac{\text{IMAGINARY part of the AMPLITUDE}}{\text{REAL part of the AMPLITUDE}}$$

To compute the s-wave phase shifts insert the following lines of code into the program CP1 at line 82.

```
"COMMENT" DECLARE E,DELO,DEL2 AS INTEGER VARIABLES, AND
NEW AS A REAL VARIABLE WITHIN MAIN PROGRAM. E IS THE
ENERGY OF THE TWO-PION SYSTEM IN MEV, DELO AND DEL2 ARE
THE I=0 AND 2 S-WAVE PHASE SHIFTS RESPECTIVELY IN DEGREES;
"FOR"NEW:=0.0 "STEP"0.1"UNTIL"12.0"DO"
  "BEGIN"E:=ENTIER(278*SQRT(NEW+1));
  "COMMENT" DELO AND DEL2 ARE GIVEN BY SUBSTITUTING
  FROM EQTN 3.3.27 INTO EQTN B3.1;
  DELO:=ENTIER(57.296*ARCTAN(-NEW*(2*B0+R*H0*NEW^(3/2)))/
  (A0-4*NC0*NEW+(8/3)*(4*F0+K0)NMW*NEW));
  DEL2:=ENTIER(57.296*ARCTAN(-NEW*(2*B2+R*H2*NEW^(3/2)))/
  (A2-4*NC2*NEW+(8/3)*(4*F2+K2)*NEW*NEW));
  "PRINT"E,SAMELINE,"S6",DELO,"S6",DEL2;
"END";
```

A set of initial values for a_2 , a_0 and nc_0 are given in Table B3.1 and the resulting solutions in Table B3.2 on the next page.

	SOLN $A_1^{(a)}$	SOLN $A_1^{(b)}$	SOLN $A_1^{(c)}$	SOLN A_2	SOLN B_1	SOLN B_2
a_2	0.04	0.04	0.04	-0.04	0.04	-0.04
a_0	0.10	0.50	0.90	-0.11	-0.05	0.1
nc_0	0.0	0.0	0.0	0.0	0.0	0.01

Table B3.1

Table B3.2

Coefficients from PGM-II

	SOLN A ₁ ^(a)	SOLN A ₁ ^(b)	SOLN A ₁ ^(c)	SOLN A ₂	SOLN B ₁	SOLN B ₂	SOLN B ₂
a ₂	0.04	0.04	0.04	-0.04	0.04	-0.04	-0.064
a ₀	0.184867	0.548594	0.881614	-0.107131	-0.052912	0.039060	0.058126
b ₀	-0.017088	-0.150478	-0.388622	-0.005738	-0.001400	-0.000763	-0.001689
b ₂	-0.0008	-0.0008	-0.0008	-0.0008	-0.0008	-0.0008	-0.002048
nc ₀	-0.005860	-0.008377	0.034627	0.003728	0.023714	-0.024829	-0.040521
c ₁	0.005725	0.024123	0.030608	-0.000928	-0.012689	0.011699	0.018484
nc ₂	0.006575	0.026432	0.033431	-0.000523	-0.013300	0.011240	0.017377
f ₀	0.000271	0.001699	0.004032	0.000116	-0.000031	-0.000021	-0.000050
f ₁	0.000144	0.001421	0.003699	0.000036	-0.000006	-0.000012	-0.000033
f ₂	0.000195	0.001532	0.003832	0.000068	-0.000016	-0.000016	-0.000040
H ₀	-0.000555	-0.001771	-0.002200	-0.000185	0.000662	0.000536	0.001314
H ₂	-0.000222	-0.000708	0.000880	-0.000074	0.000265	0.000214	0.000526
k ₀	0.000278	0.000886	0.001100	0.000092	-0.000331	-0.000268	-0.000657
k ₂	0.000111	0.000354	0.000440	0.000037	-0.000132	-0.000107	-0.000263

Table B3.3

Martin inequalities from PGM-II

I	$A_0^{00}(4) > A_0^{00}(3.155)$
II	$A_0^{00}(4) > A_0^{00}(0) > A_0^{00}(3.189)$
III	$A_0^{00}(0.2937) > A_0^{00}(2.4226)$
IV	$A_0^{00}(3.205) > A_0^{00}(0.2134) > A_0^{00}(2.9863)$

Solution $A_1^{(a)}$

I	$0.088289 > 0.084318$	✓
II	$0.088289 > 0.083994 > 0.084367$	×
III	$0.083821 > 0.083655$	✓
IV	$0.084391 > 0.083865 > 0.084105$	×

Solution $A_1^{(b)}$

I	$0.209531 > 0.174935$	✓
II	$0.209531 > 0.171935 > 0.175393$	×
III	$0.170277 > 0.168672$	✓
IV	$0.175617 > 0.170702 > 0.172933$	×

Solution $A_1^{(c)}$

I	$0.320538 > 0.229815$	✓
II	$0.320538 > 0.221813 > 0.231043$	×
III	$0.217342 > 0.213006$	✓
IV	$0.231640 > 0.216488 > 0.224453$	×

Solution A₂

I	-0.062377 > -0.063964	✓
II	-0.062377 > -0.064096 > -0.063944	×
III	-0.064167 > -0.064235	✓
IV	-0.063934 > -0.064148 > -0.064051	×

Solution B₁

I	0.009029 > 0.007768	✓
II	0.009029 > 0.007618 > 0.007792	×
III	0.007521 > 0.007424	✓
IV	0.007803 > 0.007546 > 0.007661	×

Solution B₂: $a_2 = -0.04$

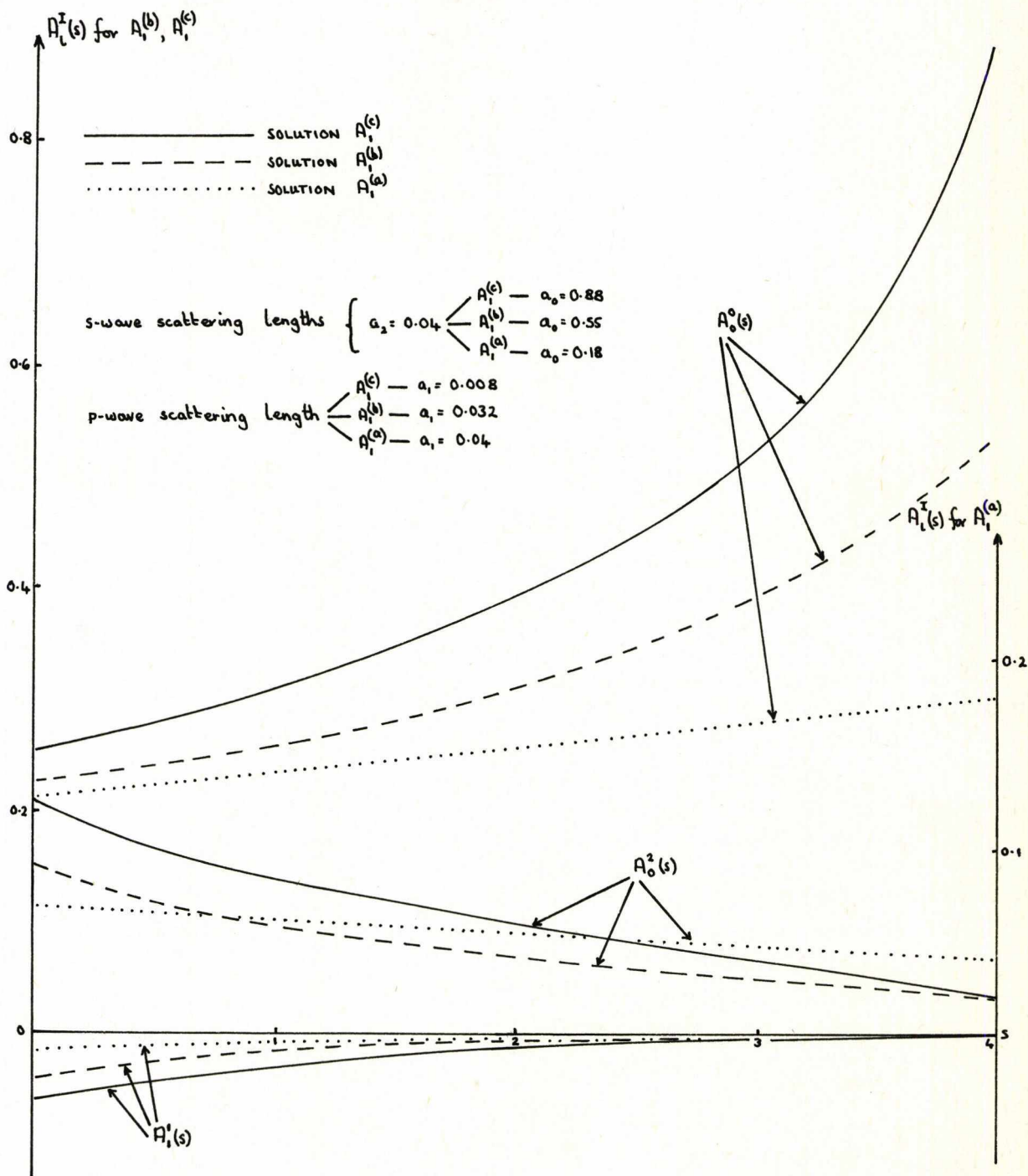
I	-0.013647 > -0.014653	✓
II	-0.013647 > -0.014773 > -0.014633	×
III	-0.014850 > -0.014928	✓
IV	-0.014624 > -0.014830 > -0.014738	×

Solution B₂: $a_2 = -0.064$

I	-0.023291 > -0.025756	✓
II	-0.023291 > -0.026050 > -0.025709	×
III	-0.026240 > -0.026430	✓
IV	-0.025686 > -0.026191 > -0.025965	×

Figure B3.1

$\pi\pi$ s- and p-wave amplitudes in $[0,4]$ from PGM-II



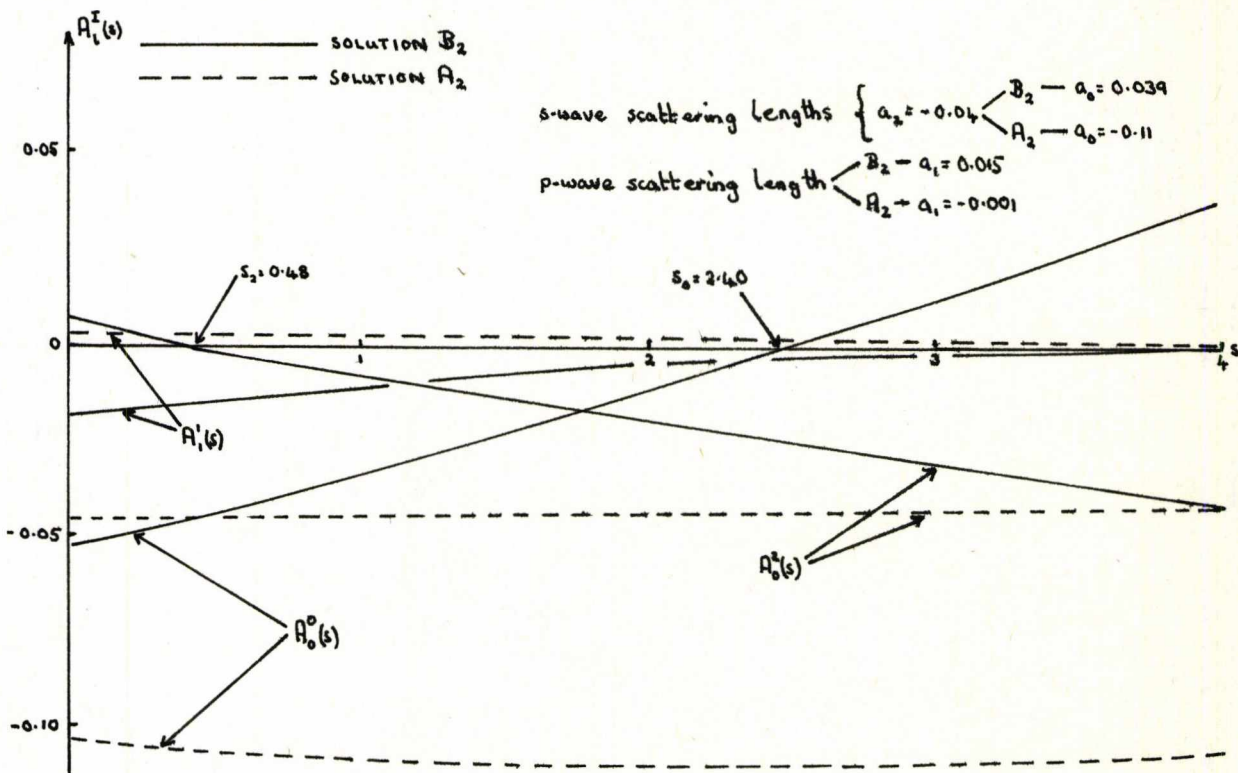
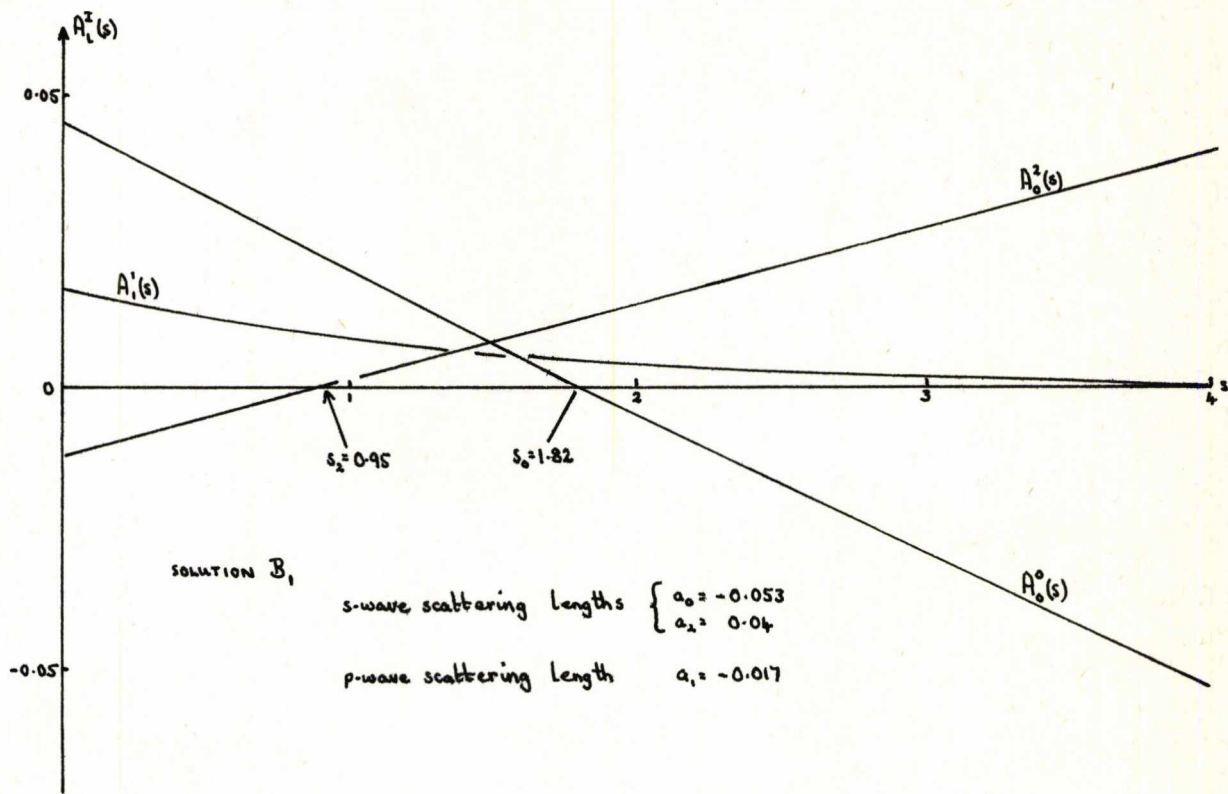
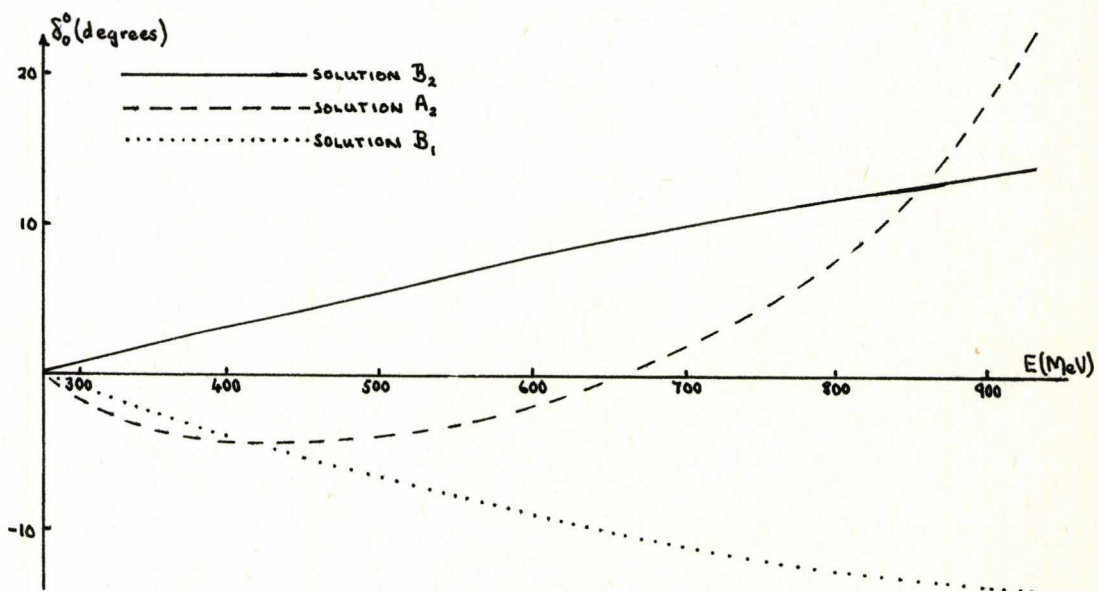
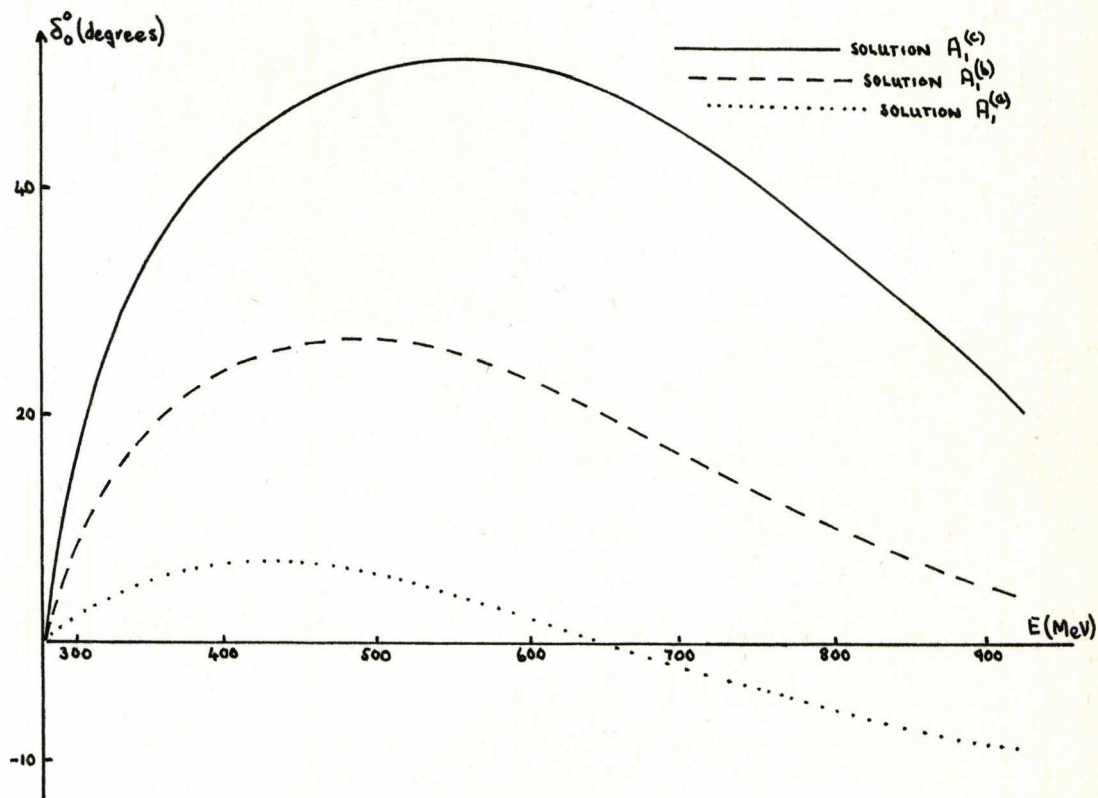


Figure B3.2

I=0 s-wave phase shifts from PGM-II



VIOLATION OF ELASTIC UNITARITY IN PGM-II

Using the formula

$$\left\{ \left| \frac{\text{Im } A_{\ell}^I(s)}{\sqrt{s-4}/s |A_{\ell}^I(s)|^2} - 1 \right| \right\} \times 100 \quad (B3.1)$$

the percentage violation of elastic unitarity in each of the s-wave amplitudes of PGM-II is given in Table B3.4 (only percentages <30% are given).

s in MeV	Solution A ₁ ^(a) a ₂ =0.04		Solution A ₂ a ₂ =-0.04		Solution B ₁ a ₂ =0.04		Solution B ₂ a ₂ =-0.04	
	I=0	I=2	I=0	I=2	I=0	I=2	I=0	I=2
284	0.5	0.3	0.4	0.3	0.3	0.1	0.4	0.3
291	1.7	0.9	1.6	1.0	1.2	0.6	1.5	0.8
298	3.2	1.6	3.1	1.7	2.4	1.1	2.9	1.5
305	4.9	2.7	4.7	2.7	3.8	1.8	4.5	2.5
312	7.8	4.0	7.7	4.0	6.3	2.6	7.3	3.8
326	13.7	7.7	13.6	7.5	10.7	4.0	12.9	7.4
340	21.0	11.0	20.7	10.7	16.3	6.1	19.7	10.5
355	-	16.4	29.7	16.0	23.0	8.3	29.1	15.5
368	-	21.6	-	21.1	29.9	12.7	-	20.4
381	-	26.2	-	25.8	-	16.4	-	24.8
393	-	-	-	-	-	20.1	-	29.1

Table B3.4

APPENDIX C3

LINEAR CONSTRAINT EQUATIONS: MODEL DCB-I

The linear constraint equations between the coefficients of Equation (3.4.3) are obtained by substituting for $A_{\ell}^I(s)$ from (3.4.3) into (3.4.12) and performing the integrations explicitly. The resulting matrix equation, of the form

$$\underline{Ax} = \underline{By} \tag{C3.1}$$

is given by

$$\begin{bmatrix} 0 & 0 & 35 & 0 & 70 & 128 \\ 210 & -525 & 280 & 0 & -700 & -960 \\ 210 & -525 & 420 & -1890 & -1050 & -1600 \\ 2310 & -5775 & 3696 & -8316 & -9240 & -12800 \\ 18018 & -45045 & 24024 & 0 & -60060 & -76800 \\ 0 & 1 & 0 & 0 & 4 & 8 \end{bmatrix} \begin{bmatrix} a_0^s \\ a_2^s \\ b_0^s \\ b_1^p \\ b_2^s \\ c_2^s \end{bmatrix} = \begin{bmatrix} 12 & 24 & -64 & 0 & 80 & 160 & 0 \\ -336 & 840 & -384 & 0 & -960 & 2400 & 0 \\ -288 & 720 & -640 & 4272 & -640 & 1600 & 0 \\ -3520 & 8800 & -5120 & 20040 & -8960 & 22400 & 0 \\ -29120 & 72800 & -30720 & 10632 & -80640 & 201600 & 0 \\ 0 & 0 & 0 & 0 & 0 & 0 & 1 \end{bmatrix} \begin{bmatrix} z_0^s \\ z_2^s \\ c_0^s \\ c_1^p \\ y_0^s \\ y_2^s \\ a_2 \end{bmatrix} \tag{C3.2}$$

To solve the system of equations which define Model DCB-I it is necessary to amend the computer program CP1, given in Appendix B3, as follows:

Computer program

The coefficients of DCB-I can be determined from the program CP1 with the modifications listed below

Replace lines 2 to 4 by

```
"REAL" A0S, A2S, B0S, B1P, B2S, C0S, C1P, C2S, Z0S, Z2S, Y0S, Y2S,
A2, DZ0S, DC0S, DC1P, DY0S, DY2S, W, RTW, DET;
"ARRAY" A[1:6, 1:6], B[1:6, 1:7], ARR[1:5, 0:5], BRR[1:5, 1:5];
```

Replace lines 10 to 15 by

```
"BEGIN" "ARRAY" C, X[1:6, 1:1], Y[1:7, 1:1];
Y[1, 1] := Z0S;
Y[2, 1] := Z2S;
Y[3, 1] := C0S;
Y[4, 1] := C1P;
Y[5, 1] := Y0S;
Y[6, 1] := Y2S;
Y[7, 1] := A2;
```

Replace lines 23 to 39 by

```
A0S := X[1, 1];
A2S := X[2, 1];
B0S := X[3, 1];
B1P := X[4, 1];
B2S := X[5, 1];
C2S := X[6, 1];
ARR[1, CYC] := C0S - (1/18) * ((A0S + 4 * B0S + 8 * C0S) ↑ 2) - (5/18) * A2 * A2;
ARR[2, CYC] := C1P + (1/18) * ((A0S + 4 * B0S + 8 * C0S) ↑ 2) - (5/36) * A2 * A2;
ARR[3, CYC] := Z0S + (1/2) * ((A0S + 4 * B0S + 8 * C0S) ↑ 2);
ARR[4, CYC] := (Z0S - (W - 4) * Y0S) * RTW + ((A0S + B0S * W + C0S * W * RTW) ↑ 2)
+ (W - 4) * ((Z0S - (W - 4) * Y0S) ↑ 2);
ARR[5, CYC] := (Z2S - (W - 4) * Y2S) * RTW + ((A2S + B2S * W + C2S * W * RTW) ↑ 2)
+ (W - 4) * ((Z2S - (W - 4) * Y2S) ↑ 2);
"IF" CYC = 0 "THEN" "PRINT" ALIGNED(1, 8), ARR[1, CYC], SAMELINE,
**S5** , ARR[2, CYC], **S5** , ARR[3, CYC], **S5** , ARR[4, CYC],
**S5** , ARR[5, CYC];
```

Note: N is now 6 and M is 5

Replace lines 52 and 53 by

```
"READ"A2,Z0S,C0S,C1P,Y0S,Y2S,Z0S,DC0S,DC1P,DY0S,DY2S;
Z2S:=- (1/2)*A2*A2;
"COMMENT"W CORRESPONDS TO S IN TEXT;
W:=4.001;
RTW:=SQRT(W);
```

Replace lines 64 to 73 by

```
CYC:=1;
Z0S:=Z0S+DZ0S;
EVCO;
CYC:=2;
C0S:=C0S+DC0S;
Z0S:=Z0S-DZ0S;
EVCO;
CYC:=3;
C1P:=C1P+DC1P;
C0S:=C0S-DC0S;
EVCO;
CYC:=4;
Y0S:=Y0S+DY0S;
C1P:=C1P-DC1P;
EVCO;
CYC:=5;
Y2S:=Y2S+DY2S;
Y0S:=Y0S-DY0S;
EVCO;
Y2S:=Y2S-DY2S;
```

Replace lines 79 and 80 by

```
Z0S:=Z0S+BRR[1,1]*ARR[1,0]+BRR[1,2]*ARR[2,0]+BRR[1,3]*ARR[3,0]
+BRR[1,4]*ARR[4,0]+BRR[1,5]*ARR[5,0];
C0S:=C0S+BRR[2,1]*ARR[1,0]+BRR[2,2]*ARR[2,0]+BRR[2,3]*ARR[3,0]
+BRR[2,4]*ARR[4,0]+BRR[2,5]*ARR[5,0];
C1P:=C1P+BRR[3,1]*ARR[1,0]+BRR[3,2]*ARR[2,0]+BRR[3,3]*ARR[3,0]
+BRR[3,4]*ARR[4,0]+BRR[3,5]*ARR[5,0];
Y0S:=Y0S+BRR[4,1]*ARR[1,0]+BRR[4,2]*ARR[2,0]+BRR[4,3]*ARR[3,0]
+BRR[4,4]*ARR[4,0]+BRR[4,5]*ARR[5,0];
Y2S:=Y2S+BRR[5,1]+BRR[1,0]+BRR[5,2]*ARR[2,0]+BRR[5,3]*ARR[3,0]
+BRR[5,4]*ARR[4,0]+BRR[5,5]*ARR[5,0];
```

Table C3.1

Coefficients from DCB-I

	Solution A ₁	Solution A ₂	Solution B ₁	Solution B ₂ ^(a)	Solution B ₂ ^(b)	Solution B ₂ ^(a)
a ₂	0.05	-0.05	0.05	-0.05	-0.05	-0.052
a ₀	0.057121	-0.059519	-0.078467	0.123091	0.318520	0.130744
a ₁	-0.006781	0.007966	-0.022584	0.025697	0.025017	0.026258
a ₀ ^S	0.110789	-0.095444	0.043059	-0.078073	-0.236979	-0.083575
a ₂ ^S	0.028639	-0.026985	-0.023535	0.024648	0.060858	0.025985
z ₀ ^S	-0.001631	-0.001771	-0.003079	-0.007576	-0.050727	-0.008547
z ₂ ^S	-0.001250	-0.001250	-0.001250	-0.001250	-0.001250	-0.001352
b ₀ ^S	-0.015168	0.007199	-0.032455	0.047219	0.126213	0.050178
b ₁ ^P	-0.002193	0.001540	-0.005661	0.007808	0.022122	0.008307
b ₂ ^S	0.004922	-0.006211	0.017563	-0.020732	-0.041771	-0.021833
c ₀ ^S	0.000876	0.000891	0.001037	0.001537	0.006331	0.001701
c ₁ ^P	0.000166	0.000150	0.000005	-0.000495	-0.005289	-0.000574
c ₂ ^S	0.000209	0.000229	0.000410	0.001035	0.007028	0.001168
y ₀ ^S	-0.000919	-0.000807	0.001923	0.005462	0.041205	0.006197
y ₂ ^S	0.000122	0.000121	0.000784	0.000726	0.000879	0.000785

Table C3.2

Martin Inequalities from DCB-I

I	$A_0^{00}(4) > A_0^{00}(3.155)$
II	$A_0^{00}(4) > A_0^{00}(0) > A_0^{00}(3.189)$
III	$A_0^{00}(0.2937) > A_0^{00}(2.4226)$
IV	$A_0^{00}(3.205) > A_0^{00}(0.2134) > A_0^{00}(2.9863)$

Solution A₁

I	$0.052374 > 0.051399$	✓
II	$0.052374 > 0.051469 > 0.51414$	✓
III	$0.051314 > 0.051174$	✓
IV	$0.051422 > 0.051350 > 0.51332$	✓

Solution A₂

I	$-0.053173 > -0.054234$	✓
II	$-0.053173 > -0.054161 > -0.054217$	✓
III	$-0.054331 > -0.054489$	✓
IV	$-0.054209 > -0.054292 > -0.054310$	✓

Solution B₁

I	$0.007178 > 0.004136$	✓
II	$0.007178 > 0.004254 > 0.004204$	✓
III	$0.003747 > 0.003125$	✓
IV	$0.004236 > 0.003871 > 0.003833$	✓

Solution B₂^(a): $a_2 = -0.05, a_0 = 0.123$

I	$0.007697 > 0.001899$	✓
II	$0.007697 > 0.002128 > 0.002029$	✓
III	$0.001141 > -0.000065$	✓
IV	$0.002092 > 0.001382 > 0.001310$	✓

Solution B₂^(b)

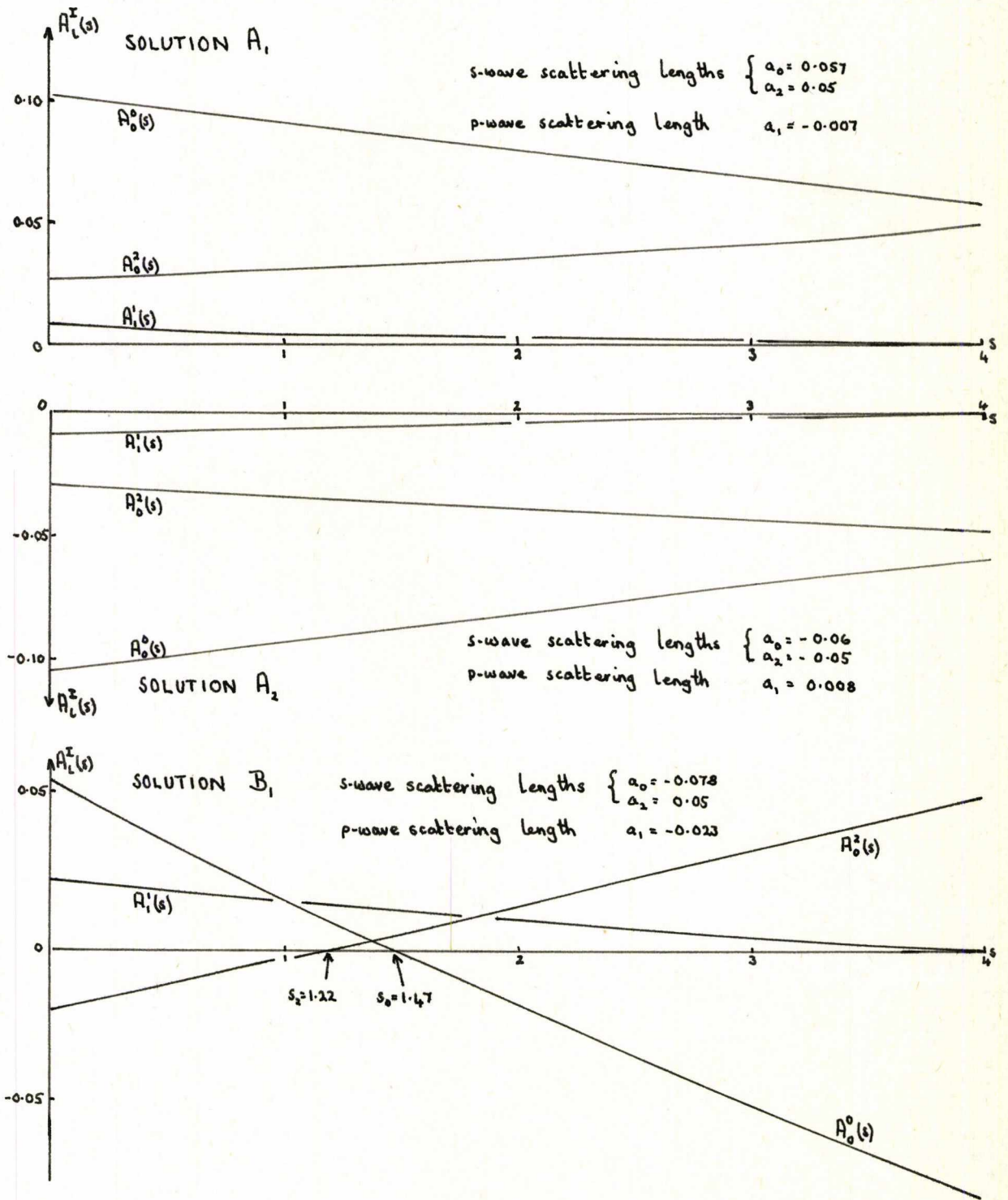
I	$0.072840 > 0.039353$	✓
II	$0.072840 > 0.040661 > 0.040120$	✓
III	$0.034864 > 0.027750$	✓
IV	$0.040490 > 0.036281 > 0.035878$	✓

Solution B₂^(a): $a_2 = -0.052, a_0 = 0.13$

I	$0.008915 > 0.002419$	✓
II	$0.008915 > 0.002676 > 0.002565$	✓
III	$0.001570 > 0.000218$	✓
IV	$0.002636 > 0.001839 > 0.001759$	✓

Figure C3.1

$\pi\pi$ s- and p-wave amplitudes in $[0,4]$ from DCB-I



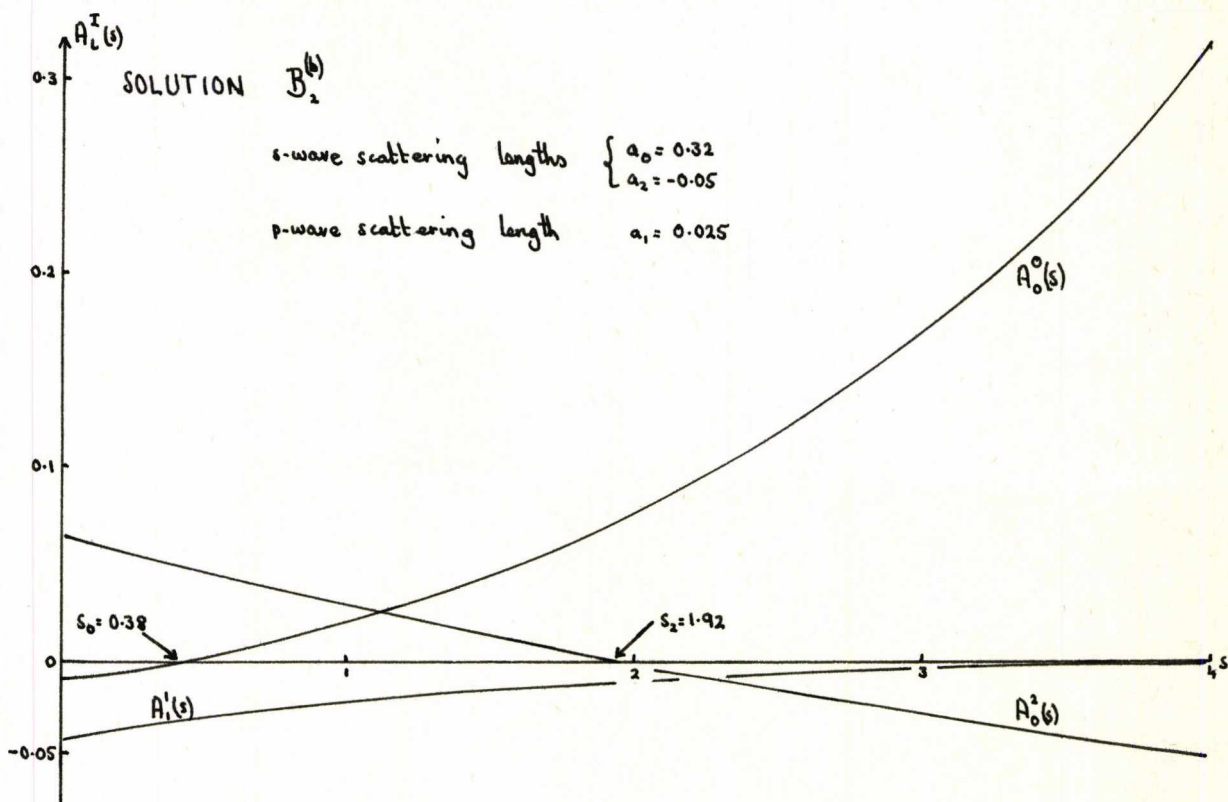
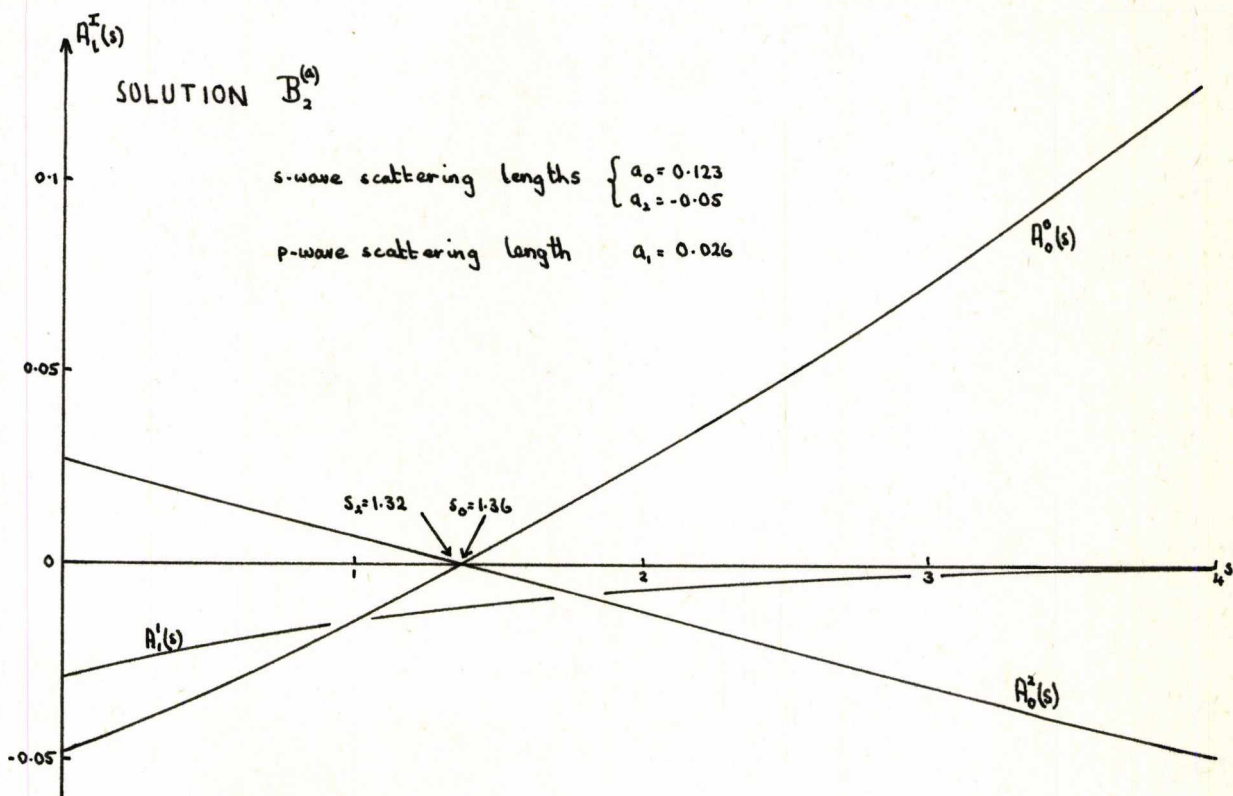
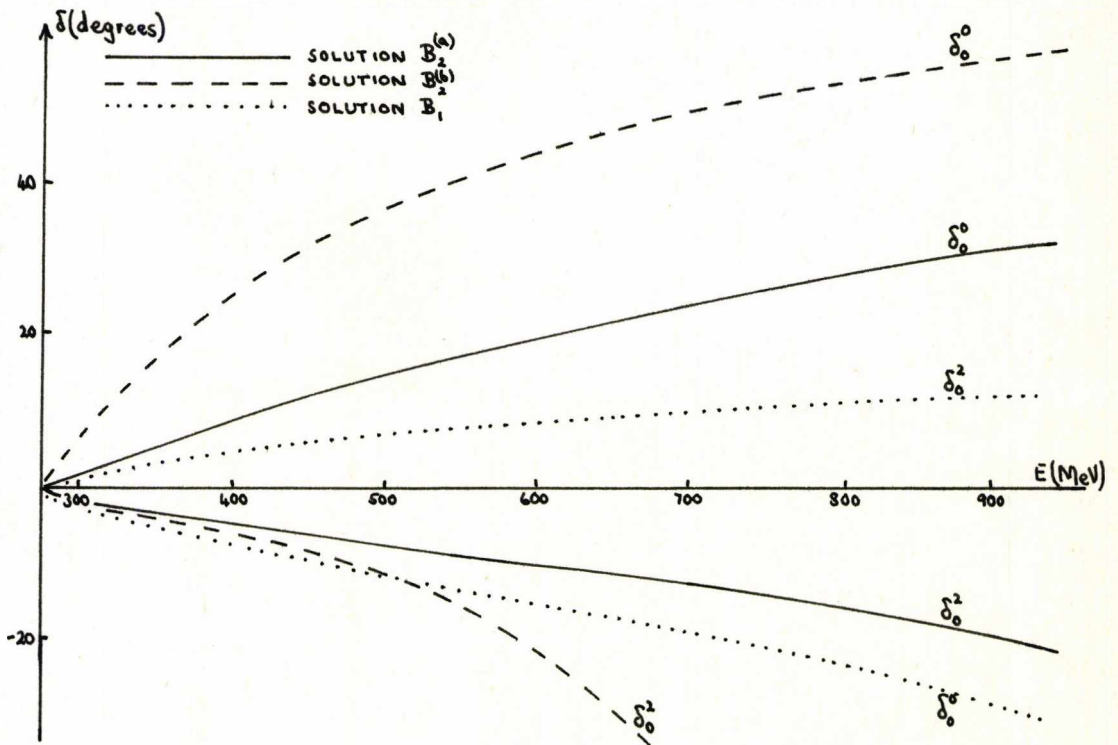
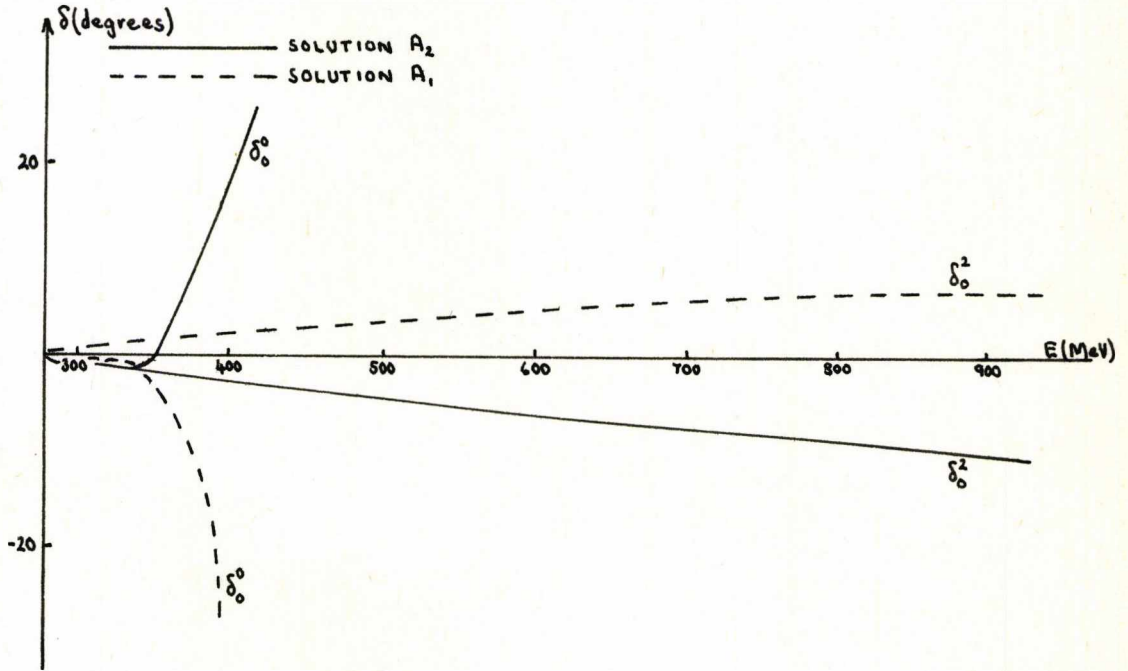


Figure C3.2

$\pi\pi$ s-wave phase shifts from DCB-I



APPENDIX A4

THE BEHAVIOUR OF $\text{Im } A_{\ell}^{\text{I}}(s)$ IN THE VICINITY OF $s=0$

One can write partial wave amplitudes in the form

$$A_{\ell}^{\text{I}}(s) = \frac{1}{4-s} \int_0^{4-s} A^{\text{I}}(s,t,u) P_{\ell} \left(1 + \frac{2t}{s-4} \right) dt \quad (\text{A4.1})$$

If s is kept fixed, small and negative, then $\text{Im } A^{\text{I}}(s,t,u) \neq 0$ for $u > 4$ or $t > 4$ and one can write

$$\begin{aligned} \text{Im } A_{\ell}^{\text{I}}(s) &= \frac{1}{4-s} \int_{4+}^{4-s} \text{Im } A^{\text{I}}(s,t,u) P_{\ell} \left(1 + \frac{2t}{s-4} \right) dt \\ &+ \frac{1}{4-s} \int_0^{-s} \text{Im } A^{\text{I}}(s,t,u) P_{\ell} \left(1 + \frac{2t}{s-4} \right) dt \quad (\text{A4.2}) \end{aligned}$$

Taking into account $s \leftrightarrow t$ and $s \leftrightarrow u$ crossing properties, (A4.2) becomes

$$\begin{aligned} \text{Im } A_{\ell}^{\text{I}}(s) &= \frac{1}{4-s} \left[\sum_{\text{I}'} \alpha_{\text{st}}^{\text{II}'} \int_4^{4-s} \text{Im } A^{\text{I}}(t,s,u) P_{\ell} \left(1 + \frac{2t}{s-4} \right) dt \right. \\ &\left. + \sum_{\text{I}'} \alpha_{\text{su}}^{\text{II}'} \int_0^{-s} \text{Im } A^{\text{I}}(u,t,s) P_{\ell} \left(1 + \frac{2t}{s-4} \right) dt \right], \quad (\text{A4.3}) \end{aligned}$$

where $\alpha_{\text{st}}^{\text{II}'}$ and $\alpha_{\text{su}}^{\text{II}'}$ are the crossing matrices of (1.7.14) and (1.7.16).

Using the analytic properties of the absorptive parts of the amplitudes one can expand $\text{Im } A^I(s, t, u)$ in terms of its partial waves. It follows from elastic unitarity and normal threshold behaviour that

$$\text{Im } A^I(s, t, u) = \sqrt{\frac{s-4}{s}} \left\{ a_I^2 + (s-4)\alpha_I \right\} + O(s-4)^{5/2}, \quad (A4.4)$$

where a_I is the s-wave scattering length with isospin I, and

$$\alpha_I \equiv \frac{d}{ds} \left\{ \left| A^I(s) \right|^2 \right\}_{s=4}. \quad (A4.5)$$

By inserting (A4.4) into (A4.3), one obtains after integration partial wave amplitudes of the form

$$A_{\ell}^I(s) = C_{3,\ell}^I s^{3/2} + C_{5,\ell}^I s^{5/2} + \dots \text{ near } s=0 \quad (A4.6)$$

where,

for the s-waves

$$C_{3,0}^0 \equiv c_0^s = \frac{1}{6} \left(\frac{1}{3} a_0^2 + \frac{5}{3} a_2^2 \right)$$

$$C_{3,0}^2 \equiv c_2^s = \frac{1}{6} \left(\frac{1}{3} a_0^2 + \frac{1}{6} a_2^2 \right)$$

$$C_{5,0}^0 \equiv e_0^s = \frac{13}{240} \left(\frac{1}{3} a_0^2 + \frac{5}{3} a_2^2 \right) - \frac{1}{10} \left(\frac{1}{3} \alpha_0 + \frac{5}{3} \alpha_2 \right)$$

$$C_{5,0}^2 \equiv e_2^s = \frac{13}{240} \left(\frac{1}{3} a_0^2 + \frac{1}{6} a_2^2 \right) - \frac{1}{10} \left(\frac{1}{3} \alpha_0 + \frac{1}{6} \alpha_2 \right)$$

for the p-wave

$$c_{3,1}^1 \equiv c_1^p = -\frac{1}{6}\left(\frac{1}{3}a_0^2 - \frac{5}{6}a_2^2\right)$$

$$c_{5,1}^1 \equiv e_1^p = -\frac{7}{80}\left(\frac{1}{3}a_0^2 - \frac{5}{6}a_2^2\right) + \frac{1}{10}\left(\frac{1}{3}\alpha_0 - \frac{5}{6}\alpha_2\right)$$

for the d-waves

$$c_{3,2}^0 \equiv c_0^d = \frac{1}{6}\left(\frac{1}{3}a_0^2 + \frac{5}{3}a_2^2\right)$$

$$c_{3,2}^2 \equiv c_2^d = \frac{1}{6}\left(\frac{1}{3}a_0^2 + \frac{1}{6}a_2^2\right)$$

$$c_{5,2}^0 \equiv e_0^d = \frac{37}{240}\left(\frac{1}{3}a_0^2 + \frac{5}{3}a_2^2\right) - \frac{1}{10}\left(\frac{1}{3}\alpha_0 + \frac{5}{3}\alpha_2\right)$$

$$c_{5,2}^2 \equiv e_2^d = \frac{37}{240}\left(\frac{1}{3}a_0^2 + \frac{1}{6}a_2^2\right) - \frac{1}{10}\left(\frac{1}{3}\alpha_0 + \frac{1}{6}\alpha_2\right)$$

APPENDIX B4

Table B4.1

Coefficients from DCB-II

	Solution A	Solution B	Solution C	Solution D
a_{00}	0.083726	0.103865	0.099388	0.117996
a_{02}	-0.05	-0.05	-0.05	-0.07
a_{11}	0.113952	0.04	0.03	0.03
a_{20}	0.026928	0.009593	0.007197	0.005903
a_{22}	0.001359	0.000425	0.000774	0.000635
a_0^s	-0.153969	0.033638	0.032923	0.062193
a_2^s	-0.061965	-0.065456	-0.060680	-0.095900
z_0^s	-0.003505	-0.005394	-0.004939	-0.006962
z_2^s	-0.001250	-0.001250	-0.001250	-0.002450
b_0^s	0.086031	-0.064589	-0.062711	-0.086632
b_1^p	-0.022963	-0.004943	-0.002151	-0.002519
b_2^s	-0.004035	0.014430	0.015366	0.036103
$c_0^{s,d}$	0.001084	0.001294	0.001243	0.002135
c_1^p	-0.000042	-0.000252	-0.000202	-0.000093
$c_2^{s,d}$	0.000459	0.000669	0.000618	0.000910
y_0^s	0.002348	0.009393	0.008640	0.012045
y_2^s	-0.000630	0.000307	0.000464	0.001557

Table B4.1 contd./ ...

Table B4.1 (contd.)

	Solution A	Solution B	Solution C	Solution D
d_o^s	-0.007931	0.020700	0.020050	0.025655
d_o^d	-0.002341	-0.001035	-0.001006	-0.001878
d_1^p	0.005785	0.000808	0.000262	0.000033
d_2^s	0.001560	-0.002038	-0.002609	-0.006607
d_2^d	-0.001132	0.000156	0.000180	0.000175
e_o^s	0.000369	-0.000405	-0.000420	-0.000788
e_o^d	0.001019	0.000371	0.000326	0.000492
e_1^p	0.000265	0.000462	0.000408	0.000502
e_2^s	-0.000016	-0.000469	-0.000437	-0.000627
e_2^d	0.000259	-0.000068	-0.000066	-0.000082
x_o^s	0.000238	-0.005620	-0.005187	-0.007326
x_1^p	-0.000406	-0.000543	-0.000499	-0.000757
x_2^s	0.003370	0.002535	0.002260	0.003184

APPENDIX C4

MARTIN INEQUALITIES FROM DCB-II

Table C4.1

Inequalities involving the s-wave amplitudes in the unphysical region

I	$A_0^{00}(4) > A_0^{00}(0) > A_0^{00}(3.189)$
II	$A_0^{00}(0.2937) > A_0^{00}(2.4226)$
III	$A_0^{00}(3.205) > A_0^{00}(0.2134) > A_0^{00}(2.9863)$

Solution A

I	$-0.005425 > -0.019311 > -0.020397$	✓
II	$-0.024788 > -0.030078$	✓
III	$-0.020148 > -0.023424 > -0.023401$	×

Solution B

I	$0.001288 > -0.016864 > -0.017228$	✓
II	$-0.021435 > -0.026806$	✓
III	$-0.016960 > -0.020290 > -0.020380$	✓

Solution C

I	$-0.000204 > -0.016043 > -0.016356$	✓
II	$-0.019973 > -0.024602$	✓
III	$-0.016124 > -0.018989 > -0.019076$	✓

Solution D

I	$-0.007335 > -0.020903 > -0.021285$	✓
II	$-0.024080 > -0.027718$	✓
III	$-0.021101 > -0.023294 > -0.023428$	✓

Table C4.2

Inequalities involving s- and p-wave amplitudes and their first derivatives in [0,4]*

I	$-\frac{1}{4} \left[2A_0^{00}(4) - A_0^{00}(2) - A_0^{00}(0) \right] > A_0^{00}'(0)$
II	$A_0^2(0) - A_1^1(0) - \frac{2}{3} \left[A_0^0(4) - A_0^2(4) \right] > 2A_0^2'(0) - 2A_1^1'(0)$
III	$4A_0^0(0) - 10A_0^2(0) - 3A_1^1(0) > A_0^0'(0) + 20A_0^2'(0) - 6A_1^1'(0)$
IV	$-A_0^0(0) + \frac{5}{2}A_0^2(0) + \frac{3}{2}A_1^1(0) > 2A_0^0'(0) + A_0^2'(0) + 3A_1^1'(0)$
V	$\frac{1}{2}A_1^1(0) > A_0^2'(0) + A_1^1'(0)$
VI	$2A_0^0(0) - 5A_0^2(0) + A_1^1(0) > -2A_0^0'(0) + 10A_0^2'(0) + 2A_1^1'(0)$

Solution A

I	-0.010416 > -0.021116	✓
II	-0.028993 > -0.108758	✓
III	-0.856075 > -1.220333	✓
IV	0.197644 > 0.036443	✓
V	-0.010917 > -0.084073	✓
VI	-0.482620 > -0.872166	✓

*The inequalities have been derived by

G. Auberson, Nuovo Cimento 68A, 281 (1970).

All other constraint equations in this paper are also satisfied by all of our solutions.

Solution B

I	-0.012246 > -0.017595	✓
II	-0.063755 > -0.085589	✓
III	-0.413801 > -0.752142	✓
IV	0.085987 > 0.022815	✓
V	-0.011642 > -0.030971	✓
VI	-0.265112 > -0.398964	✓

Solution C

I	-0.010561 > -0.015158	✓
II	-0.063478 > -0.077490	✓
III	-0.354721 > -0.648867	✓
IV	0.071423 > 0.025286	✓
V	-0.011505 > -0.023075	✓
VI	-0.234884 > -0.326122	✓

Solution D

I	-0.008924 > -0.012594	✓
II	-0.081797 > -0.088515	✓
III	-0.404614 > -0.682930	✓
IV	0.078660 > 0.057211	✓
V	-0.014996 > -0.019010	✓
VI	-0.277285 > -0.342061	✓

Table C4.3

Inequalities involving the $\pi^0\pi^0$ s- and d-wave amplitudes in $[0,4]^*$

I	$3.061 A_2^{00}(0.0730) > A_0^{00}(3.654) - A_0^{00}(0.0730)$
I'	$4.067 A_2^{00}(0.0341) < A_0^{00}(3.839) - A_0^{00}(0.0341)$
II	$1.633 A_2^{00}(0.325) > A_0^{00}(0.325) - A_0^{00}(2.463)$
II'	$1.428 A_2^{00}(0.304) < A_0^{00}(0.304) - A_0^{00}(2.543)$
III	$3.061 A_2^{00}(0.589) > A_0^{00}(0.237) - A_0^{00}(0.589)$
III'	$3.252 A_2^{00}(0.803) < A_0^{00}(0.199) - A_0^{00}(0.803)$
IV	$2.050 A_2^{00}(0.572) > A_0^{00}(0.572) - A_0^{00}(1.294)$
IV'	$1.498 A_2^{00}(0.572) < A_0^{00}(0.572) - A_0^{00}(1.087)$
V	$3.061 A_2^{00}(0.826) > A_0^{00}(2.953) - A_0^{00}(0.826)$
V'	$3.267 A_2^{00}(0.747) < A_0^{00}(3.052) - A_0^{00}(0.747)$
VI	$1.929 A_2^{00}(2.288) > A_0^{00}(2.288) - A_0^{00}(1.091)$
VI'	$1.620 A_2^{00}(2.288) < A_0^{00}(2.288) - A_0^{00}(1.244)$
VII	$1.633 A_2^{00}(2.857) > A_0^{00}(2.857) - A_0^{00}(0.377)$
VII'	$1.630 A_2^{00}(3.102) < A_0^{00}(3.102) - A_0^{00}(0.296)$
VIII	$3.061 A_2^{00}(3.536) > A_0^{00}(0.0322) - A_0^{00}(3.536)$
VIII'	$3.066 A_2^{00}(3.106) < A_0^{00}(0.0619) - A_0^{00}(3.106)$

*The inequalities are from

A. Martin, Nuovo Cimento 63A, 167 (1969).

Solution A

I	$0.008276 > 0.008289$	×	I'	$0.010978 < 0.011010$	✓
II	$0.004407 > 0.004397$	✓	II'	$0.003858 < 0.003922$	✓
III	$0.008023 > 0.005152$	✓	III'	$0.008160 < 0.008089$	×
IV	$0.005388 > 0.005380$	✓	IV'	$0.003937 < 0.004537$	✓
V	$0.007637 > 0.007598$	✓	V'	$0.008305 < 0.008265$	×
VI	$0.002127 > 0.002075$	✓	VI'	$0.001786 < 0.002743$	✓
VII	$0.000902 > 0.000940$	×	VII'	$0.000581 < 0.003104$	✓
VIII	$0.000314 > -0.005345$	✓	VIII'	$0.001084 < 0.001082$	×

Solution B

I	$0.010003 > 0.004388$	✓	I'	$0.013606 < 0.013801$	✓
II	$0.004606 > 0.004595$	✓	II'	$0.004078 < 0.004138$	✓
III	$0.007386 > 0.004388$	✓	III'	$0.006875 < 0.006951$	✓
IV	$0.004998 > 0.004964$	✓	IV'	$0.003652 < 0.004099$	✓
V	$0.006377 > 0.006359$	✓	V'	$0.007154 < 0.007141$	×
VI	$0.001184 > 0.001113$	✓	VI'	$0.000995 < 0.001789$	✓
VII	$0.000452 > 0.000392$	✓	VII'	$0.000280 < 0.002829$	✓
VIII	$0.000142 > -0.006708$	✓	VIII'	$0.000522 < 0.000656$	✓

Solution C

I	$0.008666 > 0.008629$	✓	I'	$0.011796 < 0.011982$	✓
II	$0.003974 > 0.003963$	✓	II'	$0.003519 < 0.003571$	✓
III	$0.006348 > 0.003768$	✓	III'	$0.005893 < 0.005968$	✓
IV	$0.004296 > 0.004264$	✓	IV'	$0.003139 < 0.003520$	✓
V	$0.005465 > 0.005450$	✓	V'	$0.006137 < 0.006126$	×
VI	$0.001002 > 0.000939$	✓	VI'	$0.000841 < 0.001521$	✓
VII	$0.000381 > 0.000323$	✓	VII'	$0.000236 < 0.002427$	✓
VIII	$0.000119 > -0.005807$	✓	VIII'	$0.000439 < 0.000568$	✓

Solution D

I	$0.006931 > 0.006876$	✓	I'	$0.009473 < 0.009759$	✓
II	$0.003127 > 0.003115$	✓	II'	$0.002772 < 0.002819$	✓
III	$0.004954 > 0.002982$	✓	III'	$0.004583 < 0.004708$	✓
IV	$0.003354 > 0.003305$	✓	IV'	$0.002451 < 0.002734$	✓
V	$0.004249 > 0.004232$	✓	V'	$0.004776 < 0.004765$	×
VI	$0.000789 > 0.000733$	✓	VI'	$0.000663 < 0.001179$	✓
VII	$0.000304 > 0.000216$	✓	VII'	$0.000189 < 0.001854$	✓
VIII	$0.000096 > -0.004550$	✓	VIII'	$0.000352 < 0.000557$	✓

Table C4.4

Further inequalities involving the $\pi^0\pi^0$ s- and d-wave amplitudes in $[0,4]^*$

$$\begin{aligned} \delta_1 &= A_0^{00}(0.185) - A_0^{00}(1.168) \\ \delta_2 &= A_0^{00}(3.390) - A_0^{00}(0.408) \\ \delta_3 &= A_0^{00}(3.770) - A_0^{00}(0.0758) \\ \delta_4 &= A_0^{00}(0.0871) - A_0^{00}(2.737) \\ \delta_5 &= A_0^{00}(0.537) - A_0^{00}(2.363) \\ \delta_6 &= A_0^{00}(3.904) - A_0^{00}(0.00663) \end{aligned}$$

I	$3.169 A_2^{00}(1.168)$	$+ 1.422 A_2^{00}(0.185)$	$> \delta_1$	$> 3.163 A_2^{00}(1.168)$	$+ 1.347 A_2^{00}(0.185)$
II	$3.492 A_2^{00}(0.408)$	$+ 1.632 A_2^{00}(3.390)$	$> \delta_2$	$> 3.147 A_2^{00}(0.408)$	$+ 1.632 A_2^{00}(3.390)$
III	$4.391 A_2^{00}(0.0758)$	$+ 1.633 A_2^{00}(3.770)$	$> \delta_3$	$> 3.896 A_2^{00}(0.0758)$	$+ 1.633 A_2^{00}(3.770)$
IV	$1.380 A_2^{00}(0.0871)$	$+ 3.073 A_2^{00}(2.737)$	$> \delta_4$	$> 1.303 A_2^{00}(0.0871)$	$+ 3.073 A_2^{00}(2.737)$
V	$1.510 A_2^{00}(0.537)$	$- 1.622 A_2^{00}(2.363)$	$> \delta_5$	$> 1.494 A_2^{00}(0.537)$	$- 1.623 A_2^{00}(2.363)$
VI	$6.503 A_2^{00}(0.00663)$	$- 3.061 A_2^{00}(3.904)$	$> \delta_6$	$> 4.347 A_2^{00}(0.00663)$	$- 3.061 A_2^{00}(3.904)$

*These inequalities are also from A. Martin, Nuovo Cimento 63A, 167 (1969).

Solution A

I	0.010947 > 0.010792 > 0.010731	✓
II	0.009648 > 0.009415 > 0.008723	✓
III	0.011915 > 0.010513 > 0.010577	×
IV	0.005757 > 0.005599 > 0.005549	✓
V	0.002327 > 0.002285 > 0.002284	✓
VI	0.017517 > 0.011743 > 0.011705	✓

Solution B

I	0.009604 > 0.009465 > 0.009365	✓
II	0.009514 > 0.009304 > 0.008587	✓
III	0.014344 > 0.012749 > 0.012729	✓
IV	0.005508 > 0.005305 > 0.005258	✓
V	0.002848 > 0.002830 > 0.002807	✓
VI	0.022123 > 0.015083 > 0.014787	✓

Solution C

I	0.008247 > 0.008128 > 0.008040	✓
II	0.008194 > 0.008015 > 0.007396	✓
III	0.012425 > 0.011054 > 0.011026	✓
IV	0.004747 > 0.004573 > 0.004530	✓
V	0.002462 > 0.002448 > 0.002428	✓
VI	0.019194 > 0.013113 > 0.012829	✓

Solution D

I	0.006466 > 0.006381 > 0.006302	✓
II	0.006430 > 0.006301 > 0.005803	✓
III	0.008936 > 0.008924 > 0.008817	✓
IV	0.003788 > 0.003677 > 0.003616	✓
V	0.001918 > 0.001904 > 0.001891	✓
VI	0.015468 > 0.010797 > 0.010339	✓

APPENDIX A5

DETERMINATION OF $D_0^I(v)$ FROM THE POLE APPROXIMATION TO $N_0^I(v)$

If the left-hand cut is approximated by a series of n poles,

$$N_0^I(v) = \sum_{i=1}^n \frac{\Gamma_i^I}{v+v_i^I} \quad (A5.1)$$

Substitute for $N_0^I(v)$ from (A5.1) into (5.3.4) and consider

$$P \int_0^\infty dv' \sqrt{\frac{v'}{v'+1}} \frac{1}{v'(v'-v)} \sum_{i=1}^n \frac{\Gamma_i^I}{v'+v_i^I} \quad (A5.2)$$

The summation and integration signs of (A5.2) are interchangeable and using the substitution $v' = \sinh^2 \theta$ in the integrand one obtains

$$2 \sum_{i=1}^n \Gamma_i^I \left\{ P \int_0^\infty \frac{d\theta}{(\sinh^2 \theta - v)(\sinh^2 \theta + v_i^I)} \right\} \quad (A5.3)$$

which can be rewritten in the form

$$2 \sum_{i=1}^n \frac{\Gamma_i^I}{v+v_i^I} \left\{ P \int_0^\infty \frac{d\theta}{\sinh^2 \theta - v} - P \int_0^\infty \frac{d\theta}{\sinh^2 \theta + v_i^I} \right\} \quad (A5.4)$$

Further manipulation yields the integrands in the more recognisable form

$$\sum_{i=1}^n \frac{\Gamma_i^I}{v+v_i^I} \left[\frac{1}{\sqrt{v(v+1)}} \mathcal{P} \left\{ \int_0^\infty \frac{\operatorname{sech}^2 \theta \, d\theta}{\tanh \theta - \sqrt{v/v+1}} - \int_0^\infty \frac{\operatorname{sech}^2 \theta \, d\theta}{\tanh \theta + \sqrt{v/v+1}} \right\} \right. \\ \left. - \frac{1}{v_i^I(v_i^I-1)} \mathcal{P} \left\{ \int_0^\infty \frac{\operatorname{sech}^2 \theta \, d\theta}{\tanh \theta + \sqrt{v_i^I/(v_i^I-1)}} - \int_0^\infty \frac{\operatorname{sech}^2 \theta \, d\theta}{\tanh \theta - \sqrt{v_i^I/(v_i^I-1)}} \right\} \right] \quad (A5.5)$$

The integrals can then be done explicitly (see tables of integrals) giving

$$\sum_{i=1}^n \frac{\Gamma_i^I}{v+v_i^I} \left\{ \frac{1}{\sqrt{v(v+1)}} \ln \left| \frac{1-\sqrt{v/v+1}}{1+\sqrt{v/v+1}} \right| - \frac{1}{\sqrt{v_i^I(v_i^I-1)}} \ln \left| \frac{1+\sqrt{v_i^I/(v_i^I-1)}}{1-\sqrt{v_i^I/(v_i^I-1)}} \right| \right\} \quad (A5.6)$$

and the denominator function, from (5.3.4), can be written as

$$D_O^I(v) = 1 + \frac{1}{\pi} \sqrt{\frac{v}{v+1}} \ln \left| \frac{1+\sqrt{v/v+1}}{1-\sqrt{v/v+1}} \right| + \sum_{i=1}^n \frac{\Gamma_i^I}{v+v_i^I} \\ + \frac{v}{\pi} \sum_{i=1}^n \frac{\Gamma_i^I}{v+v_i^I} \frac{1}{\sqrt{v_i^I(v_i^I-1)}} \ln \left| \frac{1+\sqrt{(v_i^I-1)/v_i^I}}{1-\sqrt{(v_i^I-1)/v_i^I}} \right| - i \sqrt{\frac{v}{v+1}} \sum_{i=1}^n \frac{\Gamma_i^I}{v+v_i^I} \quad (A5.7)$$

APPENDIX B5

DETERMINATION OF $D_0^I(v)$ FROM THE CUT + POLE APPROXIMATION
TO $N_0^I(v)$

For a finite number, say n , of poles,

$$N_0^I(v) = (v+1)^{3/2} \sum_{i=1}^n \frac{\Gamma_i^I}{v+v_i^I} \quad (B5.1)$$

Consider,

$$\mathcal{P} \int_0^\infty dv' \sqrt{\frac{v'}{v'+1}} \frac{(v'+1)^{3/2}}{v'(v'-v)} \sum_{i=1}^n \frac{\Gamma_i^I}{v'+v_i^I} \quad (B5.2)$$

Using the change of variable $x^2=v'$, (B5.2) becomes

$$2 \sum_{i=1}^n \Gamma_i^I \left\{ \mathcal{P} \int_0^\infty \frac{x^2+1}{(x^2-v)(x^2+v_i^I)} dx \right\} \quad (B5.3)$$

and writing

$$\frac{x^2+1}{x^2+v_i^I} = 1 + \frac{1-v_i^I}{x^2+v_i^I} \quad (B5.4)$$

leads to the form

$$2 \sum_{i=1}^n \Gamma_i^I \left\{ \mathcal{P} \int_0^\infty \frac{dx}{x^2-v} + (1-v_i^I) \mathcal{P} \int_0^\infty \frac{dx}{(x^2-v)(x^2+v_i^I)} \right\} \quad (B5.5)$$



The contribution from the first integral is zero and the second can be rewritten in the form

$$\begin{aligned}
 & 2 \sum_{i=1}^n \frac{\Gamma_i^I}{v+v_i^I} (v_i^I-1) \left\{ \mathcal{P} \int_0^\infty \frac{dx}{x^2-v} - \mathcal{P} \int_0^\infty \frac{dx}{x^2+v_i^I} \right\} \quad (B5.6) \\
 & = 2 \sum_{i=1}^n \frac{\Gamma_i^I}{v+v_i^I} (1-v_i^I) \left[\frac{1}{\sqrt{v_i^I}} \tan^{-1} \frac{x}{\sqrt{v_i^I}} \right]_0^\infty \\
 & = \sum_{i=1}^n \Gamma_i^I \frac{(v_i^I-1)}{(v+v_i^I)} \frac{\pi}{\sqrt{v_i^I}}
 \end{aligned}$$

so that the corresponding D-function is given by the expression

$$D_0^I(v) = 1 - v \sum_{i=1}^n \frac{\Gamma_i^I}{v+v_i^I} \frac{(v_i^I-1)}{\sqrt{v_i^I}} - i \sqrt{\frac{v}{v+1}} (v+1)^{3/2} \sum_{i=1}^n \frac{\Gamma_i^I}{v+v_i^I} .$$

(B5.7)